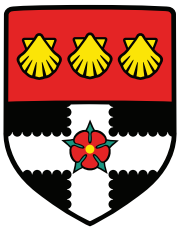

University of Reading

Department of Meteorology

Combining multiple streams of environmental data into a decision support tool for maize based systems in Sub-Saharan Africa

A thesis submitted for the degree of Doctor of Philosophy

Dagmawi Teklu Asfaw

September 2019

Declaration

I confirm that this is my own work and the use of all material from other sources has been properly and fully acknowledged.

Dagmawi Teklu Asfaw

Abstract

In sub-Saharan Africa, where agriculture is the primary sector providing a livelihood for communities, effective use of agrometeorological advisories reduces climate risks and provides guidance on impending weather-related hazards. Early warning of weather-related hazards enables farmers, policymakers and aid agencies to mitigate their exposure to risk. To address this need, this thesis developed and investigated a new framework to monitor climatic risk associated with agriculture and support decision making using available satellite environmental data sets and numerical models for sub-Saharan Africa.

TAMSAT-ALERT (Tropical Applications of Meteorology using SATellite data and ground-based measurements-AgricuLtural EaRly warning sysTem) is a new operational framework, which provides early warning of meteorological risk to agriculture. TAMSAT-ALERT combines information on land surface properties, seasonal forecasts and historical weather to quantitatively assess the likelihood of adverse weather-related outcomes, such as low yield and drought. On a shorter timescale, TAMSAT-ALERT has also been adopted to support farmer decision making on when to plant - a critically important choice. TAMSAT-ALERT incorporates a new soil moisture model simplified from the Joint UK Land Environment Simulator (JULES). The new soil moisture model runs faster and requires low computing power while providing a similar result compared to JULES soil moisture output. Evaluation against observations shows that TAMSAT-ALERT skillfully predicts the climatic risk associated with maize yield 4-6 weeks before harvest over northern Ghana and in some circumstances can anticipate agricultural drought 2-3 months in advance of the end of the season over Kenya. TAMSAT-ALERT identifies a planting date that results in a maximum yield which can be used to provide advisory to farmers in western Kenya. For this application, TAMSAT-ALERT is used to assess the tradeoff between the risk to germination and insufficient moisture for crop growth and development. Overall, the results proved that the TAMSAT-ALERT framework can be used as a tool in climate service providers across sub-Saharan Africa to produce tailored products that help to make an informed decision related to climatic risk on agriculture.

Acknowledgements

First of all, I would like to thank CIMMYT-TAMASA project and Bill and Melinda Gates Foundation for the scholarship opportunity to pursue my PhD study in the UK. I want to express my great gratitude and appreciation to my supervisors Prof. Emily Black and Dr. Ross Maidment. Emily, thank you so much for your wise advice, enthusiastic support and constant helpfulness throughout my study. Ross, thank you so much for all the encouragement and being there for me any time I need help. I am also thankful to Step Aston and One Acre Fund for providing valuable data required for my research.

I would like to thank Prof. Nigel Arnell and Dr. Rob Thompson on my monitoring committee for their guidance and encouraging comments. Many thanks to Dr. Matt Young and Dr. Ewan Pinnington for your time in supporting me with Python coding and reading my paper. I am also grateful to all the members of TAMSAT group where I learn a lot about African weather, and I am very much proud to be part of such a group.

Amsale and Melaku, I am forever grateful for helping me while I was sick, thank you for opening your home and be there with me! Paulos and Genet, I am thankful for all the support you have given me.

Finally, a special thank you to my family (Leoul Teklu, Tinebeb Teklu, Kimiya Mohammed, Mohammed Umer) for all your encouragement and prayers.

"The fear of the lord is the beginning of wisdom, and the knowledge of the holy one is understanding." Proverbs 9:10

Contents

Chapter 1

Introduction

1.1 Motivation

This thesis focuses on developing a new framework for assessing the climatic risk on agriculture within the growing season at short (two weeks) and long time (seasonal) scales and on identifying information that can be provided to end-users to make informed agricultural decisions based on available climatic data in sub-Saharan Africa.

1.1.1 Climate risks on agriculture

The increase in extreme events of weather conditions over the world, coupled with improper land management and social pressures, has exacerbated disasters related to drought and flooding (Adikari and Yoshitani, 2009). In developing countries where the economic ability to withstand disaster events like flooding and drought is low, the impact caused by such events is enhanced causing significant loss of life, economic, environmental, and social impacts that hinder the development process of these nations. From all natural disasters, drought is considered to be the most complex and affects many people when it happens. The impacts of drought are significant irrespective of the development level of the countries, even though the characteristics differ (Wilhite, 2000). In sub-Saharan Africa (SSA), where agriculture plays a significant role in the overall economy of countries and people livelihoods (Struif Bontkes and Wopereis, 2003) understanding and monitoring the climate risk on the sector is paramount. Drought and the subsequent reduction in productivity of crops and fodder, which result in food shortage and threaten the food security of

people is the main climatic risk sub-Saharan African countries face. Though low productivity of crops is not only a result of rainfall and soil moisture deficit, climate risk plays a dominant role and the impact of climate variability on crop productivity is well documented in the literature (Challinor et al., 2010; Rosenzweig et al., 2014; Lana et al., 2017; Rosenzweig et al., 2018; Vogel et al., 2019). Therefore, quantifying the climatic risk on the agriculture sector in Africa is of higher importance for adopting relevant policies and strategies towards mitigating the impacts on people in advance.

1.1.2 Climate information for agriculture

Agriculture is one of the primary economic sectors in Africa, but it is also highly exposed to impacts due to climate variability. Managing climatic risk requires reliable and useful climate information tailored to the local condition and delivered on time (Lötter et al., 2018). Cooper et al. (2008) states that the ability of decision-makers to utilise short term information and manage current climate risk is a crucial prerequisite for better management of future climate risk associated with rainfed agriculture. Jones et al. (2015) and Nidumolu et al. (2016) showed that long term climate information can improve decision making. Decision making considers many factors in addition to climate information like agronomic, social, economic, labour and individual capacity but, review of past studies indicated that climate information is provided separately from the other relevant information; hence, it alone cannot define the comprehensive decision-making process (Singh et al., 2018).

Success in the uptake of using climate information for decision making occurs when the information provided is both tailored to the local context and makes use of innovative participatory delivery processes. However, climate information has not been well integrated into the national development program and decision-making process in African countries (Singh et al., 2018). Though there is a considerable effort made by scientists in improving coverage, quality and accessibility of climate information there are still significant barriers in using the available information. Singh et al. (2018) generalise these barriers as:

a. Relevance to be useful for decision making at the local level.

b. The manifestation of the local phenomena to be translated to variables and processes that

matter to the end-user (water supply, crop production, floods, drought etc.)

c. Level of interaction between end-users and information provider is also crucial in the uptake of the information.

d. Inadequate understanding of how and why end-users make a decision.

Overall, farmers decision-making process is very complex, involving interactive process and alterations based on their assets and assumptions, socio-economic culture and perceptual environment (Singh et al., 2016). This means more agricultural decisions taken by farmers focus on a short time scale of a season or year rather than decades that impact climate change (Singh et al., 2018). Therefore, climate services that support short term decision-making are likely to be of greatest value to farmers (Lobo et al., 2017).

1.2 Background

1.2.1 Drought and its impact on agriculture

1.2.1.1 Drought definition

Drought has no universally agreed precise definition and lack of such a consistent agreement on the definition for the term contributes to its complexity resulting in subjectivity of the impacts associated with it (Zargar et al., 2011). The meanings of drought usually are region and impact–specific, resulting in many interpretations of drought events (Wilhite, 2000). The existing definitions can be categorised as either conceptual or operational. Conceptual definitions are more general and are based on defining the boundaries of the concept of drought like the definition given by Encyclopedia of Climate and Weather: *"A prolonged period during which the amount of precipitation falling over a particular area is markedly less than the amount that usually falls in that place over the same period"* (Allaby, 2007). Operational definitions, on the other hand, are subjected to specific sectors and expanded in describing its beginning, end and severity depending on the operation identified (e.g. agriculture or hydrology) (Zargar et al., 2011). These operational definitions allow for analysing drought frequency, severity, and duration for a defined period (Wilhite, 2000). For example, the definition of agricultural drought evaluates the soil moisture deficit as a ratio and describes the impact on various crops at a different stage. Based on

the operational definition drought can be classified as meteorological, agricultural, hydrological and socioeconomic.

Meteorological drought: is defined as a shortage of precipitation over a specific location compared to the long term historical amount available for the location. Many of the analyses for meteorological drought are based on precipitation and are only expressed as an anomaly from historical records. It measures the degree of dryness in comparison to some normal or average amount within a specific period of intervals (Wilhite and Glantz, 1985; WMO, 2006).

Agricultural drought: is defined as a period with declining soil moisture level resulting in lack of crop growth and production. It is mostly concerned with soil moisture deficiency and the impact it has on crop production. A decrease in soil moisture depends on several factors like lack of precipitation and increased evaporation due to high temperature. The impact on the crop is also very specific as the evapotranspiration demand of crops varies depending on type, variety and growth stage of the crop itself as well as the properties of the soil. Several drought indices, based on a combination of precipitation, temperature and soil moisture, have been derived to study agricultural droughts (Wilhite and Glantz, 1985; WMO, 2006).

Hydrological drought: is related to a period where there is insufficient surface and subsurface water resources for water uses of a given water resources management system like water supply for urban areas or irrigation system. Hydrological droughts usually lag from the occurrence of meteorological and agricultural droughts as it takes a longer time for precipitation deficiencies to manifest in components of the hydrological system such as soil moisture, streamflow, and groundwater and reservoir levels (Wilhite and Glantz, 1985; WMO, 2006).

Socioeconomic drought: is associated with failure of water resources systems to meet water demands and thus associating droughts with supply and demand for an economic good (Mishra and Singh, 2010; WMO, 2006). It involves the components from meteorological, hydrological, and agricultural drought but it is unique from the others as its occurrence depends on the supply and demand of economic goods like water, forage, food grains fish and hydroelectric power which are directly or indirectly related to weather condition in a specific location. Socioeconomic drought

is a product of increased demand for an economic good due to reduced supply as a result of a weather-related loss in the water supply (Mishra and Singh, 2010).

The drought types mentioned above occur in the same order given. Meteorological drought is the first to occur as a result of precipitation deficit compared to the climatology within a short time scale of weeks to months. This deficit of precipitation will result in a substantial decrease in soil moisture, which results in agricultural drought within a time scale of three months to a year. As the deficit of precipitation continues for extended period water supply in reservoirs like rivers and lakes and groundwater decline, causing the hydrological drought with a time scale of over a year. Finally, socioeconomic drought occurs as a result of the combination of all these droughts severely damaging the socioeconomic fabric of the society affecting the supply and demand of economic goods like food grains, animal fodder and hydroelectric production (WMO, 2006; Mishra and Singh, 2010; Spinoni et al., 2014). Figure 1.1 shows the sequence of drought occurrence where all drought type begins from lack of precipitation for a prolonged time (Meteorological drought) leading to soil moisture deficiency (Agricultural drought) resulting in reduced streamflow and reduction in water levels of water bodies (Hydrological drought) and the combination of all these finally causing economic, social and environmental damage (Socioeconomic drought).

All types of drought defined above can be characterised by the severity, duration and spatial distribution (Zargar et al., 2011). Identifying drought before it develops into a severe socioeconomic drought can reduce impacts and save lives and resources; hence, monitoring of meteorological, agricultural and hydrological drought is vital. Existing systems that monitor just one type of drought do not provide a full picture. For instance, one can base drought monitoring only on recorded precipitation, and this can only tell how dry it is and tell nothing about the impacts. If one only tries to monitor drought based on crop harvested, it might lead to a conclusion that the climatic conditions cause all crop failures. Therefore, a combination of drought monitoring tools needs to be used to accurately identify the onset, severity and extent of the drought to deliver relevant information to decision-makers who are involved in preparing emergency plans and resource allocation for the mitigation drought impact. This study will help to address this applied need through the development of a new framework to predict and monitor the likelihood of drought occurrence throughout the growing season (chapter 4).

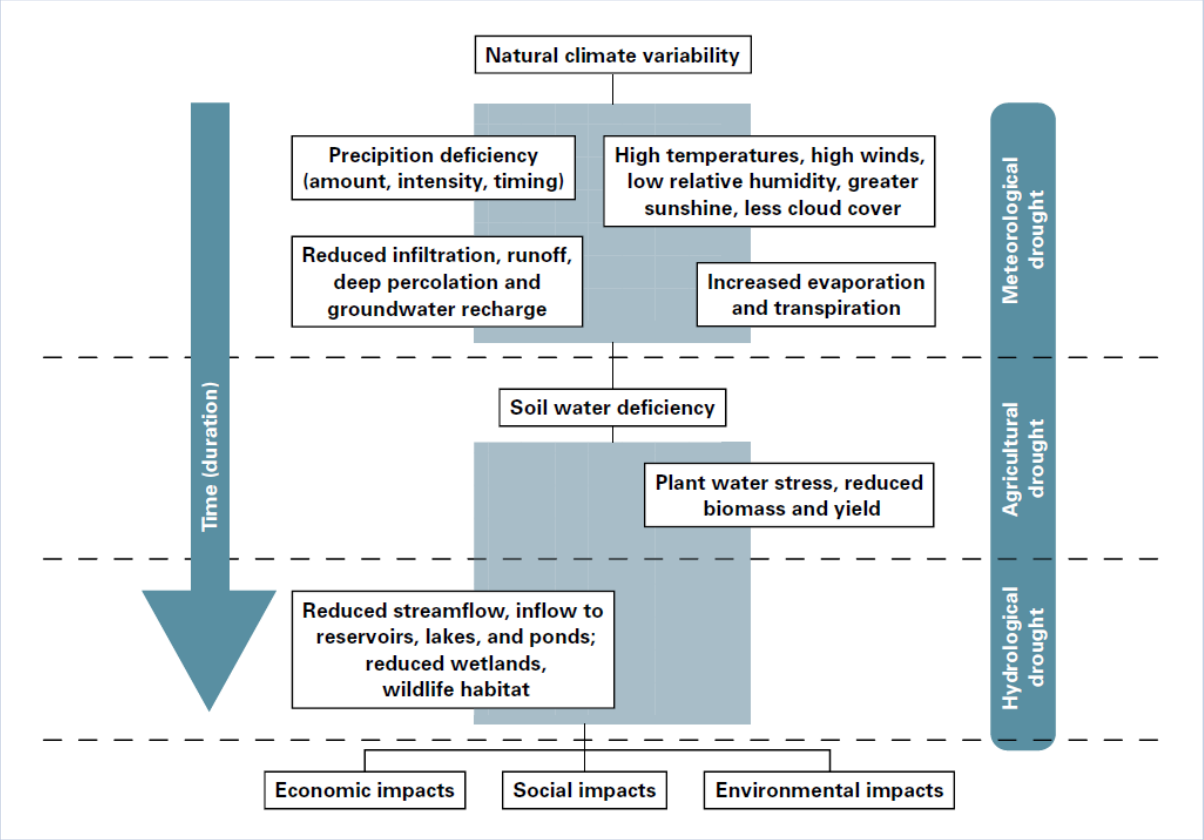

Figure 1.1: Sequence of drought occurrence and impacts for commonly accepted drought types. All droughts originate from a deficiency of precipitation or meteorological drought but other types of drought and impacts cascade from this deficiency. (Source: National Drought Mitigation Center, University of NebraskaLincoln, USA, `https://drought.unl.edu/Education/DroughtIn-depth/TypesofDrought.aspx`)

1.2.2 Drought monitoring tools and indices

Drought monitoring tools are tools which allow monitoring of the different characteristics of a possible drought event using various indicators based on quantitative climate data such as precipitation, temperature and model-based data like soil moisture and evapotranspiration or river discharge. Drought indices are single values that combine the raw data, which is the main cause of the drought to occur and provide a general idea about the drought to be used in decision making for mitigating it (Zargar et al., 2011). There are many drought indicators (>80) that are utilised throughout the world to make decisions and help people cope with the impacts caused by drought (Niemeyer, 2008). These drought indices are variable on their approach of approximating the drought condition and use of driving data set. These indices also describe different types of droughts; meteorological, agricultural, hydrological and socioeconomic. They try to explain the severity, onset and end of the drought at different spatial and temporal scales. They are

also used at various operational levels for planning, early warning and mitigation of drought (Zargar et al., 2011). Drought is a very complex phenomenon, as discussed in earlier paragraphs. Hence, there is no universally accepted definition of drought and in the same manner, there is no universal drought indicator method (Niemeyer, 2008). All the methods developed have their way of explaining the characteristics of the drought; therefore, one has to use a combination or modify the tools to fit the condition in the local region. Some of the drought indices transform the raw data to a single value indicator which can be compared and analysed at different temporal and spatial scale for decision-making (Zargar et al., 2011). A brief description of some of the drought indicators that are commonly used in Africa to monitor drought are described below to indicate the similarities and differences among them.

Most commonly used drought monitoring indices in Africa include Standardized Precipitation Index (SPI) which is based on the precipitation anomaly of an area and uses a statistical approach to put an index for the drought condition of the area in question (Mckee et al., 1993). Standardized Precipitation Evapotranspiration Index (SPEI) is a modified form of the SPI where the concept is the same but the data used to determine the drought index is different. SPEI involves the use of the difference between precipitation and the potential evapotranspiration (PET) rather than using only precipitation values. The difference between precipitation and PET produces a fuller view of the water balance, and converting the anomaly to a standard Z-score will allow a better estimation of the drought as it also takes the temperature of an area into account (Vicente-Serrano et al., 2010). The Palmer Drought Severity Index (PDSI) is based on the conceptual framework of calculating the water balance of an area and deriving the deviation from climatological normal moisture value of the area in question (Agnew, 2000). Multivariate standardized drought index (MSDI) is a drought index based on the concept of ensemble streamflow prediction (ESP). It combines precipitation and soil moisture to give an estimation of both meteorological and agricultural drought. It combines the Standardized Precipitation Index (SPI) and Standardized Soil Moisture Index (SSI). It helps to connect the conditions from both the precipitation and soil moisture (Hao and AghaKouchak, 2013). Soil Moisture Deficit Index (SMDI) and Evapotranspiration Deficit Index (ETDI) which are agricultural drought indices based on the anomaly of available soil water deficit and the anomaly of water stress to the long term average (Narasimhan and Srinivasan, 2005). Aggregate Drought Index (ADI) is a multivariate drought index that comprehensively considers all physical forms of drought (meteorological, hydrological, and agricultural) through inclusion

of variables that are related to each drought type (precipitation, evapotranspiration, streamflow, reservoir storage, soil moisture content, and snow water content) and uses principal component analysis to derive a single index (Keyantash and Dracup, 2004). Water Requirement Satisfaction Index (WRSI) is the ratio of cumulative actual crop evapotranspiration to the cumulative potential evapotranspiration over a defined growing period. It compares the amount of water available for plants, with the amount required to grow without water stress (Senay and Verdin, 2003).

1.2.2.1 Drought impact on agriculture

Drought causes a significant impact on people's livelihood in Africa, mainly through crop failure. Lower productivity of crops and fodder due to moisture deficit result in food shortage and raise the risk of food insecurity at household and community level. Even though there are additional factors for reduced productivity of crops, climate risk is a major contributor to the problem. Studies have shown that climate variability exacerbates crop productivity loss in Africa. For instance, Schlenker and Lobell (2010) showed by mid-century (2046-2065), the mean estimates of aggregate production in SSA decrease by 8 - 22 % for the major crops maize, sorghum, millet, groundnut, and cassava. Another study on climate change impact on crop productivity in Africa indicates that mean yield changes of 17%, 5%, 15% and 10% for wheat, maize, sorghum and millet were estimated respectively from the baseline period (1961-1990) for the projected climate changes based on various general circulation models (GCM) and a timescale up to the 2080 (Knox et al., 2012). Challinor et al. (2007) showed that even though climate change and variability impact on agriculture productivity in Africa is mostly negative farmers ability for adaptability in short and long term variation to the environment is proved to be high with the critical factor of accessing relevant knowledge and information. Much of the African continent is going to get drier and hotter with a subsequent adverse effect on crop yield and this requires a strong adaptation strategy involving people relocation, structure change of production, and crop patterns as well as government providing information incentives and economic environment to facilitate these changes (Collier et al., 2008). In general, agriculture in Africa is subjected to a variety of risks from changing climate and variability that exist throughout the continent. The challenges faced require a strong commitment and tailored information for making informed decisions in many of the everyday farming practices and at a country level policy formulation and strategies for risk aversion emanating from

climate variability.

1.2.3 Weather and climate data for risk assessment

Integrating scientific information from weather and climate data create many opportunities to make informed decisions (Adams and Vaughan, 2015). Due to the changing climate, many of developing countries are faced with a vast climatic risk associated with essential sectors like agriculture and water resources. This calls for the incorporation of climate information in the decision-making process for the long term and short term actions that are taken to enhance the sectors. There are many opportunities to utilise available climate information as input to make critical decisions. This fact lies in the ability of scientists and decision-makers abilities to integrate all the information into a ready to use and relevant tool that support decision making (e.g. Ranger et al., 2010; Daron, 2015). The relevance of information on climate and weather is dependent on the nature of the risk, such as economic sector affected or governance structure. There is an abundance of local anecdotal evidence in using climate information for making decisions in the agriculture sector over sub-Saharan Africa (Singh et al., 2018). But, developing this knowledge and integrating it with scientific knowledge that could easily be transferable to other regions and making part of the overall decision-making process is vital. Many studies reviewed the main factors that affect the uptake and use of climate information. Some of the factors include lack of reliable historical information to understand the current climate and evaluate models (Tarhule and Lamb, 2003), the coarse-scale of climate projections (Taylor et al., 2012), disconnect between users and procedures of climate information and inadequate capacity to use and deliver climate information (Singh et al., 2016).

To properly comprehend the use of climatic information in the decision-making process, understanding the climate information type and availability is vital and the technological and scientific challenges of producing this information must be understood and explained well. The predictability of the future climate and ability to understand the past climate affects the information provided that is relevant to sectors like agriculture and water. For instance, Troccoli (2010) states that seasonal forecast has more value for guiding management decision in agriculture even though they have low skill. In the use of climate information, there is a difference between a climate variable (e.g. temperature, rainfall, wind) and climate-related variables (river flow and

soil moisture) where non-climate variables influence the latter. Climate-related variables are generated from numerical methods (hydrological models, crop models, land surface models) to predict changes in climate-related variables and generate information that can be used in the decision-making process. Besides producing the information, sharing it with users is even more vital. In this regard, dissemination of climate information has improved through time with access to the internet and the willingness of several institutes like National Aeronautics and Space Administration (NASA), Climate Prediction Center (CPC), and Postdam institute climate impact to hold data portals that can easily be accessed all over the world (Singh et al., 2018). The major scientific challenge is to post-process this raw data into useful and impact-oriented information. This task requires skills and experience in computation and analysis tools making many of the users researchers and impact modellers. Despite this, there are efforts to translate climate information to more user-oriented advisories for farmers (e.g. Dorward et al., 2015). In addition to converting climate information to usable format, the dissemination through effective communication channels in an equally important aspect for widespread uptake. The global challenge of such endeavours is ensuring quality, consistency, and appropriate interpretation of climate information (Singh et al., 2018).

African countries operate their meteorological agencies and despite their differences in capacity, most provide weather and climate information, collect data and provide this information to communities and other users. Regional institutes and collaborations also support this effort (e.g. Intergovernmental Authority on Development Climate Prediction and Applications center-ICPAC, Agrometeorology, Hydrology, Meteorology-AGRHYMET, Southern African Development Community Climate Services Centre-SADC-CSC, African Center of Meteorological Application for Development-ACMAD) (Singh et al., 2018). These regional institutes are mainly engaged in providing seasonal forecasts, early warning related to extreme events and crop productivity. ICPAC, for instance, has collaborations with regional and international institutes to develop tools supporting the use of climate information in different sectors like agriculture, food security, livestock, and water resources risk assessment and management.

1.2.4 Climate services in Africa

Climate services are becoming an integral part of adaptation in the agricultural sector of many countries providing vital information about local climate, supporting institutional and local farming decisions and supporting resilience-building interventions in addition to creating the platform for climate-smart agriculture (Hansen et al., 2019). Developing effective agricultural climate services at a national scale requires balance between specific needs of local farmers and providing cost-effective service at scale. The challenge of doing this is associated with the fact that farmers need for climate service varies depending on the experience, wealth, gender and livelihood activities (Hansen et al., 2019). On the other hand, climate service providers are faced with resource constraints and broad multi-sector mandates not to focus on tailored climate service provision. For example, the regional climate outlook forums Greater Horn of Africa Climate Outlook Forum (GHACOF, `http://www.icpac.net/`), Southern African Regional Climate Outlook Forum (SARCOF, `https://www.sadc.int/`), and Climate Outlook Forum for West Africa (PRESAO, `http://www.acmad.net/new/`) are primary providers of such information in Africa. In any agricultural activity, farmers make management decisions in response to the weather so that they can optimise productivity and minimise the risk associated. However, their decisions on farming are based on their indigenous knowledge accumulated over a long time (Mafongoya and Ajayi, 2017). In many countries, farmers believe their insights on the outlook of the climate and follow a more conservative strategy which leads to sacrificing productivity to reduce risk of loss (Nesheim et al., 2017).

Farmers' knowledge can be supported and integrated with scientific data available from ground measurements, satellite observation and numerical model output (e.g. weather forecasts and land surface conditions) to facilitate weather-sensitive decisions regarding agricultural management and climatic risk (FAO, 2019; Mafongoya and Ajayi, 2017). The main climate services supporting the agriculture sector include weather forecasting, seasonal climate forecasting, statistical assessments of the future frequency of extreme weather and climate events, agrometeorological crop monitoring and agrometeorological advisories (FAO, 2019). Agrometeorological advisories provided by national or regional climate service agencies are used for planning the crop season and making strategic decisions related to the type of crop, planting time and water requirement for irrigation (FAO, 2019). Using operational decision-making tools to extract information from available

climatic data set from ground-based measurements, automatic weather stations and freely available satellite observations outlooks about season onset, cessation, crop harvest and drought are provided. Efficient use of agrometeorological advisories helps to reduce climatic risks on farming communities and provide enough time for authorities to respond to adverse events (FAO, 2019). For these to be operational and provide consistent advisory, decision support tools are key elements that every climate service provider need to have. These decision support tools integrate available information (weather data, forecasts, and land surface conditions) to anticipate agronomic conditions on which mitigating management actions could be taken.

1.2.5 Decision support tools

Climate information generated from global and regional climate models and satellite and ground-based measurements is critical information for farmers. However, such raw information has little significance for farmers and the formats are not presented in such a way that farmers can understand or utilise. Therefore, this raw climate information is mainly used within computer models to generate simplified, easy to understand and relevant information for making practical decisions at farmer scale and country level often in the form of drought indices (section 1.2.2). In sub-Saharan Africa, decision support tools can assist with diagnosis and analysis of problems and opportunities related to the risks farmers are facing. Agricultural decision support tools (DST) are computer software that can be used to support complex decision making based on available evidence to improve agricultural productivity (Shim et al., 2002; Rose et al., 2016). DSTs are designed to help users make more effective decisions by leading them to clear decision stages and presenting the likelihood of various outcome resulting from different options (Dicks et al., 2014). DSTs can be dynamic software tools that provide an optimal decision path. For example, it can facilitate effective farm management through recording data, analysing and generalising a series of options that are based on objective evidence synthesis (Rose et al., 2016). Though there are a variety of DSTs many of them include database management holding the necessary data, simple to complex numerical modelling functions and simple graphical user interface enabling interactive inputs, reports and graphics (e.g. Shim et al., 2002).

There have been many DSTs developed with the advancement in weather and climate forecast, knowledge of social frameworks and computing power. These DSTs range from complex com-

puter models to simple table and charts that help farmers to make an informed decision. DSTs are very useful for developing site-specific recommendations for different challenges and risk farmers face throughout a growing season. DSTs also allow for accounting the diversity and dynamics of farmers reality. DSTs are very suitable to be used in participatory development and dissemination of relevant information however, DSTs have not been widely used in SSA. Walker (2002) provides the major constraints in the use of DSTs for agriculture in SSA as follows:

a. DSTs fail to capture the complexity of smallholder agriculture of SSA.

b. Require data that are not available or are of poor quality.

c. Lack of knowledge on DST prevents the use.

d. Institutes that usually use DSTs promote the use of single tools but, the complexity of risks and challenges require the use of multidimensional DSTs.

e. The problem of handling data collection, problem identification, application of tools and making appropriate and relevant conclusions from it.

Decision making in agriculture can be of different time scales; short term (when to plant?), medium (what variety to plant?) and long term (what is the likelihood of drought occurrence?). Therefore, the ultimate goal of using DSTs is to help farmers, but other primary users include scientists and experts in the field of risk assessment, agriculture and climate, planners and higher level decision-makers. In general, DSTs are designed to help users make more effective decisions by leading them to clear decision stages and presenting the likelihood of various outcome resulting from different options (Dicks et al., 2014), however, understanding the limitations associated with DST is also equally crucial. The effectiveness of DST is measured whether it addresses the fundamental question, its availability, the requirements to use it, and the availability of the required data to run the system. Many regional and national climate service centres in SSA utilise different DSTs to provide climate information for farmers and government for better decision making regarding the understanding of the climatic risk and outlook of a growing season.

1.2.6 Gaps in climate service provision

Though there is a significant improvement in climate data gathering, analysis and interpretation, the challenge still faced is regarding the communication of the information to a standard required

by users. There is also a gap among users concerning the information available, where to find it and how to use it for agricultural management decisions (FAO, 2019). For the SSA context, the value of climate and weather information is held in the ability to be used in agriculture management practice to safeguard or improve productivity; otherwise, their value is lost. Despite the efforts in improving climate and weather information, most of the information is not reaching local farmers due to poor communication, including from not being adapted to the local scale (GCOS, 2006). GCOS (2006) presents four main challenges concerning the use and dissemination of climate information:

- Some policies regarding free data sharing are restrictive due to financial issues or low budget.
- Archives of long term climate data are not digitised and quality controlled.
- Gaps in real-time-data for operational systems and early warning use.
- Inadequate understanding of how to make the best use of satellite data.

Harvey and Singh (2017) also identified insufficient staffing and technical expertise, delays in data transfer resulting delayed early warning, the need for greater strengthening of observational capacity and the need for greater financial resources as gaps in Burkina Faso climate service. Hansen et al. (2019) discusses farmers climate information needs over SSA and found that the information provided by regional outlook forums generally is a probabilistic estimate of the seasonal rainfall and temperature as tercile forecast from the historical distribution. These tercile forecasts are presented in a map covering a large area and do not include information regarding interannual and spatial variability of the local climate. These forecasts are found to be poor matches for farmers decision-making needs and do not improve the estimation of climatic risk on crops (Asfaw et al., 2018). The tercile seasonal forecasts do not directly provide information about anticipated climate conditions at a local scale of farmers decision-making, forecast categories are arbitrary, and acting on probabilistic forecast information requires an understanding of the uncertainty of the forecasts (Hansen et al., 2011, 2019). Farmers need more than just the average conditions during the season, such as the timing of season start and end, risk of damaging dry spells and other extremes. Therefore, providing the information in a probability of exceedance format along the historical values helps first with connecting the forecast with the historical condition which increases awareness about the past condition and allows the information to be used in the absence

of forecasts. Second, it provides information in association with thresholds that are relevant to decision options instead of arbitrary tercile boundaries and lastly, it conveys the uncertainty in a clear manner (Hansen and Indeje, 2004; Hansen et al., 2011, 2019). Mafongoya and Ajayi (2017) states that the information dissemination ability of Regional Climate Outlook Forum (RCOF) for smallholder farmers is inadequate due to:

- Forecasts are not specific enough for the needs of end-users.
- Poor interpretation and communication of forecasts, which leads to misunderstanding.
- Farmers inability to respond to forecasts due to their lack of access to seed, fertiliser, labour and credit, which would allow them to make adjustments in relation to the expected seasonal climate.
- Poor distribution of the forecast due to lack of communication channels.

The capacity of end-users like agricultural extension workers and farmers is also very minimal. However, work in Zimbabwe (Patt et al., 2005), Mali (Hellmuth et al., 2007), and Nigeria (Isaac et al., 2009) have shown that efforts to translate and localise the information can influence farmers decision-making processes. However, results from a paper by Luseno et al. (2003), in Ethiopia and Kenya show the contrary due to weak link between rainfall and pastoralist risk and the information being more directed towards crop production than pastoral production system. Venkatasubramanian et al. (2014) also indicate that climate services help farmers to use the best adaptation practices and improve the management of climate-related agricultural risks.

The use of historical data directly and in conjunction with simulation models, to analyse the risk and support decision-making, is well established in agricultural research and practice. But, climate service providers in SSA are very slow in recognising the value of local historical climate data in agricultural climate services. Historical data helps in understanding the seasonality, variability and trends of the local climate and also it helps to manage risk and adaptation to climate change (Hansen et al., 2019). Farming communities understand their local climate and use observable indicators to anticipate upcoming weather conditions, and integrating analysis of historical climate enables farmers and decision-makers to better understand and adapt to variability, seasonality and any trends that characterise their local climate (Hansen et al., 2019). In principle, translating raw information into agricultural impacts and management advisories

increases the relevance for farmers decision-making. Agricultural climate services employ both quantitative and model-based tools and subjective consultative processes to translate climatic information tailored to specific crops and management decisions.

Climate service providers have the potential to serve more using their capacity and knowledge of the climate, especially in the areas of water resource management, agriculture and early warning for disaster risks associated with climate (GCOS, 2006). The experience across many African countries suggest that routinely provided climate information and farmers need is strongly incompatible and require a significant improvement for their effectiveness (GCOS, 2006; Hansen et al., 2019; FAO, 2019). One way of improving their capability is providing them with simple systems that can be run with their limited resources at their disposal to generate more information out of climate data available and enhancing their capacity to do the analysis by themselves so that they can integrate their local knowledge and produce a tailored climate information for their primary users. The new tools should also be helpful for farmers to make farm management decisions in response to the climate conditions.

1.3 Research questions and thesis objectives

Research questions

Drought and subsequent yield decrease are the primary climate risks faced by farmers in SSA (section 1.2.3). Increased climate variability and lack of access for relevant climate information tailored to the local condition exacerbate the climate risks on agriculture (section 1.1.2). Therefore, the need for monitoring climatic risk on agriculture is paramount and climate service providers need to take a significant role in making usable climate information available on time for end-users like farmers, government and aid agencies as well as private sectors to make an informed decision. In light of this, the overall aim of this thesis is to assess meteorological risk on agriculture within the growing season at short and long time scales and to derive information that can be provided to end-users to make informed agricultural decisions (section 1.1). This thesis will, therefore, address this overarching aim by focusing on the following primary questions:

1. What information about meteorological risk on agriculture can be derived from local and regional meteorological observations and forecasts? (chapter 2)

2. Can simplified versions of a complex land surface model be used to represent an agricultural risk decision metrics? (chapter 3)

3. How robustly do model outputs such as soil moisture and Water Requirement Satisfaction Index (WRSI) represent agricultural drought compared to meteorological based metrics such as Standardized Precipitation Index (SPI)? (chapter 4)

4. How can historical weather information and numerical models be integrated for deciding on the optimal planting date? (chapter 5)

Thesis objectives

To address the the research questions described above the thesis include the following objectives:

1. Developing a new framework of assessing climatic risk on agriculture which uses historical climatic data and seasonal forecasts and demonstrate the use of the system to evaluate the risk of low maize yield over Ghana.

2. Developing a soil moisture model based on the principle of a more complex land surface model and evaluate the ability to use less complicated numerical model outputs to assess climatic risk on agriculture.

3. Evaluate how the new framework can be used for assessing climatic risk at a seasonal timescale, where it is used for drought monitoring and its ability compared to conventional drought monitoring tool SPI over Kenya.

4. Developing a new methodology to determine an optimum planting date (short timescale critical decision) in western Kenya based on the concepts of the new framework accounting for available soil moisture and WRSI.

The following sections provide a brief background on the research questions and thesis objectives.

1.3.1 Developing a new framework for assessing climate risk on agriculture

There are many climatic data sets available from satellite and ground observations in Africa, and most African countries provide weather and climate information through their national meteorological agencies. Even though these raw data sets can provide information that users are interested

in (Lobo et al., 2017), the climate information is required in a more tailored fashion to the local conditions to manage climate risk (Lötter et al., 2018). There is an increased demand for timely climatic information which is relevant to practical decision support (section 1.1.2) and mostly users compare the current season with past to intuitively assess risk (Tarhule et al., 2009). Climate service centres in Africa also use DSTs available to them to provide more detailed and user-relevant information; however, there are many challenges in using existing DSTs (section 1.2.5). One major issue related to climatic risk assessment DSTs is that most of them are instantaneous reflecting only on the existing condition at the time of evaluation hence, requiring more improvement for their effectiveness (GCOS, 2006; Hansen et al., 2019; FAO, 2019) (section 1.2.6). Nevertheless, the climate risk on agriculture is dependent on what happened throughout the growing season rather than a single time condition that occurs within the season. Therefore, the first research question attempts to develop a new framework for assessing climate risk on agriculture, considering climate risk as a function of what happened in the whole season (past and future). Through this new concept, it tries to identify the information that can be derived from existing climatic data and forecasts through continuous monitoring of the growing season (chapter 2).

1.3.2 Developing soil moisture model

The second research question deals with developing a simplified version soil moisture model based on the concepts and mathematical description of a well-tested land surface model (LSM). DSTs use numerical models to process weather data sets to determine the impact of climate risk on the agriculture sector (section 1.2.5). For instance, drought monitoring tools utilise weather data and numerical soil moisture output to estimate the drought severity and extent (chapter 4), however, the capacity of climate service centres in African countries is very limited in using complex numerical models and the accessibility of already existing tools is limited (section 1.2.4). There are many challenges associated with the use of a complex land surface model like the knowledge gap between the model producers and users, lack of capacity at the local level to modify complex land surface models, scale issues related to the output of LSMs (section 3.1.2, section 3.1.3). Complex LSMs are also difficult to adopt for new relevant metrics. Therefore, in this thesis a new soil moisture model was developed based on the Joint UK Land Environment Simulator (JULES) model description for further studies in chapter 4 and chapter 5 regarding drought monitoring and optimum planting time identification. The research question addresses how much the simpli-

fied version of soil moisture code can represent the output of a well tested complex land surface model to be used for climate risk assessment on agriculture. (chapter 3)

1.3.3 Drought monitoring within the growing season

Drought is a common risk that farmers in Africa face within every growing season (section 1.2.1). The impact of a drought is very devastating to local communities that are dependent on rainfed agriculture for their livelihood. Hence, anticipating and monitoring the occurrence of drought ahead of time is crucial information that many government authorities, farmers and aid agencies would like to receive. There are several drought monitoring tools available (section 1.2.2) and the SPI is one of the meteorological drought monitoring tools (section 4.2.3). The third research question arises to evaluate the use of the new framework developed to monitor climate risk on agriculture (chapter 2) in monitoring agricultural drought using Water Requirement Satisfaction Index (WRSI) (section 3.2.3). Meteorological drought indicators like SPI indicate only the deficit on precipitation whereas soil moisture based WRSI allows to monitor agricultural drought. Therefore, chapter 4 discusses the improvement in using WRSI as an indicator for agricultural drought compared to SPI and evaluate how early the new framework can anticipate agricultural drought within the growing season. (chapter 4)

1.3.4 Identifying optimum planting date

One of the critical decisions every farmer make each season is the time of planting. This decision of planting time is important as it determines subsequent farming practices (Hassan, 1996; Wolf et al., 2015). The planting time is also one of the adaptation measures to get the best use of rainfall in a growing season and the decision is solely in the hands of the individual farmers with no costs to incur (Tubiello et al., 2000). The methods available to identify optimum planting time are based on the onset of the rainfall and the others depend on specific soil moisture derived from numerical models; others use crop models to identify the planting time with the highest yield (Stehfest et al., 2007; Liu et al., 2007; Sacks et al., 2010; Waha et al., 2012). All these methods have one common character, which is that they are not operational but rather provide a planting window for a region once. Nevertheless, planting time is always variable depending on the condition of the season (Harrison et al., 2000; Chmielewski et al., 2004). Farmers in Burkina Faso, for instance, base their decision of planting time on past year experience with some adjustment for the season

based on the weather forecast (Ingram et al., 2002). Therefore, the last research question for this thesis emanates from the quest for developing an operational optimum planting date decision making for SSA by modifying the decision making framework developed to monitor climate risk on agriculture (chapter 2). The new approach for identifying optimum planting time for maize crop over western Kenya utilises historical weather data and soil moisture forecasts and combine them to identify criteria for selecting an optimum planting time and identify the advisory service that could be given for farmers. (chapter 5)

1.4 Thesis approach

To achieve the overall thesis theme and objectives discussed above, the thesis employed two models; the Global Large Area Model (GLAM) and a soil moisture model. For the demonstration of climatic risk on low yield using the new framework for agricultural decision support the system uses a pure crop model GLAM (chapter 2). GLAM requires minimal input data and it is a well-established model for crop yield estimation. Using GLAM avoids the complexity that could result from using many input data and helps solely see the value of the new framework in its ability to estimate climate risk on agriculture (low yield). However, the crop model only focuses on yield estimation and is not capable of estimating major climate risk like drought. Therefore, the thesis used a new soil moisture model (chapter 3) which outputs WRSI that can be used as a proxy to determine agricultural drought occurrence and the subsequent crop yield loss due to the higher correlation between WRSI and crop yield (chapter 4). Using WRSI will help to combine both risks on agricultural drought and low yield rather than using two separate models for crop yield and drought. The thesis also aims for the new approach of assessing climate risk on agriculture to be easily accessible and used by African climate service centres. Sharing of the new system requires avoiding the use of models such as GLAM and JULES that are under a licence which is one of the rationales for the development of a new model that combines both yield and drought risk assessment.

The thesis evaluates the new framework using GLAM over northern Ghana and the drought prediction was assessed over Kenya where the climate is spatially variable with high rainfall and humid environment in the west and more arid and semi-arid weather in the east. This helps to see the value of the new framework ability in predicting drought risk within the growing season.

Overall, applying the framework over different environments and modelling tools helps to show the versatility of the new climate risk assessment framework.

1.5 Thesis structure

In light of the need to provide climate risk monitoring in the agricultural season, chapter 2 presents a new approach to monitoring climate risk on agriculture that considers agricultural risk as a function of historical and future climate. Chapter 3 explains the soil moisture model development used in the thesis and evaluates the usability of a simplified land surface model in agricultural decision making related to climate risk. In chapter 4, the role of monitoring drought within a growing season (a seasonal timescale) is discussed and comparison with standard drought monitoring tools of SPI and WRSI is provided. Chapter 5 then describes the application of the concept to make a critical decision on planting date (a short timescale) using the new decision-making framework. Chapter 6 summarises the principal conclusions and identifies possible areas of future work.

Chapter 2

TAMSAT-ALERT: a new framework for agricultural decision support

This chapter describes the basic concept of a new agricultural decision support framework - Tropical Applications of Meteorology using SATellite data and ground based measurements-AgricuLtural EaRly warning sysTem (TAMSAT-ALERT); it's setup and its application in relation to meteorological risk on maize yield. This chapter lays the foundation for the subsequent works done in in this project and has been published in (Asfaw et al., 2018).

Asfaw, D., E. Black, M. Brown, K. J. Nicklin, F. Otu-larbi, E. Pinnington, A. Challinor, R. Maidment, and T. Quaife, 2018: TAMSAT-ALERT v1: A new framework for agricultural decision support. Geoscientific Model Development, (February), 128, doi:10.5194/gmd-2017-316.

> *Contribution=80%*
> *D.A developed the TAMSAT-ALERT code and incorporated GLAM into the system with the assistance of E.B. and R.M. E.B, M.B, F.O worked on the initial concept of TAMSAT-ALERT system. K.J.N and A.C provide the GLAM code. T.Q and E.P helped with data assimilation of crop yield into the system (not included in the final paper). D.A carried out the analysis and led the writing of the paper, with input from E.B., R.M., A.C, and valuable contributions from reviewers.*

The key points that are made in this chapter include:

1. Describing the concept of TAMSAT-ALERT and its place with regard to other risk metrics available.

2. Application of the framework for assessing meteorological risk to maize yield.

3. Describing the information contained in seasonal forecasts that are provided for users in Africa in relation to decision making of users on agricultural risk emanating from climate variability.

Abstract

Early warning of weather-related hazards enables farmers, policymakers and aid agencies to mitigate their exposure to risk. We present a new operational framework, Tropical Applications of Meteorology using SATellite data and ground-based measurements-AgricuLtural EaRly warning sysTem (TAMSAT-ALERT), which aims to provide early warning for meteorological risk to agriculture. TAMSAT-ALERT combines information on land surface properties, seasonal forecasts and historical weather to quantitatively assess the likelihood of adverse weather-related outcomes, such as low yield. This article describes the modular TAMSAT-ALERT framework and demonstrates its application to risk assessment for low maize yield in northern Ghana (Tamale). The modular design of TAMSAT-ALERT enables it to accommodate any impact or land surface model driven with meteorological data. The implementation described here uses the well-established General Large Area Model (GLAM) for annual crops to provide probabilistic assessments of the meteorological hazard for maize yield in northern Ghana (Tamale) throughout the growing season. The results show that climatic risk to yield is poorly constrained at the beginning of the season, but as the season progresses, the uncertainty is rapidly reduced. Based on the assessment for the period 2002-2011, we show that TAMSAT-ALERT can estimate the meteorological risk on maize yield 6 to 8 weeks in advance of harvest. The TAMSAT-ALERT methodology implicitly weights forecast and observational inputs according to their relevance to the metric being assessed. A secondary application of TAMSAT-ALERT is thus an evaluation of the usefulness of meteorological forecast products for impact assessment. We show that in northern Ghana (Tamale), the tercile seasonal forecasts of seasonal cumulative rainfall and mean temperature, which are routinely issued to farmers, are of limited value because regional and seasonal temperature and rainfall are poorly correlated with yield. This finding speaks to the pressing need for meteorological forecast products that are tailored for individual user applications.

2.1 Introduction

Many African people depend on rainfed agriculture and are thus vulnerable to drought and other weather-related hazards exacerbated by climate change (Muller et al., 2011). Anticipation of hazard enables farmers and aid agencies to plan ahead, averting disaster (Boyd et al., 2013). Here, we present a new framework for early warning of high meteorological risk to agriculture, the Tropical Applications of Meteorology using SATellite data and ground based measurements-AgricuLtural EaRly warning sysTem (TAMSAT-ALERT). TAMSAT-ALERT integrates an assessment of climatological weather-related risk with forecasts and real-time monitoring of environmental conditions. The framework is intended to be a decision support system, which when combined with socioeconomic assessments, can be used by governmental agencies and NGOs to help farmers manage agricultural risk.

The need for timely information on agricultural risk has motivated the development of a number of drought early warning systems and decision support platforms. The Rainwatch-AfClix early warning system (RWX) (`http://www.rainwatch-africa.org/rainwatch/`, last access: June 2018), for example, provides time series of cumulative rainfall, which are compared against historical time years. Users value the facility to compare the current season against past years, finding that it enables them to intuitively gauge risk (Tarhule et al., 2009). The severity of drought, however, depends not only on rainfall. It is furthermore not straightforward to translate information on meteorological drought (deficit rainfall) into warning of agricultural drought (deficit soil moisture) (Black et al., 2016a). The need to consider a range of variables and to compare data from a variety of sources is addressed by more comprehensive platforms, such as the Famine Early Warning Systems Network Early Warning Explorer (FEWSNET-EWX)(`https://earlywarning.usgs.gov/fews/ewx/index.html`, last access: June 2018) and International Research Institute (IRI) data library and map rooms (`http://iridl.ldeo.columbia.edu/index.html?Set-Language=en`, last access: June 2018), which enable users to compare meteorological data with land surface remote sensing products, such as the Normalized Difference Vegetation Index (NDVI) and soil moisture. Such platforms are aimed at expert users capable of interpreting complex, multivariate data. An alternative approach is to use a land surface model driven with meteorological time series to derive snapshots and forecasts of soil moisture. The Africa Flood and Drought Monitor (AFDM)

(http://stream.princeton.edu/AWCM/WEBPAGE/interface.php, last access: June 2018), for example, estimates soil moisture using a land surface model. The model is driven with satellite data for monitoring current conditions with bias-corrected, downscaled forecasts for predicting future conditions (Sheffield et al., 2014). The Africa Flood and Drought Monitor is implemented continent wide, with the aim of monitoring and forecasting metrics related to drought and flood (soil moisture and streamflow). The AFDM does not, however, attempt to predict crop yield at particular localities. There have been several attempts to forecast yield using crop models driven by seasonal forecasts (e.g. Hansen and Indeje, 2004; Semenov and Doblas-Reyes, 2007). Mismatches between the scales of the input agronomic and climate data and the lack of skill of the seasonal forecasts proved challenging for these early systems (Hansen and Indeje, 2004). In the last few years there have, however, been marked improvements in the skill of sub-seasonal to seasonal forecasts, leading to greater success for forecasting yield, even in the extratropics where predictability is low. A recent study, for example, demonstrated significant skill for predicting wheat yield in France using a wheat growing model driven with seasonal forecasts (Canal et al., 2017). Previous operational attempts to predict yield using crop models have mainly focused on issuing predictions in advance of sowing. A weather generator approach to providing continually updated assessments was, however, successfully demonstrated for UK winter wheat yield (Bannayan et al., 2003), indicating the potential of this type of approach for operational risk assessment.

TAMSAT-ALERT complements existing systems by providing a means of continually updating yield predictions as the season progresses, in a manner similar to that proposed in Hansen et al. (2006) for characterizing the simulated uncertainty in yield resulting from climatic variability. The TAMSAT-ALERT methodological approach combines the use of historical information, as encapsulated in the RWX methodology, with a land surface or impact model, as demonstrated in the Africa Drought and Flood Monitor. The system can output any variable or metric that can be generated by the land surface or impact model. The impact model output and the weather risk associated with the output that can be obtained from TAMSAT-ALERT can be used by governmental and nongovernmental organizations involved with providing farming information and aid, as well as by weather index insurance providers, who require continuously updated assessment of the risk.

In this study, TAMSAT-ALERT is demonstrated through continually updated seasonal assess-

ments of the meteorological risk to agriculture for Ghana. Although an application of TAMSAT-ALERT has been described elsewhere (Brown et al., 2017), this paper is the first formal description and validation of the methodological approach. Section 2.2 describes the design of the framework and gives brief notes about its implementation. Section 2.3 describes the implementation of the framework for the assessment of meteorological risk to yield in Ghana. The chapter concludes with a discussion of the place that TAMSAT-ALERT has in early warning systems of meteorological hazards and wider decision-making processes (section 2.4).

2.2 Framework concept and design

2.2.1 Concept

The TAMSAT-ALERT framework provides a means of deriving quantitative agricultural risk assessments from information on the climatology, historical time series and (optionally) meteorological forecasts. In essence, the system addresses this question:

Given the climatology, the state of the land surface, the evolution of the growing season so far, and (optionally) the meteorological forecast, what is the risk of some adverse event?

The "adverse event" is any metric that can be derived either directly from meteorological data or using a model driven with meteorological data. TAMSAT-ALERT is designed to be modular and flexible, enabling users to choose models and datasets to suit their application. So far it has been applied to risk assessments of agricultural drought using the Joint UK Land Environment Simulator (JULES) model (Brown et al., 2017) and to risk assessments of low yield using the General Large Area Model (GLAM) for annual crops (section 2.3.2.2).

At a given location and for a given season, the likelihood of an adverse event may depend on past and future weather. Midway through the growing season, for example, the likelihood of low yield depends both on weather in the past and on the likelihood of unfavorable conditions in the coming weeks. In TAMSAT-ALERT, past weather is based on observations, and future weather is based on the climatology. Thus, a 30-year climatology generates a 30-member ensemble of

possible yields based on 30 possible weather futures, each of which can be driven through a crop model and used to derive a possible yield. Statistical comparison between the forecast ensemble yield and the climatological ensemble yield leads to quantitative assessments of the risk of unfavorable conditions.

In its default setup, for which meteorological forecast information is not included, TAMSAT-ALERT treats all weather futures as equally likely. The risk assessments can, however, be refined by weighting the ensemble members based on probabilistic forecast information, for example tercile forecasts of cumulative rainfall or mean temperature cumulated and averaged over a 90-day period. Specifically, the value of the metric being forecasted for each ensemble is used to assign that ensemble member to a particular tercile. Each ensemble member is then weighted by the appropriate tercile probability (section 2.2.2). If there is a weak link between the metric being forecast (for example, regional seasonal rainfall) and the risk being assessed (for example, local low yield), then the forecast will have little impact on the risk assessments. Conversely, if the link is strong, skillful forecasts can significantly reduce the uncertainty in the risk assessments. TAMSAT-ALERT is thus both a method for downscaling and bias-correcting meteorological input into impact models and a method for accounting for mismatch between forecast variables and metrics of risk. There are several sources of potential predictive power in TAMSAT-ALERT. Firstly, as the season progresses, the amount of observational information included in the forecast increases, and the range of possible outcomes is thus reduced. Secondly, the antecedent state of the land surface (especially root zone soil moisture) has a significant effect on the likelihood of drought and hence low yield (Brown et al., 2017). Thirdly, local information on the climatology determines the likelihood that meteorological conditions will be sufficiently favorable during the remainder of the season to offset less favorable past meteorological and land surface conditions. Finally, skillful meteorological forecasts provide direct information on the likelihood of adverse weather conditions in the remainder of the season. The relative importance of these sources depends on the metric being predicted, along with the local climate and land surface conditions. The effect of forecast information depends both on the precision of the forecast and the relevance of the meteorological forecast metric for the metric of hazard assessed by TAMSAT-ALERT.

2.2.2 Model implementation

The TAMSAT-ALERT framework is illustrated in Figure 2.1. The user provides a time series of driving data, which is long enough to generate a statistically meaningful ensemble and climatology. The driving meteorological data are used in several ways: to generate an ensemble of predictions; to assess the progress of the period of interest so far and to derive initial conditions for the future period (if required for the ensemble predictions); and to generate a climatology against which the forecast ensemble can be compared. Once the climatology and ensemble have been produced, meteorological forecast information is optionally introduced to weight the ensemble members. The system is modular and thus easily adapted for different impact models, metrics of risk and meteorological forecasts.

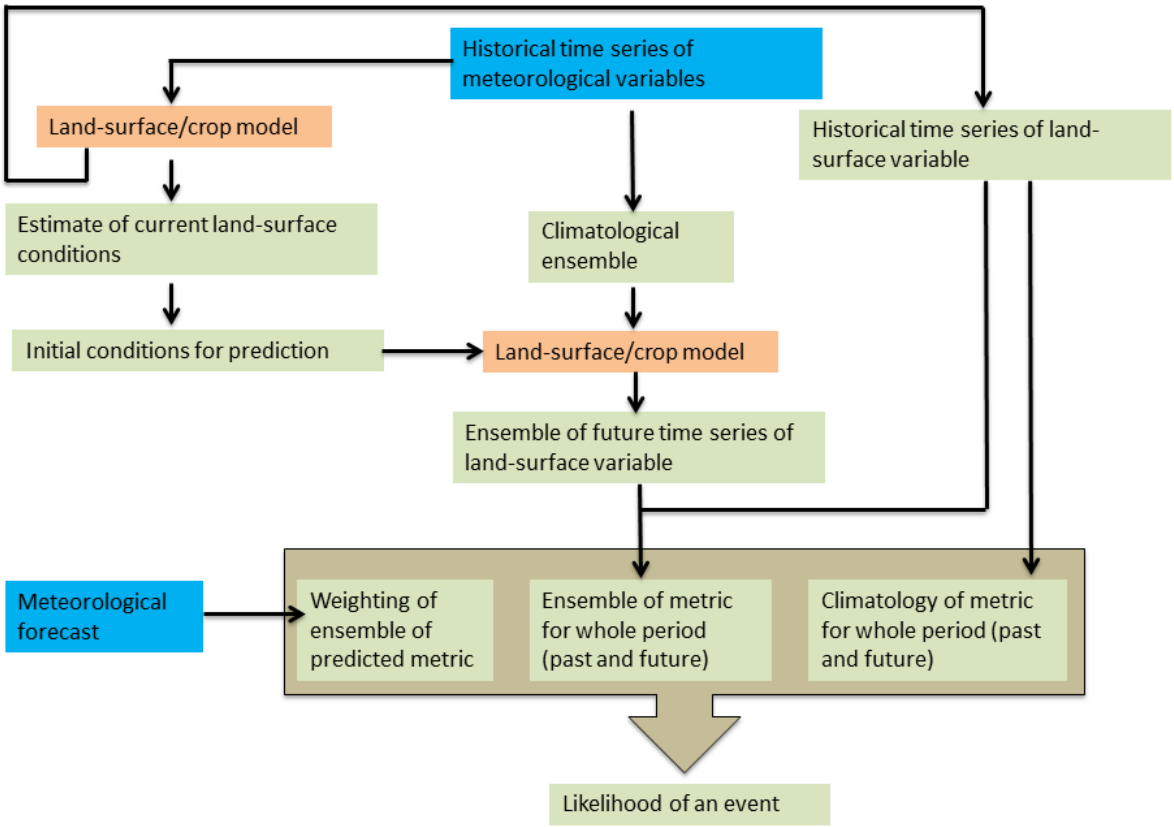

Figure 2.1: Conceptual overview of the TAMSAT-ALERT system. The blue boxes represent input data sources, the orange boxes represent the processes involved in the system and the green boxes show the outputs from TAMSAT-ALERT system.

The steps for deriving probabilistic assessments of the risk of some adverse event on a particular day (the day in question) can be summarized as follows.

1. The user prepares a file containing historical time series of driving data, along with any other parameter files (e.g., agronomic or soil parameters). These should extend at least until the day in question. Note that TAMSAT-ALERT version 1.0 only supports daily input. Support for higher or lower resolution data will be introduced in future versions of the framework.

2. The user converts the long daily time series of driving data into the appropriate format for their impact model and carries out a historical run in order to derive an annual historical time series of their chosen risk metric. This enables a baseline assessment of climatological risk. The risk metric time series should be presented as an annual time series of the form <year ><data >. Here, we will call this time series file *"historical_metric.txt"*.

3. For the probabilistic risk assessments, the impact model is driven with an ensemble of meteorological forcing data generated by TAMSAT-ALERT. As described earlier, the period of interest might contain both the past and the future.

   (a) For the past, the meteorological driving data for ensemble member includes identical time series taken from observations.

   (b) For the future, the meteorological driving data for each ensemble member is based on the historical climatology. Specifically, for a given day of year (DoY), the driving data are taken for that DoY for a year in the past. To maintain the daily weather statistics and the consistency between variables, each ensemble member is based on a particular past year. Thus, ensemble member x is based entirely on year y.

   To accomplish this, the system converts the daily time series of driving data into multiple files, each containing driving data for one ensemble member. The user is allowed to set the period over which the ensemble system will be run. This is distinct from the period over which the metric is calculated (the metric period). The metric period is the period on which the weighting will be done, and the probabilistic risk is calculated. For example, if one wants to estimate the meteorological risk on available soil moisture the ensembles can be run for a much longer period to allow the spin-up of the model to equilibrium values for the initial condition required, but the main interest for the user might be the first 90 days. Hence, the length of the metric period is only the first 90 days and all risk analysis is done on this metric period. The period over which the ensemble will be run should include sufficient time before the metric period to allow for spin-up. The user makes any format changes necessary to convert these TAMSAT-ALERT driving data files into driving data specific to

their impact model. The user then carries out the ensemble prediction runs, outputting the time series of driving data through the impact model and outputting the user defined metric over whatever period is relevant for that metric. Because of the nature of the TAMSAT-ALERT method, each ensemble member is associated with the year for which the possible weather future was derived (see above). The output can thus be presented in a single file with two columns, <year ><data >, for file name *"ensemble_metric.txt"*.

4. The risk assessment is derived by comparing the mean and standard deviation of the climatological baseline distribution (*historical_metric.txt* derived in point 2) with the mean and standard deviation ensemble distribution (*ensemble_metric.txt* derived in point 3). Note that an alternative approach employing an empirical cumulative distribution function can be specified by the user. The empirical cumulative distribution function (ECDF) approach is suitable for non-Gaussian variables but can result in noisy predictions if the ensemble is relatively small.

   At this point, meteorological forecast data are incorporated (if available).

   (a) An annual historical time series of the metric being forecast (e.g., cumulative JuneAugust rainfall) is provided by the user for file name *weighting_ metric.txt*, which is of the form <year ><data >. The data series should be provided for the years used to generate the weather future aspect of the ensemble (i.e., *ensemble_metric.txt* as described in 3b). The TAMSAT-ALERT version 1.0 release includes a utility function for extracting forecast metrics from the historical driving meteorological data file supplied by the user.

   (b) The annual time series of forecast metric is then ranked. Based on this ranking, each historical year is assigned to a forecast category. In the case of terciles, for example, the bottom third is assigned to tercile 1, the middle third to tercile 2 and the top third to tercile 3.

   (c) As was noted in 3b, each ensemble member is associated with a historical year and *ensemble_ metric.txt* is presented in the form <year ><data >. Each data point in this file can thus be associated with a quantile category using the year assignments described in 4b.

   (d) When calculating the mean and standard deviation, the ensemble is weighted by the

user-supplied categorical forecast probabilities, which are assigned to each member during 4c.

The TAMSAT-ALERT code is written in Python. All code and documentation (including a user manual) for TAMSAT-ALERT have been released on GitHub (`https://github.com/tamsat-alert/v1-0`, last access: June 2018). However, users need to have their own working installations of their chosen impact model. The TAMSAT-ALERT version 1.0 release consists of scripts to:

- convert meteorological time series into driving data for both the ensemble forecasts,
- calculate quintile predictions for user-defined risk metrics based on the input files *historical_metric.txt*, *ensemble_ metric.txt* and *weighting_metric.txt*, and
- produce a set of plots comparing the ensemble and climatological distribution.

In the GitHub release, in addition to the general TAMSAT-ALERT framework scripts listed above, scripts are provided that set TAMSAT-ALERT up for (i) for the GLAM crop model (the implementation demonstrated in section 2.3 of this chapter) and (ii) for assessments based purely on time means and cumulations of meteorological variables. A test case is provided so that users can be assured that the system is working as expected.

2.3 Demonstration of the system: a case study of maize yield prediction in Ghana

This case study demonstrates the use of the TAMSAT-ALERT system for forecasting the risk of poor maize harvest harvest in Ghana. The first and second part of the case study describe the study area and the implementation and evaluation of a mechanistic crop model, GLAM. The third part demonstrates the implementation of GLAM as part of the TAMSAT-ALERT system for continually updated risk assessments.

2.3.1 Study area

Ghana is located on the southern coast of West Africa, between latitudes 4° 44′ N and 11° 11′ N and longitudes 3° 11′ W and 1° 11′ E. Rainfed agricultural systems are the major component of

the Ghanaian economy, accounting for 30 % of the GDP and employing half of the labour force (PARI, 2015). The country is divided into six agro-ecological zones, each with a distinct rainfall pattern (Figure 2.2). The Northern part is dominated by Guinea Savannah with average annual rainfall of 10001100 mm from one rainy season spanning May to September, while in the southern part, moist semi-deciduous agro ecology dominates, with an average annual rainfall of 1500 mm, falling within two rainfall seasons (Owusu and Waylen, 2009, 2013). Most of the cereal crops (primarily Sorghum, Millet and Maize) are produced in the northern part of Ghana (Martey et al., 2014). Table 3.3 shows the six agro-ecological zones with the average annual rainfall and major crops grown in the agro-ecological zones.

Maize is one of the major crops produced in Ghana. The production area and the amount of yield has been increasing since 1994 (Figure 2.3). Figure 2.4 shows a time series of maize yield in Ghana (expressed in kgha^{-}1). From 1994 2006 there is no observed trend, but after 2007 there is a step change in yield coinciding with the introduction of a new variety by the Crop Research Institute (CRI) of the Council for Scientific and Industrial Research (CSIR) of Ghana in 2007 (Ragasa et al., 2013).

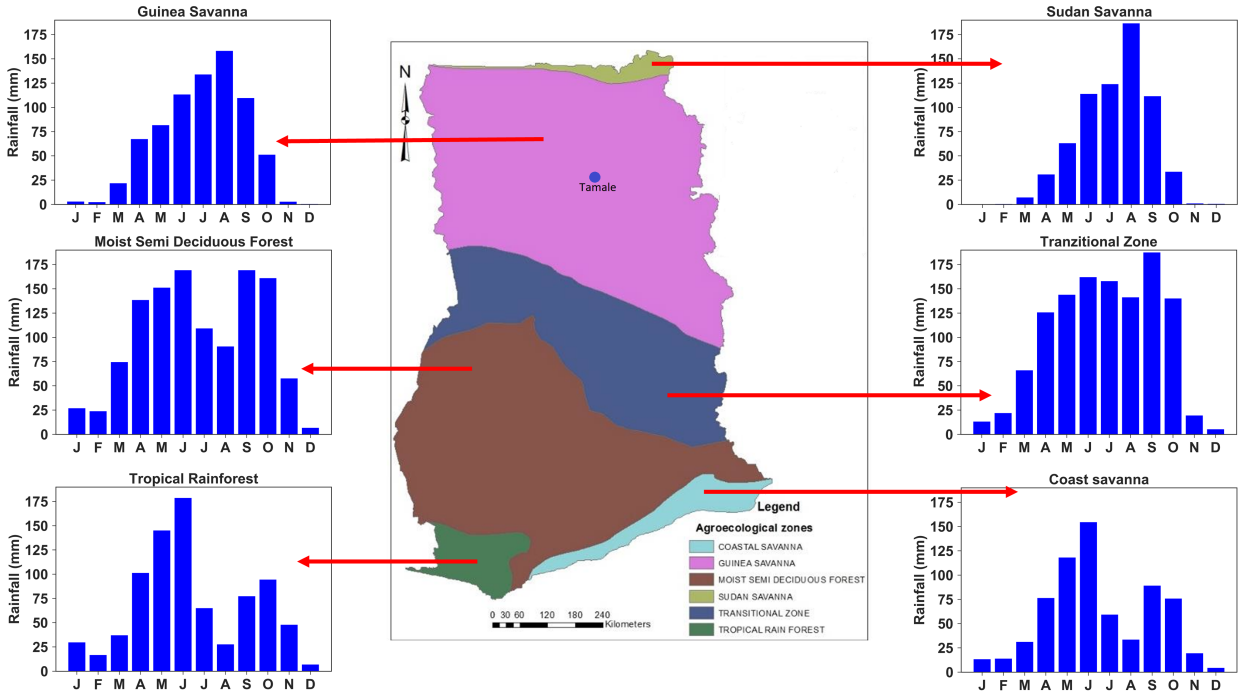

Figure 2.2: Agroecological zones of Ghana (source: (Sidibé et al., 2016)) and average seasonal rainfall pattern of each agroecological zone based on TAMSAT rainfall estimates.

Table 2.1: Characteristics of agroecological zones in Ghana (source: http://www.fao.org/nr/water/aquastat/countries_regions/GHA/, last access: June 2018).

Agro ecological zone	Rainfall (mm year^{-}1)	Number of seasons	Major crops
Sudan savannah	1000	1	Millet, Sorghum, Maize
Guinea savannah	1100	1	Maize, Sorghum
Transition zone	1300	1	Maize, Roots, Plantain
Moist semi deciduous forest	1500	2	Roots, Plantain
Costal savannah	800	2	Roots, Maize
Rainforest	2200	2	Roots, Plantain

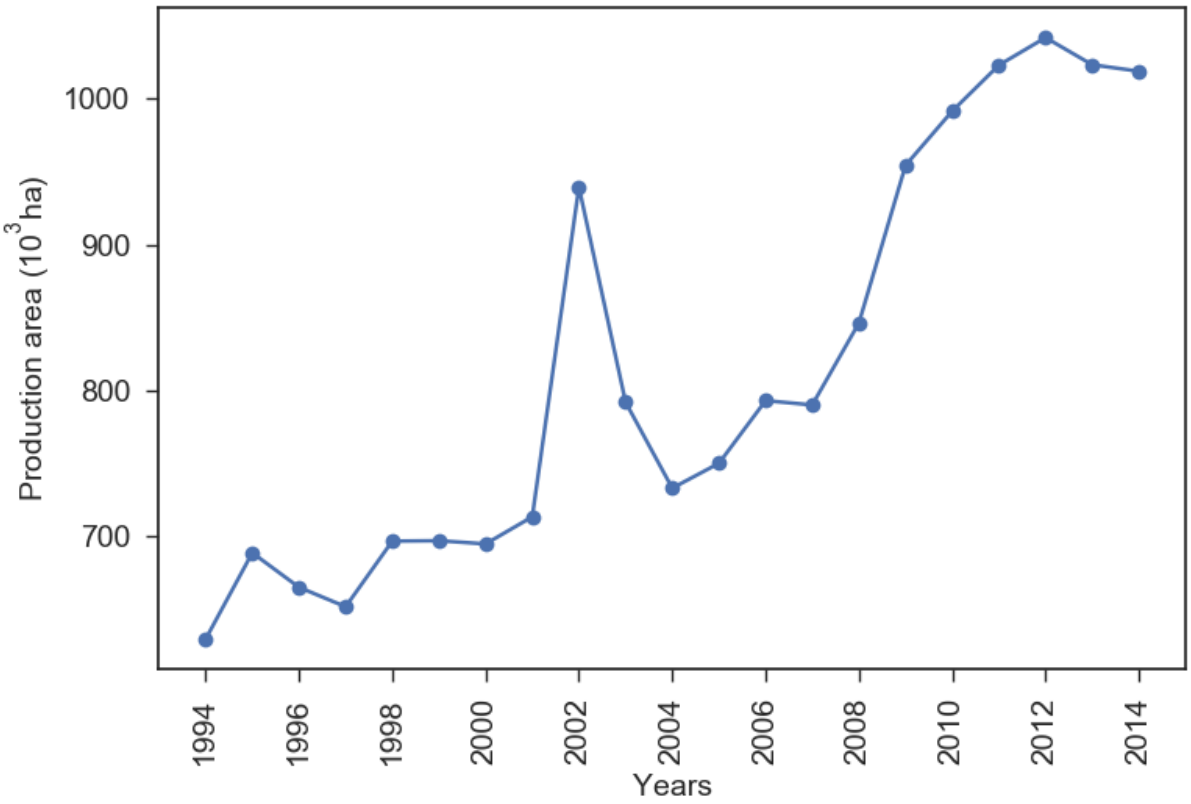

Figure 2.3: Maize production area over Ghana from 1994 to 2014.

2.3.2 Data and methods

2.3.2.1 Datasets used

The driving weather datasets for the evaluation of the model were daily time series extracted from the Watch Forcing Data ERA-Interim (WFDEI) (Weedon et al., 2014) for shortwave radiation, maximum temperature, minimum temperature and rainfall. For the demonstration of the system at a point, the driving data were based on daily, quality-controlled station data provided by the

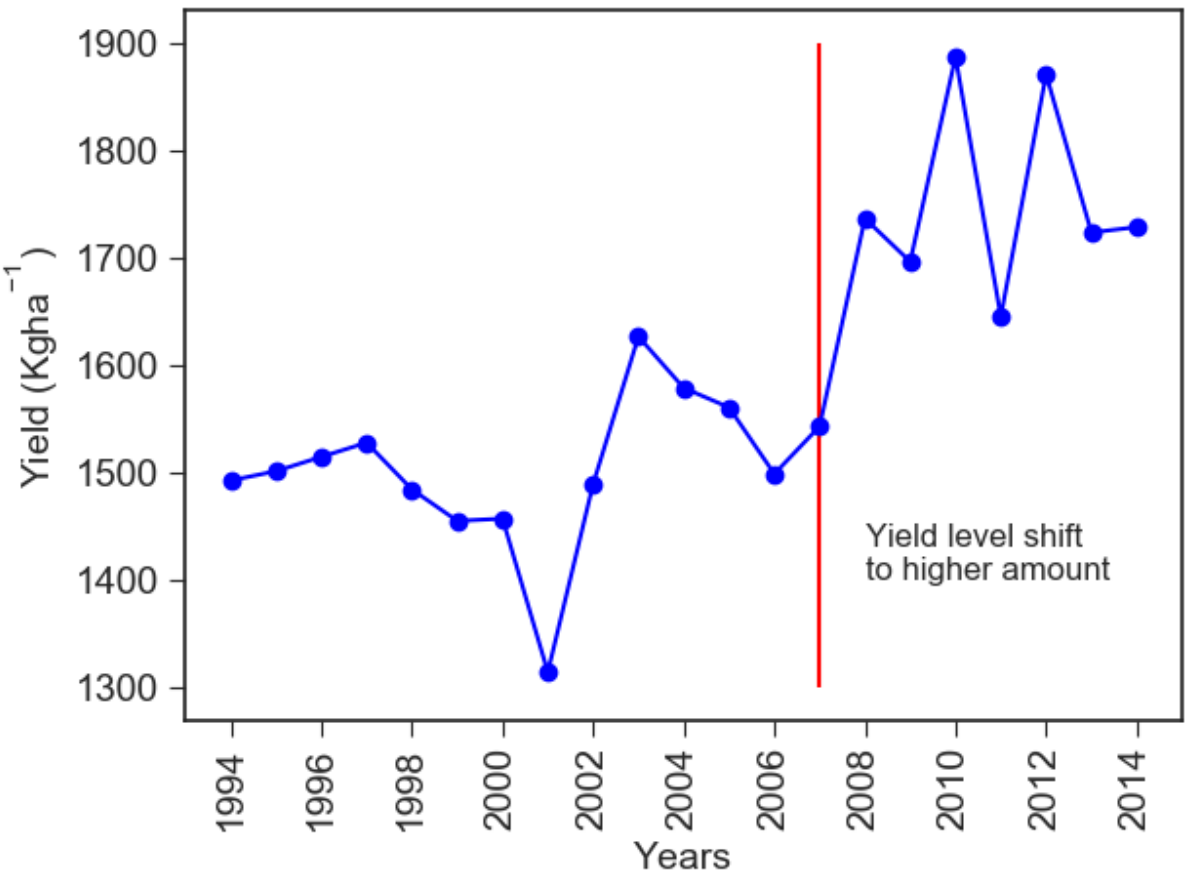

Figure 2.4: Maize yield in Ghana 1994-2014. There are two separate periods marked by the red lines during which we observe changes in yield. For 1994-2006 there is no clear trend in the yield produced and for 2007-2014 there is a shift in the production in which a higher yield is observed.

Ghana Meteorological Agency. The station used is Tamale, which is located in northern Ghana (9.41°N, 0.85°W; Figure 2.2). Precipitation and maximumminimum temperature were measured directly, and shortwave radiation was derived from sunshine hours.We chose to use Tamale because it is in the northern part of Ghana (Figure 2.2) where most of the maize is grown. The station in Tamale also has a long-term record of the driving data for the crop model. It should be noted that TAMSAT-ALERT can in principle be run using any gridded meteorological data, like satellit-erainfall estimates (e.g., TAMSAT (`https://www.tamsat.org.uk/data/rfe/index.cgi`, last access: June 2018), with a resolution of 4 km (Maidment et al., 2017).

Tercile forecast data were downloaded from the publicly available IRI regional forecasts (`http://iri.columbia.edu/our-expertise/climate/forecasts/seasonal-climate-forecasts/`, last access: June 2018). The IRI forecasts are based on a hybrid dynamicalstatistical method developed by the U.S. National Oceanographic and

Atmospheric Administration North American Multi-Model Ensemble Project (NOAA-NMME) (Kirtman et al., 2014). The seasonal forecasts are issued at the beginning of each month for precipitation and temperature at a global scale with a spatial resolution of 2.5° for precipitation and 2° for temperature (Barnston and Tippett, 2014). The IRI forecasts were chosen for this analysis because of their wide use by African meteorological services and regional climate outlook forums. In this study the seasonal forecast data were used in the form they are supplied to farmers, i.e., tercile probabilities of 3-month cumulative rainfall and 3-month mean temperature at a regional level.

In addition to meteorological time series, GLAM requires data on soil type and the agronomic properties of maize (section 2.3.2.2). For this study, the soil texture was set to be sandy loam and the planting date was set to start from the 124^{th} day of the year to the 154^{th} day of the year, which allows for a 30-days planting window. Additional maize agronomic properties were taken from the published literature. GLAM was evaluated against national level maize yield data released by the FAOSTAT (`http://www.fao.org/faostat/`, last access: June 2018; Figure 2.4). Although the FAO issues guidance on the compilation of these datasets, in practice there is little quality control and the data should be treated with caution.

2.3.2.2 The GLAM crop model

As described in section 2.2.1, the TAMSAT-ALERT system can be used to assess any metric of risk that can be output by a model driven with meteorological data. In this study, the General Large Area Model (GLAM) for annual crops is used to simulate maize yield and subsequently to monitor the probabilistic risk of poor harvest as the growing season progresses.

GLAM is a process-based crop simulation model, which incorporates sufficient processes to capture the impact of climate variability on crop yield (Challinor et al., 2004; Ramirez-Villegas et al., 2015). GLAM uses a limited number of driving datasets and an intermediate complexity of crop development process representation. Nevertheless, previous studies have demonstrated that GLAM has skill in capturing the impact of weather on crops (Challinor et al., 2005, 2006). Such information enables users to translate time series of weather into a time series of yield estimates (Challinor and Wheeler, 2008). GLAM has also been used to model weather and climate change

impact on crop yield and adaptation strategies (Parkes et al., 2015; Ramadas and Govindaraju, 2015; Ramirez-Villegas and Challinor, 2016).

GLAM requires daily values of precipitation, shortwave radiation, maximum temperature and minimum temperature as driving weather data with additional inputs of soil properties and planting window (Watson and Challinor, 2013). GLAM accumulates the aboveground biomass, which is a product of daily transpiration and a predetermined transpiration efficiency value, within the growing season to determine total biomass production, which is converted into yield using a harvest index (Osborne et al., 2007). The planting date is either prescribed by the user or determined using GLAMs intelligent planting date system (the approach taken in this study). It is important to note that GLAM does not account, in a process-based fashion, for non-meteorological influences on crop growth, such as pests, diseases and fertilizer use. Rather, these factors are encapsulated in the yield gap parameter (YGP), which is determined by calibrating the model yield with observed yield (Challinor et al., 2004). The YGP is assigned a value between 0 and 1, where 1 represents the potential yield given the weather conditions, soil texture and crop development parameters (Challinor et al., 2005).

2.3.2.3 GLAM evaluation

GLAM was used to simulate the yield from 1994 to 2014 using the WFDEI as a driving dataset. The WFDEI has a 0.5° by 0.5° resolution and so GLAM was output at this resolution. The simulated yield at each grid point was then weighted by the year 2000 season fraction of production area over each grid point to make a country average yield (Weedon et al., 2014; Monfreda et al., 2008).This country average yield was then compared with the FAO maize yield dataset for the same period. It is shown in Figure 2.4 that maize production can be split into two distinct periods: 1994-2006 and 2007-2014. Because of the reported changes in agronomic practice and drought-tolerant maize variety introduction through the drought-tolerant maize for Africa (DTMA) project (Obeng-Antwi et al., 2013; Ragasa et al., 2013) the transpiration efficiency (TE) value was increased from 7.0 for the period 1997–2006 to 8.0 for the period 2007-2014.The YGP was maintained at 0.4 for the whole simulation period.

The results of the simulated crop yield are presented in Figure 2.5 and the statistical values of the

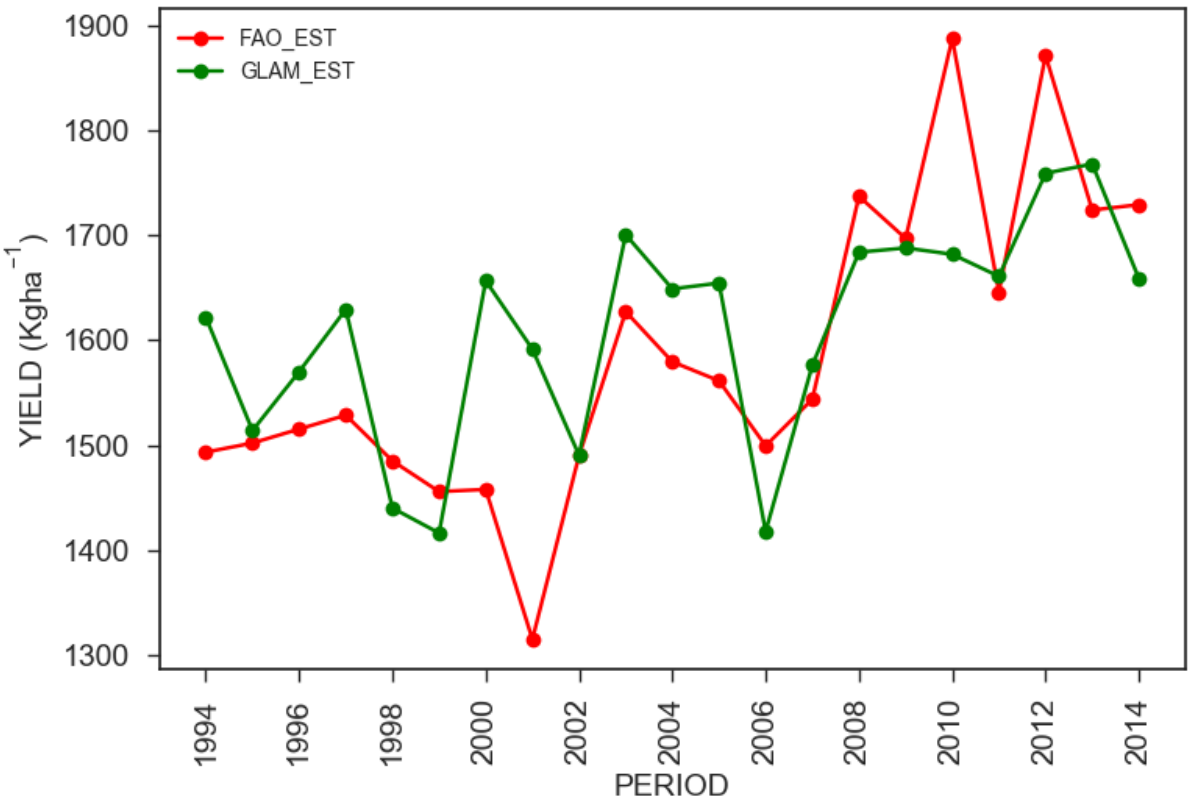

Figure 2.5: Time series of FAO yield (red line) and GLAM-simulated yield (green line).

comparison are presented with the scatter plot in Figure 2.6. GLAM was able to maintain the overall mean yield and, and as a result the normalized root mean square error (NRMSE) is very low (0.07). The overall correlation value is found to be 0.67 (Pearson) and the Spearman correlation, which is less affected by outliers, is 0.8. The difference in the Spearman and Pearson correlation coefficients is mainly due to the severe overestimation of 2001 season yield, probably resulting from a long dry spell, the impact of which on farming practices was not fully accounted for by GLAM (FAO/WFP-GIEWS, 2002). Some of the correlation strength is due to capturing the change in mean yield from the 1994-2006 to 2007-2014 period, and this is done by changing the transpiration efficiency (TE) value for the two periods. The strength of the correlation of yield suggests that the link between Ghana-wide weather and yield is moderate an important consideration for policy makers when they make use of information from TAMSAT-ALERT. This is primarily due to the myriad of factors that can affect yield, including agronomic practice, pests and disease, and socioeconomic problems. Nevertheless, in vulnerable regions, the meteorological risk to yield is, in itself, an important consideration for agricultural agencies because action can be taken to mitigate the hazard. This might include subsidizing drought-resistant varieties or encouraging early planting and replanting.

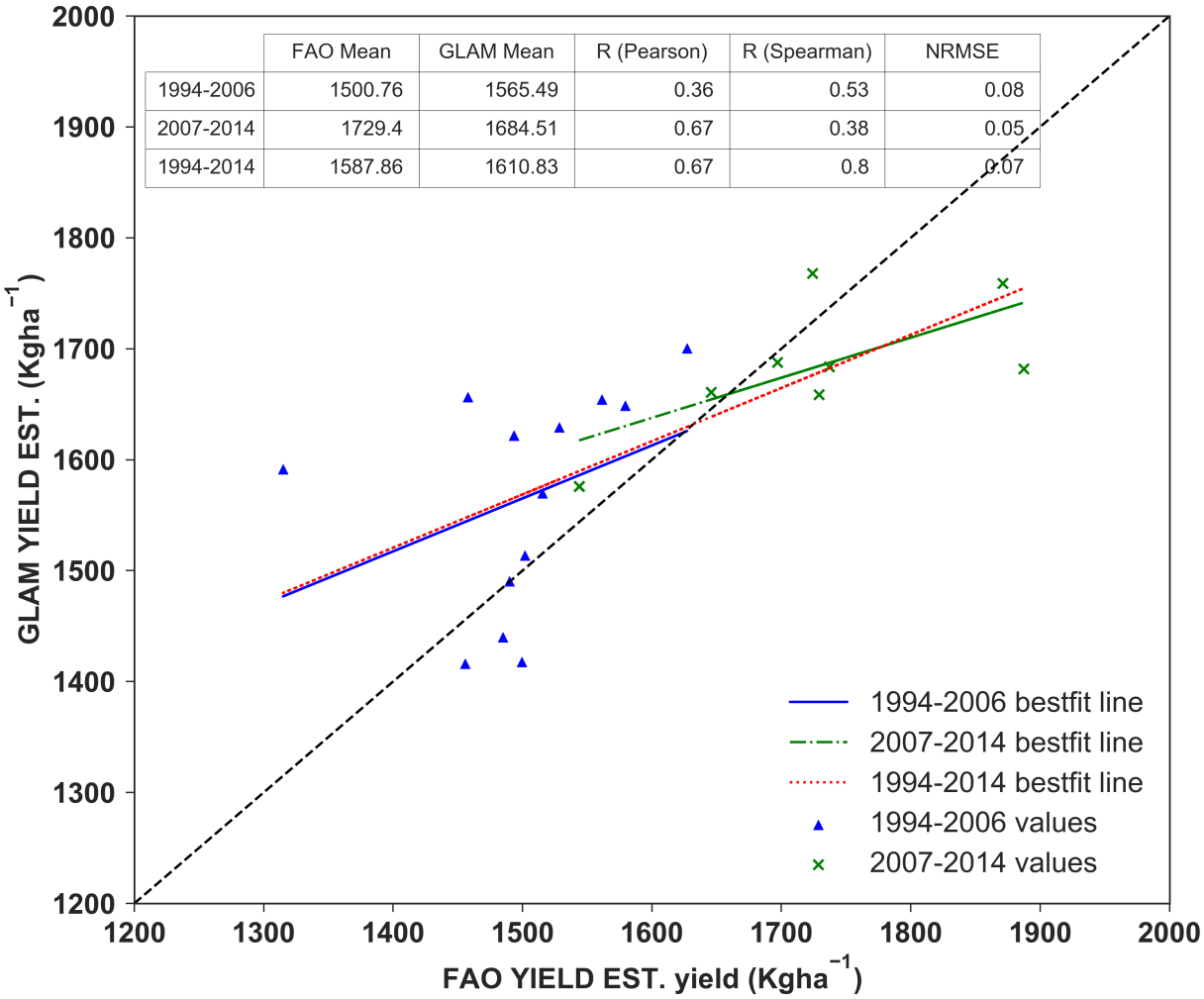

Figure 2.6: Scatter plot between FAO yield and GLAM-simulated yield. The red dotted line is the best-fit line for the whole period considered (1994-2014). The blue solid line shows the best-fit line for the period 1994-2006. The green line shows the best-fit line for the period 2007-2014.

2.3.2.4 Incorporation of GLAM into TAMSAT-ALERT

Figure 2.7 shows how GLAM has been incorporated into the TAMSAT-ALERT system. As described in section 2.2, time series of driving data based on historical observations are used both to derive climatological yield and to generate an ensemble of predicted yield. Individual planting dates are determined for each ensemble member using GLAMs intelligent planting date system, and the crop is harvested when the growing degree-day requirement is fulfilled (Challinor et al., 2004; Challinor and Wheeler, 2008). Because of the way TAMSAT-ALERT is set up to incorporate observational data continually as the season progresses, once the optimum planting time has passed for the year being hindcast, the planting date for each ensemble member converges. Analogously, once the harvest date for the hindcast year has passed in the observations, the harvest date, and indeed the predicted yield, for each ensemble member is identical. In this implementation of

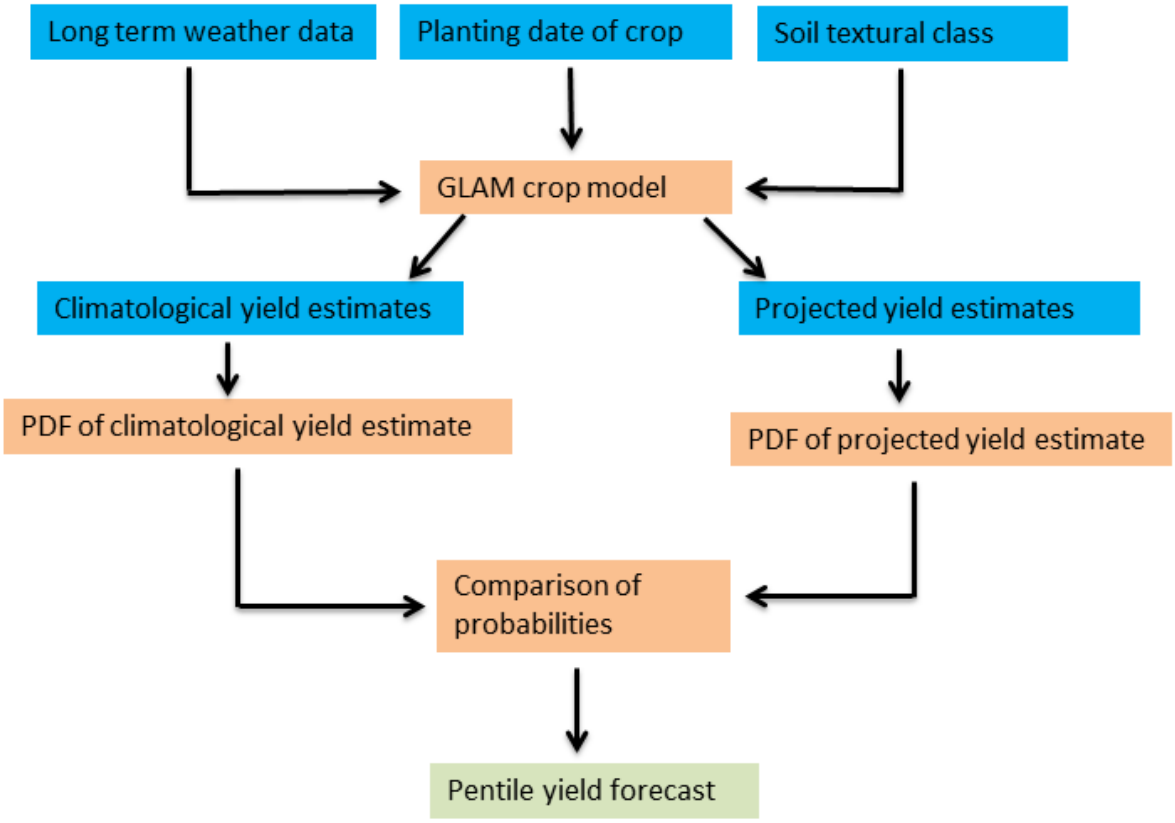

Figure 2.7: Process flowchart for crop yield forecasting within the TAMSAT-ALERT system. The blue boxes represent input data sources, the orange represents the processes involved in the system and the green box shows the final probabilistic forecast for the crop yield.

GLAM, a climatological period of 30 years (1980-2009) was used for the yield forecast.

2.3.3 Case study results

2.3.3.1 Yield forecasting using GLAM: 2011 season example

Figures 2.8, 2.9 and 2.10 illustrate the implementation of TAMSAT-ALERT for the 2011 growing season, which nationally was a low yield year compared to other post-2007 years (noting that we do not have yield data for Tamale). The hindcasts were initiated every 5 days. GLAM infers that planting occurred on 4 June and harvesting on 15 September to 20 September. Figure 2.8 depicts all ensemble members in the context of the climatological spread in yield. Figure 2.9 shows histograms of ensemble members at monthly intervals, starting 10 days after planting. Figure 2.10 shows a time series of ensemble spread (standard deviation of ensemble yield predictions).

At the outset of the season, the yield estimates are derived only from the meteorological climatology; no in-season observational data are incorporated. The spread is thus large (equivalent to the climatology). During the season, as inseason data are incorporated by TAMSAT-ALERT, the meteorological time series driving GLAM become progressively more similar. As a result, the ensemble rapidly converges. In this example, for instance, 2 months after planting, the ensemble standard deviation is 34% of the climatology. The yield forecasts can be communicated with end users in a probabilistic form, with the ensemble expressed as quintiles representing the following categories: above the $80^{th}, 60^{th} - 80^{th}, 40^{th} - 60^{th}, 20^{th} - 40^{th}$ and below 20^{th} percentile.

These categories can be equated to very high, high, average, low and very low yield, respectively. An example of such quintile forecasts at monthly intervals during the 2011 growing season is shown in Figure 2.11. Consistent with Figures 2.8 and 2.9, at the outset of the season, the categories are equally likely except the extreme categories, the difference in probability coming from the change in planting date for some years in the climatological period considered (1980-2009). As the season progresses, the average and low categories become more likely and the extreme categories (very high and very low) less likely.

It is evident from Figure 2.11 that the ensemble mean tends towards average or low values, even 2 months ahead of the harvest date during 2011, suggesting a degree of precision, even towards the beginning of the growing season. Section 2.3.3.3 presents a formal evaluation of skill for the 2002-2011 period.

2.3.3.2 Incorporation of meteorological forecasts

As described in section 2.2.1, the TAMSAT-ALERT framework can use probabilistic information from meteorological forecasts to weight the yield forecast ensemble, providing a means of incorporating forecast information into the decision support system. In this study, we consider tercile forecasts of cumulative 90-day rainfall and mean 90-day temperature to reflect the information currently available to the Ghana Meteorological Agency. The forecasts are commonly issued at the start of every month. Hence, we have applied the forecasts only to the meteorological season being forecasted with the remaining season not included in the weighting estimation. For example, for running TAMSAT-ALERT on 4 June, the seasonal forecast of June-July-August is

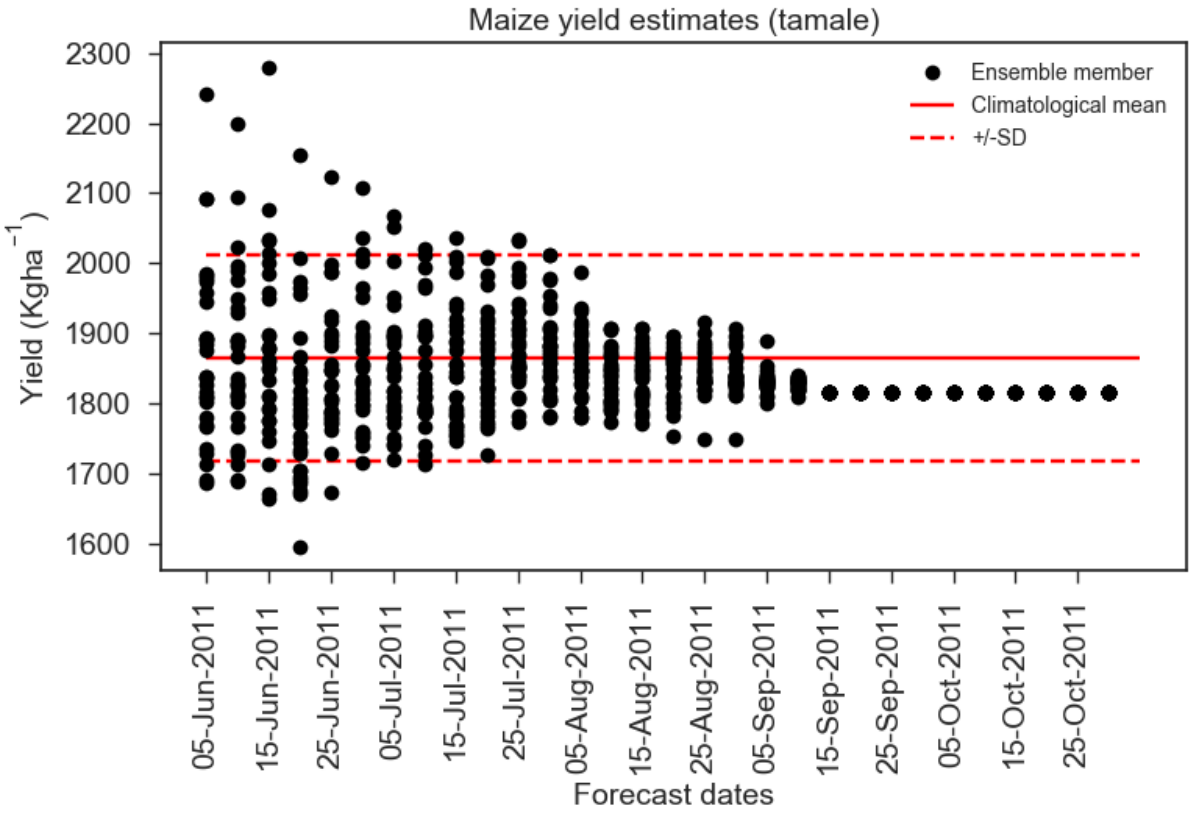

Figure 2.8: An example hindcast of maize yield using GLAM implemented into the TAMSAT-ALERT system. Black dots represent individual ensemble members and red lines are the climatology.

applied. To illustrate the process of including forecasts, we continue with the 2011 case study. We have used idealized tercile seasonal forecasts for total June-July-August (JJA) precipitation to weight the forecast on 4 June 2011, July-August-September (JAS) precipitation to weight the forecast on 4 July 2011, August-September-October (ASO) precipitation to weight the forecast on 4 August 2011 and September-October- November (SON) precipitation to weight the forecast on 4 September 2011.

To assess the potential value of tercile rainfall and temperature seasonal forecast information, we have weighted the ensemble as if the next 90 days of temperature and cumulative rain are known (i.e., perfect forecast experiment). So, we consider three probabilistic forecasts: tercile weightings of [0,0,1] for the lower, middle and upper tercile, respectively (perfect wet forecast), [0,1,0] for the lower, middle and upper tercile, respectively (perfect normal forecast), and [1,0,0] for the lower, middle and upper tercile, respectively (perfect dry forecast). The ensemble was weighted by these perfect tercile forecasts according to the actual total rainfall (perfect rainfall forecast) or the actual

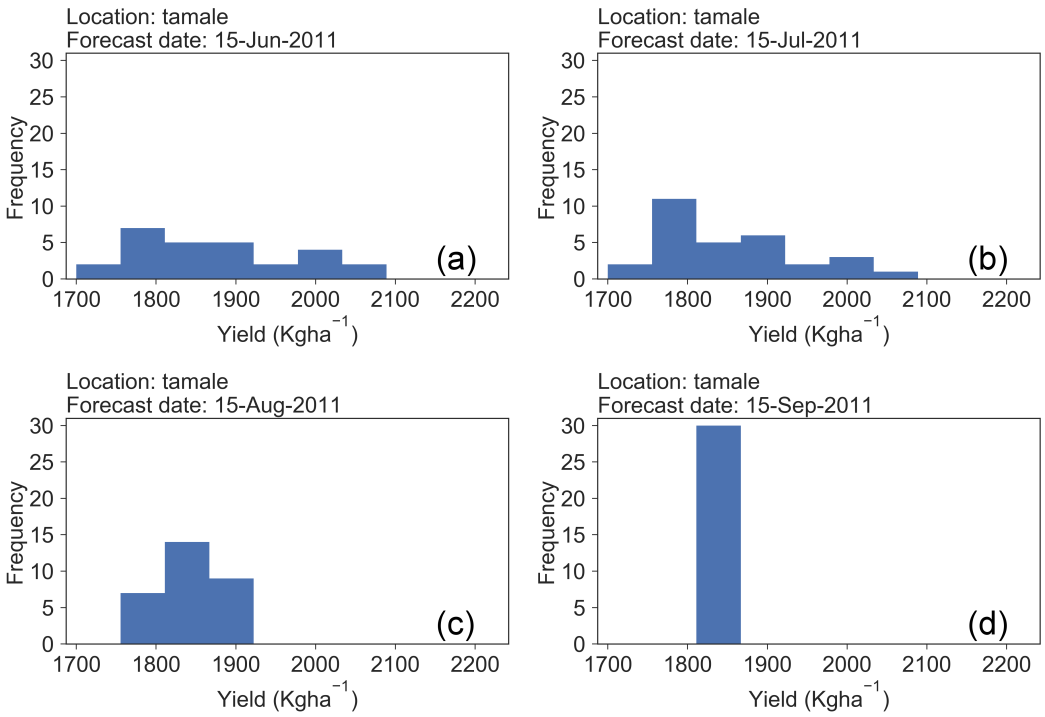

Figure 2.9: Histograms of yield forecast for (a) 15 June 2011, (b) 15 July 2011, (c) 15 August 2011 and (d) 15 September 2011.

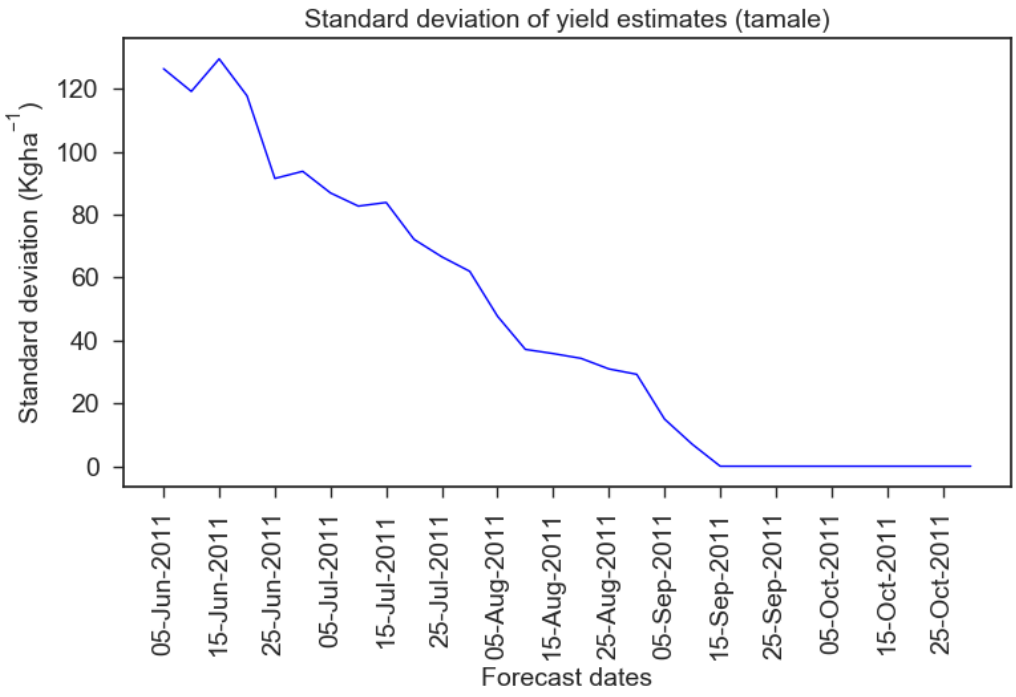

Figure 2.10: Standard deviation of the yield estimate initiated on the dates displayed on the x axis.

mean temperature (perfect temperature forecast) that ensued in the next 90 days following each TAMSAT-ALERT hindcast.

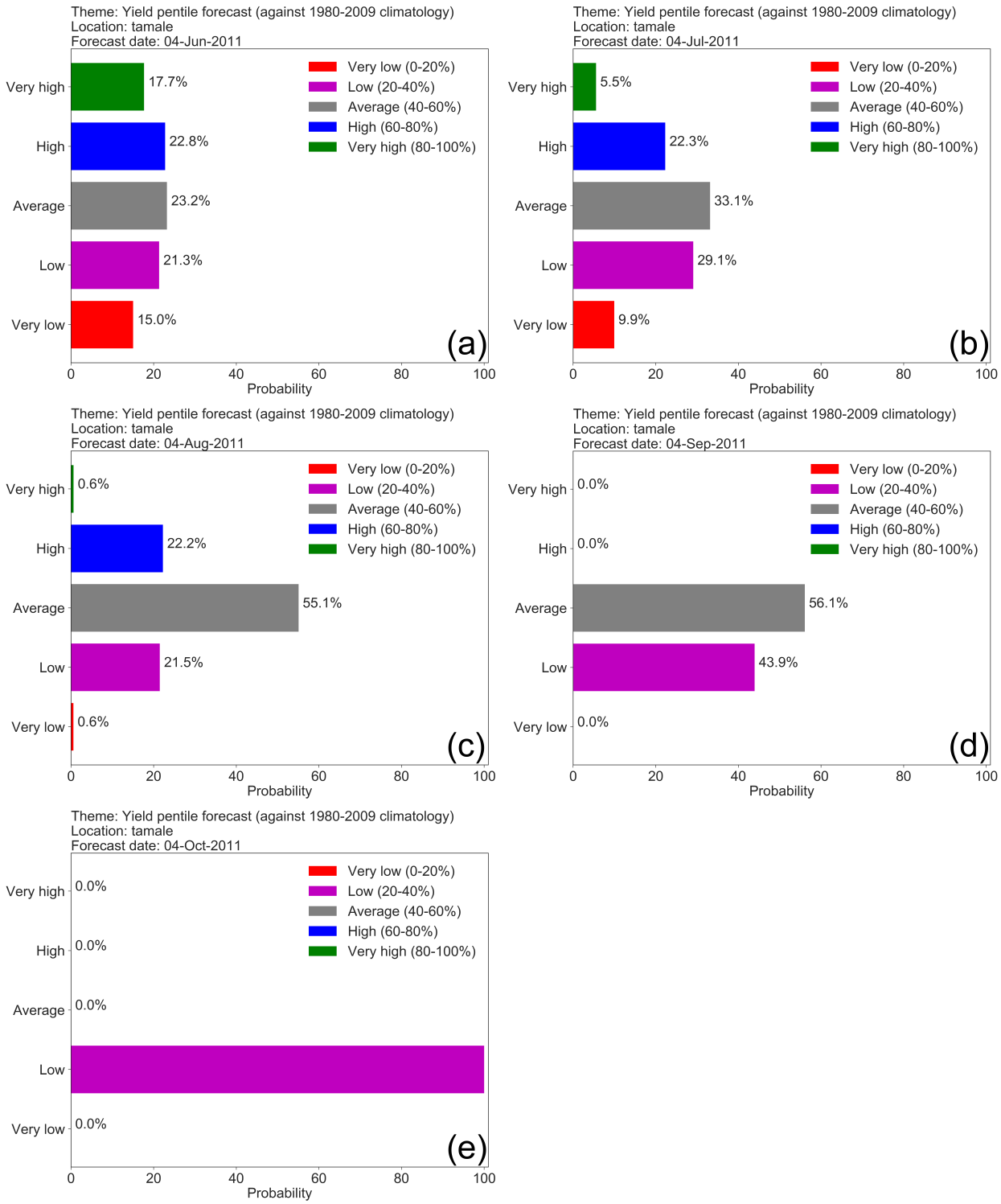

Figure 2.11: Probabilistic forecasts for maize yield in northern Ghana (Tamale) for five dates: (a) 4 June 2011, (b) 4 July 2011, (c) 4 August 2011, (d) 4 September 2011 and (e) 4 October 2011. The planting date was 4 June 2011. In the first day of planting the impact of the weather is not well indicated that the yield probabilities are spread more or less equally in all categories, but after 1 month on 4 July 2011 it is indicated that 62% of the ensembles fall in the average and low categories. After 2 months on 4 August 2011, 76% of the ensembles indicate an average and low yield estimate compare to the climatological yield. A few days before harvest on 5 September 2011, 100% of the yield is estimated to be in the average and low quintile category.

Table 2.2: IRI tercile seasonal forecast for the 2011 season.

Season	Rainfall			Temperature		
	Below normal	Normal	Above normal	Below normal	Normal	Above normal
JJA	25	35	40	30	40	30
JAS	33.3	33.4	33.3	30	40	30
ASO	33.3	33.4	33.3	45	35	20
SON	33.3	33.4	33.3	33.3	33.4	33.3

Figure 2.12 shows the yield forecast probabilities when the perfect rainfall forecast is used. When a perfect rainfall forecast is used to weight the ensemble, the probabilities of the quintile forecast show more rapid convergence, especially 2 months into the season. The improvement is less noticeable in June and July, perhaps reflecting the fact that, at least in the GLAM crop model, cumulative rainfall in this part of the season is comparatively less strongly correlated with yield.

An alternative approach is to use temperature forecasts to weight the ensemble. To investigate the effect of temperature forecasts, the ensemble was weighted using idealized June-July-August (JJA) tercile temperature forecasts to weight the forecast on 4 June 2011, July-August-September (JAS) tercile temperature forecasts to weight the forecast on 4 July 2011, August-September-October (ASO) tercile temperature forecasts to weight the forecast on 4 August 2011 and September-October-November (SON) tercile temperature forecasts to weight the forecast on 4 September 2011. As with rainfall, the upper, middle and lower terciles are weighted [1,0,0] for a ”perfect cold forecast”, [0,1,0] for a ”perfect normal forecast” and [0,0,1] for a ”perfect warm forecast”. Figure 2.13 shows the forecast for the 2011 cropping season with a perfect average temperature forecast. Due to a negative correlation of the average temperature with maize yield, a warmer temperature forecast is associated with predictions of lower yield. Comparison between Figures 2.12 and 2.13 suggests that temperature forecasts have a greater effect on the risk assessments than rainfall forecasts.

So far, only idealized forecasts have been considered. In the next section, we demonstrate the effect of using actual tercile forecast information issued by the International Research Institute (IRI) for rainfall and temperature. The seasonal forecasts from IRI for 2011 in northern Ghana are shown in Table 3.4.

Figure 2.14 shows the yield forecast probabilities based on weighting the yield ensembles by sea-

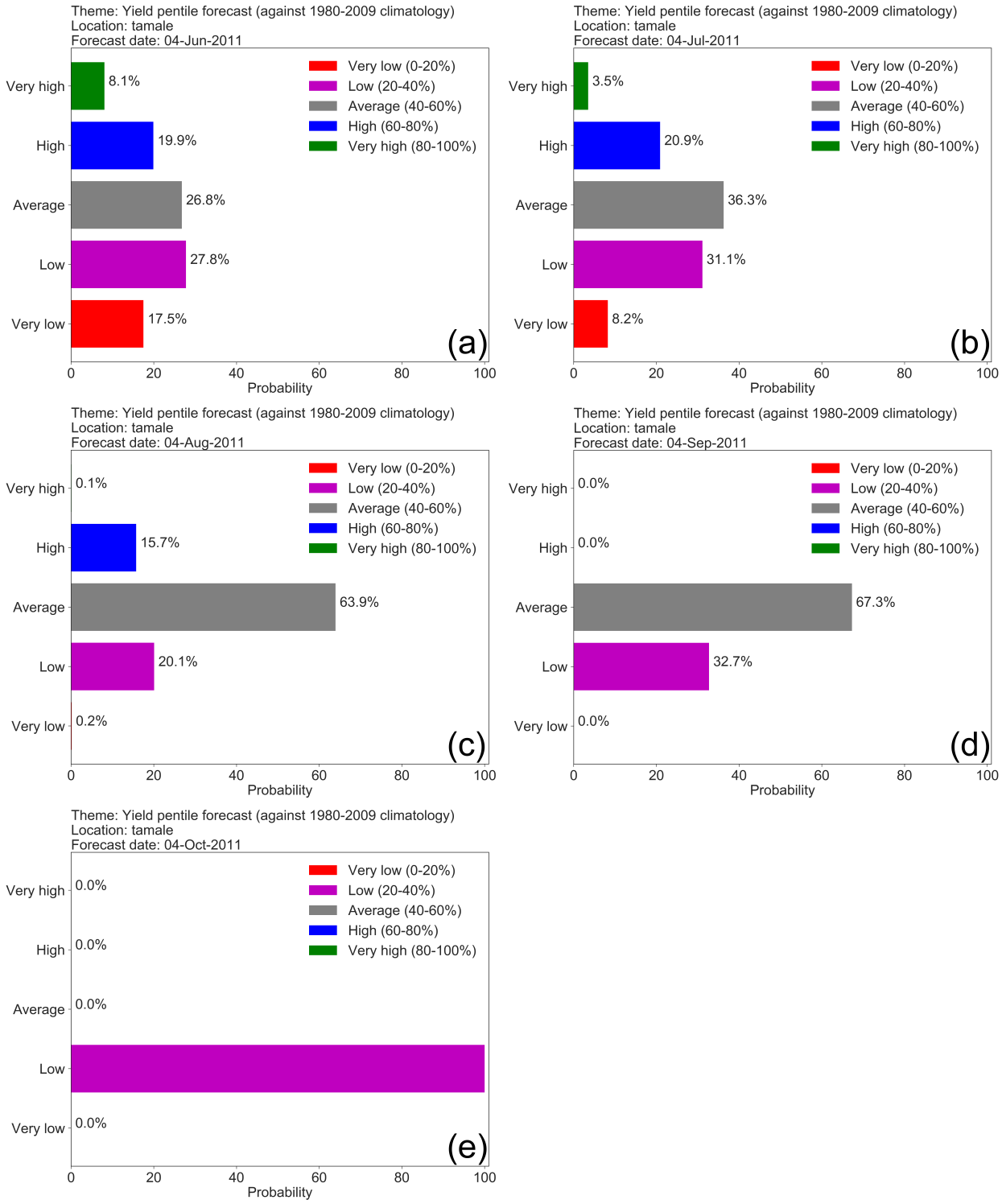

Figure 2.12: Yield probability forecast for the year 2011 for five forecast dates, (a) 4 June, (b) 4 July, (c) 4 August, (d) 4 September and (e) 4 October, when ensembles are weighted by a perfect tercile seasonal rainfall forecast.

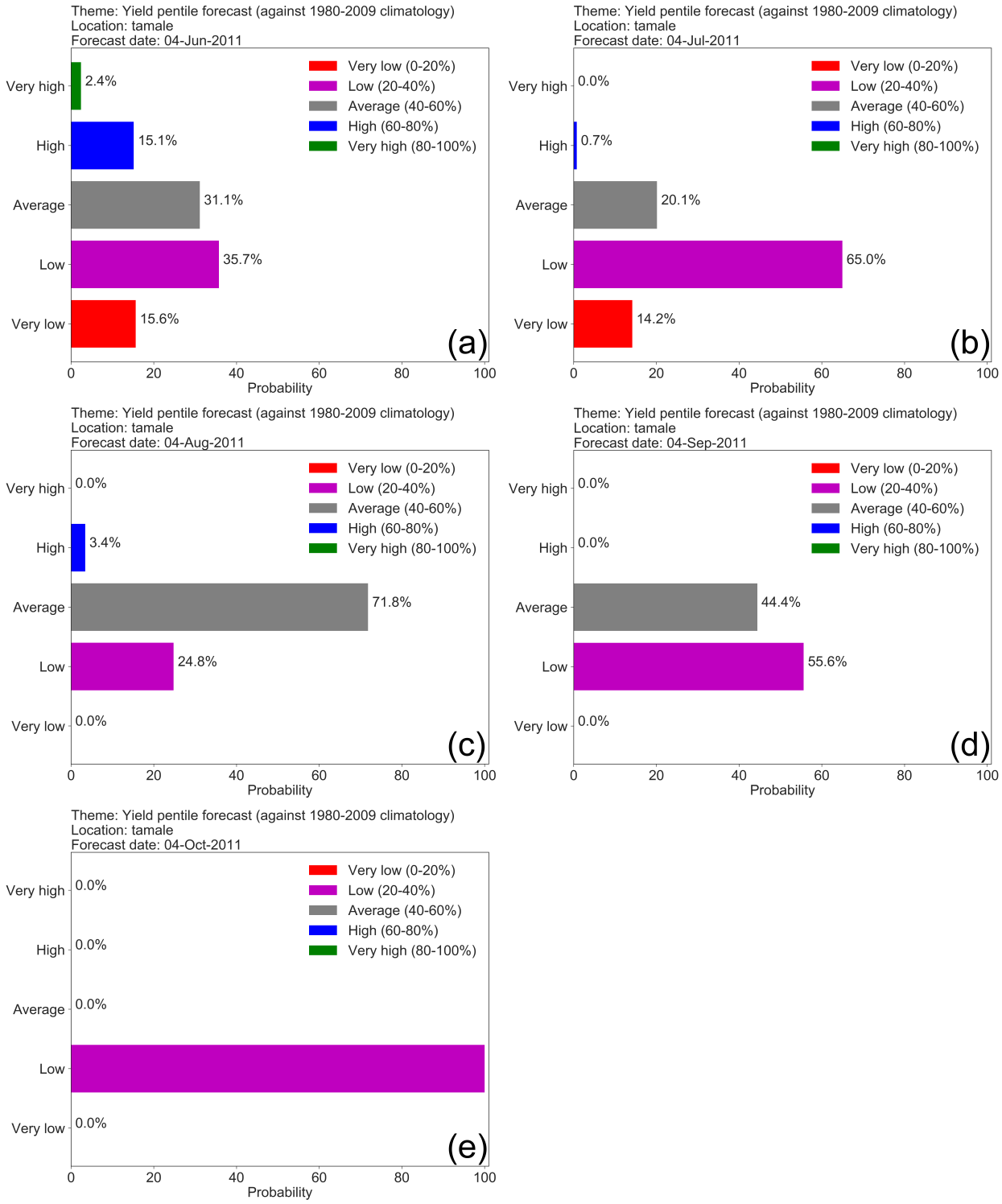

Figure 2.13: Yield probability forecast for the year 2011 for five forecast dates, (a) 4 June, (b) 4 July, (c) 4 August, (d) 4 September and (e) 4 October, when ensembles are weighted by a perfect average temperature of seasonal forecast.

sonal rainfall forecasts from IRI. Comparison with Figure 2.11 suggests that the weighting has little effect. Figure 2.15 shows the quintile yield predictions when temperature forecast weightings from IRI are applied. As with rainfall, comparison with Figure 2.15 shows that the weighting has little effect. The results are summarized in Figure 2.16, which represents the probability of each yield pentile at different lead times in the 2011 season yield forecast with no seasonal forecast, precipitation forecast or temperature forecast applied. For all lead time periods indicated, weighting by IRI seasonal forecast for the 2011 season showed no improvement in predicting the final yield compared to the non-weighted values. This is not surprising because the relationship between the seasonal cumulative rainfall and seasonal mean temperature with maize yield is very low (Figure A.1.1 and Figure A.1.2). The tercile weightings for the IRI forecast (Table 3.4) are close to climatology, and the previous discussion showed that even a perfect and precise seasonal forecast has relatively little impact.

In summary, Figures 2.12 and 2.13 indicate that if meteorological forecasts have sufficient accuracy and precision, they can add information to the decision-making process, especially in the middle to later part of the growing season. However, Figures 2.14–2.16 show that the tercile forecasts currently issued in northern Ghana do not have sufficient precision information to yield risk assessments. A further application of TAMSAT-ALERT could be to investigate the level of skill that is required for meteorological forecasts to contribute useful information to such decision-making processes.

2.3.3.3 Formal skill evaluation

The objective of TAMSAT-ALERT is to provide early warning of the meteorological risk to yield, which is not an observable quantity. For this reason, evaluations of TAMSAT-ALERT skill are carried out in a "perfect model" framework, in which we attempt to forecast the yield simulated by GLAM forced with observed weather data. It is important not to confuse these skill assessments with evaluation of GLAM (section 2.3.2.3), although the usefulness of the framework depends to a large extent on the quality of the model and data incorporated within it.

Figure 2.17 shows GLAM hindcasts at four approximate lead times (i.e., ∼3, ∼2, ∼1, ∼0.5 months ahead of harvest) for 5 years. Towards the outset of the season, the hindcasts for each year are similar and close to the climatology, with the minor differences explained by variation in planting

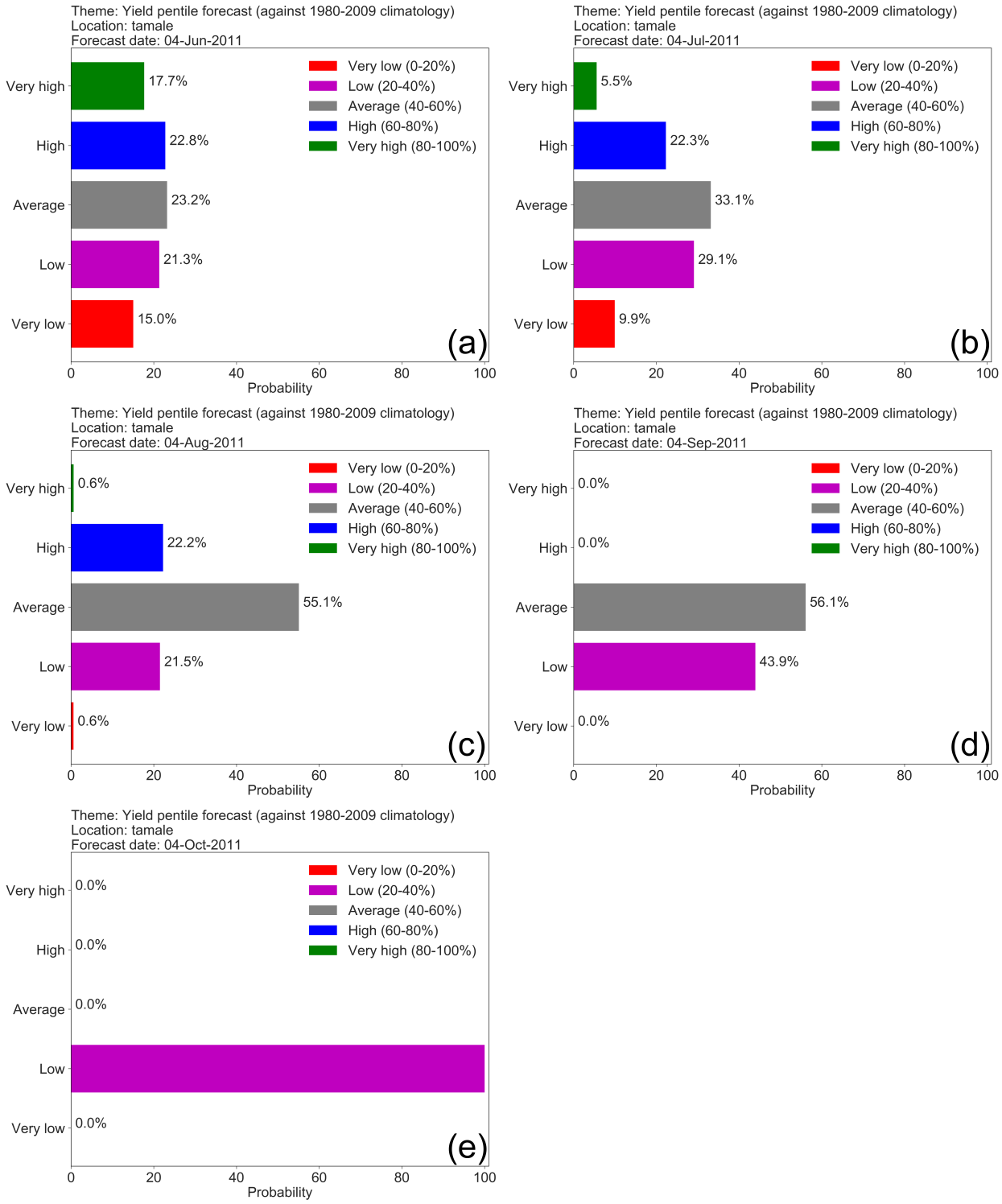

Figure 2.14: Yield probability forecast for the year 2011 for five forecast dates, (a) 4 June, (b) 4 July, (c) 4 August, (d) 4 September and (e) 4 October, when ensembles are weighted by IRI seasonal rainfall forecast.

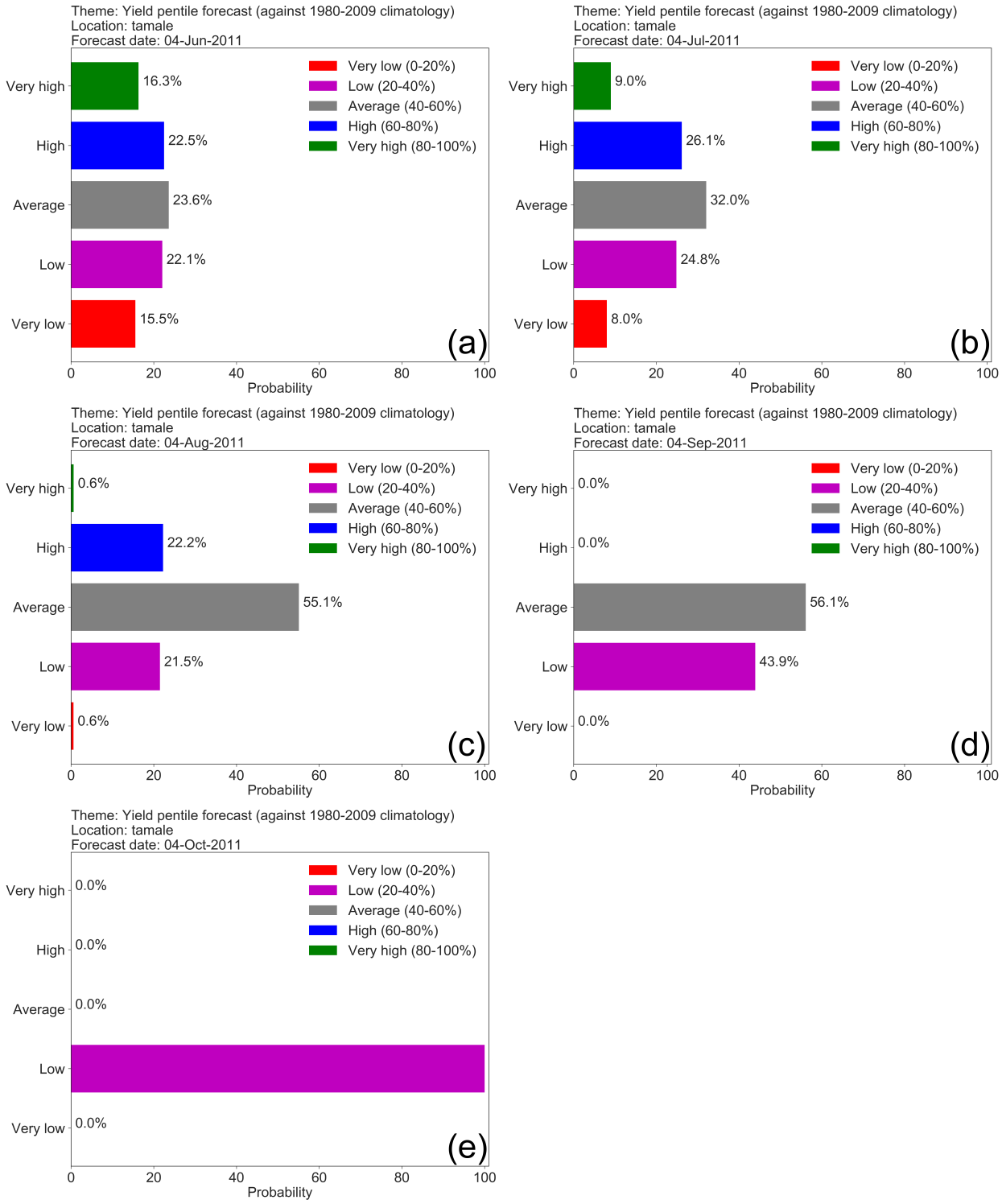

Figure 2.15: Yield probability forecast for the year 2011 for five forecast dates, (a) 4 June, (b) 4 July, (c) 4 August, (d) 4 September and (e) 4 October, when ensembles are weighted by IRI seasonal forecast average temperature.

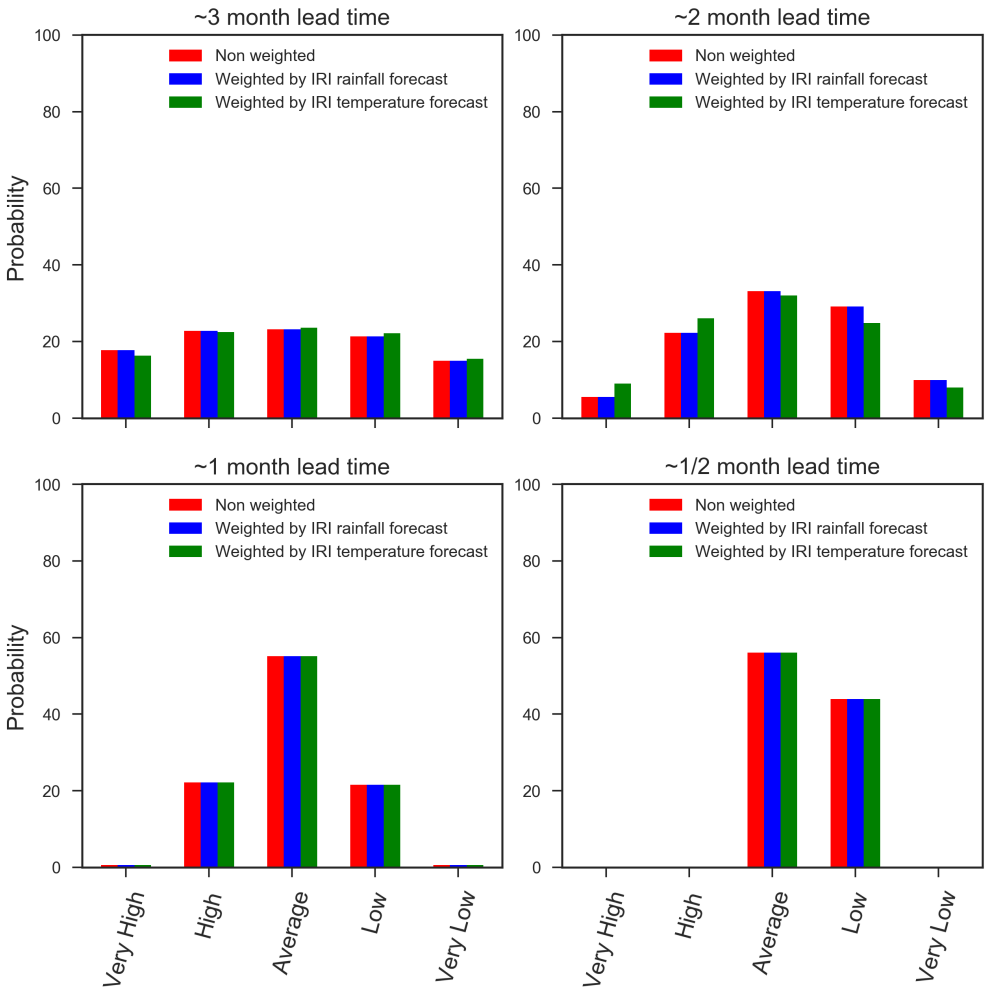

Figure 2.16: Probability of yield forecast for the 2011 growing season when weighted by IRI seasonal forecast of rainfall (blue), when weighted by IRI seasonal forecast of temperature (green) and when no weightings are used (red). The x axis represents the pentile categories used in the yield forecast.

date. For all the lead times considered the spread of the ensembles is reduced as the season progresses. Only the years 2007-2012 are presented in Figure. 2.17 because the maize variety changed in 2007, making the hindcasts of these years more relevant to the present day than the 1994-2006 period (Figure A.1.3).

As described in section 2.3.3.1, the probabilistic ensemble forecasts will be presented as the likelihood of quintile categories. The skill of the probabilistic forecast was assessed using the ranked probability skill score (RPSS). The RPSS is a skill score formulated from the ranked probability score (RPS) that compares the cumulative squared probability error for climatological forecasts in each category identified. The RPSS is negatively biased with smaller ensemble sizes

(<40) and due to this a correction was done on the reference RPS used before calculating the final RPSS. The biascorrected RPSS is called the discrete ranked probability skill score (RPSSD). Details on the calculation and bias-correction are given in Muller et al. (2005) and Weigel et al. (2007). Positive values indicate better skill than the climatology; a unit value represents a perfect score and zero or below-zero values indicate no skill in the forecast.

The RPSSD for Tamale was derived for the period 2002- 2011. This period is used because IRI seasonal forecasts for precipitation and temperature issued on a monthly basis are only available from 2002. Figure 18 indicates the skill scores for the four lead times for the forecasts made using the TAMSAT-ALERT system. The skill scores are generally above 0.4 for ∼2-month lead time and over 0.6 for ∼1- month lead time over the 10-year period considered. There are some years in which the skill score was lower than the stated values and this is mainly because of shifts in forecast categories towards the end of the season, which tends to happen if the yield is near a category boundary. For example, the 2011 final yield was in the low category, but 1 month earlier than harvest the ensembles indicate 56% in the average category and 44% in the low category (Figure. 2.11), which results in a low skill score for that year. The overall skill of the system is presented in Figure 2.19, which shows a good skill even 2 months ahead of harvest. The average $RPSS_D$ shows an increase in skill as the lead time decreases, which is expected. Comparison of similar period skill scores for yield forecasted weighted by the IRI seasonal weather forecast of rainfall and temperature showed a similar result to that of the non-weighted forecast. This indicates that the seasonal forecasts have little impact in predicting the maize yield in the region, which is associated with both the low correlation of seasonal weather values and maize yield and with the vague nature of the forecasts.

2.4 Discussion and conclusions

The TAMSAT-ALERT framework complements and extends previous systems by driving impact models with ensembles based on observed weather rather than weather generators or direct forcing with seasonal forecasts. This provides a simple means of combining information at different scales and bias-correcting seasonal forecasts. The framework is thus capable of integrating multiple sources of environmental observations and forecasts into continually updated assessments of the likelihood of a user-defined adverse event, such as unfavorable weather conditions

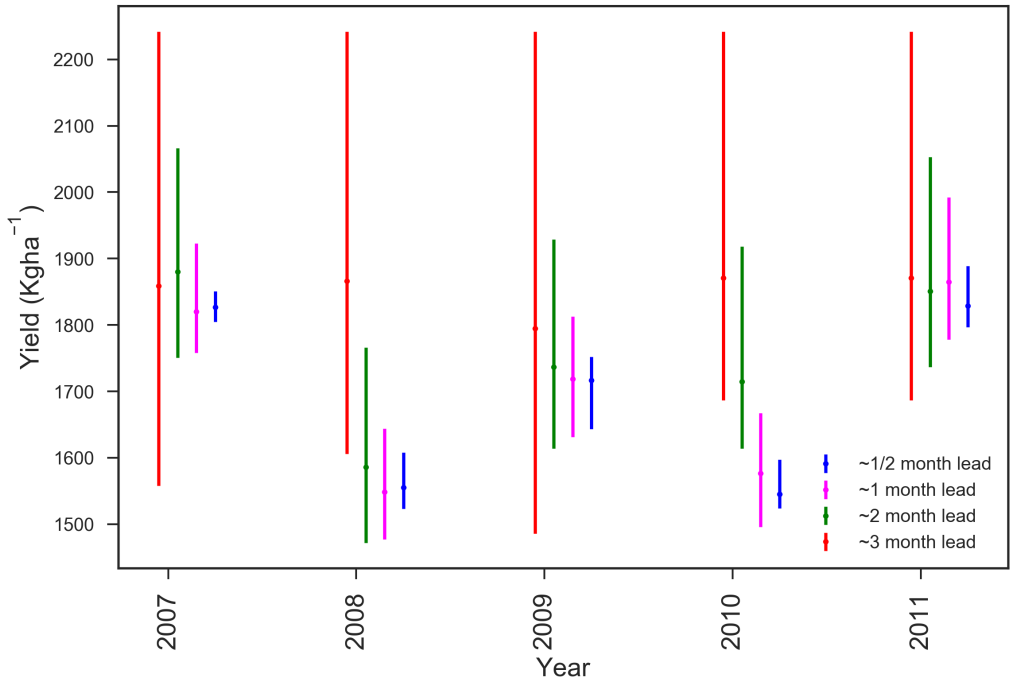

Figure 2.17: Time series of maize yield forecast in Ghana from 2007 to 2011 with four lead times of forecast. This is done using a hindcast for each year and comparing the plots of ∼3-month lead time (red), ∼2-month lead time (green), ∼1-month lead time (magenta) and ∼0.5-month lead time (blue).

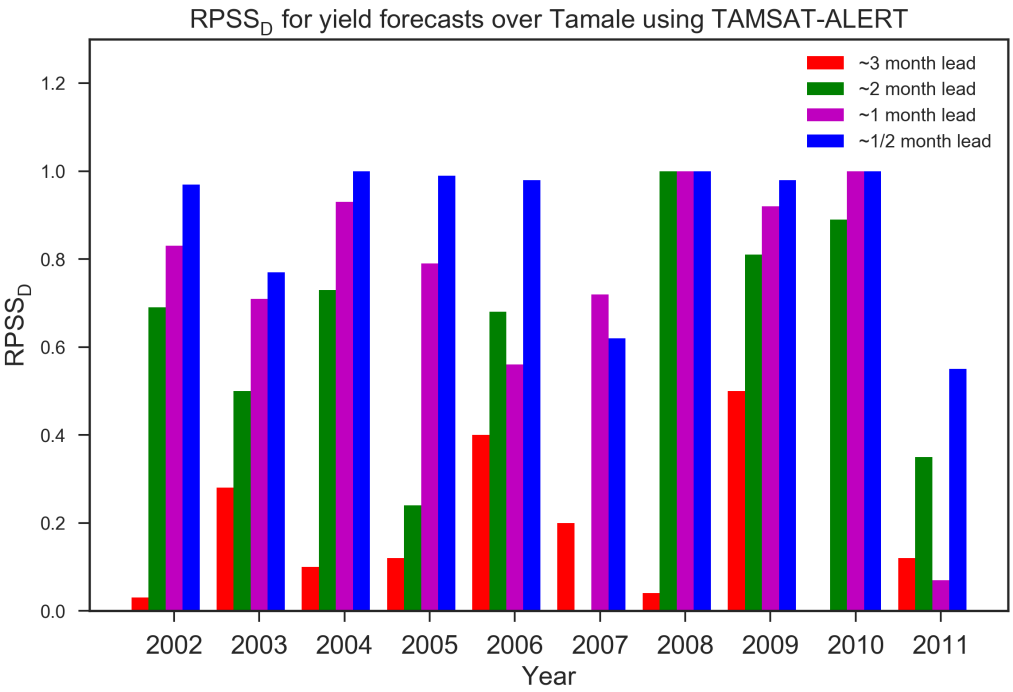

Figure 2.18: Discrete ranked probability skill score for the yield forecasts over Tamale using the TAMSAT-ALERT system at different lead times.

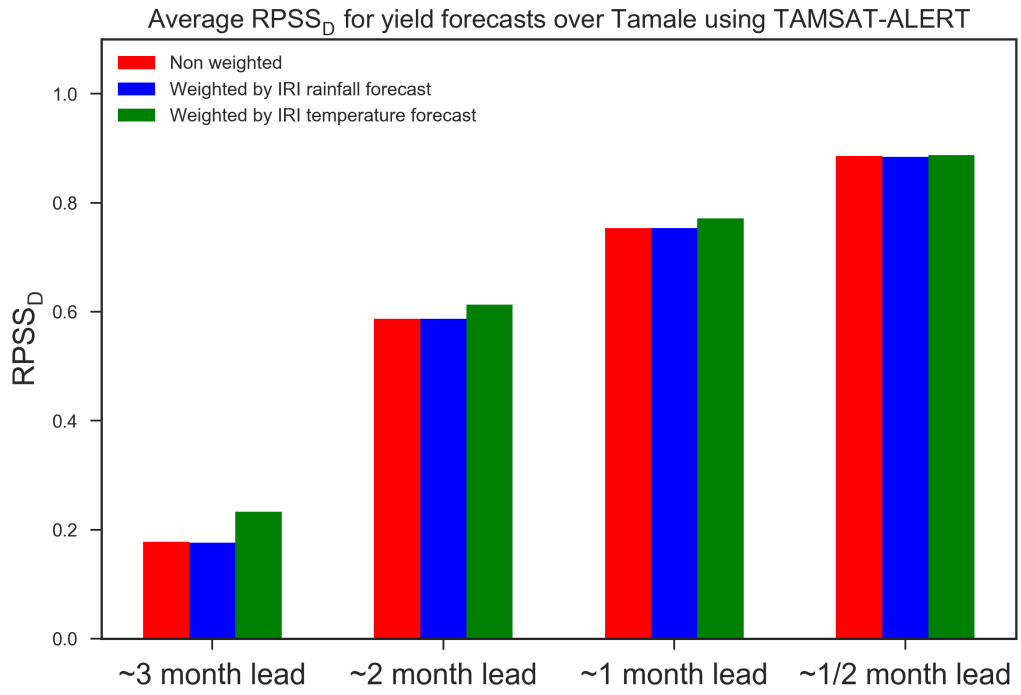

Figure 2.19: Discrete ranked probability skill score for the yield forecasts over Tamale using the TAMSAT-ALERT system at different lead times averaged for 20022011.

for maize yield. While the emphasis of our study has been on forecasting adverse events, such as low yields, it should be noted that TAMSAT-ALERT is also capable of anticipating favorable conditions, enabling decision makers to maximize the benefits of such years, for example by managing post-harvest storage and markets. The system can, moreover, work at any spatial scale for which driving data are available, including for individual communities.

The use of decision support tools for agricultural activities in Africa is low because of low capacity for model use, lack of funding from governments in the development of agricultural decision support tools, lack of data availability for the validation and calibration of models, and low knowledge among decision makers about the use of decision-making tools (MacCarthy et al., 2018). Nevertheless, the demand for meteorologically driven crop models, such as the Decision Support System for Agrometeorology Transfer (DSSAT), World Food Studies (WOFOST) and Crop Environment Resource Synthesis-Maize (CERES-Maize) for sub-Saharan Africa, speaks to a need for the quantification of the meteorological hazard to yield (Dzotsi et al., 2003; Kassie et al., 2014, 2015; MacCarthy et al., 2017). The implementation of TAMSAT-ALERT described in this study quantifies the meteorological risk to agriculture, and as such potentially provides information for government, aid agencies and nongovernmental organizations working in

agriculture. A key result is that, even in the absence of meteorological seasonal forecasts, low yield can be anticipated 6–8 weeks before with some skill.

In the example described in this paper, we have used the GLAM crop model. It is clear from the validation of GLAM against national yield statistics presented in section 2.3.2.3 that the models ability to simulate year to year variation in Ghana-wide maize yield is moderate. Nevertheless, previous studies have demonstrated that GLAM can capture the meteorological hazard to yield (Challinor et al., 2007, 2010; Osborne et al., 2013) when the model is driven with highquality meteorological data and is compared against robust information on yield. The provision of the scripts for the GLAM implementation will enable further studies to be carried out at locations with more robust information on yield and agronomic characteristics.

This study used the GLAM crop model as an illustration of the implementation of the system. The strength of TAMSAT-ALERT, however, is its modularity. TAMSAT-ALERT can be implemented for any impact model driven with meteorological data. There is now demand for TAMSAT-ALERT in locations throughout East and West Africa, with the system adapted to implement trusted metrics and models. This modularity and flexibility is important, since the skill of the TAMSAT-ALERT system is constrained by the quality of the model and its calibration. In this study, for example, the evaluation and calibration of GLAM was hampered by quality-control issues with the available yield data. The system would be much improved if used in house by agencies with access to high-quality yield data and locally calibrated models. Nevertheless, it is important that model error is taken into account in the decision-making process, and forecasts should therefore be issued in the context of model evaluations like the one presented in this study. TAMSAT-ALERT's modular structure, moreover, permits forecasts to be produced using an ensemble of crop models and crop model parameterizations, facilitating formal analysis of model uncertainties.

A key finding from our study is that tercile seasonal forecasts have little impact on TAMSAT-ALERTs skill for the case study considered. This is not unexpected. The correlation of 90-day total rainfall with GLAM-simulated maize yield in this region is low. The low correlation means that we do not expect precipitation seasonal forecasts to improve the yield forecasts even if they are

skillful. Our results do not suggest that there is no information available from seasonal forecasts. However, we do show that 90-day tercile forecasts of temperature and rainfall, even if perfectly skillful, provide comparatively little information for risk assessments of low maize yield. This could be because the sensitivity of crops to moisture is on a specific period of their growth and the sensitivity of crops to temperature is also not similar throughout their growth stage. In other words, our findings highlight the necessity of more specific and localized forecasts if users are to benefit from the inherent skill contained in the forecasts. These findings are consistent with anecdotal evidence that the tercile seasonal forecasts of rainfall routinely issued by forecasting organizations are of little practical benefit for decision-making. A secondary application of TAMSAT-ALERT could be to provide guidance on forecasts that would potentially be of use for decision makers should they have sufficient skill. Such analyses are currently underway as part of a major national capability program being carried out at the National Centre for Atmospheric Science.

In summary, TAMSAT-ALERT is a lightweight system, which can be run either using the computing facilities available in house at meteorological services or on the cloud. Its modular design enables it to work alongside existing systems to combine multiple sources of data into quantitative assessments of risk. Together with socioeconomic assessments, this information could be of significant value for governments, policy makers and humanitarian service providers tasked with mitigating the effect of drought on Africa's poorest farmers.

Chapter 3

Soil moisture model development

This chapter describes the soil moisture model used to evaluate the use of the TAMSAT-ALERT method for drought monitoring (chapter 4) and develop a planting date decision-making tool (chapter 5). The first part provides general background about a land surface model, the use of the land surface model in agricultural decision making and its utilisation in Africa and explains the need for extracting parts of the Joint UK Land Environment Simulator (JULES) model. Next, description of the fundamental equations used in the model is explained, including an account of the modification of JULES. Finally, a comparison of soil moisture outputs from the new model with JULES is given to evaluate how the new model performs relative to JULES. The objective of this chapter is, therefore focused on answering the following question:

Can simplified versions of a complex land surface model be used to represent an agricultural risk decision metrics?

The chapter addresses the following objectives:

- Describing the fundamental mathematical equations of the soil moisture model.
- Explaining the modifications made on the part of the JULES soil hydraulics to simplify and develop a new soil moisture model.
- Describing the additional specific outputs introduced in the new soil moisture model relevant for agricultural decision making.
- Evaluating the soil moisture outputs from the JULES model and the new soil moisture

model.

The chapter evaluated the soil moisture model and showed that the modified soil moisture model use less number of input data, with faster run time and requiring less computational power and adapted to integrate additional outputs to be used as metrics to indicate adverse events caused by climate risk. The model being freely available also add usability by African climate services to add value on current weather advice they provide to move to impact-oriented forecast and provide actionable information to end users.

3.1 Land surface modelling approach

3.1.1 Land surface models

Land surface models (LSMs) are numerical models used to represent physical process on earth such as energy flow, the water cycle and the carbon cycle (Abramowitz et al., 2008). These LSMs are critical components in global and regional climate models that simulate the atmosphere as they represent the processes on the surface that interact with the atmosphere and provide outputs regarding sensible and latent heat, available water, runoff and evaporation, and simulate carbon exchange (Abramowitz, 2005). The earlier LSMs were very simple, accounting only for surface energy and water balance, and the level of complexity has increased through time by adding more complex physical processes such as the carbon cycle, use of multi-dimensional soil temperature and moisture schemes, runoff routing, dynamic evolution of snowpack, land use representation such as urban, lake, and biogeochemical processes (Pitman, 2003; van den Hurk et al., 2011). The additional complexity of LSMs increases driving data requirements, computational power and skill required to utilise the models; however, they can provide a more realistic representation of the global and regional changes of the climate and the subsequent response of the land surface as indicated by studies involving LSMs (Leipprand and Gerten, 2006; Betts et al., 2007; Steiner et al., 2009). These studies show that changes in the land surface and the atmosphere will influence the climate in general and the outputs from climate models at a global and regional scale reveal the differences. Even though a good representation of physiological and biological processes is vital for a realistic prediction of changes in the land surface (Betts et al., 2007) such increased physical process representation to improve LSMs pose significant challenges regarding parametrising essential aspects of the land surface such as hydrological process, root process, and biodiversity

within simulation grid scale (Pitman, 2003; Sato et al., 2015). Furthermore, incorporation of all these complex processes within LSMs need multi-disciplinary teams representing a range of skills, increasing the challenge for developing LSMs (Pitman, 2003).

3.1.2 Utilising land surface models for agricultural decision making in Africa

Linking scientific knowledge with decision making that leads to effective action to meet the development needs of human is a difficult task and these difficulties present problems for decision makers not getting the necessary scientific information to make informed decisions (Cash et al., 2003b). Evidence-based decision making is paramount and increased demand for information that allows making an informed decision on complex environmental issues drive the science (Matthies et al., 2007). There are a wealth of research outputs that utilise LSMs and climate models to evaluate a different aspect of the environment at global and regional scale such as water resource management (Liu et al., 2007), rainfall and hydrological variability (Cook and Vizy, 2006; Li et al., 2005), energy and carbon exchange (Sellers et al., 1997) and effects of CO_2 increase (Leipprand and Gerten, 2006). Despite all these advanced research outputs on environmental science, the link between the knowledge and its support for decision making is still a major challenge (Cash et al., 2003a; Reichert et al., 2007). The challenges of utilising research outputs come from many directions and the first one being a poor mutual understanding between result producers and users for decision making, this occurs due to differences in values, interest, apprehensions and perceptions among them (Jacobs, 2002; McNie, 2007). The second reason is poor correlation between the product from scientific research and the demand by decision makers. The mismatch could be in a form of a wrong result, unusable format or poor clarity of results (Jacobs et al., 2005; Cash et al., 2003a). The third one is the uncertainty associated with the results coming out of the scientific community make decision makers reserved from fully utilising the outcomes for their decision making (Refsgaard et al., 2007; Xu et al., 2007).

In Africa where most people's livelihoods depend on subsistence agriculture and animal husbandry, the risk associated with climate change and variability is far more devastating (Boko et al., 2008; Makondo et al., 2014). Hence, the regional climate service providers are more focused on providing information regarding drought risk, seasonal weather outlook and implications on agriculture. These meteorological service providers base their outlooks on results from numerical

weather forecast systems involving land surface models at different time scales (Graham et al., 2015). For example, Greater Horn of Africa Climate Outlook Forum (GHACOF) run by Intergovernmental Authority on Development Climate Prediction and Applications Centre (ICPAC) provide seasonal climate outlooks for eastern Africa and similarly Southern African Development Community (SADC) climate service centre provides weather and climate information for southern Africa. Graham et al. (2015) on Climate Information and Service for Africa (CIASA) argues that the services offered are more focused on food security and agriculture within a time scale of 3–6 months but agricultural activity such as identifying season onset and cessation, timing of heavy rains and dry spells require sub-seasonal information which is mostly absent from services provided by the regional climate service providers. Moreover, the uptake of climate information to guide policy and decision making is limited even with guidance on climate risk is available to the decision-makers (Graham et al., 2015). The capacity of many of the African meteorological services is also quite limited in providing basic climate information rather than the interpretation of a large set of data and inferring implication in sectors of agriculture and water resources. Hence, effective utilisation of results from large scale land surface models or climate models require a capacity building in managing the results or should be more simplified and tailored to the specific needs of each user. This chapter provides a simple soil moisture model which can be run in local computers with minimum skills available at African climate service centres and generate soil moisture estimates and drought metric WRSI at a spatial scale of the available climatic driving data. Such additional variables allow African climate service centres to provide information regarding impending drought and subsequent yield reduction in a growing season (chapter 4) and advice farmers on critical decisions like planting time (chapter 5) in addition to the routine climate forecasts.

3.1.3 Rationale for modification of JULES and objective

Outputs from complex large scale land surface models are useful in analysing results at a global and regional scale. However, to make use of the results from these land surface models, there is a need to modify them to fit the demand of end-users like farmers, government and humanitarian agencies. In this chapter, the soil hydraulics part of the JULES model was simplified to develop a new soil moisture model. The new soil moisture model developed is used for monitoring drought within the growing season (chapter 4) and decision-making tool development for

planting time (chapter 5) of crops based on a new framework of agricultural decision support – TAMSAT-ALERT (chapter 2). The choice of the JULES model comes as it has been extensively used in many researches related to climate change impact studies and the fundamental equations are well described and tested.

The need for the modification of the soil moisture model arises from two fundamental reasons, the scientific challenge of modifying large and complex models like JULES and the practical difficulty of running these models in African meteorological service centres. JULES model is very complex and mostly used within global scale numerical weather forecast models. This complexity is associated with high requirement of skill and understanding in the utilisation of the very many input parameters and side processes (e.g. photosynthesis, energy balance, soil thermodynamics) that need to be run in parallel even though those outputs are not to the interest of users. Practically the JULES model takes a longer time to run and require more computational power which is not commonly available in most African countries and any decision-making tools developed based on JULES need legal permission to share as the model is under copyright making it difficult to share any newly developed system easily. Hence, extracting a single part of the JULES model representing the soil hydraulics and modifying the inputs to simulate soil moisture was found to be more applicable to the studies conducted in this thesis and will have a wider utility. The thesis developed a new decision support framework for assessing climatic risk on agriculture (chapter 2) and a demonstration of the system was done based on the Global Large Area Crop Model (GLAM) (Challinor et al., 2004). The new framework was also used to monitor drought risk within the growing season (chapter 4) and development of a planting date decision-making criteria (chapter 5). GLAM is a pure crop model focused on yield estimation, whereas JULES is a land surface model focused on large scale physical land surface processes. Therefore, there was a need to use a unified system to monitor agricultural risk (low yield and drought) within the growing season and Water Requirement Satisfaction Index (WRSI) was found to be a metric that accomplished this task (chapter 4). In both GLAM and JULES, the WRSI is not part of the output emphasising the need for the development of a new model that calculates WRSI value.

In general, the above facts lead to the choice of modifying the JULES model to develop a new soil moisture model that will help to accomplish the desired aims of this thesis. Here, the goal is not

to replicate the JULES model but rather have a simple modified soil moisture model written in Python based on the concepts described in the JULES technical documentations (Cox et al., 1999; Best et al., 2009, 2011) with the additional output WRSI required for further study in chapter 4.

3.2 Soil moisture model description

The soil moisture model used in this work is adopted from JULES soil hydraulics which uses the Met Office Surface Exchange Scheme (MOSES) for modelling water and energy balance. Figure 3.1 shows the schematic of MOSES. There are ten meteorological forcing variables required to run the model; downward short and longwave radiation, precipitation, air temperature, wind speed (zonal and meridional), air pressure, specific humidity, and diurnal temperature and total snow. JULES can provide several outputs related to hydrology, carbon, soil moisture and temperature, and dynamic vegetation. The calculation is done based on grid boxes which can be represented by nine land surfaces, of which five are vegetative and four are non-vegetative. These tiles can be represented with different proportion within each grid and results can be generated as aggregate or separate for each section of the grid. JULES uses a default soil layer with 0.1, 0.25, 0.65, and 2.0 m depth. The Darcy law (Equation 3.10) and Richards equation (Equation 3.7) describes the flux between each soil layer. The model allows the use of heterogeneous soil types which are represented by the texture of the soil from which important soil hydrothermal properties are calculated. JULES simulates fluxes in the vertical direction and lateral flows are considered to be zero (Cox et al., 1999; Best et al., 2011). All the equations discussed in this section are similar in the modified soil moisture model, except for those modifications which are described in section 3.2.2.

3.2.1 Summary of JULES soil hydraulics

The fundamental equations describing the soil hydraulics presented are adopted from (Cox et al., 1999; Best et al., 2009, 2011). The soil hydraulics in the JULES model uses the Darcy flow and Richards equation to generate the soil moisture at each soil layer. Precipitation that falls to the ground is reduced by the canopy water which is the amount of water that will be intercepted by vegetation canopy, and the throughfall is the amount reaching the ground. Throughfall is then divided in to surface runoff and the remaining water will infiltrate to the soil.

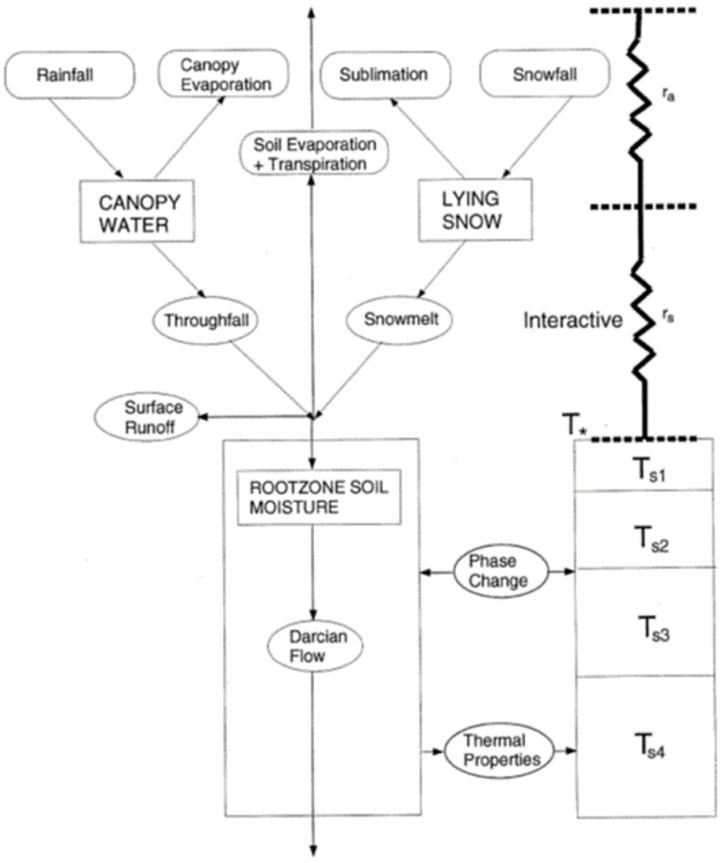

Figure 3.1: Schematic representation of the Meteorological Office surface exchange scheme (MOSES). Figure adopted from (Cox et al., 1999)

$$T_f = R\left(1 - \frac{C}{C_m}\right)\exp\left(\frac{-\epsilon_r C_m}{R\Delta t}\right) + R\frac{C}{C_m} \tag{3.1}$$

$$C_m = 0.5 + 0.05(\Lambda) \tag{3.2}$$

Equation 3.1 represents how the throughfall is calculated. Where T_f is the throughfall, R is the precipitation, C is canopy water, C_m is maximum canopy water, fraction of grid box covered by rainfall (ϵ_r) represents how much of the precipitation falling comes from convective rainfall and how much of it comes from large scale rainfall, and Δt is the time step of model run. The maximum canopy water represents the maximum amount of precipitation that a canopy can intercept and it is calculated using Equation 3.2 where Λ is the leaf area index.

$$Y_s = \begin{cases} R\frac{C}{C_m}\exp\left(\frac{-\epsilon_r K C_m}{RC}\right) + R\left(1-\frac{C}{C_m}\right)\exp\left(\frac{-\epsilon_r C_m}{R\Delta t}\right) & K\Delta t \leq C \\ \\ R\exp\left(\frac{-\epsilon_r(K\Delta t + C_m - C)}{R\Delta t}\right) & K\Delta t > C \end{cases} \tag{3.3}$$

$$C^{n+1} = C^n + (R - T_f)\,\Delta t \tag{3.4}$$

$$K = K_s * I_v \tag{3.5}$$

Equation 3.3 is used to calculate the amount of runoff from the throughfall and Equation 3.4 updates the amount of canopy water C at each time step. Y_s is the amount of precipitation that goes as a surface runoff and K is the surface infiltration rate. K calculated using Equation 3.5 where K_s the saturation hydraulic conductivity of the soil, which is dependent on the soil type and it is estimated based on the soil texture. I_v is infiltration enhancement factor, which is different for the land surface conditions used in the model (Table 3.1).

Equation 3.6 is used to calculate the available soil moisture factor for each soil layer where β_k is the available moisture factor at each soil layer, k is the soil layer, θ_k is the soil moisture content at each soil layer, θ_c and θ_w are the critical soil moisture level and the wilting soil moisture level respectively. The soil moisture availability factor (β_k) is the fraction representing the available soil moisture within the root zone. The value is range between zero and one indicating dry and wet soil, respectively. It is determined based on θ_c which is the moisture level below which plant

Table 3.1: Infiltration enhancement factor(I_v)

	Iv
Broadleaf trees	4
Needelleaf trees	4
C_3 grass	2
C_4 grass	2
Shrubs	2
Urban	0.1
Water	0
Soil	0.5
Ice	0

transpiration is affected (it is set to be the moisture level at matrix water potential of -33 KPa) and θ_w which is the moisture level below which plants will not survive (it is set to be the moisture level at matrix water potential of -1500 KPa) (Best et al., 2011).

$$\beta_k = \begin{cases} 1 & \theta_k \geq \theta_c \\ (\theta_k - \theta_w)/(\theta_c - \theta_w) & \theta_w \leq \theta_k < \theta_c \\ 0 & \theta_k \leq \theta_w \end{cases} \tag{3.6}$$

Soil moisture content is calculated using Equation 3.7. Where M represent soil moisture, ρ_w is density of water, Δz is the depth of soil layer, Θ_s represents the saturated moisture content of the soil, and S_u and S_f represent the unfrozen and the frozen fractional soil moisture content compared to the saturation soil moisture content respectively. Equation 3.8 helps to calculate the fractional soil moisture content at each time step of the model run.

$$M = \rho_w \Delta z \Theta_s (S_u + S_f) \tag{3.7}$$

$$S_u = \frac{\Theta_u}{\Theta_s} \tag{3.8}$$

Where S_u represent the unfrozen fractional soil moisture content compare to the saturation soil moisture content, Θ_u unfrozen soil moisture content and Θ_s is the saturated soil moisture content (Cox et al., 1999).

$$\frac{dM_n}{dt} = W_{n-1} - W_n - E_n \tag{3.9}$$

The soil moisture at each time step in the model is updated using the difference in input and output moisture. The input moisture is the flow from the upper layer for the lower layers and the infiltration for the top layer. The outflow is the moisture flowing down to the lower layer and the evapotranspiration that is extracted by plant roots. Equation 3.9 represents how the change in soil moisture at each soil layer is calculated. W represent the soil moisture flux, n represent the

time step and E represent the evapotranspiration. Soil moisture fluxes between each soil layer are calculated according to Equation 3.10, which is based on Darcy water flow equation. $\partial\Psi$ is the matrix potential difference calculated using Equation 3.11, ∂z is the change in soil depth and K is the hydraulic conductivity of the soil calculated using Equation 3.12.

$$W = K\left(\frac{\partial\Psi}{\partial z} + 1\right) \tag{3.10}$$

$$\Psi = \Psi_s S_u^{-b} \tag{3.11}$$

$$K = K_s S_u^{2b+3} \tag{3.12}$$

The flow of water between the layers W depends on the matrix potential difference Ψ and water is not allowed to flow upwards. The soil has a maximum capacity to hold water and excess water at each layer is drained as a subsurface flow and directed up-wards when all the soil layers are saturated. K denotes the hydraulic conductivity of the soil calculated using Equation 3.12 where K_s the saturated hydraulic conductivity, b the Brooks and Corey $b - parameter$ and Ψ_s the saturated hydraulic conductivity are all empirical soil dependent constants determined based on the soil texture (Best et al., 2009).

The flow of water into the top layer of the soil is represented by Equation 3.13 where the flow is the difference between the throughfall (T_f) and runoff (Y_s) calculated using Equation 3.1 and 3.3 respectively. The lower layer boundary flow is kept similar to the saturated hydraulic conductivity of the soil K_N, as shown in Equation 3.14 (Cox et al., 1999).

$$W_0 = T_f - Y_s \tag{3.13}$$

$$W_N = K_N \tag{3.14}$$

The amount of water extracted from the soil at each time step is a total of soil evaporation from

the surface layer and the transpiration from each sub-surface layers which is calculated based on the fraction of the root depth available at each soil layer (Equations 3.26, 3.27, 3.28, and 3.29). Evapotranspiration is calculated from the potential value and potential evapotranspiration is the amount of evapotranspiration subjected to the aerodynamic resistance only.

$$E_o = \frac{\rho_{air}}{r_a}(q_{sat}(T_*) - q_1) \tag{3.15}$$

Equation 3.15 is used to calculate potential evapotranspiration where E_o is the potential evaporation, ρ_{air} is air density, r_a aerodynamic resistance, $q_{sat}(T_*)$ saturation specific humidity evaluated at surface temperature (T_*) and measured specific humidity (q_1).

JULES uses an iterative estimation of q_{sat} at each time step accounting the first soil layer temperature (T_1) in addition to the present time step surface temperature (T_*). Equation 3.16 represents the estimation of $q_{sat}(T_*^{n+1})$ in JULES. The next time steps q_{sat} is estimated using an additional term D, which is given by Equation 3.17. This term accounts for the impact of the first soil layer temperature in the estimation of q_{sat}. The additional term will result in a different value of q_{sat}, which determine the potential evaporation given by Equation 3.15.

$$q_{sat}(T_*^{n+1}) = q_{sat}(T_*^n) + D(T_*^{n+1} - T_*^n) \tag{3.16}$$

$$D = \frac{q_{sat}(T_*^n) - q_{sat}(T_1^n)}{T_*^n - T_1^n} \tag{3.17}$$

Potential evapotranspiration mostly occurs on free water surfaces (lakes) and in a canopy fully covered with water. For all the other conditions the potential evapotranspiration is reduced by surface resistance due to plant and bare soil which is governed by the canopy conductance (g_c), surface conductance (g_s), wind speed and atmospheric stability in the area (Best et al., 2009). The evapotranspiration from the soil E is the actual amount of evapotranspiration from the soil storage and represented as a portion of the potential evapotranspiration E_o as described in Equation 3.18 where ψ is the factor that represents the portion.

$$E = \psi E_o \tag{3.18}$$

$$\psi = f_a + (1 - f_a)\frac{g_s}{g_s + (C_H U_1)} \tag{3.19}$$

ψ has a maximum value of one representing potential evapotranspiration from the soil water storage and it is calculated based on Equation 3.19. Where f_a represent the wet fraction of the canopy and calculated using Equation 3.20, g_s represent the stomatal conductance and calculated using Equation 3.25, C_H represent the surface exchange coefficient and U_1 is the wind speed.

$$f_a = \frac{C}{C_m} \tag{3.20}$$

where f_a is the wet fraction of the canopy, C is the canopy water and C_m is the maximum canopy water capacity.

$$f_{par} = \frac{1 - \exp(-0.5 * \Lambda)}{0.5} \tag{3.21}$$

$$f_r = 1 - \exp(\frac{-\Lambda}{0.5}) \tag{3.22}$$

where f_{par} is a parameter dependent on leaf area index used to determine the canopy conductance, f_r is the radiative fraction and Λ is the leaf area index. Equation 3.23 is used to calculate the bare soil surface conductance where g_{soil} is bare soil surface conductance, θ_1 is the soil moisture on the first layer and θ_c is the critical soil moisture level.

$$g_{soil} = 0.01 * \left(\frac{\theta_1}{\theta_c}\right)^2 \tag{3.23}$$

$$g_c = g_l * f_{par} \tag{3.24}$$

Equation 3.24 is used to calculate the canopy conductance g_c where g_l leaf conductance and f_{par} is the parameter determined using Equation 3.22. In the JULES model, the leaf conductance g_l is

calculated based on the level of photosynthesis rate at each time step. This part has been modified in the new soil moisture model (section 3.2.2).

$$g_s = g_c + (1 - f_r)g_{soil} \tag{3.25}$$

Equation 3.25 is used to calculate the total surface conductance g_s by adding the canopy conductance g_c and the bare soil surface conductance g_{soil}.

Evapotranspiration depletes the soil moisture by extracting a certain amount of water from each soil layer depending on the fraction of the plant root at each soil layer. The plant root follows an exponential function distribution in the soil and it might extend beyond the rooting depth of the plant specified (Best et al., 2011). Equation 3.26 represent the calculation of root fraction in each soil layer where r_k is the fraction of the root at each soil layer, z_k is the depth of the soil layer, d_r represent the plant root depth and p is the power describing depth dependence of root density profile and is considered one in the model used.

$$r_k = \frac{e^{-pz_{k-1}/d_r} - e^{-pz_k/d_r}}{1 - e^{-pz_t/d_r}} \tag{3.26}$$

$$e_k^0 = \frac{r_k \beta_k}{\Sigma_k r_k \beta_k} \tag{3.27}$$

Based on fractions of the root at each soil layer r_k a factor will be generated from the ratio of the product of root fraction r_k and the available moisture factor at each soil layer β_k. Equation 3.27 is used to estimate the flux extracted from the soil layer k by plant roots. This value is dependent on the root fraction on each soil layer r_k and the available soil moisture in the layer β_k.

$$e_1 = \frac{g_c e_1^0 + (1 - f_r)g_{soil}}{g_s} \tag{3.28}$$

$$e_k = \frac{g_c e_k^0}{g_s} \tag{3.29}$$

The soil moisture to be extracted from each soil layer is then the actual evapotranspiration E cal-

culated using Equation 3.18 multiplied by the root fraction factors at each soil layer from Equation 3.28 and Equation 3.29. e_1 in Equation 3.28 represent the evaporation from the first soil layer plus the transpiration from the layer whereas e_k in Equation 3.29 only account the transpiration from the subsequent soil layers where there is no direct evaporation.

3.2.2 What modification has been done?

The modified new soil moisture model is a simple soil moisture model written in Python based on the JULES model soil hydraulics described in section 3.2. Figure 3.2 shows the schematics of the new soil moisture model. Comparing it with the JULES model schematics on Figure 3.1, the major difference is that the new soil moisture model is a pure soil hydraulic model that does not include soil thermodynamics, full energy balance and photosynthesis. The new model includes additional data variables like surface temperature to account for energy balance and parametrisation of values like stomatal conductance (g_l) to account for photosynthesis.

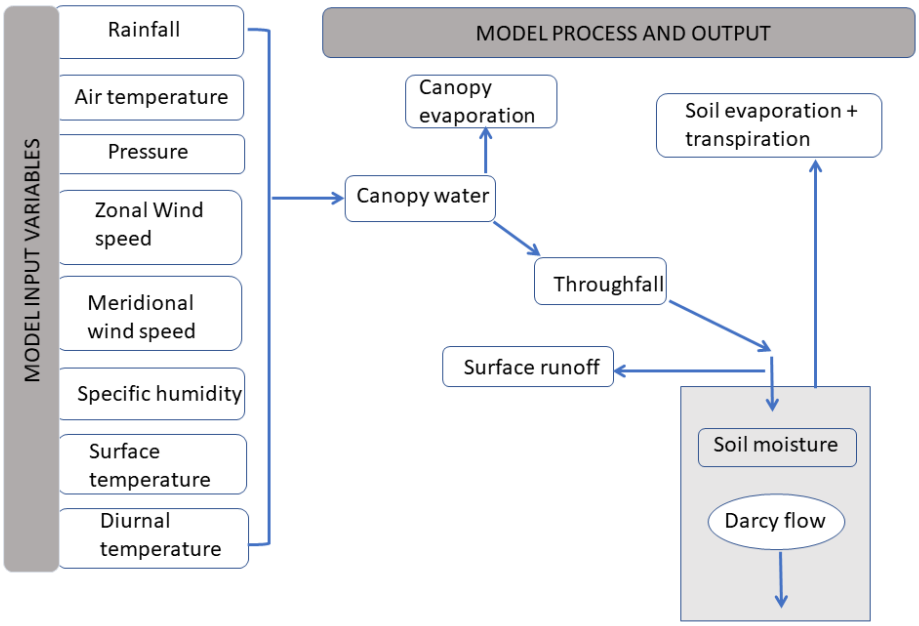

Figure 3.2: Schematic representation of the new modified soil moisture model

3.2.2.1 Difference in estimation of potential evaporation

The main modification to simplify the new soil moisture model was done in the use of an additional input variable surface temperature (T_*) as the new model does not calculate the energy

balance explicitly. Direct input of surface temperature is used to account for the energy balance in the new soil moisture model, unlike JULES, which estimates the surface temperature internally based on Equation 3.16 described in section 3.2.1. The implication of this difference is on the estimation of potential evaporation (E_o) calculated using Equation 3.15; the new model does not account for the soil layer temperature since there is no thermodynamic representation of the soil layers. Therefore, the q_{sat} is only evaluated based on the surface temperature (T_*) directly provided as input data from National Center for Environmental Prediction (NCEP) reanalysis data. This difference in the estimation of E_o in part attributes to the differences in soil moisture between the new model and JULES. Section 3.3.3 discuss the result in modelling bare soil moisture.

3.2.2.2 Modification of stomatal conductance

The JULES model explicitly represented the vegetation and carbon model (Raoult et al., 2016; Cox et al., 1999). This representation determines the transpiration of water and carbon through the stomatal openings as well as the rate of photosynthesis. Equation 3.30 shows the JULES model representation of photosynthesis.

$$A = \frac{g_s}{1.6 * R * T_*}(c_c - c_i) \tag{3.30}$$

where A is net leaf photosynthesis, g_s stomatal conductance to water vapour, R is the perfect gas constant, T_* is the leaf surface temperature,and c_c and c_i represent the leaf surface and internal CO_2 partial pressures respectively. In Equation 3.30 three values , A, g_s and c_i, are unknown. The initial c_i is then approximated by Equation 3.31 where the internal CO_2 is dependent on the external CO_2 concentration (c_c) and the specific humidity deficit (D), f_o and D_* are vegetation specific parameters (Cox et al., 1999).

$$\frac{c_i - c_*}{c_c - c_*} = f_o\big(1 - \frac{D}{D_*}\big) \tag{3.31}$$

Leuning model represented by Equation 3.32 is the basis for estimating stomatal conductance at each time step depending on the photosynthesis rate (A) and vapour pressure deficit (D_s).

$$g_l = \frac{a * A}{(c_c - c_*)\big(1 - \frac{D_s}{D_*}\big)} + g_o \tag{3.32}$$

D_s is the vapour pressure deficit, a and D_* are empirical coefficients which will be parameterised, g_o is the initial minimum stomatal conductance value (Wang et al., 2009). The term $\left(1 - \frac{D_s}{D_*}\right)$ represents the response of humidity on stomatal conductance- physically it means that when there is very low humidity the stomata will close reducing leaf conductance (g_l). g_l is also related to the leaf photosynthesis (A) and in JULES this term is directly related to the soil moisture availability factor (β) as the net photosynthesis (A_1) is a function of β as shown in Equation 3.33.

$$A_1 = A * \beta \tag{3.33}$$

JULES uses the photosynthesis rate to increment the g_l at each time step based on Equation 3.32 however; the new model does not have such photosynthesis description forcing the use of a single value as initial stomatal conductance to estimate g_l. The initial stomatal conductance ($g_{initial}$) used in the new soil moisture model requires tunning for C_4 plant hence the soil moisture output from JULES and the new soil moisture model were used to find a value that match. Based on this, a $g_{initial}$ value of 0.025 was used for C_4 plant. Furthermore, a new adjusted leaf conductance parameter $g_l(modified)$ was introduced as given in Equation 3.34. The modification was done by multiplying $g_{initial}$ with moisture availability factor (β) and the ratio of specific humidity to saturation humidity ($\frac{q1}{q_{sat}}$).

$$g_l(modified) = g_{initial} * \beta * \frac{q1}{q_{sat}} \tag{3.34}$$

$$g_c(modified) = g_l(modified) * f_{par} \tag{3.35}$$

Plant stomatal closure is largely governed by humidity at the leaf surface and water availability to roots in the absence of light limitation (Bond and Kavanagh, 1999; Bauer et al., 2013). Stomata tend to close with reduced moisture availability and increased vapour pressure deficit (VPD) while stomata open with increased moisture availability and decreased VPD (McAdam et al., 2016) (also shown in Equation 3.32). Therefore, the multiplying factors β and ($\frac{q1}{q_{sat}}$) were used to account the dependence of stomatal conductance for soil moisture availability and vapour pressure deficit. Modifying the stomatal conductance g_l with the soil moisture availability factor (β) limits transpiration depending on available moisture while the ratio of specific humidity to saturation humid-

ity ($\frac{q1}{q_{sat}}$) accounts for stomatal closure and reduction of transpiration due to humidity. Therefore, Equation 3.24 in JULES is modified to Equation 3.35 in the new modified soil moisture model. Section 3.3.4 discuss the model result comparison of a C_4 plant.

3.2.3 Additional output to monitor drought: WRSI

One of the reasons for modifying the soil moisture model was to be able to add new outputs that can be used to generate user relevant metrics related to agriculture in Africa. Based on this, the new soil moisture model described in this chapter has an additional feature to output Water Requirement Satisfaction Index (WRSI) which is used to monitor drought. WRSI is the ratio of cumulative actual crop evapotranspiration to the cumulative potential evapotranspiration over a certain growing period (Senay and Verdin, 2003). WRSI describes how much water is available for plants to grow without water stress and the value of WRSI run from 0 to 100 where a value of 100 indicate no water stress and 0 value indicate complete dryness.

$$WRSI = \left(\frac{\sum_{t=1}^{t} ET_t}{\sum_{t=1}^{t} PET_t} \right) * 100 \tag{3.36}$$

$$ET_t = \frac{SM_t}{SWC_t} * PET_t \tag{3.37}$$

Equation 3.36 is used to calculate the WRSI values where t is the time period, ET_t actual evapotranspiration of the crop for time t and PET_t potential evapotranspiration of the crop for time t. The evapotranspiration is calculated as a ratio of the soil moisture at the specific time SM_t and the soil water content SWC_t, which is the critical soil water amount below which plants will experience stress. Equation 3.37 is used to calculate the evapotranspiration value ET_t (McNally et al., 2015).

The mean soil moisture availability factor β defines WRSI in the modified soil moisture model as expressed in Equation 3.38. β_t is the soil moisture availability factor at time t and t is the period in days starting from planting to harvesting.

$$WRSI_\beta = \bar{\beta_t} * 100 \tag{3.38}$$

The reason for using β as a measure of WRSI arise since the value β represents the availability of moisture which is similar to that of the ratio between SM_t and SWC in Equation 3.37. The derivation for the similarity between β and WRSI is given below:

(a) Substituting Equation 3.37 into Equation 3.36 results in Equation 3.39.

$$WRSI = (\frac{SM_t}{SWC_t}) * 100 \tag{3.39}$$

(b) Equation 3.40 calculates β where, θ_t is the soil moisture content at time t, θ_w the wilting soil moisture content and θ_c the critical soil moisture content below which plants show stress.

$$\beta = \frac{\theta_t - \theta_w}{\theta_c - \theta_w} \tag{3.40}$$

(c) Equation 3.41 indicates the moisture content available for plants at time t (SM_t) is equal to the difference between the soil moisture content of the soil at time t (θ_t) and the wilting soil moisture content (θ_w).

$$\theta_t - \theta_w = SM_t \tag{3.41}$$

(d) Equation 3.42 indicates the soil water content below which plants show stress (SWC_t) is the same as the amount of soil moisture between critical soil moisture content below which plants show stress (θ_c) and the wilting soil moisture content (θ_w).

$$\theta_c - \theta_w = SWC_t \tag{3.42}$$

(e) Therefore, based on the above derivation Equation 3.43 indicates that WRSI is the same as β.

$$WRSI = \beta \tag{3.43}$$

Based on the above derivation, the $WRSI$ values from Equation 3.36 can be represented similarly by $WRSI_\beta$ values from Equation 3.38. The notation β in Equation 3.38 is just to indicate the WRSI is calculated from β.

WRSI values are crop specific and if one wants to monitor drought occurrence within a cropping season, it is crucial to estimate the actual and potential evapotranspiration of the crop. It is needed to have a crop model within the soil moisture model to determine the actual evapotranspiration. In the modified soil moisture model, an additional simple estimation of rooting depth growth, leaf area index and plant height growth model has been set up. The representation of crop growth is done first by estimating the total length of the growing period using the growing degree days (GDD). GDD is used as a measure of the accumulated heat unit for different crops and is used to determine the crop growth rate (Mcmaster and Wilhelm, 1997; Lee, 2011). Equation 3.44 is used to calculate the daily GDD value from planting until harvesting time. T_{base} refers to the base temperature below which the crop will not grow and T_{mean} refer to the daily mean temperature.

$$GDD = \begin{cases} (T_{mean} - T_{base}) & T_{mean} > T_{base} \\ 0 & T_{mean} \leq T_{base} \end{cases} \tag{3.44}$$

Crops typically have four growing stages which are initial stage where it takes from planting to 10% ground cover (growing stage 1), development stage where the plant reaches up to 80% ground cover (growing stage 2), middle stage from full vegetative growth to seed setting (growing stage 3) and late stage which take from seed setting to maturity (growing stage 4). All these stages will have a different amount of growing degree days (GDD) depending on the crop type and variety. In the new soil moisture model, by providing the total GDD values for these four stages of crops, we determine the length of time required to grow the crop from planting to harvesting using Equation 3.44.

Once the number of days for each growing stage is estimated based on GDD, the model will determine plant root, height and LAI growth. Every crop has a maximum rooting depth (d_r^{max}), height (h_{max}) and LAI (Λ_{max}). Based on this assumption a linear plant root, height and LAI growth model are implemented from the period of planting to end of development stage (growing stage 2) after that the root, height and LAI will remain constant till harvesting. Equations 3.45, 3.46 and 3.47 are used to determine the rooting depth, plant height and LAI from planting to harvesting respectively;

$$d_r = \begin{cases} \sum_{planting}^{stage2} \frac{d_r^{max}}{LGP_{planting}^{stage2}} & stage \leq 2 \\ d_r^{max} & stage > 2 \end{cases} \tag{3.45}$$

$$h = \begin{cases} \sum_{planting}^{stage2} \frac{h_{max}}{LGP_{planting}^{stage2}} & stage \leq 2 \\ h_{max} & stage > 2 \end{cases} \tag{3.46}$$

$$\Lambda = \begin{cases} \sum_{planting}^{stage2} \frac{\Lambda_{max}}{LGP_{planting}^{stage2}} & stage \leq 2 \\ \Lambda_{max} & stage > 2 \end{cases} \tag{3.47}$$

In the new soil moisture model switching to *"crop mode"* lets the use of temporally variable rooting depth, plant height and LAI rather than assuming constant value throughout the year. Therefore, modelling soil moisture as bare soil outside of the growing season and switching to vegetative condition using the temporally varying root depth, plant height and LAI, within the growing season, will help to calculate the WRSI at any time within the growing season. Figure 3.3 shows an example of the root depth, plant height and LAI representation when the *"crop mode"* is switched on in the model. The root, height and LAI will have a linear increase until the end of the second stage while retaining maximum value for the rest of the growing period until harvest. In JULES, crop growth starts from the date of sowing and passes through three stages (sowing – emergence, emergence – flowering, flowering – maturity) to be harvested at maturity. The rate of crop development is determined based on the thermal time (growing degree days) (Osborne et al., 2015). This approach is similar to what the new soil moisture model in this thesis also used for crop growth. The main difference between JULES and the new soil moisture model is JULES simulated crop growth and net primary productivity is accumulated over a day then partitioned into the different parts of the plant (root, stem, leaves, and harvest organ) (Osborne et al., 2015). The partitioned amount determines the rooting depth, plant height and LAI day by day whereas, in the new model, this is replaced by linear growth models as described in Equations 3.45, 3.46 and 3.47. Reducing the complexity of crop growth in the new model helps to avoid the many parametrisations required by JULES. Besides Osborne et al. (2015) found that by improving the partitioning of JULES crop growth does not lead to improving modelling sensible and latent heat fluxes.

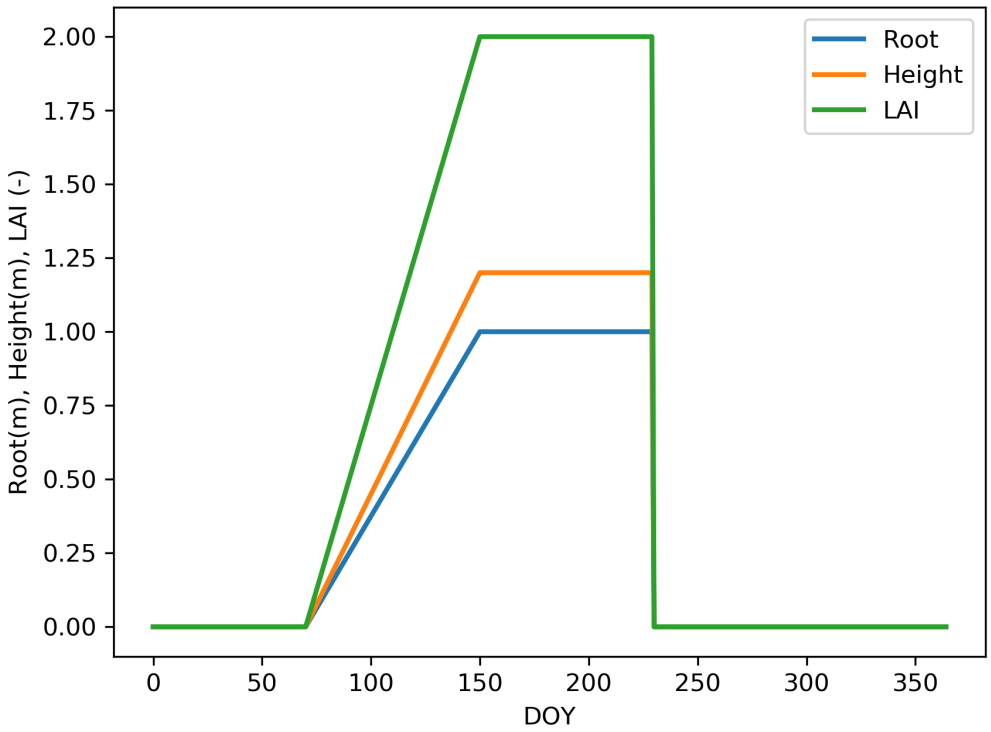

Figure 3.3: An example of root depth, plant height and LAI representation for a maize crop planted on day 70 with a total growing period of 160 days with a maximum rooting depth of 0.8m, plant height of 0.7m, and LAI of 2.0.

3.3 Comparison of new soil moisture model with JULES

3.3.1 Model driving datasets

The JULES model requires the meteorological forcing data described in section 3.2. The model can ingest these driving data sets at different time scales ranging from minutes to daily. Using a higher resolution timescale (<60 minutes) is vital for the numerical stability of the JULES model; hence, JULES normally runs at an hourly time step or less. If the driving data is longer than hourly timescale, it conducts an internal disaggregation to higher resolution timescales to maintain the numerical stability. In this study, the model time step was one hour and all driving data sets were disaggregated to the same temporal scale. The new soil moisture model, on the other hand, uses eight driving data sets where shortwave radiation, longwave radiation and snow were removed and surface skin temperature introduced as a new data variable. In the process of simplifying the soil hydraulics from the JULES model, the energy balance was removed and to account for this in

the estimation of evaporation and transpiration processes the new soil moisture model uses the surface skin temperature from the NCEP data set directly (section 3.2 and section 3.3).

NCEP reanalysis data provide a long term global analysis of atmospheric and land surface fields to support research in the field of climate monitoring (Kistler et al., 2001). The reanalysis used past data from 1979 to 2018 for data assimilation and produce different atmospheric and land surface variables estimates on a global scale for a 4-times daily and daily average time scale (Kanamitsu et al., 2002). The NCEP data was designed with the main objectives of providing climatic and land surface outputs, which allow for comprehensive budget studies to be done and availing easily accessible data to users (Kalnay et al., 1996). The reanalysis includes a total surface energy balance, hydrological budget and top-of-atmosphere radiation budget and it uses data assimilation technique to generate different variables and also provide model output variables which do not include observational data sets. The NCEP data is classified into three categories (Kalnay et al., 1996):

1. Group A: the data which is highly influenced by observational data like wind and upper air temperature.
2. Group B: variables which include observation but also influenced by the model used in the reanalysis these include variables like humidity and surface temperature.
3. Group C: this category involves all variables which are a direct output of model reanalysis and do not include any observational dataset examples include all the surface fluxes and precipitation.

NCEP data set production consists of extensive quality control with a three-step process involving data quality control module, analysis module and output module. Despite all the quality control care in using these datasets is vital (Kistler et al., 2001), but the NCEP reanalysis is approved to be a useful and easily accessible data set in the research field for climate studies and more. The product is provided with a 2.5° spatial resolution at a global scale.

A time series of precipitation data from the climate hazards infrared precipitation Tropical Applications of Meteorology using SATellite and ground-based observations (TAMSAT-v3) was used for locations in western Kenya (Kitale; 1.0N, 35.0E) and eastern Kenya (Wajiri; 1.73N, 40.09 E). TAMSAT rainfall dataset is one of the widely used rainfall product in Africa (Maidment et al.,

2017). The product provides daily rainfall estimate for Africa at a 0.0375° spatial resolution from 1983 to present. TAMSAT uses Meteosat satellite thermal infrared (TIR) imagery to produce cold cloud duration (CCD) fields, which are calibrated against rain gauge observations to produce rainfall estimates. Version 3.0 also employs a spatially and temporally variable bias adjustment on the calibration (Maidment et al., 2017). TAMSAT has been used for applications such as drought risk management and drought monitoring (Black et al., 2016a; Enenkel et al., 2016), development of improved precipitation estimation (Ceccherini et al., 2015) and season onset and cessation estimation (Dunning et al., 2016).

3.3.2 Model setup

To evaluate the new soil moisture model performance compare to JULES, simulations of soil moisture for locations in western Kenya-Kitale (1.0° N and 35.0° E) and eastern Kenya-Wajiri (1.73° N and 40.09° E) were performed. The two locations represent different agro-ecology where Kitale in the west is more humid high rainfall area whereas Wajiri in the east is a semi-arid environment with low rainfall condition. Figure 3.4 and Figure 3.5 show the mean rainfall pattern in Kitale and Wajiri, respectively. Kitale has a prolonged seasonal rainfall and Wajiri has a distinct two season rainfall with a lower amount. The choice to evaluate the soil moisture model in Kenya is because further studies in this thesis regarding drought monitoring (chapter 4) and planting date decision making (chapter 5) were conducted in Kenya and observed ground data required for evaluation (maize yield and farmers planting time) was available from the country.

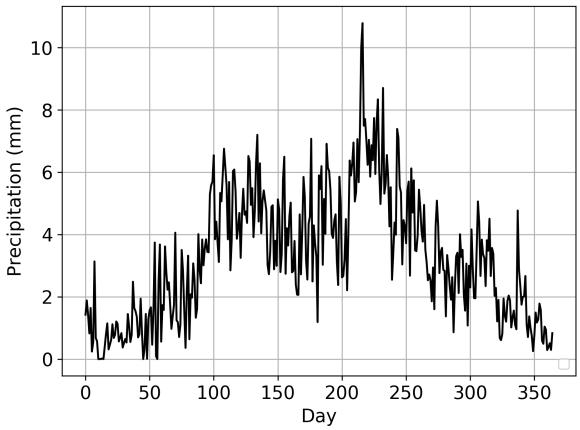

Figure 3.4: Average daily rainfall of Kitale western Kenya (2003-2017)

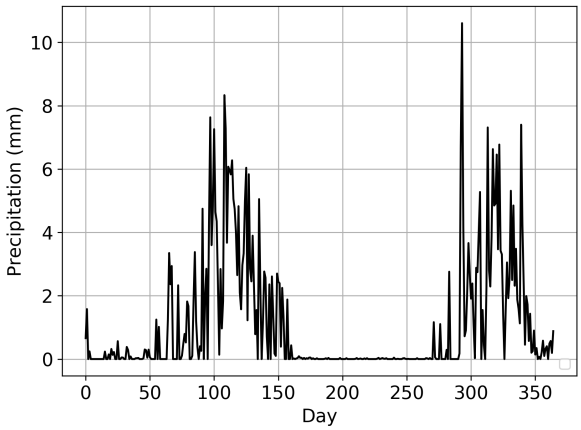

Figure 3.5: Average daily rainfall of Wajiri eastern Kenya (2003-2017)

JULES version 4.1 with driving data sets from NCEP (radiation, pressure, temperature and spe-

cific humidity) and TAMSAT-v3 (rainfall) was used to model soil moisture. The driving data set has a daily temporal scale; however, the soil moisture is modelled at an hourly time step and aggregated back to daily value. Data were disaggregated using the internal disaggregation method in the new soil moisture method (Appendix B.1). Both models were set up with four soil layers having constant soil characteristics and a depth of 0.1, 0.25, 0.65, and 2.0 meter for layer-1, layer-2, layer-3 and layer-4 respectively. A radiative canopy with heat capacity (can_model=3) and multilayer approach for radiation interception which uses a vertically varying light limited leaf photosynthesis rate with an exponential decline in leaf number according to canopy height (can_rad_mode=4) was used for JULES. Soil moisture was modelled for bare soil and a C_4 grass, since the interest of the subsequent chapters in this thesis are the development of planting date decision-making tool which uses bare soil moisture of the topsoil layer and drought monitoring within growing seasons for Maize crop which is a C_4 plant. Table 3.2 shows the soil and canopy radiation model parameters used. The results for the comparison between the new soil moisture model and JULES are discussed in section 3.3.3 and section 3.3.4.

Table 3.2: Soil and canopy radiation model parameters

Parameter	Description	Value
albsoil	Soil albedo	0.11
b	Exponent in soil hydraulic characteristics	4.641
hcap	Dry heat capacity ($Jm^{-3}K^{-1}$).	1139708.013
hcon	Dry thermal conductivity ($Wm^{-1}K^{-1}$).	0.278
satcon	Hydraulic conductivity at saturation ($kgm^{-2}s^{-1}$)	0.009
sathh	Absolute value of soil matric suction at saturation (m)	0.133
sm_crit	Soil moisture content at the critical point (m^3m^{-3})	0.207
sm_sat	Soil moisture content at saturation (m^3m^{-3})	0.413
sm_wilt	Soil moisture content at the wilting point (m^3m^{-3})	0.091
sm_levels	Number of soil layers	4
d_z	Soil layers depth (m)	0.1, 0.25, 0.65, 2.0
PFT	Plant functional type	Soil and C_4 grass
h	Plant height (m)	1.26
d_r	Rooting depth (m)	0.5
Λ	Leaf area index	4.0
can_model	Canopy model for vegetation	3
can_rad_mode	Canopy radiation treatment	4

3.3.3 Bare soil moisture modelling

A comparison between the JULES model and the new soil moisture model was made to evaluate the difference in the model output of soil moisture. Figure 3.6 and Figure 3.7 show the time series and seasonal soil moisture values from Kitale respectively. Figure 3.8 and Figure 3.9 shows a similar soil moisture plot for the dry region of Wajiri in eastern Kenya. The Figures indicate that the new model estimates represent the seasonal variability similar to the output from JULES. The new model soil moisture values are higher compared to JULES, especially in the bottom layers. Figure 3.10 and Figure 3.11 show the evaporation from the JULES model and new soil moisture model for Kitale and Wajiri respectively. The evaporation from JULES is higher compared to the new model for Kitale, which inturn reduces the soil moisture of JULES and increases soil moisture from the new model, as shown in Figure 3.7. For Wajiri where there is lower rainfall and higher temperature compare to western Kenya the impact of the evaporation is even more visible especially in the lower layers where the JULES model dries out very fast compared to the new model. During the dry periods, there is higher evaporation from JULES and lower evaporation from the new model.

The difference soil moisture between the new model and JULES could be attributed to many reasons. The first could be the way how the evaporation is estimated between the JULES model and the new model where JULES considers additional parameters based on the soil thermodynamics where the soil temperature from the soil layers are combined in the estimation of evaporation whereas the new model only accounts surface temperature. The difference is even more visible between the two locations wherein a wet, humid environment of western Kenya (Kitale) the soil dries out slowly and in the semi-arid region of eastern Kenya (Wajiri) there is fast drying of the subsurface layer. This fast drying could also be related to the higher surface temperature (T_*) in the eastern region compare to a colder environment in the western part (Kitale). The surface temperature (T_*) in JULES is calculated at each time step of the model and in the new soil moisture model, the value is directly given from NCEP reanalysis data. T_* values from JULES are lower than that of NCEP on average by 3K for Kitale and 6K for Wajiri (Figure B.2.1 and Figure B.2.2), where the difference could be attributed to the use of different precipitation rate (Figure B.3.1 and Figure B.3.2) and soil parameters by JULES and NCEP reanalysis data. The new soil moisture model uses direct reanalysis surface temperature from NCEP whereas JULES internally

estimates the values based on the driving data provided, hence the overall difference in soil moisture between the new soil moisture model and JULES in part be the result of this difference.

JULES assumes that there will always be a small amount of transpiration hence considers a rooting depth of 0.1m (Cox et al., 1999)- this will result in the growth of plants leading to more transpiration from the bottom layer. The new model used a similar approach; however the LAI and plant height are kept very low, unlike JULES where the values are calculated at each time step, the difference in LAI and plant height could be the second reason leading to lower transpiration from the bottom layer resulting in the difference in the amount of soil moisture. Jiménez et al. (2013) compared soil moisture from JULES and satellite observation and indicated that JULES soil moisture estimation main driving data is precipitation and when there is no precipitation (dry periods) the internal calculation continues to drain water from the lower layers and drift the soil moisture from the satellite observation and result in lower soil moisture value. This condition of extracting soil moisture from the lower layer during the dry period is visible in the dry location (Wajiri) where the soil moisture is very low during the distinct dry periods in the subsurface layers for JULES compare to the new model. JULES also tends to dry down faster, resulting in lower soil moisture compared to satellite observed soil moisture (Pinnington et al., 2018). Furthermore, JULES overestimates evaporation and falls too quickly during extended dry periods (Blyth et al., 2010), but the new soil moisture model does not show such behaviour resulting in higher soil moisture compared to JULES. JULES is not "perfect" and the use of NCEP sensible heat flux might be attributed to the improvement in the new soil moisture model.

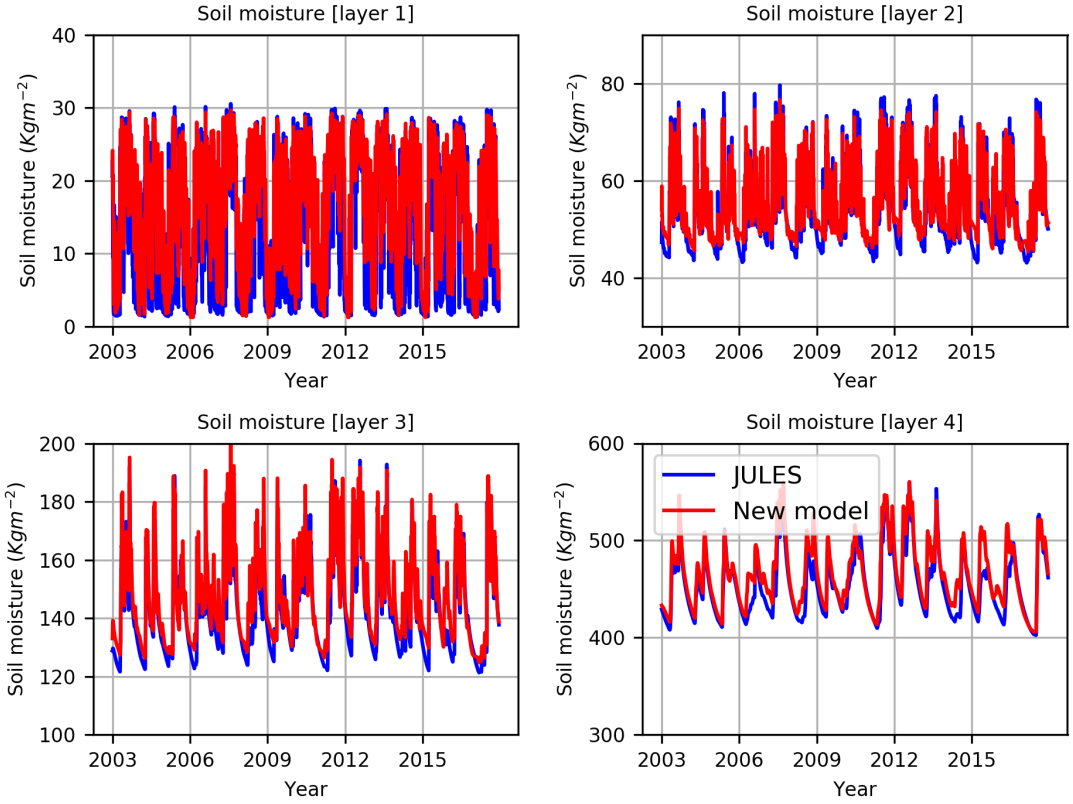

Figure 3.6: Soil moisture output from JULES and new model with bare soil (Kitale).

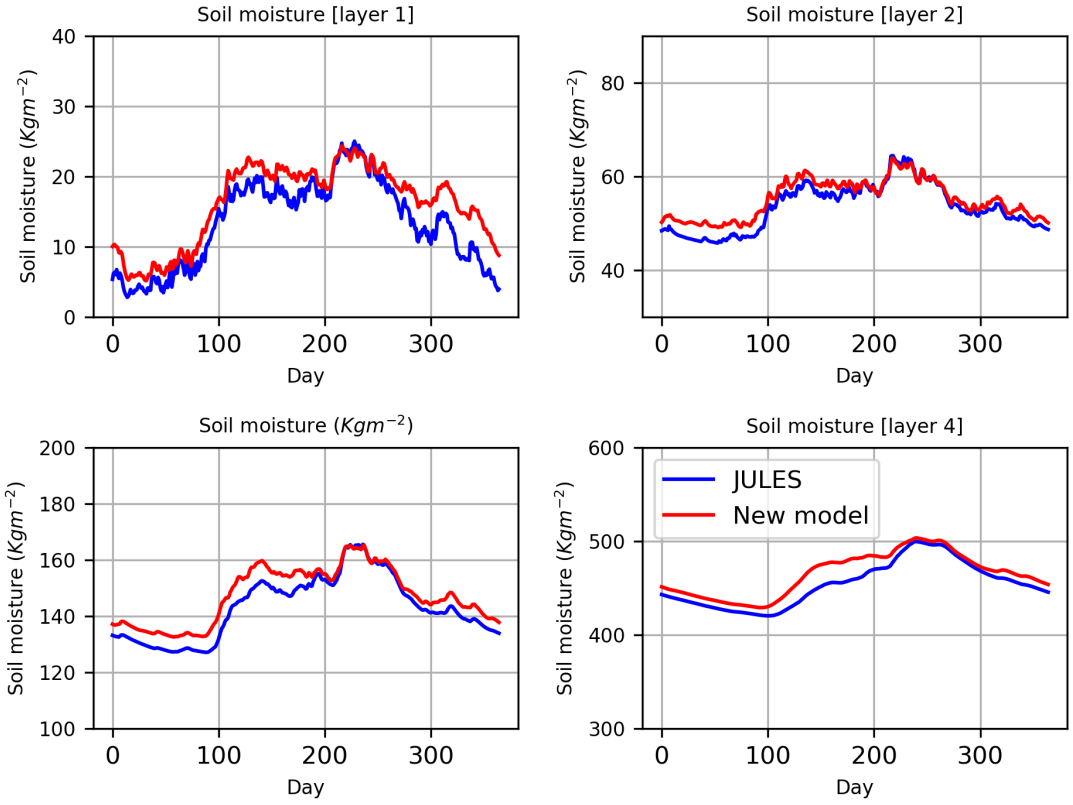

Figure 3.7: Seasonal mean soil moisture from JULES and new model with bare soil (Kitale).

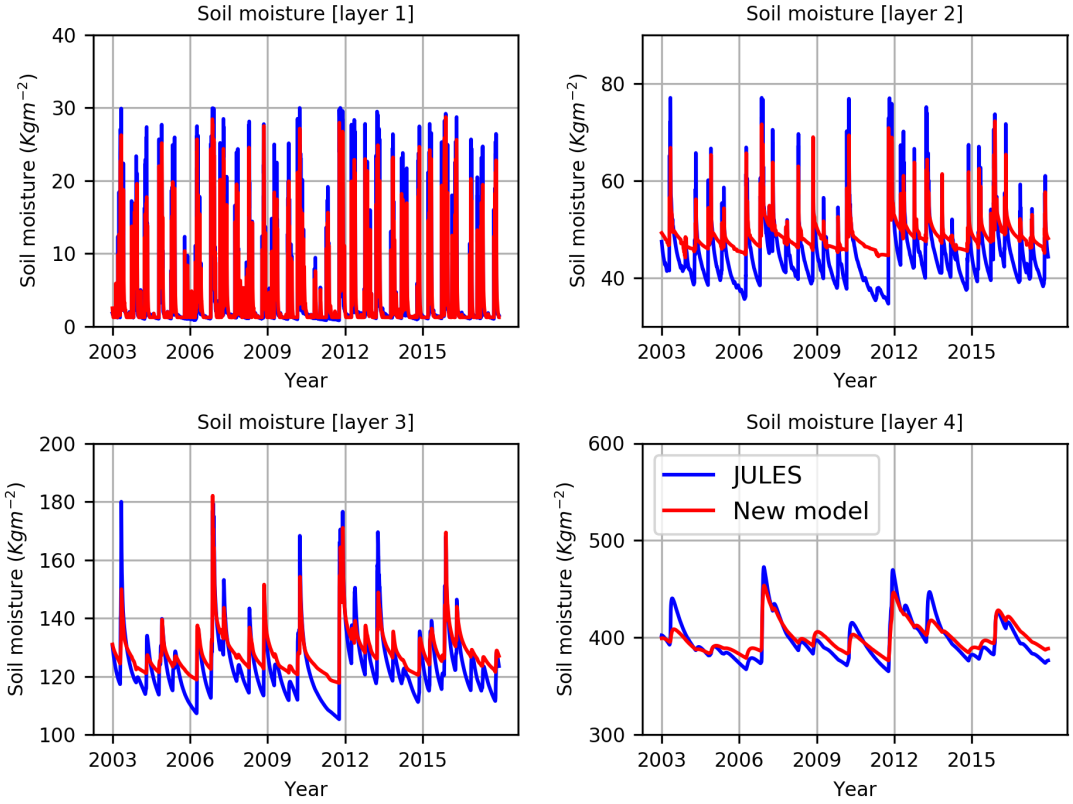

Figure 3.8: Soil moisture output from JULES and new model with bare soil (Wajiri).

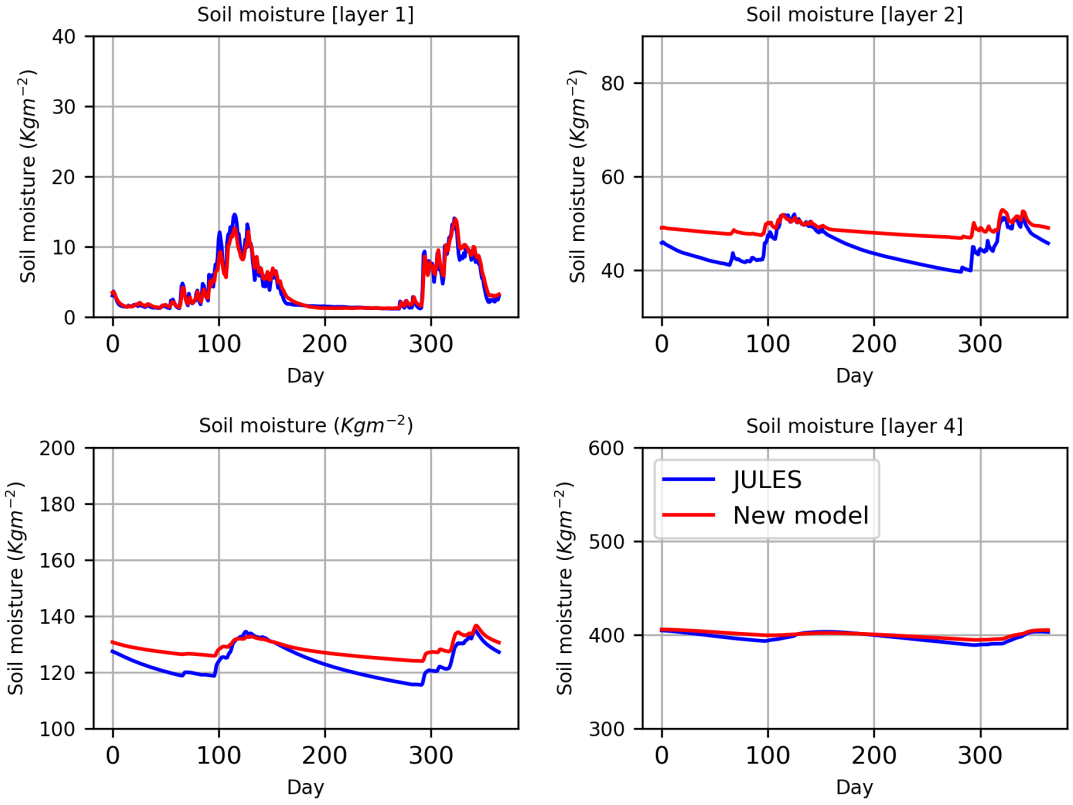

Figure 3.9: Seasonal mean soil moisture from JULES and new model with bare soil (Wajiri).

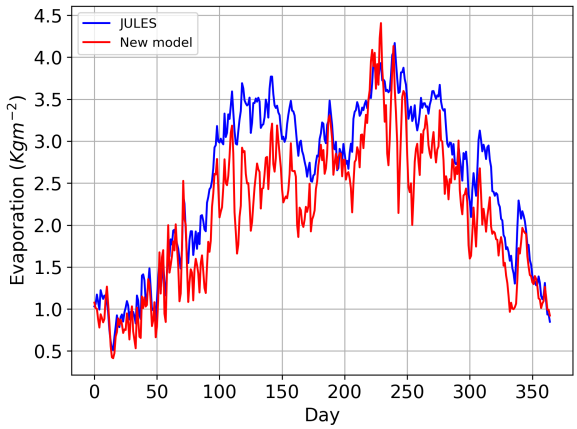

Figure 3.10: Average daily evaporation from JULES and new soil moisture model (Kitale).

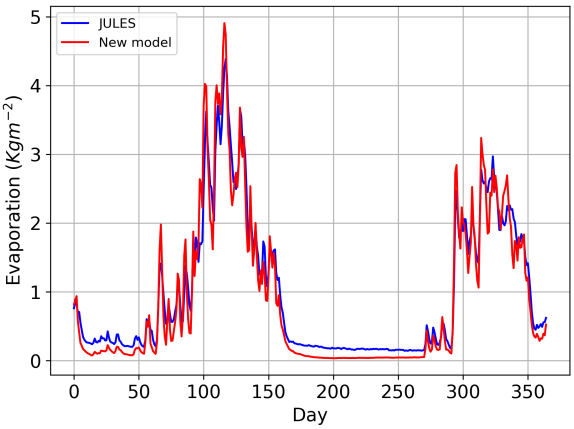

Figure 3.11: Average daily evaporation from JULES and new soil moisture model (Wajiri).

Table 3.3 gives the statistical comparisons between the JULES model and the new soil moisture model outputs. The soil moisture output is strongly correlated in all soil layers with R^2 values above 0.8 except for the second layer in Wajiri, which has an R^2 value of 0.79. The normalised root mean square errors (NRMSE) are also very small, except for the first soil layer, which has a significant error of 0.34 in Kitale and 0.55 in Wajiri. Though there is a difference in the output of the new model and JULES the central reason of comparison is not to perfectly match the soil moisture results instead it is to evaluate the new model is not highly drifted from the results given by a well-tested land surface model like JULES. The differences are expected as the new model parameterisations differ significantly from JULES.

Table 3.3: Statistical comparison between JULES and new model for bare soil moisture

	Layer-1		Layer-2		Layer-3		Layer-4	
	Kitale	Wajiri	Kitale	Wajiri	Kitale	Wajiri	Kitale	Wajiri
ME (kg/m2)	2.77	0.04	1.70	3.95	4.30	4.50	10.67	2.76
MAE (kg/m2)	3.40	1.13	2.55	4.52	5.03	5.69	11.77	7.78
RMSE (kg/m2)	4.53	2.23	3.20	5.24	6.46	6.59	15.83	9.55
NRMSE	0.34	0.55	0.06	0.12	0.05	0.05	0.03	0.02
R	0.92	0.93	0.93	0.89	0.95	0.94	0.94	0.93
R^2	0.85	0.87	0.86	0.79	0.90	0.89	0.88	0.86

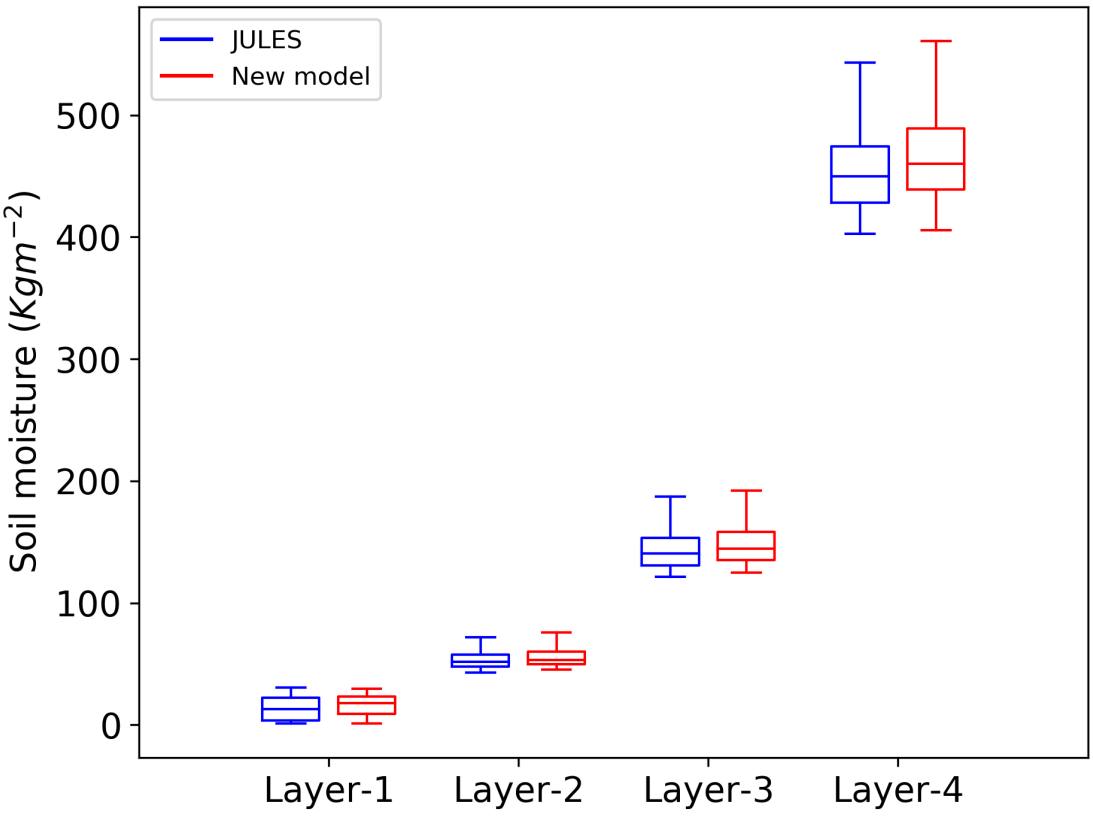

Figure 3.12: Box plot of soil moisture from JULES and new model with bare soil (Kitale).

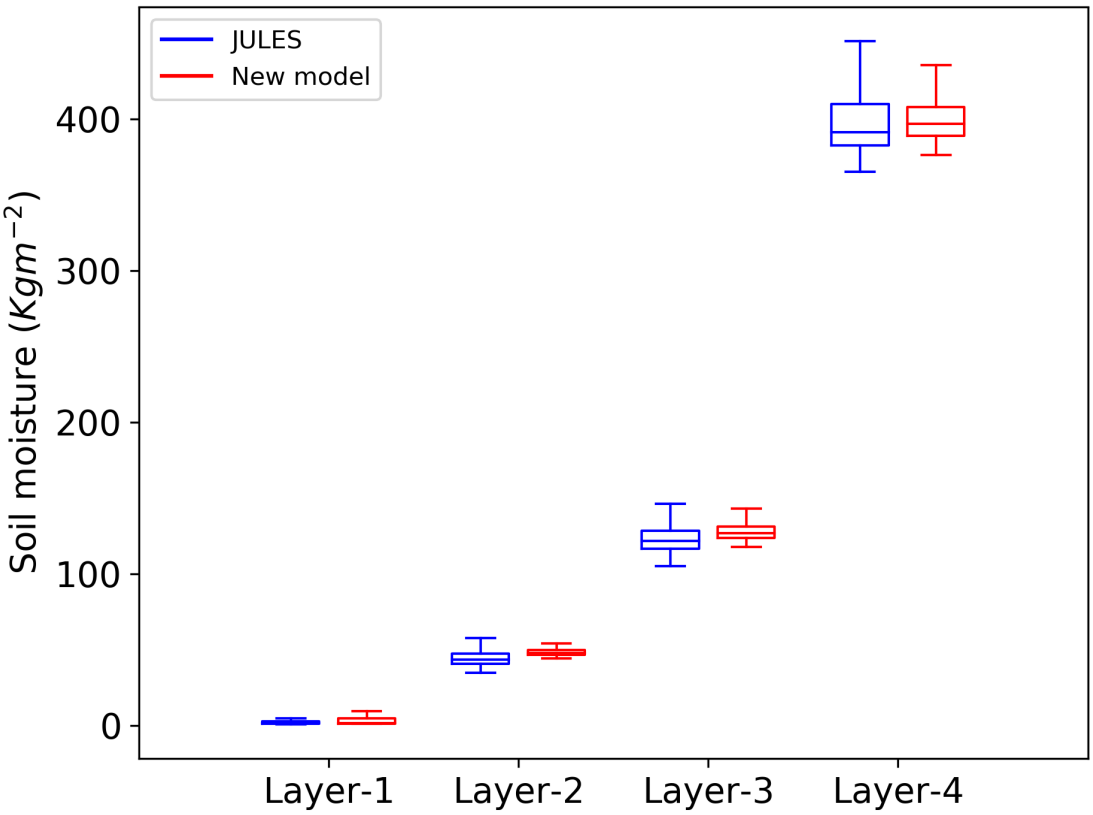

Figure 3.13: Box plot of soil moisture from JULES and new model with bare soil (Wajiri).

Figure 3.12 and Figure 3.13 show the box plots of the soil moisture output from JULES and new model for Kitale and Wajiri. In both locations the new model was able to replicate the mean and variability of soil moisture in all the soil layers as that of JULES. This bare soil moisture model is used to develop planting date decision making tool which is discussed in chapter 5. The main interest is in the top two soil layers where the soil moisture forecasts to be made are compared with climatological values of soil moisture hence the soil moisture anomalies are more important to make agricultural decision. Figure 3.14 and Figure 3.15 show the total soil moisture anomaly for the first two layers of six years (2012-2017). Figure 3.16 and Figure 3.17 show the soil moisture anomaly for the season March-April-May (MAM) from 1988 - 2017. These anomalies are used as decision making criteria and in both locations it indicates that the anomalies from the new model and fully run JULES are more or less the same despite the difference in actual values for many of the years considered. Therefore, the results of the new soil moisture model can be used for monitoring climatic risk on agriculture and developing additional agricultural decision-making tools.

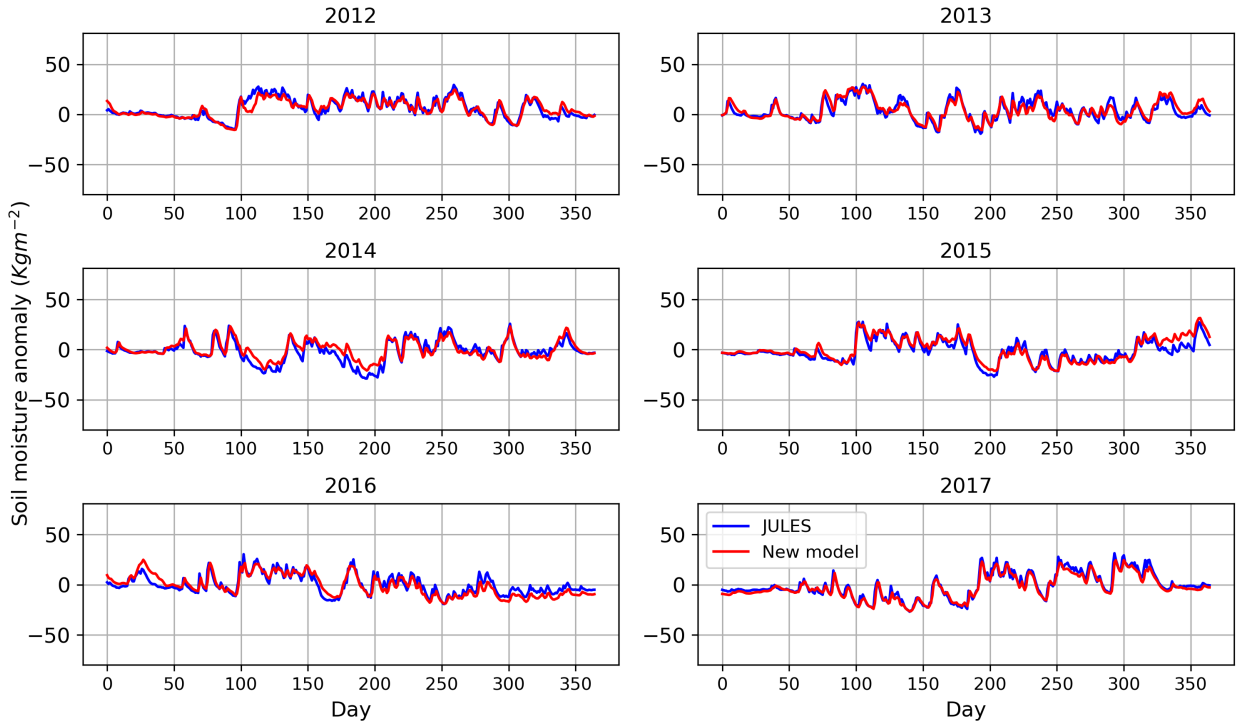

Figure 3.14: Soil moisture anomaly for the sum of top two layers (Kitale).

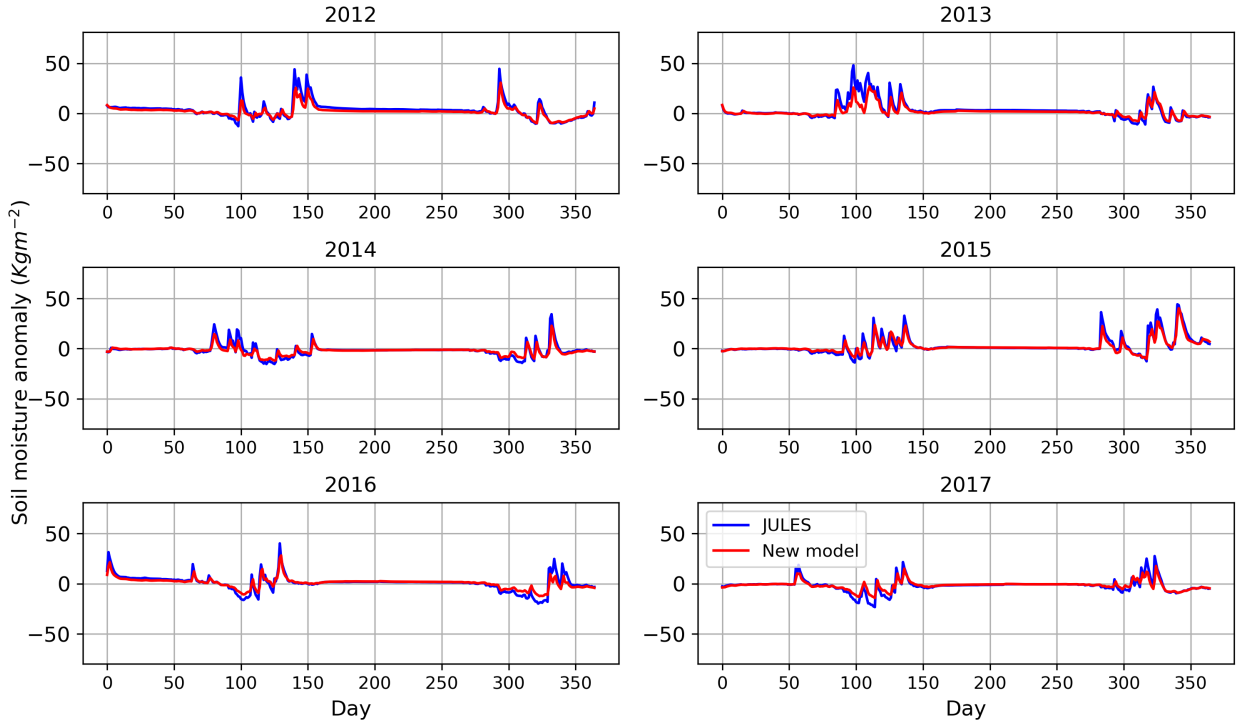

Figure 3.15: Soil moisture anomaly for the sum of top two layers (Wajiri).

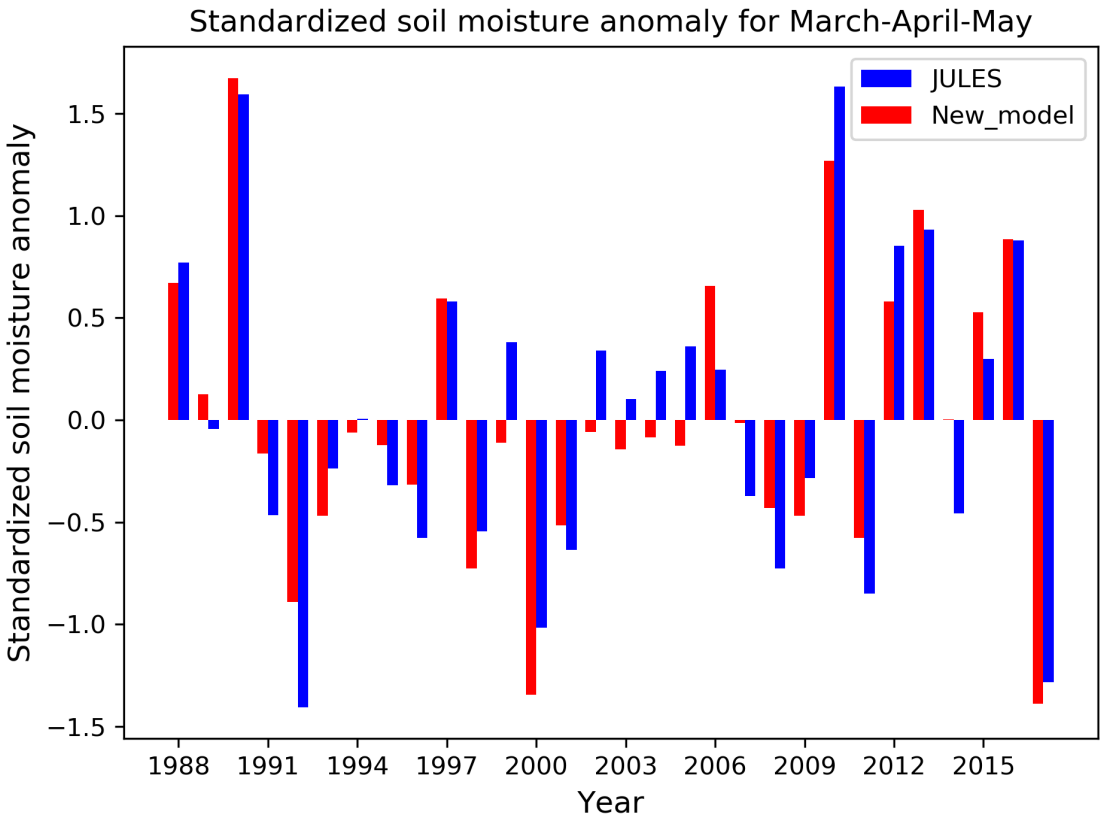

Figure 3.16: Standardized soil moisture anomaly for the top two layers for the season MAM (Kitale).

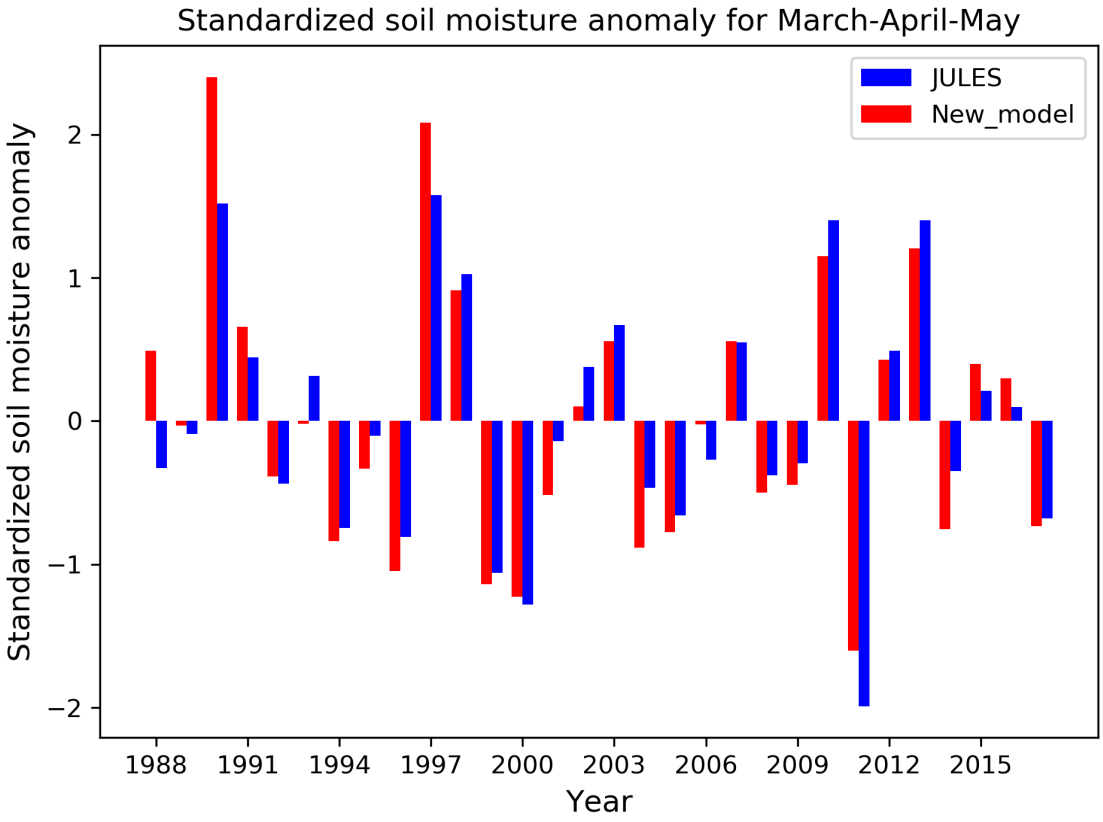

Figure 3.17: Standardized soil moisture anomaly for the top two layers for the season MAM (Wajiri).

3.3.4 Soil moisture modelling with vegetation

Figure 3.18 and Figure 3.19 show the time series and seasonal average soil moisture modelled with a 100% cover of vegetation by a C_4 grass for Kitale from JULES and new soil moisture model. Similarly, Figure 3.20 and Figure 3.21 show the results for Wajiri. The two locations have different soil moisture levels where Kitale indicates higher moisture and Wajiri has lower soil moisture; this is due to the environment difference between the locations. Especially in the third and fourth layer, there is minimal variability in soil moisture level in Wajiri compare to Kitale. Wajiri being in the dry region of eastern Kenya with lower rainfall amount the rainfall is not reaching the lower layers resulting in a more constant soil moisture level. The figures indicate that the soil moisture with a full cover of a C_4 vegetation is well represented except in the fourth layer where the new model underestimate the moisture.

Figure 3.22 and Figure 3.23 show the box plots of the new model and JULES soil moisture outputs for Kitale and Wajiri, respectively. The figures indicate that the new soil moisture model well represents the variability in soil moisture in a similar way like JULES. However, the new soil moisture model tends to underestimate the amount in the fourth layer at Kitale and third soil layer at Wajiri. The underestimation could be a result of the modified initial stomatal conductance level ($g_{initial}$) as discussed in section 3.2.2. Since there is no representation of a full photosynthesis process the $g_{initial}$ used in the new soil moisture model was tuned based on the moisture from the JULES model for a C_4 grass and was found to be 0.025. However, in JULES, this initial stomatal conductance is calculated at each time step depending on the amount of photosynthesis. The use of a single constant initial stomatal conductance level ($g_{initial}$) value could be one reason for the underestimation of soil moisture in the lower layers as JULES internally calculate this value and progressively increase it depending on the vegetation growth. Table 3.4 shows the statistical comparisons between the JULES model and the new soil moisture model with full coverage of C_4 vegetation. The values indicate that there is a strong correlation ($R^2 > 0.8$ for all soil layers except layer 3 in Wajiri) between the results from JULES and the new model.

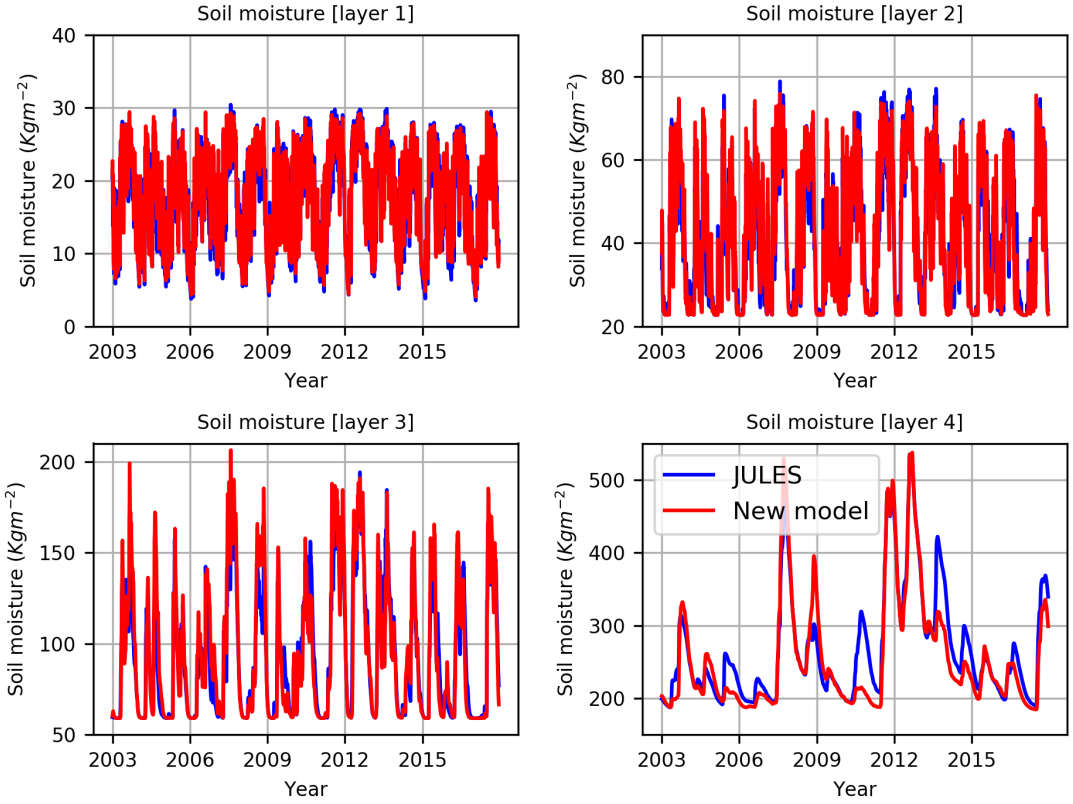

Figure 3.18: Soil moisture output from JULES and new model with full cover of C_4 vegetation (Kitale)

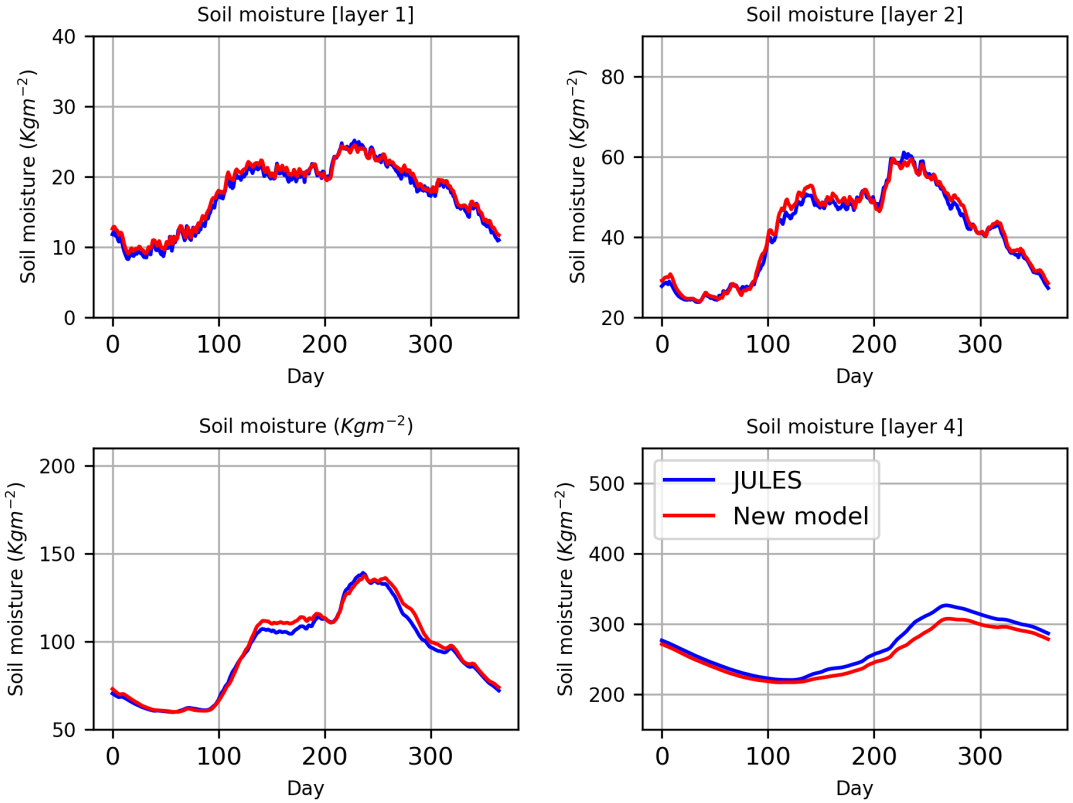

Figure 3.19: Seasonal mean soil moisture from JULES and new model with full cover of C_4 vegetation (Kitale)

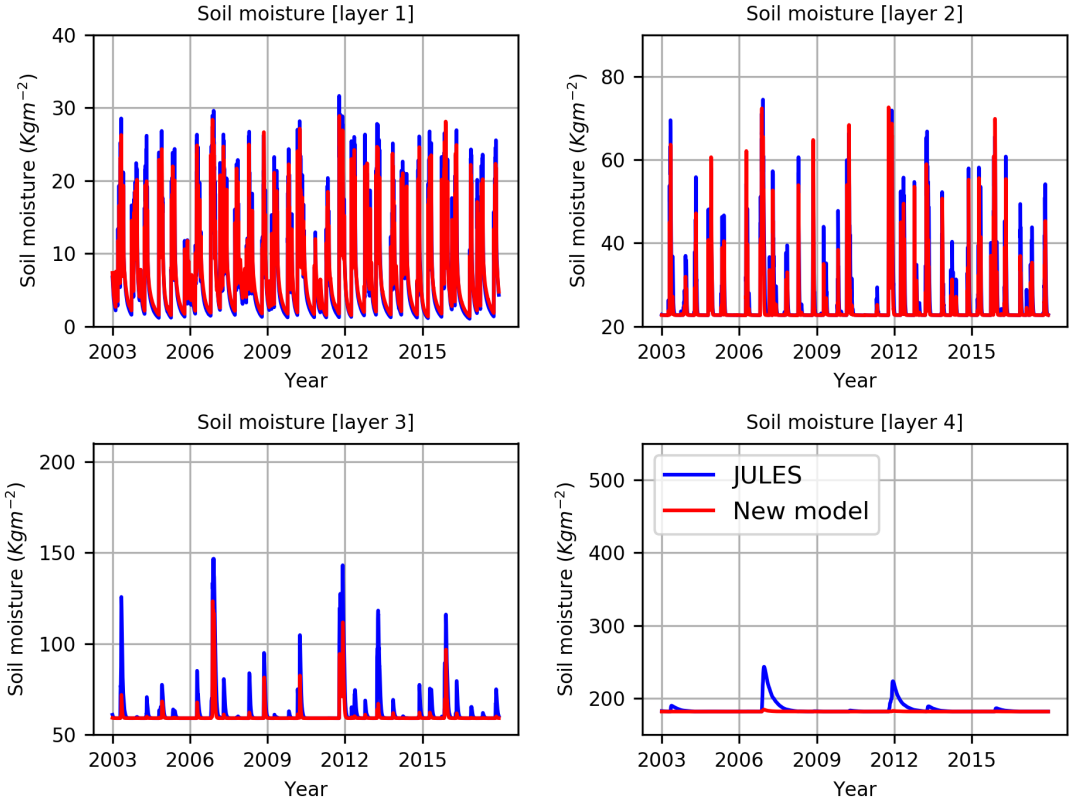

Figure 3.20: Soil moisture output from JULES and new soil moisture model with a fully covered C_4 plant (Wajiri).

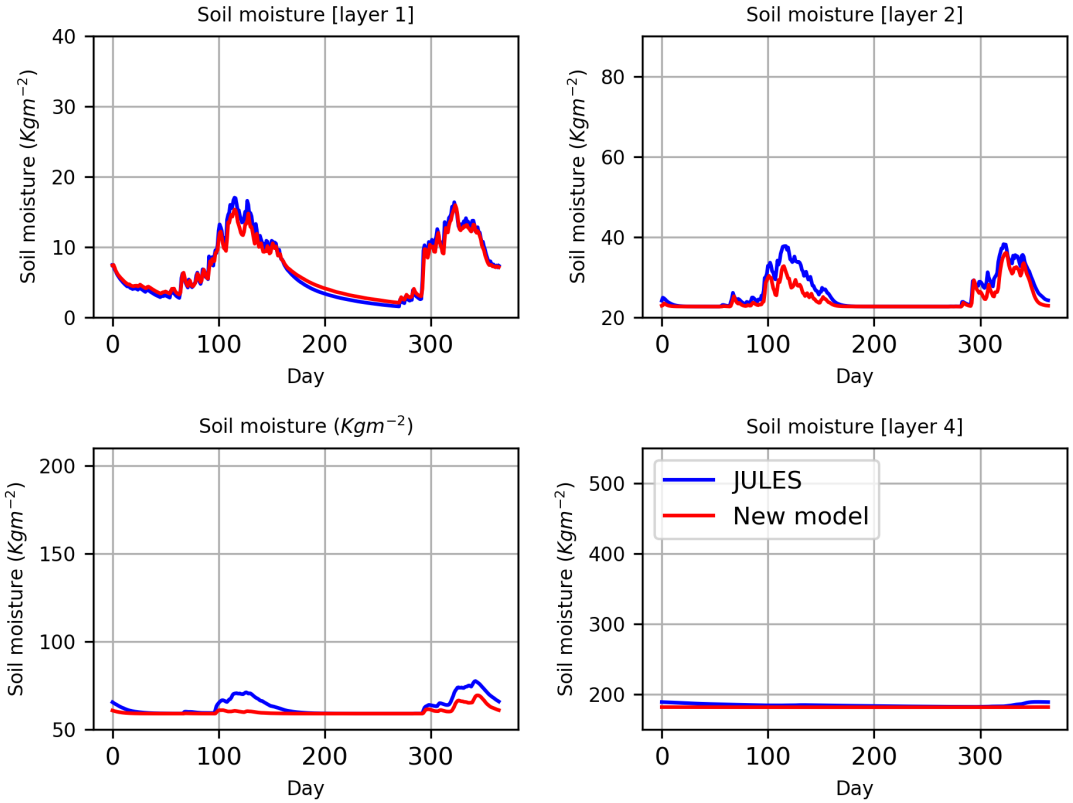

Figure 3.21: Seasonal mean soil moisture from JULES and new soil moisture model with a fully covered C_4 plant (Wajiri).

Table 3.4: Statistical comparison between JULES and new model soil moisture with full cover of C_4 vegetation

	Layer-1		Layer-2		Layer-3		Layer-4	
	Kitale	Wajiri	Kitale	Wajiri	Kitale	Wajiri	Kitale	Wajiri
ME (kg/m2)	0.41	-0.01	0.64	-1.37	1.67	-2.65	-10.18	-2.84
MAE (kg/m2)	1.33	0.94	3.29	1.50	8.05	2.65	20.45	2.85
RMSE (kg/m2)	1.77	1.63	4.54	3.57	12.02	7.47	30.48	8.45
NRMSE	0.10	0.24	0.11	0.14	0.13	0.12	0.11	0.05
R	0.96	0.97	0.96	0.91	0.95	0.87	0.93	0.94
R^2	0.93	0.94	0.92	0.83	0.90	0.75	0.87	0.89

3.3.5 Evaluation of drought metrics

The soil moisture model with the C_4 vegetation is used as a part for the development of agricultural drought monitoring, which could be used by African meteorological service providers. The monitoring of agricultural drought (chapter 4) is based on the soil moisture availability (β) hence the slight difference in soil moisture amount between the JULES model and the new soil moisture model is less pronounced in the decision to be made regarding the drought. For example Figure 3.24 and Figure 3.25 show the average soil moisture availability (β) values in Kitale and Wajiri. The figures show that the new model underestimates β values especially during the wet period within the season, but the difference in the absolute amount does not matter in decision-making about drought rather the standardised values compare to the climatology is more important. Looking Figure 3.26 and Figure 3.27 for the season March-April-May (MAM) the standardised anomalies of β values from the new model are close to values from JULES though there is a year to year variability. However, the new model well represents the dry and wet years; hence, the decision that would have been made based on these anomalies will not be different whether we use the new soil moisture model or the JULES model. In general, the criteria to be used in drought monitoring which is the standardised anomalies of soil moisture availability (β) coming out of both the new model and JULES are similar making no difference in the final decision that could be made. The new model uses less number of input data, it runs much faster, requires less computational power, it can be easily adapted to integrate additional outputs, requires no license and can use freely available driving data. Hence, with all these extra benefits using the new soil moisture model is preferred for use in SSA context where National Meteorological Service Centres move into impact-based forecasting.

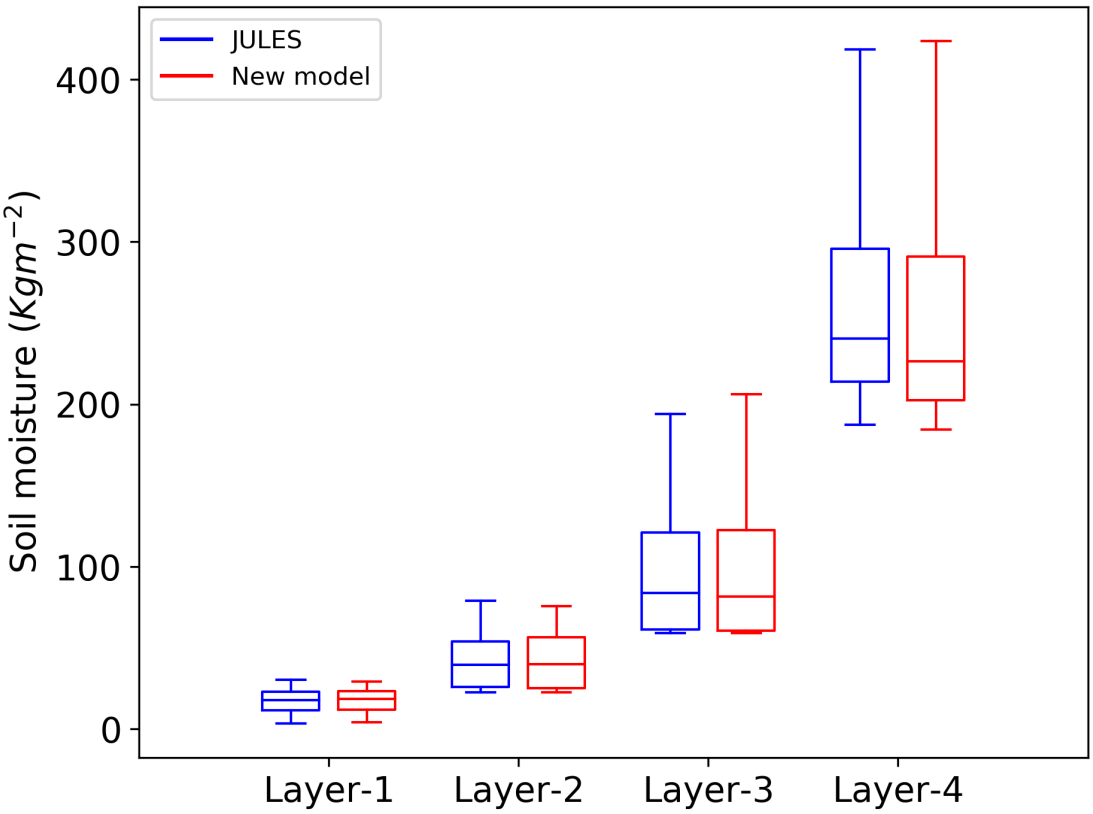

Figure 3.22: Box plot of soil moisture from JULES and new soil moisture model with full cover of C_4 vegetation (Kitale).

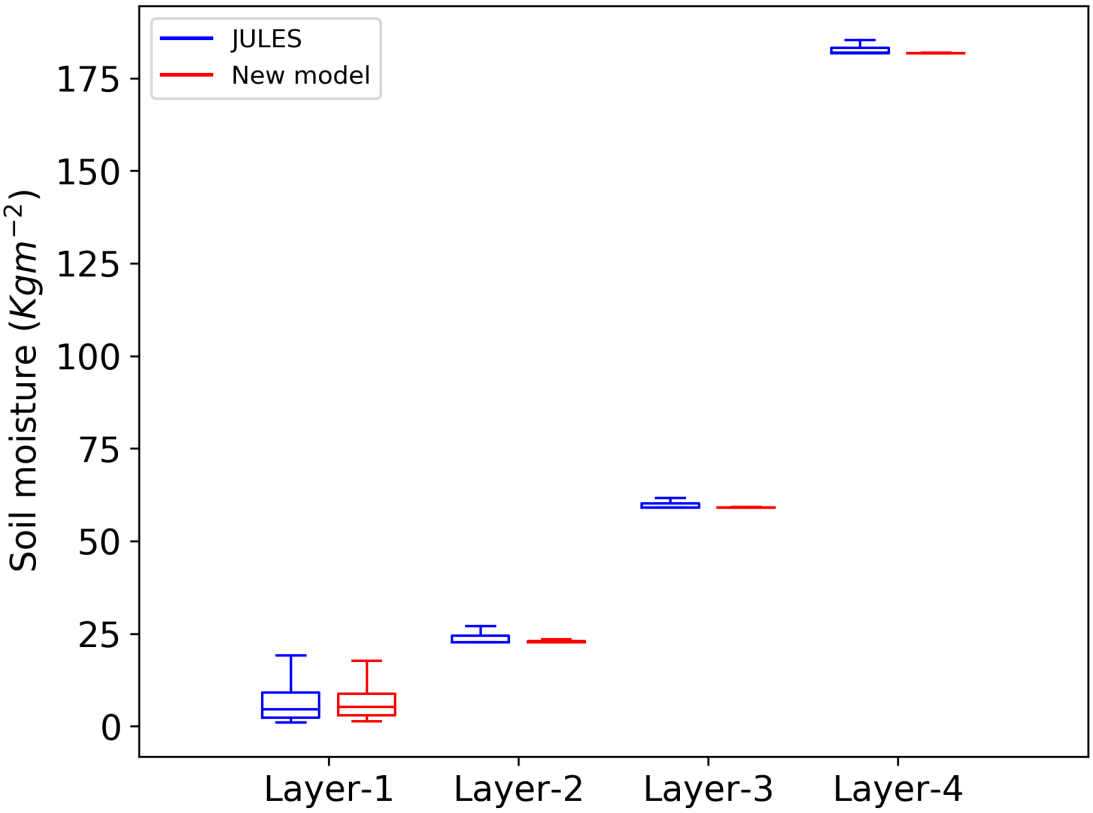

Figure 3.23: Box plot of soil moisture from JULES and new soil moisture model with full cover of C_4 vegetation (Wajiri).

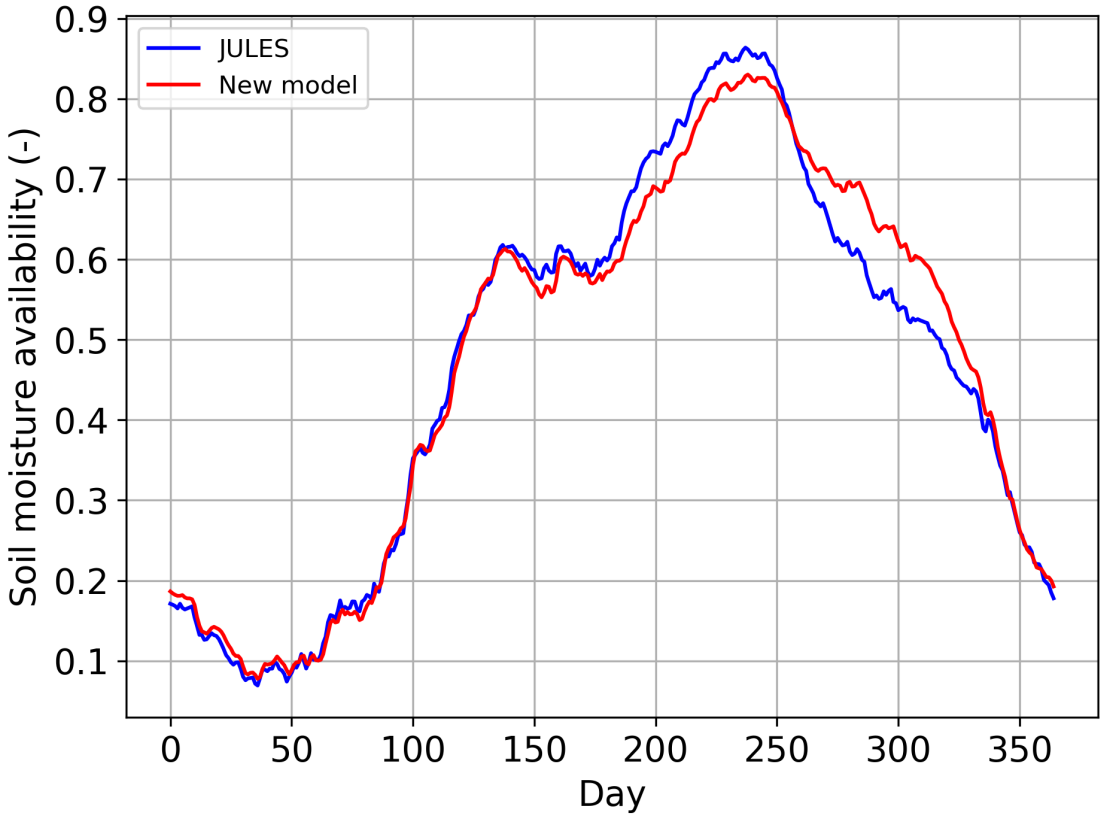

Figure 3.24: Seasonal mean soil moisture availability factor (β) (Kitale).

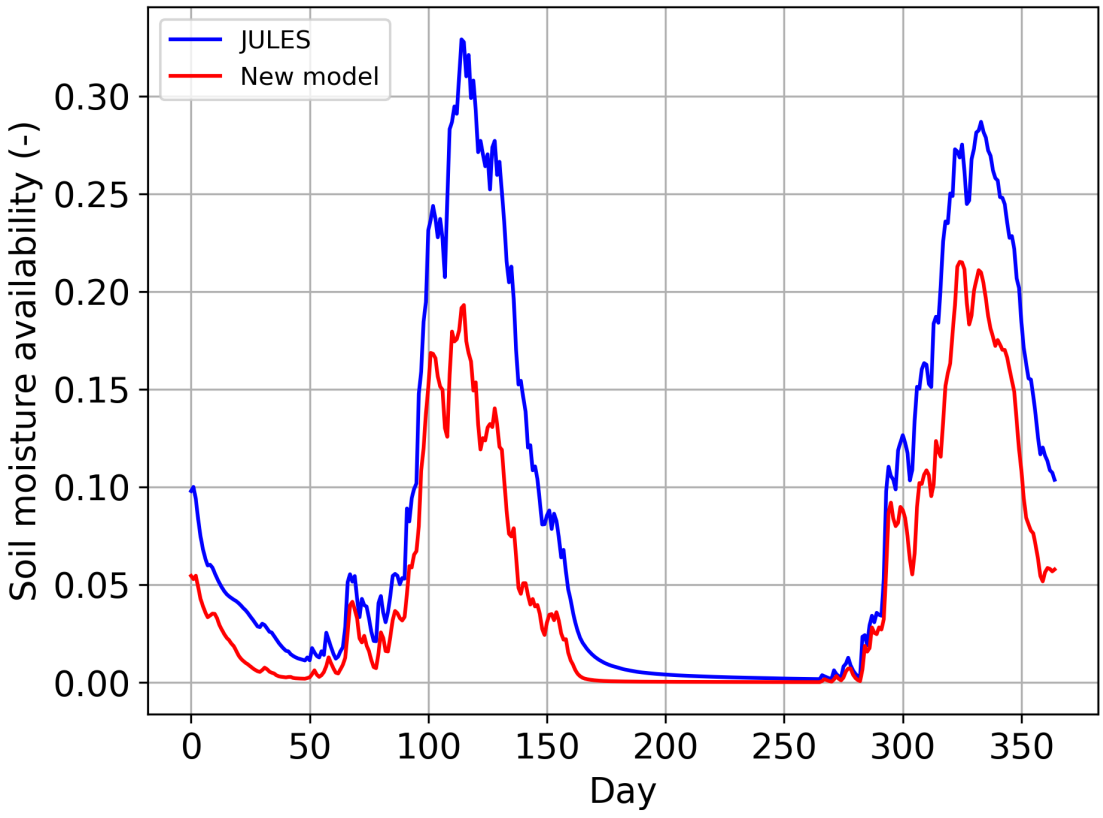

Figure 3.25: Seasonal mean soil moisture availability factor (β) (Wajiri).

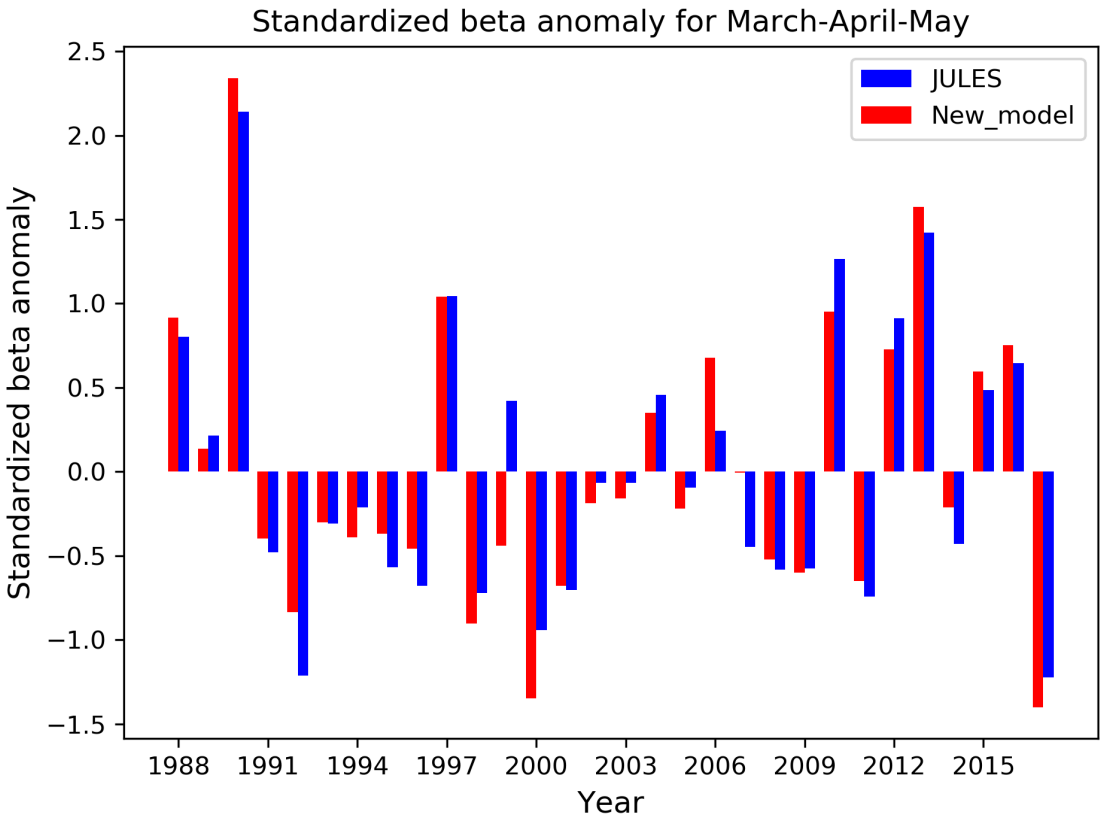

Figure 3.26: Standardized soil moisture availability factor (β) anomaly for the period MAM (Kitale).

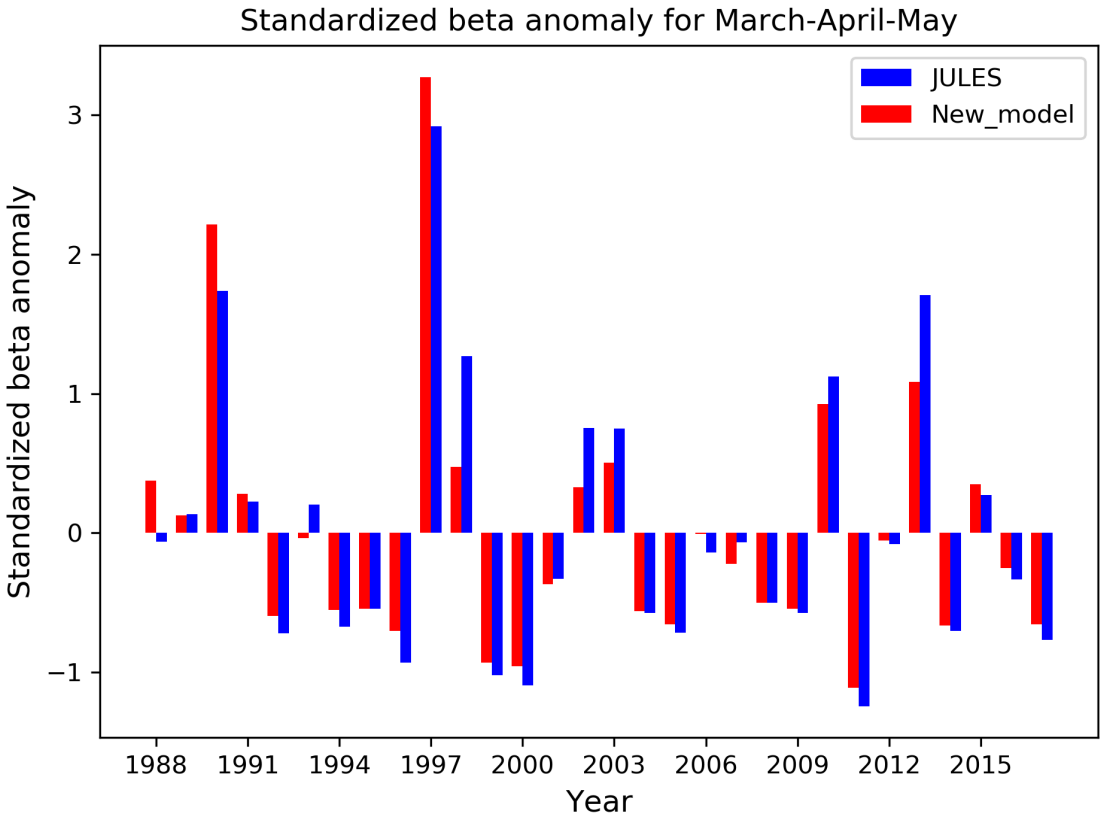

Figure 3.27: Standardized soil moisture availability factor (β) anomaly for the period MAM (Wajiri).

3.4 Summary

Land surface models (LSMs) have helped to represent many of the land surface processes and generate several important outputs which can be used to study climate and the impact of climate on sectors such as agriculture and water resources. However, the complexity of LSMs presents a challenge to be used in many African countries where the meteorological service providers have little capacity and engaged only in providing basic climate information. This challenge of providing relevant climate information that fits the needs of the end user in African countries could be done by producing easy to use decision-making tools which can be shared and used by the meteorological service providers. This chapter explains a new soil moisture model developed based on the concepts described in the JULES model soil hydraulics. The need for the modification of the soil moisture model arises from the fact that this research was conducted to share the methods with end users in Africa. Therefore, it was essential to avoid the use of a very complex model such as JULES in the decision-making tools developed (chapter 4 and chapter 5), also requires easy manipulation of the soil moisture model to adapt to the framework designed (chapter 2) as well as provide relevant metrics to end users.

The new soil moisture model is written in Python and can run fast on a standard computer with spatial resolutions comparable to the driving data sets provided. The code is also freely available, unlike GLAM and JULES which are under license making to use these models operationally difficult. The simplicity of the new model will allow meteorological services and agricultural advisory providers to produce user-relevant metrics based on their requirement using freely available driving data(e.g NCEP and TAMSAT). The results of soil moisture between JULES and the new soil moisture model was also found to be equal as the new model represents the amount and variability of the soil moisture. The new soil moisture model is not a replication of JULES instead the comparisons were made to evaluate that the new soil moisture model is not producing unrealistic soil moisture values which might distort decisions to be made related to agricultural activities (such as planting date and drought occurrence). The results of the new model indicated that the new soil moisture model outputs are within a similar value range of the well-established land surface model JULES, hence the new soil moisture model is suitable for the development of agricultural decision-making tools for drought monitoring and planting date.

Chapter 4

TAMSAT-ALERT for seasonal applications: Agricultural drought monitoring and seasonal prediction

This chapter discusses the use of TAMSAT-ALERT framework (chapter 2) for seasonal applications in predicting and monitoring agricultural drought within a crop growing season in sub-Saharan Africa. Drought is a significant risk that farmers face in a growing season and predicting and monitoring the likelihood of this risk as early as possible is crucial for preparing in advance for interventions and provide the necessary support to the vulnerable communities. This chapter addresses the use of model output soil moisture and WRSI to represent agricultural drought and compare it with SPI. The objectives include evaluating the relationship of meteorological drought index SPI and maize yield, demonstrating the WRSI metric as an early drought warning system and evaluate the predictive potential of WRSI due to the incorporation of historical soil moisture in the drought prediction rather than using seasonal weather forecasts only (section 4.1.2). The study area is Kenya where there have been many drought occurrences in the past and required data are available for the study. The agricultural drought prediction and monitoring method used in this chapter is TAMSAT-ALERT drought prediction method (section 4.2.4) where the approach involves using WRSI forecasts within a crop growing season. The results indicate that comparing SPI with soil moisture only the 3-month and 6-month aggregated SPI values have better correlation with soil moisture rather than the 1-month or 12-month aggregated SPI values. The better correlation of the 3-month and 6-month SPI values with soil moisture is because the soil moisture

responds to the rainfall condition at these time scales. However, SPI is rainfall based metrics and can not be a direct indicator of agricultural drought. Comparing end of season WRSI values with SPI showed the 6-month aggregated SPI is better correlated with WRSI values than the 3-month aggregated SPI indicating the latter is not an efficient way to be used as a proxy for agricultural drought (section 4.3.1). Similar results were also found comparing county-wide maize yield with 3-month and 6-month aggregated SPI values, however, the WRSI value of a growing season is much better correlated with country-wide maize yield indicating the potential to be used as a proxy for predicting agricultural drought within a growing season (section 4.3.2). The demonstration of drought prediction within the growing season using TAMSAT-ALERT showed that anticipating drought condition 2-3 months earlier than the harvest of crops is possible and comparison of this result with Famine Early Warning Systems Network (FEWSNET) showed the method used in this chapter could provide an early outlook of the season (section 4.3.3). In general, the results of this study showed that using TAMSAT-ALERT methods added relevant information on top of the routinely issued seasonal weather forecasts for decision-makers and farmers to be used as a proxy of seasonal progress and impact on crop yield. The findings of this chapter offer the potential of a new actionable drought outlook product to be added to already existing climate service products and help in the mitigation of drought impact on vulnerable communities.

4.1 Introduction

4.1.1 Background

Extreme and widespread droughts are expected to increase in the African continent with more devastating effects due to increased population and land and environmental degradation and this calls for a new approach on drought monitoring forcing to move from crisis management to risk management (Masih et al., 2014). This shift in paradigm can be accomplished through the development of early warning systems that are easy to be used by climate service providers over Africa. A recent study on climate services to support African farmers suggest that presenting climatic information in comparison to the historical conditions will help to connect routinely issued climate forecasts with historical climate variability (Hansen et al., 2019). In drought monitoring and prediction the choice of drought indices depend on the availability of data, the consistency of the indices for the specified region, the suitability of the indices for the specified purpose, clarity,

cost, and the existence of well defined threshold for the indices (Zargar et al., 2011). Drought indices developed based on a single or multivariate variables are used only to specific purposes and do have their own drawbacks. To increase the effectiveness of drought indices the idea of combining different indices together is becoming prominent allowing the positive sides of each indices to be combined and comprehensively explain the drought condition in an area (Zargar et al., 2011).

Considering its simplicity and requirement of a single parameter, (precipitation) SPI is a commonly used drought metric in Africa. However, SPI is a meteorological drought measure indicating precipitation deficit at different timescale aggregate (Mckee et al., 1993) and translating the concept of a meteorological drought to an agricultural drought remains problematic (Black et al., 2016b). In addition, it only provides a single snapshot of the season outlook on a monthly timescale rather than assessing the consequences of the associated risks. Drought monitoring products need to have the ability to predict agricultural drought as early as possible, utilize already existing operational satellite data and should be easy to implement in addition to being crop specific (Niemeyer, 2008). In Sub-Saharan Africa, National Climate Service Centers provide some information on drought situation in the country or region , but products are least developed, operational and utilized at the optimum level (AMCOMET, 2013). Efforts like ENACTS (Enhancing National Climate Services) demonstrate innovations to improve climate service provision by African National Climate Centers through developing derived climate information products and disseminate through online "Maprooms" (Dinku et al., 2014). The new TAMSAT-ALERT framework for agricultural decision support is one way to enhance early warning systems through utilization of historical satellite data in combination with numerical models for evaluating climatic risk associated on crops throughout the growing season. Results over Ghana showed ability to estimate climatic risk on maize yield 6–8 weeks ahead of harvest and evaluate impact of regularly issued seasonal forecast of rainfall and temperature on maize yield estimation (Asfaw et al., 2018). Chapter 2 moreover, showed that most predictive skill emanates from evaluation of the season progress, rather than the seasonal forecasts. This chapter therefore focuses on, the application of the TAMSAT-ALERT system for monitoring agricultural drought throughout the growing season using Water Requirement Satisfaction Index (WRSI) estimated from soil moisture model (chapter 3) and tries to associate agricultural drought risk in comparison to historical conditions.

4.1.2 Study objectives

This chapter aims to produce a comparison between meteorological and agricultural drought measures with validation against observed maize yield. It demonstrates the use of the TAMSAT-ALERT framework (chapter 2) as a prediction tool for agricultural drought within the growing season. Therefore, the chapter focuses on the following research question:

How robustly do model outputs such as soil moisture and Water Requirement Satisfaction Index (WRSI) represent agricultural drought compared to meteorological based metrics such as Standardized Precipitation Index (SPI)?

To address the research question the following objectives are set:

- To evaluate how meteorological drought index SPI relates to maize yield over Kenya.
- To demonstrate the WRSI metric as early drought warning system by comparing it with country wide average yield for maize and evaluate the improvements from using SPI as a measure of agricultural drought.
- To evaluate the predictive potential of WRSI due to the incorporation of the historical soil moisture in drought prediction rather than only using seasonal forecast of weather as a means of indicating the season outlook.

4.2 Data and methods

4.2.1 Study area

The study was conducted in Kenya located between -4.87° N and 5.87° N latitudes and 33.12° E and 41.87° E longitudes (Figure 4.1).The choice of the location was due to availability of data and the region is being affected by continuous drought. The country's climatic zones also consist the western part which is more humid and wet whereas the north and eastern part is semi-arid and dry allowing to see the performance of the TAMSAT-ALERT system in predicting and monitoring drought within a crop growing season. Additionally, the study use maize and this crop is a staple in Kenya. The topography of the country signifies low lands (<1200 masl) in the northern and eastern part of the country while high lands and mountains dominate (>1800 masl) in the central

and western part of the country. The country has a diverse climate where the western part is dominated by humid to sub-humid climate with average annual rainfall of about 1000 to 2000 mm with a bi-modal seasonal cycle with no distinct dry period between the seasons (see Figure 4.3(a) and Figure 4.3(c)), the average temperature is 15°C–18°C and a growing period of 180–270 days for sub-humid and above 270 days for humid regions (Kamoni et al., 2007; Kinyanjui et al., 2014). The climate of the eastern part is predominantly semi-arid with characteristically erratic and unreliable rainfall. Mean total annual rainfall ranges from as low as 300 mm to 1000 mm. The rainfall in the eastern part of the country follows a distinctly bi-modal with the main rainy season being March to May and second season October to November (see Figure 4.3(b) and Figure 4.3(d)). The average annual temperature is also higher than the western part of the country ranging between 24°C–30°C. Figure 4.2 shows the annual mean precipitation and temperature for the period 1983–2018.

East Africa rainfall is generally extremely heterogeneous due to topography, presence of Lakes, the maritime influence and seasonal tropical circulation (Nicholson, 2017). The typical explanation of the seasonal cycle of precipitation in the eastern Africa region is due to the seasonal migration of the Intertropical Convergence Zone (ITCZ) where the long rains occur as the ITCZ migrates northward and the short rains occur as it travels southward (Hession and Moore, 2011). But this is not the only explanation for the rainfall variability in the region rather, investigation of the wind regime in the region suggests differences in the seasonal cycle, large-scale teleconnections, and spatial patterns of variability play greater role too (Nicholson, 2017). Features like Lake Victoria for instance plays a greater role in creating mesoscale circulation system triggering strong night-time rainfall in the western side and afternoon rainfall eastern side (Nicholson, 2017) which is one reason western Kenya has a higher rainfall. The El-Nino Southern Oscillation (ENSO) also influences east African rainfall and it is associated with prevalent positive rainfall anomaly conditions over the eastern Africa region (Schreck III and Semazzi, 2004).

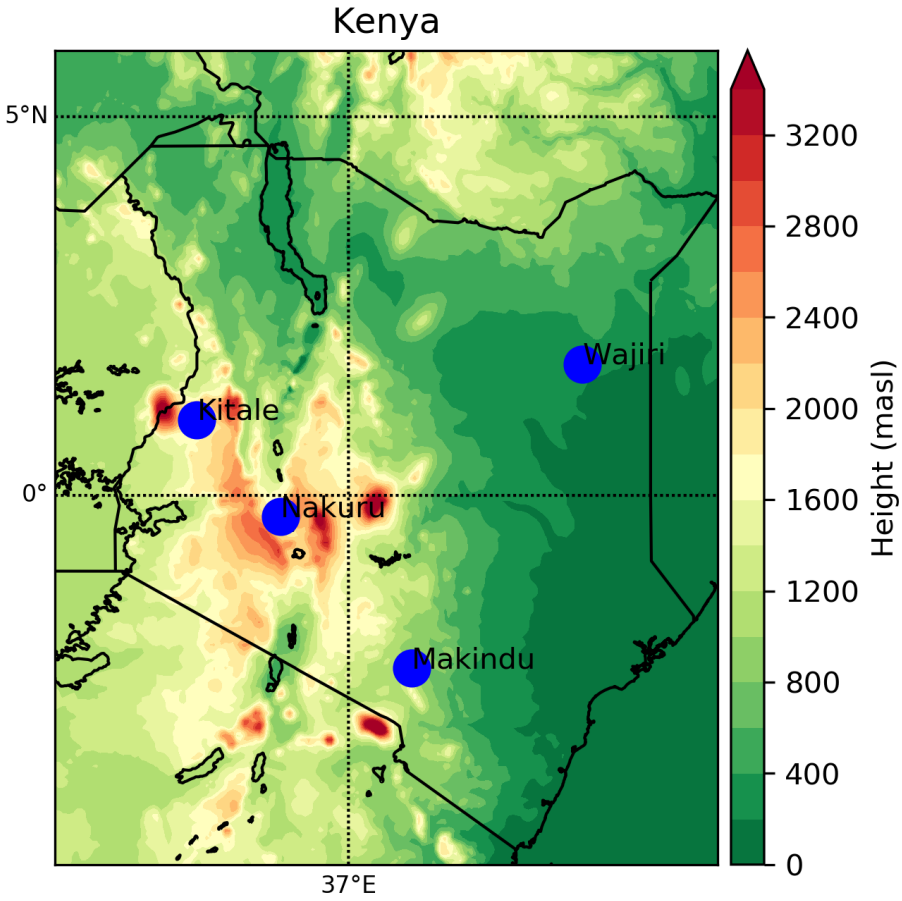

Figure 4.1: Study area with the topography of the region (color representing height above sea level in meters). The blue dots represent four locations in different part of the country where further analysis is done.

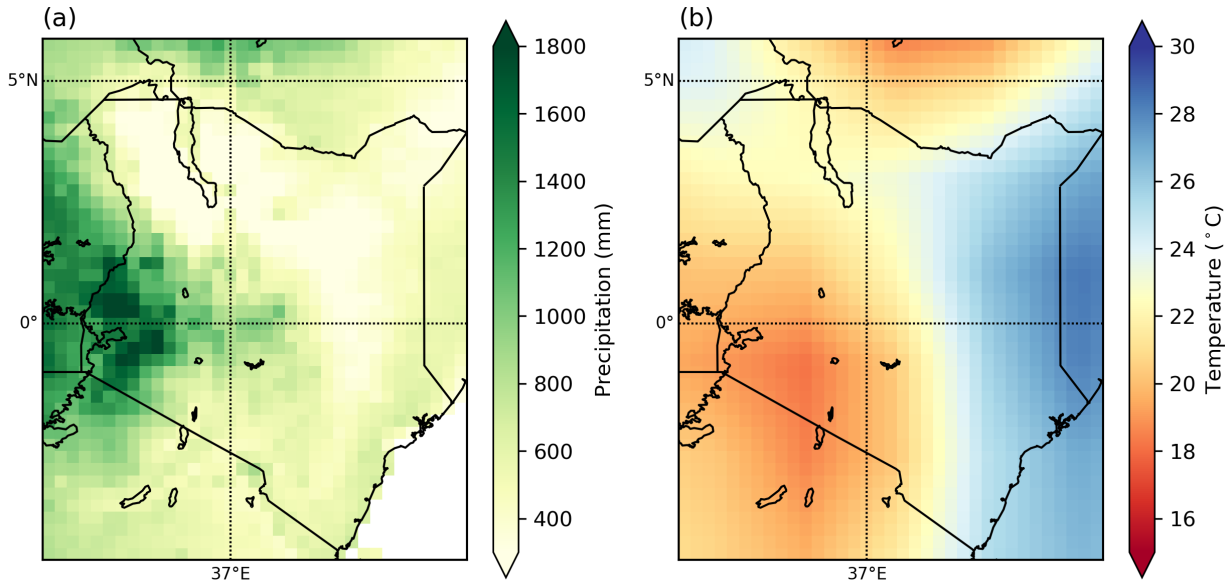

Figure 4.2: (a) Mean annual precipitation and (b) mean annual temperature in the study area.

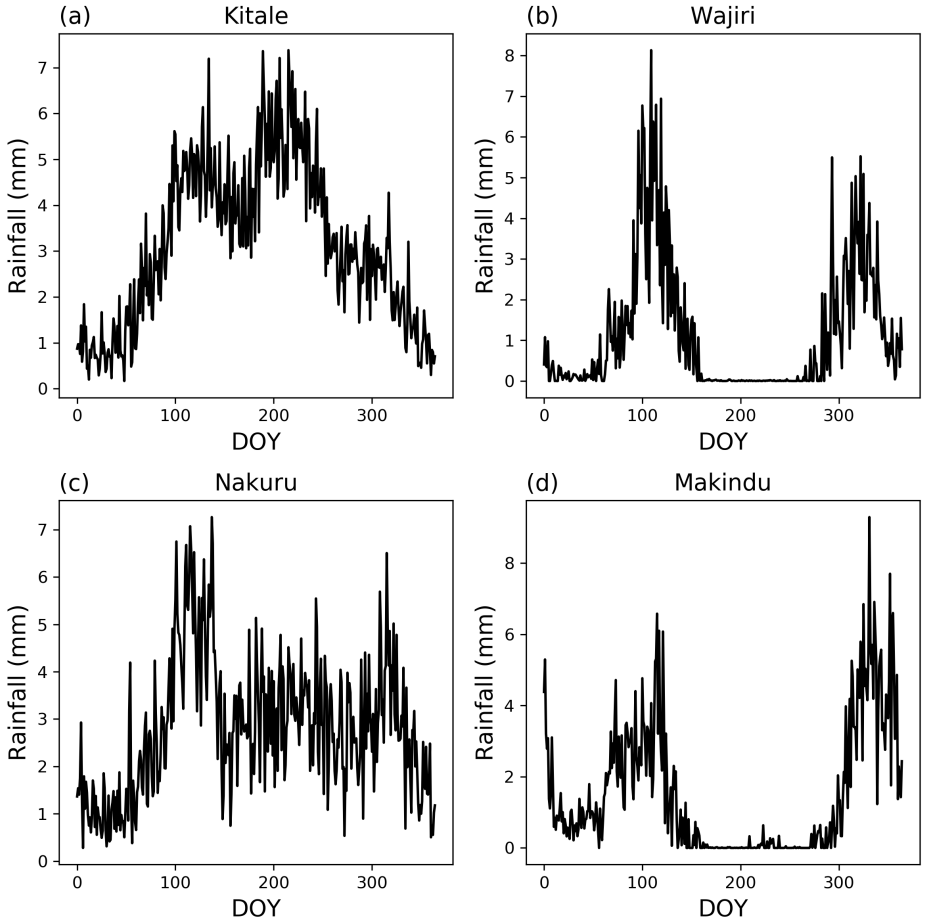

Figure 4.3: Daily rainfall average (1983–2018) for four locations specified in Figure 4.1. Rainfall has two seasons but in the western part there is no distinct dry period between the long rains and short rains.

4.2.2 Data used

The data set required to run the TAMSAT-ALERT system for estimating soil moisture is explained in chapter 3. For this study, daily precipitation data from Tropical Applications of Meteorology using SATellite and ground-based observations (TAMSAT-v3) was used by re-scaling the grid size to 0.25° spatial resolution. Other climatic data sets required for TAMSAT-ALERT were taken from NCEP reanalysis data (Kistler et al., 2001) which is provided with a 2.5° spatial resolution at a global scale and re-scaled to a 0.25° spatial resolution and daily temporal scale. In addition, to run the model maize crop which was planted March 1^{st} is used having a maximum rooting depth, plant height and leaf area index of 0.8 m, 0.7 m and 2.0 respectively. Details of the model driving dataset and setup is described in section 3.3.1 and section 3.3.2.

4.2.3 Standardized Precipitation Index (SPI)

SPI is the most widely used drought indices globally. This index utilises a long term monthly precipitation time series to compute SPI values. The method takes the time series of long term precipitation and fits a gamma distribution for the specific location and time step. After determining the cumulative density function (cdf) of the gamma distribution, it converts it into a normalized Z-score value in order to make the values comparable to each other (Mckee et al., 1993). SPI values range between -4 (extreme dry condition) and +4 (extreme wet condition) where, the negative values indicate drought conditions and the positive values indicate wet conditions. These values are arranged in a way to give a descriptive value for the drought and it is considered that the drought is sever if the SPI index falls below -1.5. The calculation of SPI values can be done over a different time scale starting (e.g. 1-, 3-, 6-, 12-, 24-, 48 months) and each time scale can help to determine from short term important indication like soil moisture to a longer term impact on ground water supply (Haied et al., 2017).

SPI values are calculated by fitting a gamma probability density function to a precipitation total of a specific location. The distribution function is given by Equation 4.1.

$$g(x) = \frac{1}{\beta^{\alpha}\Gamma(\alpha)} x^{\alpha-1} e^{-x/\beta} \tag{4.1}$$

where α is shape parameter and β is the scale parameter. Both values α and β are greater than zero. x is the precipitation amount ($x > 0$). The gamma function $\Gamma(\alpha)$ is calculated based on Equation 4.2 where $\Gamma(\alpha)$ represent the gamma function.

$$\Gamma(\alpha) = \int_0^{\infty} y^{\alpha-1} e^{-y} dy \tag{4.2}$$

the shape parameter α and scale parameter β are given by Equation 4.3 and Equation 4.4 respectively.

$$\alpha = \frac{1}{4A}(1 + \sqrt{1 + \frac{4A}{3}}) \tag{4.3}$$

$$\beta = \frac{\bar{x}}{\alpha} \tag{4.4}$$

$$A = \ln(\bar{x}) - \frac{\Sigma \ln(x)}{n} \tag{4.5}$$

The simplicity and robustness of the method makes it more preferable and used widely to describe the drought condition globally. SPI is considered by the World Meteorological Organization (WMO) as the benchmark index for measuring meteorological drought (WMO, 2012) but, since it only base on the precipitation values only it does not take into account climatic condition such as the temperature which also has a large impact on drought conditions of an area.

4.2.4 TAMSAT-ALERT drought prediction method

TAMSAT-ALERT drought prediction works based on the framework described in (Brown et al., 2017; Asfaw et al., 2018). The main concept of using the framework for drought monitoring lies on the use of Water Requirement Satisfaction Index (WRSI) as explained in chapter 3. WRSI is used rather than direct soil moisture estimates as the WRSI value is estimated for the growing season of a crop unlike the soil moisture thus accounting for the variability in crop type while monitoring agricultural drought. In order to use TAMSAT-ALERT for drought prediction over Kenya, the soil moisture model was run using the driving weather data set and four layers of soil with depth 0.1 m, 0.25 m, 0.65 m, and 2 m respectively. Here the *"crop mode"* was activated allowing a variable plant root depth, plant height and leaf area index to be used. Outside the growing season, the model ran a bare soil moisture model with the minimum planting root, plant height and leaf area index of 0.1 m, 0.1 m, and 0.006 respectively. These minimum values were given as the soil is not going to be completely devoid of vegetation and transpiration (chapter 3). After the planting date of the crop, which is set to be March 1^{st}, the model will run according to the variable crop parameters at each four stages of the crop (initial, development, middle and late stages). The end of each stage is determined according to the accumulated growing degree days (GDD) for maize crop estimated from the model.

The soil moisture model output WRSI values calculated within the period of interest which

is the period from planting to harvesting and determined by the cumulative GDD. Initially TAMSAT-ALERT system runs the soil moisture model to obtain historical values and then it runs the soil moisture model again from the specified forecast date till the end of the period of interest (harvesting date) using historical weather data from the climatology. Here the climatology period was set to 1983–2012, hence, the model ran using 30 years of data from the forecast date till the crop harvesting date resulting in 30 ensembles of soil moisture values and soil moisture availability factor (β). The soil moisture availability factor (β) is used to calculate the WRSI value (chapter 3), where WRSI is the average β with in the growing period (the period planting to harvesting) resulting in a single annual quantity unlike that of β which is a daily value. Figure 4.4 shows an example of a total soil moisture prediction for a single location in Kenya (Nakuru). This output is used to determine the soil moisture availability factor and the WRSI values hence can be presented as an example on how the drought prediction method works with in TAMSAT-ALERT system.

The following points explain what is represented in Figure 4.4:

a) The vertical green lines indicates the period of interest. The period of interest is always between the user defined planting date and spatially variable climatological harvesting date of the crop. Here the crop was planted on March 1^{st} 2009 and harvested September 22^{nd} 2009. This period is used to calculate the ensemble mean and standard deviation later.

b) The red vertical line represents the forecast date (April 1^{st} 2009). The forecast date could be any date within the period of interest (between the green lines) and the ensemble forecasts are made from this date to the end of the interest period.

c) The solid black line shows the historical moisture (what already happened in the year).

d) The colored lines between the forecast day and the end of interest period are the percentiles of the ensemble forecasts. The values are from the 10^{th} to 90^{th} percentile. Actually there are 30 ensemble values resulting from the 30 years of climatology driving data used.

e) The dark gray shade represent the climatology range with in unit standard deviation and the light gray shade shows the climatological maximum and minimum.

Based on the historical WRSI values, the system generates a distribution using climatological mean and standard deviation. Then a second probability distribution is created using the mean of the and standard deviation calculated from the WRSI values within the period of interest. Here it should be noted that the mean and standard deviation are based on both the historical values within the period of interest and the ensemble forecasts within the period of interest. This helps to account for the antecedent moisture and the impact it has on the overall outcome of the whole season.

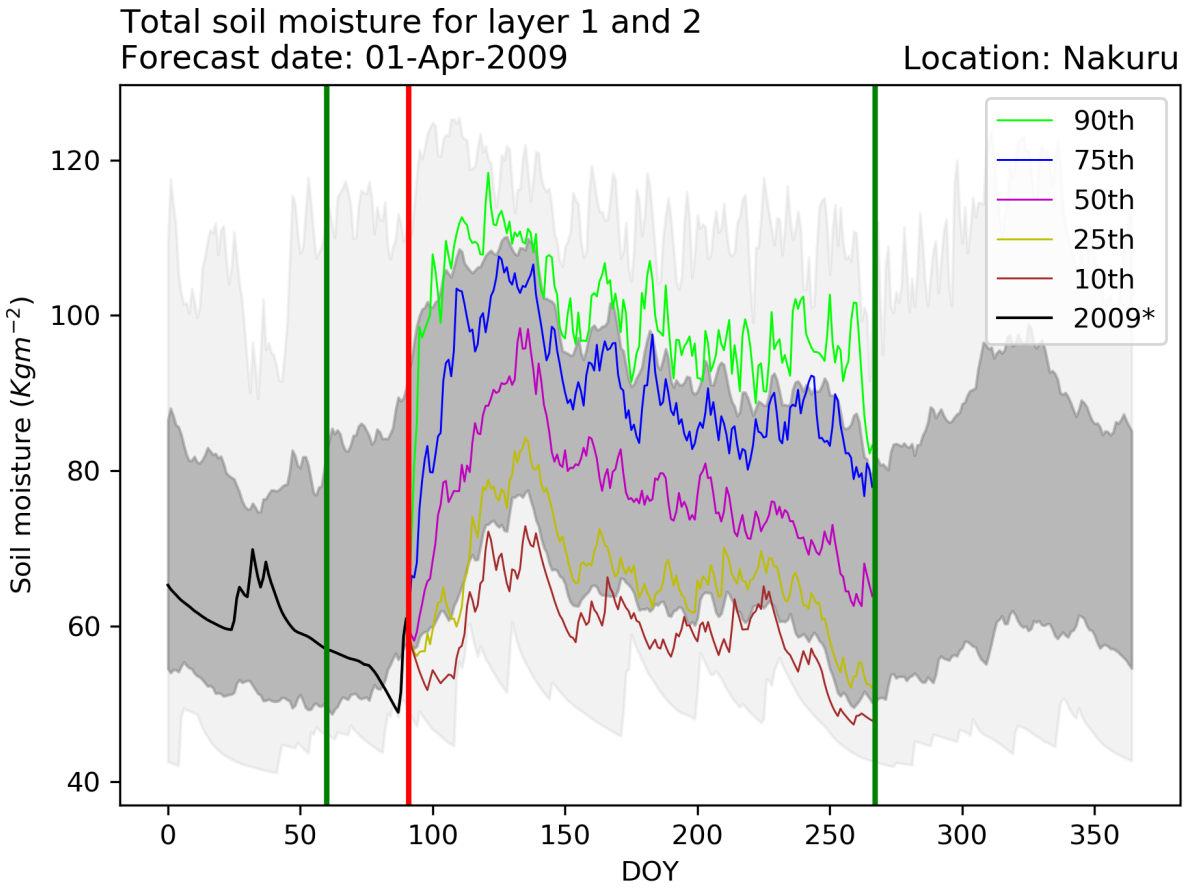

Figure 4.4: Total soil moisture for the first two layers at Makuru. The green vertical lines represent the planting and harvesting dates of maize, the red vertical line shows the date the forecast was made, the dark gray shade is the climatological value with +/-1 standard deviation, the light gray shade shows the climatological maximum and minimum value. The solid black line indicates the historical soil moisture and the percentile lines are derived from the 30 ensemble values and each line represent the percentile values indicated in the legend.

The two distributions; one from the climatology and the other from the combined historical and ensemble within the period of interest, are then compared to determine the probability of the WRSI being below average (<0.5 probability) and well below average (<0.25 probability) against the climatology at each location. These two probability thresholds signify the drought conditions

in the area where if the well below average probabilities indicate a severe drought levels in the area and the below average probability indicate a lesser drought level. These probabilities only indicate the climatic risk due to agricultural drought but does not consider the many other factors that might cause the damage on crops such as pest, disease and poor soil fertility.

4.3 Results

4.3.1 Comparison of SPI and soil moisture metrics

Soil moisture availability (β) is used to estimate the WRSI in the growing season (chapter 3) which serves as an indicator for agricultural drought in TAMSAT-ALERT system. Therefore, the correlation between the soil moisture availability (β) and SPI values at different time scale are presented to see how the meteorological drought and agricultural drought are related. First, the monthly time series of SPI was calculated and scaled from zero to one. Secondly, the daily soil moisture availability factor was weighted by the fraction of crop harvested area for each grid cell (Figure 4.9). The weighted daily β values were then converted into monthly average values. These monthly values were correlated with the monthly SPI values for the different aggregation periods (1-, 3-, 6- and 12-months). The result indicated in Figure 4.5 shows that the meteorological drought indicator SPI aggregated to three and six months are more correlated to soil moisture availability than the one month and 12 months aggregated SPI. A similar comparison of SPI and agricultural drought indicator - Soil Moisture Deficit Index (SMDI) over the Blue Nile river basin in Ethiopia showed that SPI-3 is highly correlated with SMDI (Bayissa et al., 2018). This mainly occurs as the 3-months and 6-months SPI aggregates rainfall condition over a more extended period and within this period the soil moisture responds to the rainfall condition. However, SPI is a rainfall-based metrics and soil moisture responds not only to rainfall but also to the evaporation in the region; therefore, the 3-months and 6-months SPI values are not a direct representation of the agricultural drought. Tian et al. (2018) showed that in the south-central United States soil moisture is better represented with a drought index that accounts for rainfall and potential evapotranspiration.

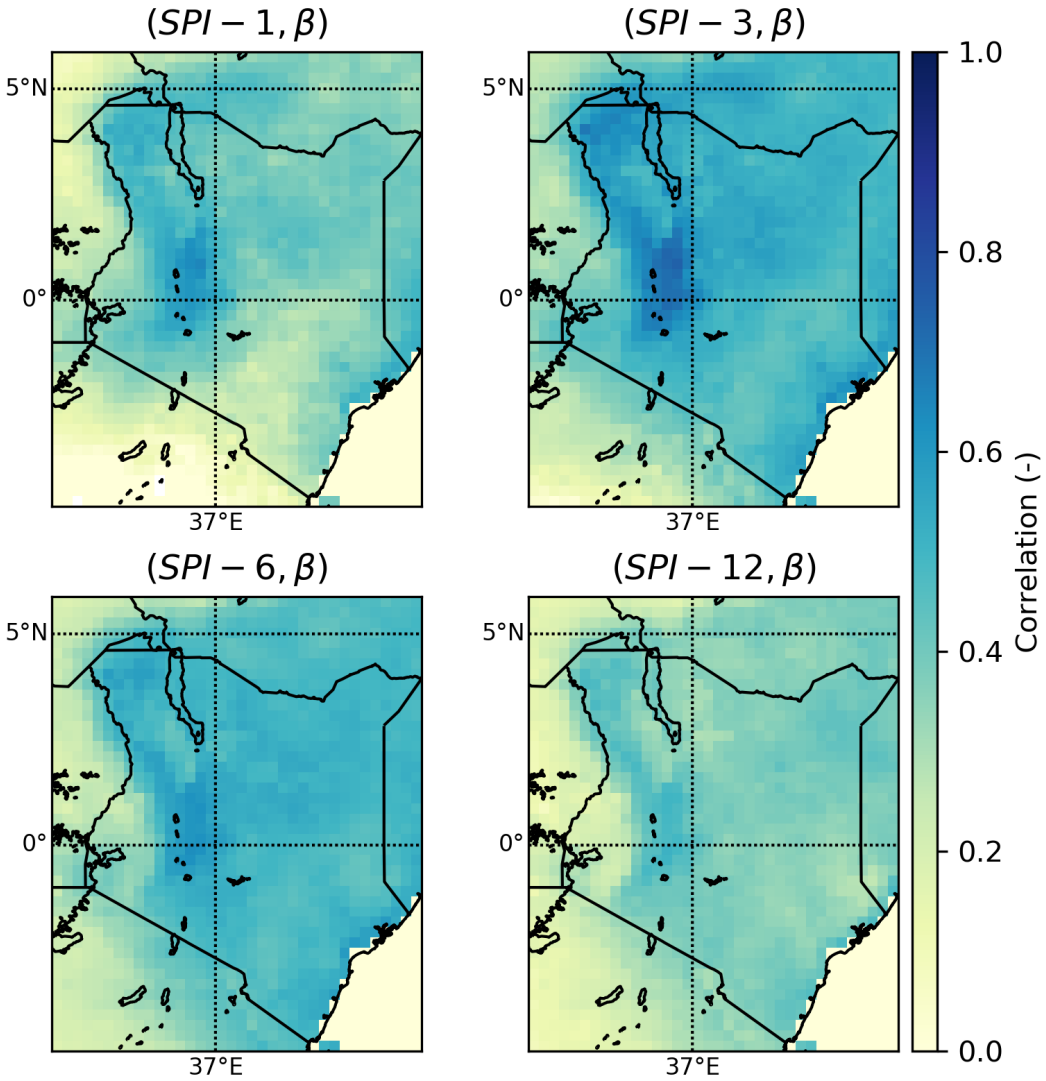

Figure 4.5: Correlation of SPI-1, SPI-3, SPI-6, and SPI-12 with Soil moisture availability (β). Comparison of SPI for 1, 3, 6, and 12 months and Soil moisture availability factor (β) values was done by taking the monthly average of value weighted by the harvest fraction for maize (Figure 4.9).

Meteorological drought indicator SPI is calculated on monthly basis using different aggregation timescales, but WRSI value is calculated only for the growing season as an average value hence direct comparison of SPI values of different aggregation time with WRSI can not be done. However, considering the 3-months and 6-months timescale SPI values for the end of growing season month (September) correlation was done with WRSI value. Figure 4.6 shows the correlation value for SPI-3 and SPI-6 with WRSI for the end of the season. The values of the correlation indicate that end of season SPI-3 is poorly connected to WRSI while SPI-6 is better correlated. This represents

using SPI-3 as a proxy for agricultural drought indication is not viable.

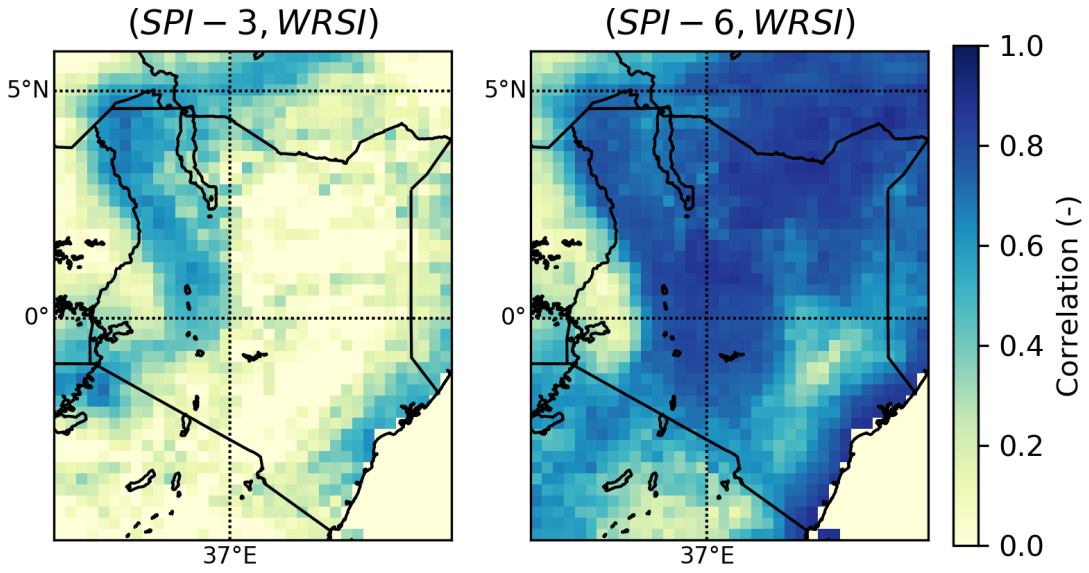

Figure 4.6: Correlation of SPI-3 and SPI-6 with WRSI. Comparison was done using end of season (September) SPI values.

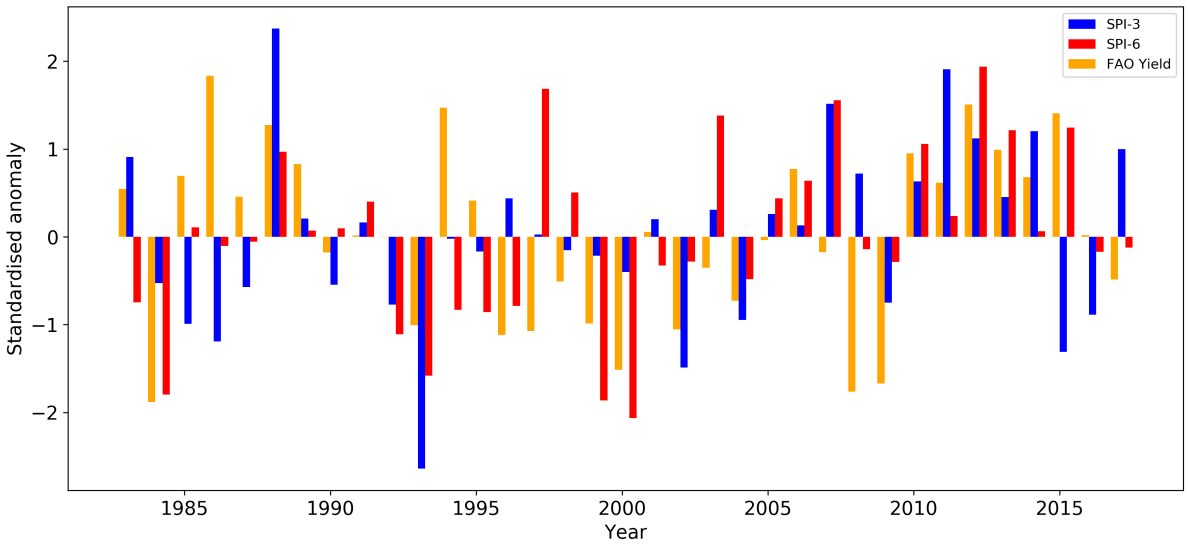

Figure 4.7: Standardise anomalies of SPI-3 and SPI-6 of September with maize yield over Kenya. The Figure indicates that SPI-3 is less correlated with season yield and SPI-6 is better correlated with season yield.

Similarly, a comparison of SPI-3 and SPI-6 values with countrywide average maize yield obtained from FAOSTAT (`http://www.fao.org/faostat/en/#data`) was done. Figure 4.7 compares the standardized anomaly of SPI-3 represent a drought period in years where the yield was high and SPI-6 on the other had better replicate the yield pattern. Figure 4.8 shows the correlation

between countrywide maize yield and SPI values at three and six months aggregate, where SPI-3 has a 0.26 correlation and SPI-6 has a 0.46 correlation. This shows that longer time aggregates are better representatives of the overall countrywide yield outlook that the SPI-3. In the south-central United States, maize yield was highly correlated with June SPI value as this is the period where maize yield most sensitive to water supply (Tian et al., 2018). Therefore, the weak correlation of SPI-3 could be associated with the fact that the maize in Kenya was not sensitive to three months aggregate rainfall as the growing season is nearly six months long from March to September. This result tells the fact that only using the rainfall does not reveal much about the yield outcome of a season; hence monitoring yield and drought impact on agriculture should be based on the soil moisture condition throughout the season.

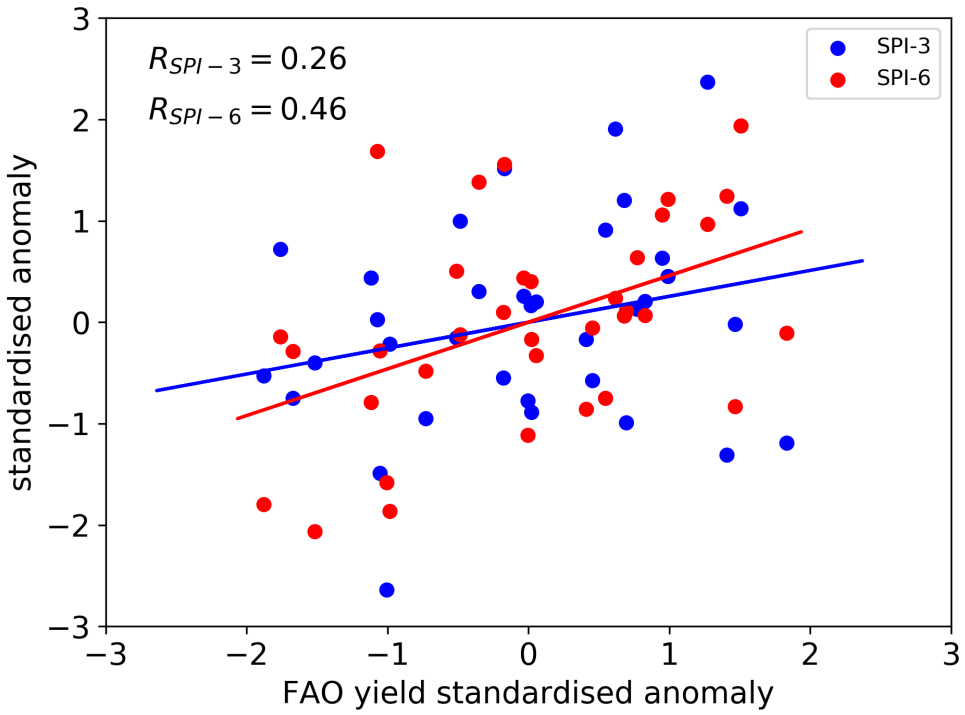

Figure 4.8: Scatter plot of SPI-3 and SPI-6 with maize Yield over Kenya. The September SPI value for 3-month and 6-month timescale was used. The blue line represents the best fit line for SPI-3 with correlation coefficient of 0.26 indicating poor correlation. The red line represents the best fit line for SPI-6 with correlation coefficient of 0.46 indicating improved correlation.

4.3.2 Comparison of WRSI with crop yield

Figure 4.10 indicates the anomalies of countrywide WRSI and maize yield. Maize grown during the primary rainy season, planted in March and harvested in September, was used for this analysis for which WRSI was estimated. The county crop yield data of maize of 35 years (1983-2017) were

taken from FAOSTAT (http://www.fao.org/faostat/en/#data). The figure shows that WRSI is related to the maize yield harvest for many of the years. For example, in 1985–1990 both WRSI and maize yield have positive anomalies indicating there was no intense drought in the country in that period, data from EM-DAT (https://www.emdat.be/) also supports this as there was no record of drought during this period. The year-to-year variability is high, but WRSI represents the overall pattern in countrywide maize yield over Kenya. The observed discrepancies between the WRSI and yield could be associated with many factors like the use of single planting time for all years, soil type and the weighting of maize harvest area fraction. A correlation analysis was also done (Figure 4.11) with the WRSI values which are spatially weighted by harvest area fraction for each grid cell shown in Figure 4.9 and countrywide average maize yield data weighted by total harvested area to analyse if WRSI affects the country maize yield. The result shows that the overall correlation is about 60%. Other studies have shown that WRSI well represents maize yield over Ethiopia, especially in identifying water limited and water-unlimited districts (Senay and Verdin, 2003) and in Zimbabwe where WRSI was used to estimate maize yield and showed a significant correlation (Verdin and Klaver, 2002). Looking at Figure 4.11 and Figure 4.8 WRSI value correlation improved by 14% from SPI-6 values of September. This indicates that the use of soil moisture is a better indicator for agricultural drought impact on maize yield rather than using rainfall as a single indicator. Although countrywide yield is not only related to soil moisture deficit but also other factors like soil fertility, pests, and diseases (Machado et al., 2002), there is still a strong correlation with WRSI. Hence, WRSI could be used as a proxy to predict the outlook of the season related to drought and its consecutive impact on overall crop production.

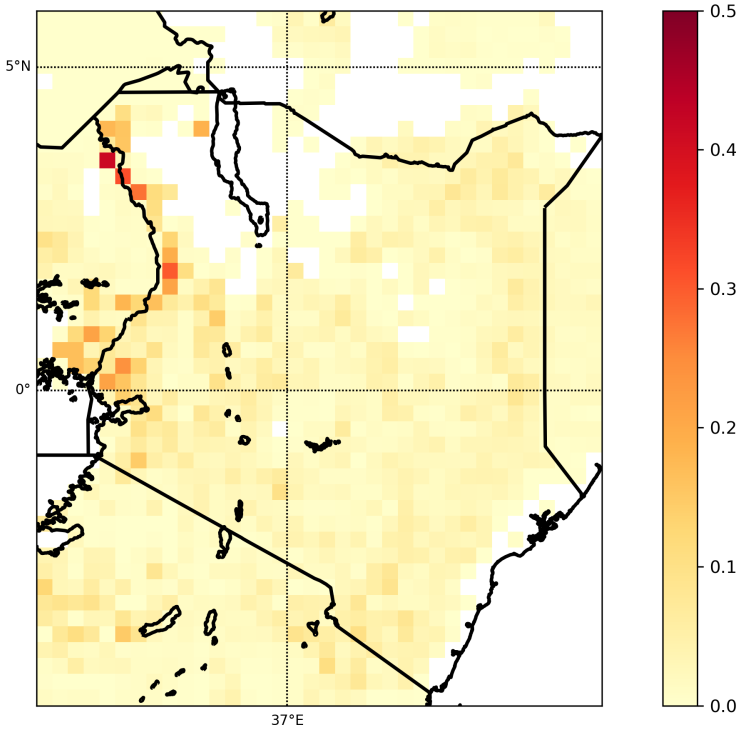

Figure 4.9: Average fraction of grid cell for maize harvested from 1997–2003 in Kenya (Monfreda et al., 2008). This fraction of harvested area fraction was used to weight the WRSI values for further analysis.

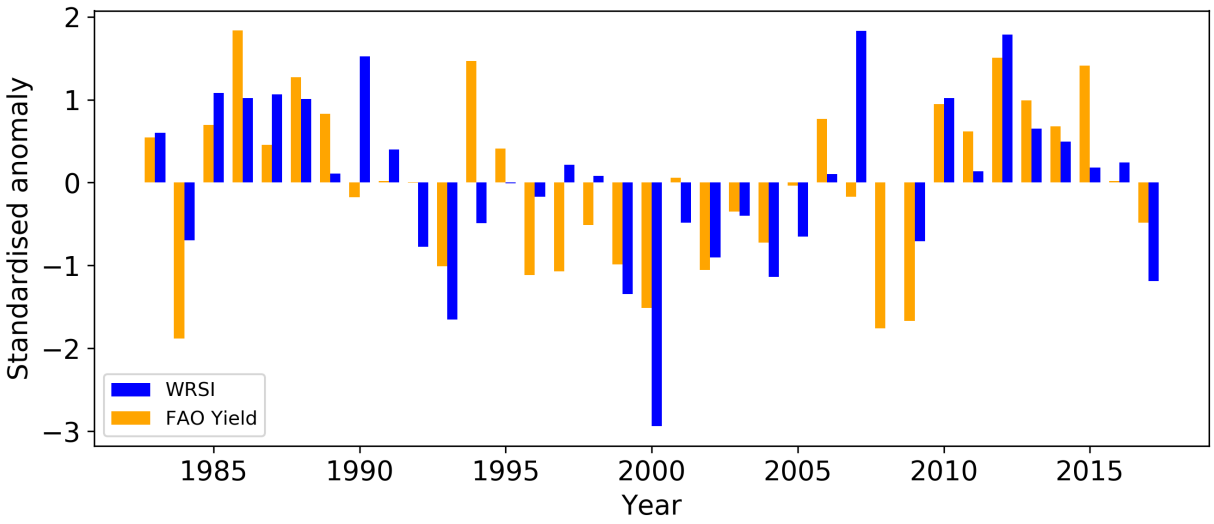

Figure 4.10: Standardise anomalies of WRSI and maize yield over Kenya.

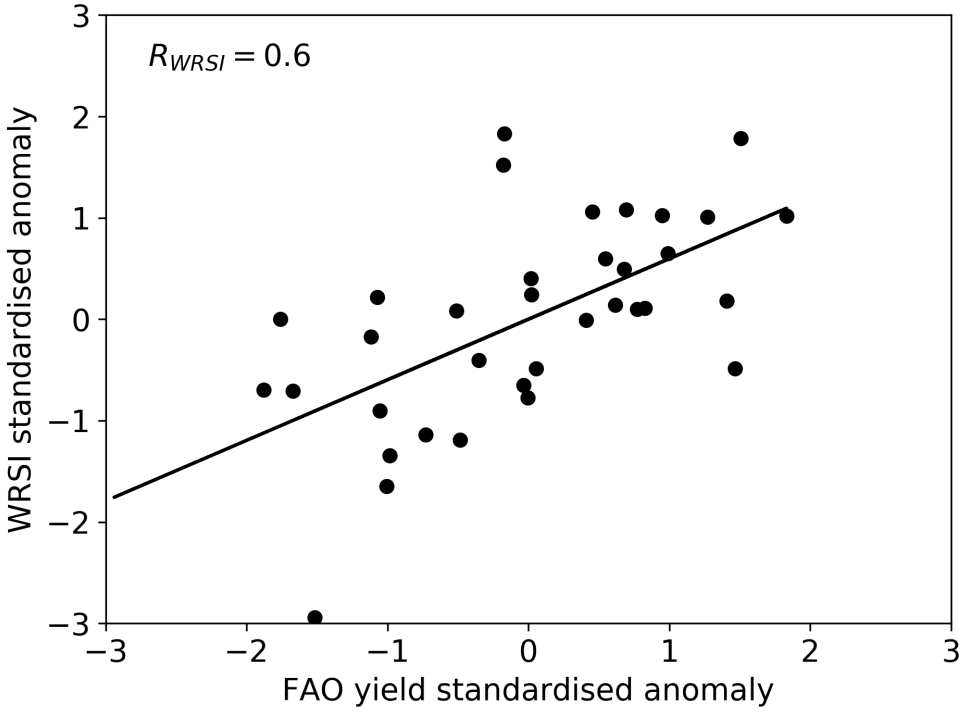

Figure 4.11: Scatter plot of WRSI and maize Yield. The black line represents the best fit line with a 0.6 correlation coefficient.

4.3.3 Demonstration of TAMSAT-ALERT: drought forecast case study over Kenya

Over the past 35 years (1983–2017), Kenya has faced many years of severe droughts of which 2009 was one year where the average countrywide maize yield was very low (Figure 4.10) (Masih et al., 2014). This year was associated with relatively low rainfall during the primary growing season (March-April-May) resulting in a strong meteorological drought. Figure 4.12 indicates the SPI-1, SPI-3, SPI-6 for March, April and May of 2009. The 3- and 6- months aggregate SPI values indicate that there was a meteorological drought in the growing season due persistent below average rainfall. The 3-months and 6-months aggregate SPI usually is taken as a proxy to show a deficiency in soil moisture which is considered agricultural drought but, as shown in section 4.3.1 and 4.3.2, SPI-3 is less correlated with maize yield over Kenya and SPI-6 was not as highly correlated as WRSI with maize yield. Therefore, WRSI is used as an early indicator of season yield and the impact of the climate over agriculture. Based on the forecasts of WRSI made for the season at the beginning of each month the overall season outlook was associated with intense agricultural drought as indicated in Figure 4.13. The figure shows the probability of well below average (<0.25 probability) and below average (<0.5 probability) values for the WRSI

of the growing season based on maize crop planted at the beginning of March. March 1, 2009 forecast indicates that at the start of the season the outlook is that the eastern part of the country is going to face a lower WRSI value indicated by the higher probability, but there is a minor chance that the WRSI value of the season is going to fall well below average (<0.25 probability) compared to the climatology. April 1, 2009 forecast, one month into the growing season, the outlook suggests that southern part of the country will face strong drought probability indicated by the well below average WRSI value and almost all part of the country will face a below average WRSI compared to the climatology. High probability shows that 2–3 months before the harvest period (September) that the overall indication is that there will be a poor harvest in the season. May 1, 2009 forecast, two months into the season it is evident that the season will be associated with a significant drought which leads to crop failure.

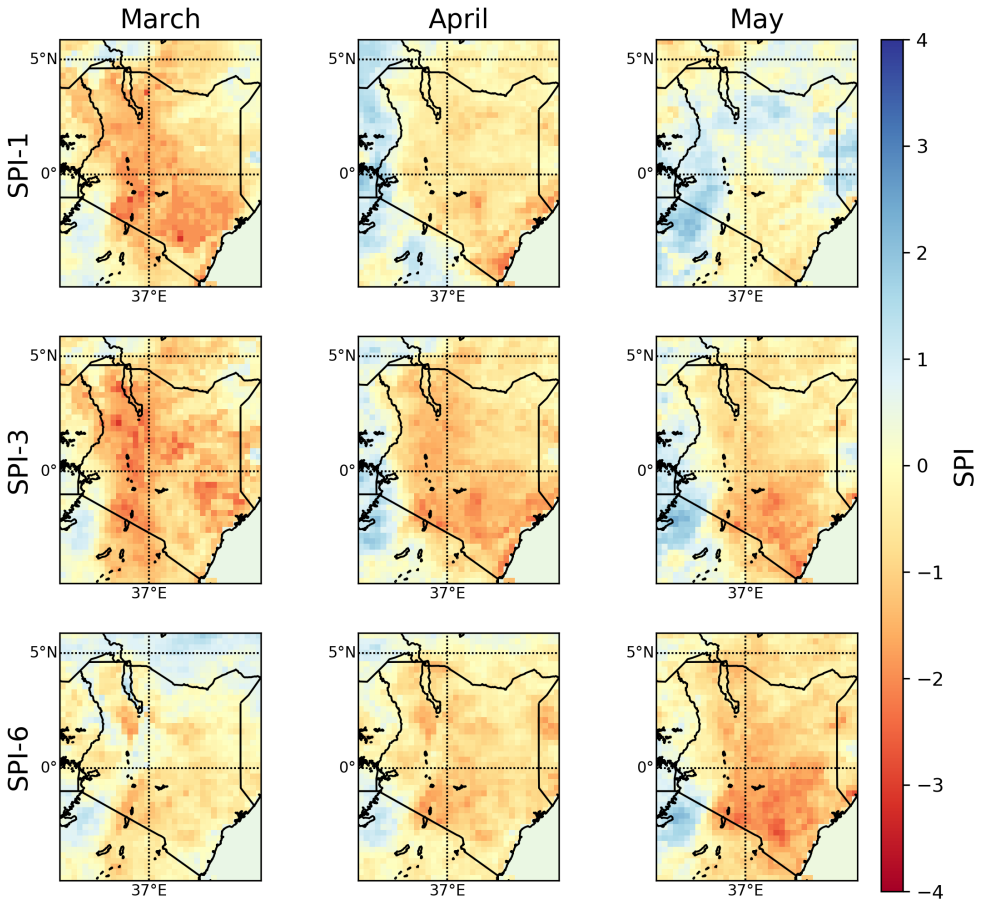

Figure 4.12: SPI-3 for March, April, May of 2009 in Kenya. The three-month aggregate SPI indicates the persistence of the rainfall shortage which also used as an indicator for a decrease in soil moisture level due to a prolonged lack of rainfall. SPI-6 of the main rainy period in Kenya March-April-May for the 2009 season shows that the season is associated with intense drought over the country which persisted over the past six months for each month. This persistence of the meteorological drought is the one that is associated with the agricultural drought leading to lower soil moisture availability.

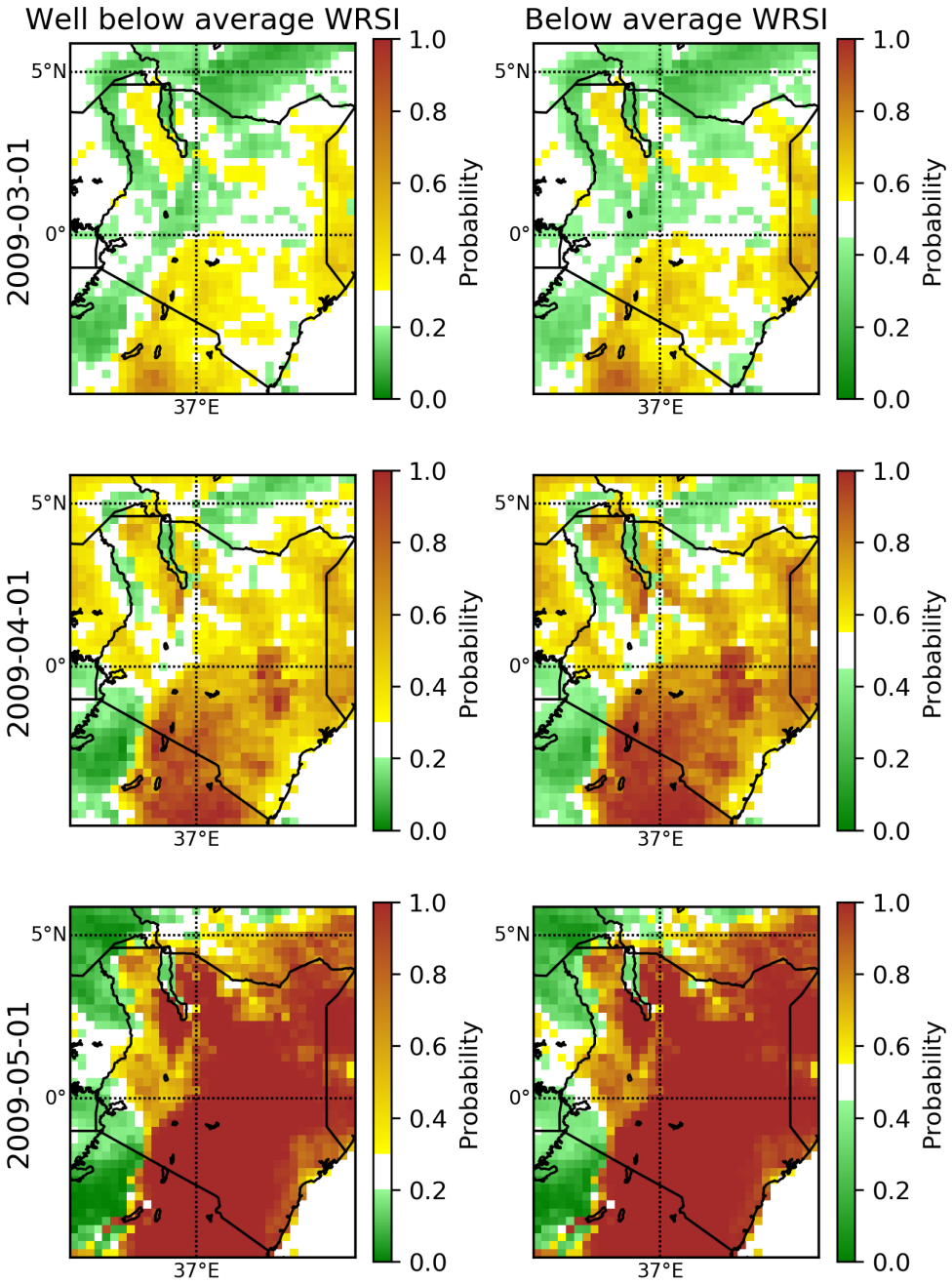

Figure 4.13: WRSI forecast at the beginning of each month for the primary growing season March-April-May for 2009 season. Green color indicate the regions with lower chance of WRSI value being below the threshold indicated and the brown color indicate those region having high chance of being above the threshold probability.

Figure 4.14 shows the WRSI forecasts at the end of each month in the primary growing season and the results indicate that there is even a strong probability of getting below average and well below average water requirement satisfaction for the crop. At the end of each month, the forecast indicates that three months into the season there will be a 100% chance that the WRSI values will be well below the average compared to the climatology. This indicates that the main rainy

period has failed and no matter what happens after this the crop failure is imminent. In 2009 the overall country average yield was low as shown in Figure 4.10 which supports the forecasts from TAMSAT-ALERT as early as 2–3 months. Hence, TAMSAT-ALERT can anticipate, 2–3 months ahead, that there will be a very poor season harvest at the end of the season as the main rainy season period is strongly associated with high probabilities of below average WRSI.

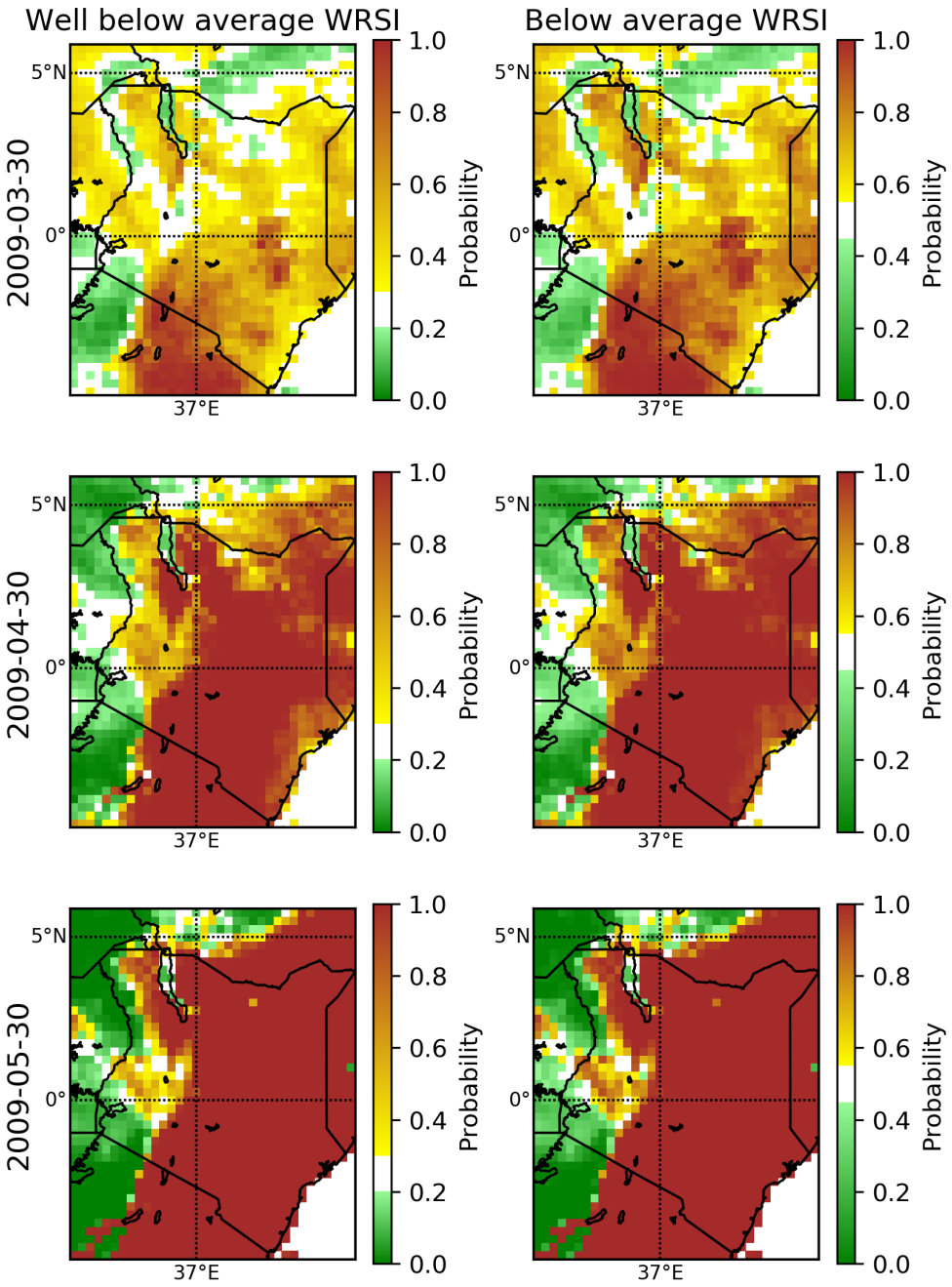

Figure 4.14: WRSI forecast at the end of each month for the primary growing season March-April-May for 2009 season. in Kenya at the end of the main rainy season there was a 100% chance that the WRSI will be well below average.

Seasonal weather forecasts and outlooks are issued at the beginning of each month (e.g. GHACOF), but the impact of the climate is generally delivered at the end of the season. Hence, it would be difficult to take appropriate measures in reliving the impact especially in the case of drought. TAMSAT-ALERT system is beneficial with this regard as it allows to monitor the condition as the season progress. Figure 4.15(a) shows the FEWSNET estimated outlook on food security which is issued in August 2009 for Kenya (FEWS, 2009) and Figure 4.15(b) shows a similar outlook of the season in terms of WRSI probability for Kenya forecasted at the end of May 2009. It clearly indicates that the 2009 season crop production in Kenya is going to be severely affected and it is confirmed that at the end of August by FEWSNET that most of the country except western region near Lake Victoria are highly or extremely food insecure. This shows that based on the TAMSAT-ALERT system of following the season outlook it is possible to anticipate climatic impacts as early as 2–3 months and the spatial variability is well captured.

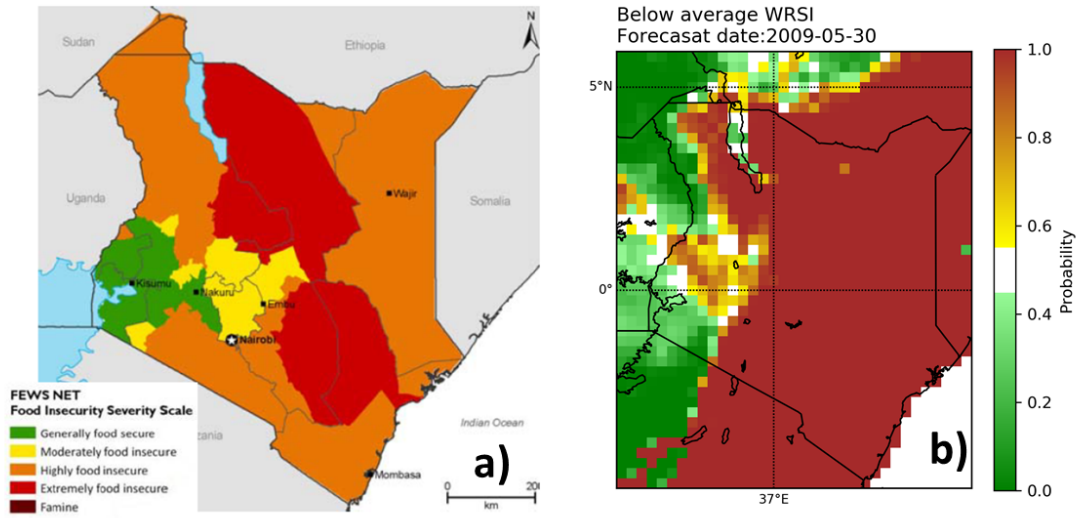

Figure 4.15: (a) FEWSNET estimated food security condition issued in August 2009 (Source: (FEWS, 2009) and (b) Below average WRSI probability forecast for May 2009.

One of the recommendations for climate services in sub-Saharan Africa is that the climatic forecast should include probabilistic impacts on agriculture which are updated through the growing season enabling a range of decision-makers to take multiple climate risk management interventions (Hansen et al., 2011). TAMSAT-ALERT is such a tool that helps to monitor climatic risk (e.g. drought) through the growing season. Figure 4.16 shows the WRSI forecast ensembles for four

locations in Kenya (Kitale, Nakuru, Wajiri and Makindu). In the western part of Kenya at the end of May, the probabilities are very low for falling well below average values of WRSI climatology indicating that the drought condition in the region is not as strong as that of the eastern and southern part of the country. In the eastern and the southern part, we can see that there is a 100% chance that the WRSI values will fall well below average from the climatology indicating that no matter what happens after this period that drought is imminent which will lead to lower crop yield harvest at the end of the season. In addition to the low rainfall over the MAM season, the eastern and southern part of the country (locations like Wajiri and Makindu) are located in the semi-arid environment and follow a distinct two season rainfall. Therefore, the use of long growing maize is not a preferred choice which pushes the growing season to include the dry period. However, TAMSAT-ALERT accounts for the climatology which also include the dry season hence provide a reasonably reliable estimate of the growing season as shown by the comparison with the FEWSNET season outlook issued in August 2009 (FEWS, 2009). A similar result of the top two layers (0.35 m depth) of soil moisture results presented in Figures C.1.1 and C.1.2 (Appendix C.1) indicate that for the eastern and southern locations a dry period follows after the MAM season.

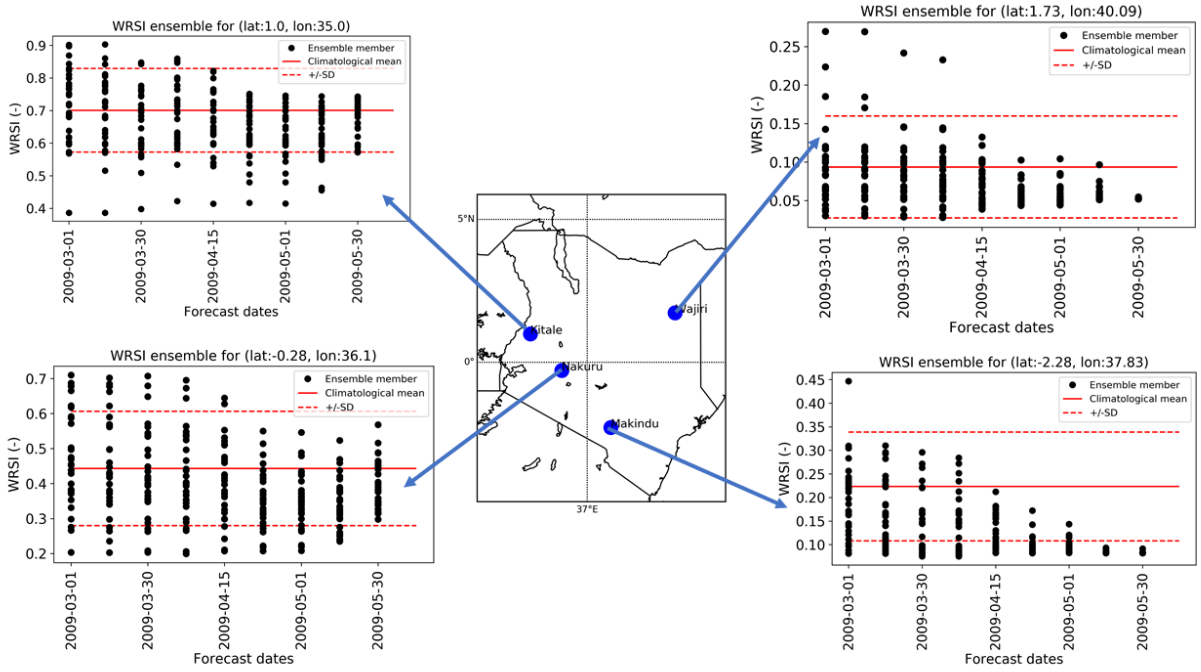

Figure 4.16: Ensemble of WRSI forecast for specific locations over Kenya for 2009 season. The result indicates that in the western part of Kenya (Kitale and Makurdu) even at the end of the season the outlook for drought occurrence cannot be definitively determined instead there is a strong chance that the WRSI values are going to be below average. Whereas in the eastern and southern part of the country (Wajiri and Makindu) it can be seen that all the ensembles are below one standard deviation from the climatological mean indicating that there is a high chance of drought occurrence in the season.

4.4 Discussion and Summary

This study evaluated the performance of TAMSAT-ALERT system in monitoring agricultural drought through the growing season using WRSI and compared it with the performance of commonly used meteorological drought indicator-SPI over Kenya. Maize is one of the primary crops grown in Kenya and this study examined the relationship between maize yield and the drought indices SPI and WRSI using the period (1983–2017). The results indicate that SPI-3 has a weak correlation with maize yield while SPI-6 and WRSI are better correlated with maize yield over Kenya with 46% and 60% correlation coefficient respectively. Despite the many factors that could affect annual maize yield in a region like sowing date, maize variety, soil texture, elevation and disease (Machado et al., 2002; Bonelli et al., 2016), WRSI values were observed to track the variation in maize yield over Kenya well. A similar implication of WRSI value based on the FAO calculations was also found in Ethiopia where WRSI is highly correlated with maize yield and helps to identify water limited and water unlimited districts (Senay and Verdin, 2003). Moreover, maize yield estimated by regression using WRSI as an independent variable showed a strong agreement in Zimbabwe (Verdin and Klaver, 2002). Comparing it with SPI, which is a retrospective approach; where we only see the drought after it occurs the use of TAMSAT-ALERT method, can estimate the likelihood of agricultural drought occurrence ahead of season harvest. In addition, SPI is calculated on a monthly scale and it is hard to follow the progress of the season before the end of each month, but the TAMSAT-ALERT system using WRSI can be used to evaluate the condition of the season at any time within the growing period using sub-monthly data. Based on the case study presented for 2009 season over Kenya, it is shown that TAMSAT-ALERT predicts WRSI as early as 2–3 months ahead of season harvest (Figure 4.15). Since there is a significant connection between WRSI and annual maize yield over Kenya, the implication for an early warning system on the outlook of the season for food shortage is paramount as conventional crop surveys are available few months after harvest and this delays decision that needs to be taken on necessary measures if there is a poor harvest.

Despite the interest of farmers in receiving seasonal forecasts combined with additional information from climate service providers; Regional Climate Outlook Forums and National Climate Service providers tend to gravitate towards safe forecasts by giving higher probabilities to the middle tercile and this tendency is partly responsible for the failure to indicate the below-normal

rainfall that occurred in major growing seasons (Hansen et al., 2011; Walker et al., 2019). For example, at the end of May 2009 for Kenya the season was considerably dry resulting a strong meteorological as well as agricultural drought (Figure 4.12 and Figure 4.14) but this information is not contained within the seasonal forecast. A further drawback of depending on forecasts for seasonal decision-making relates to the fact that it does not consider the historical observations (Hansen et al., 2019), but TAMSAT-ALERT system allows to compare the forecasts with historical observations and provide ongoing monitoring of the season in a form exceedance from the historical climate distribution. A combination of monitoring and forecasting is required for assessing risks of the climate on agriculture because occurrence of an adverse event depend both on the past and the future weather within the growing season. The new system connects the forecast with historical variability which add the value of past conditions awareness and allows decision-makers to use the system even in the absence of seasonal forecasts. In addition, the forecasts made by TAMSAT-ALERT can be compared with user defined thresholds for instance the values below average (<0.5 probability) and well below average (<0.25 probability) for the WRSI are thresholds to indicate the significant agricultural drought levels.

This study showed that TAMSAT-ALERT adds relevant information on top of the seasonal weather forecast to decision-makers and farmers regarding the seasonal progress and its impact on crop yield. The findings and methods presented here offer the potential for a new actionable product of drought outlook for food security analysis. Further developments will include a rigorous assessment of forecast skill and improved functionality, including variable planting date and crop type.

Chapter 5

TAMSAT-ALERT for short term applications: Planting date decision making

This chapter explains and demonstrates how the TAMSAT-ALERT framework (chapter 2) is modified to develop a decision making criteria to identify an optimum planting date for maize crop over western Kenya. Choice of planting time is one of the critical decisions made by farmers every year it is paramount to get the optimum date as it determines further farming practices like fertiliser application, harvesting time and second crop planting. The chapter explains how historical weather and numerical models can be integrated for identifying an optimum planting time for maize in western Kenya and evaluate the decision-making criteria. The main objectives were designing operationally viable planting date decision-making methodology using TAMSAT-ALERT framework, exploring links between environmental conditions and optimal planting date and demonstrate the application (section 5.1.2). Western Kenya is chosen as there were farmers field data on planting time and maize yield to evaluate the new decision-making criteria and allowed for further operational trials as this work was done in collaboration with an institute that works in advising farmers on agricultural practices in the region (One Acre Fund (`https://oneacrefund.org/`)). Using satellite estimate of weather data from Climate Hazards Group InfraRed Precipitation with Station data (CHIRPS) rainfall estimate and National Center for Environmental Prediction (NCEP) reanalysis the chapter used three methods of planting date decision making for the region including local recommendation by agricultural advisory ser-

vice provider (One Acre Fund method), an objective rainfall season start identification method (Onset method) and the newly developed TAMSAT-ALERT planting date method (TAMSAT-ALERT PD) and evaluate the methods for two growing seasons (2016 and 2017) for which field data were available (section 5.2.3). The first two methods are solely based on the rainfall, while the new method explained in this chapter include the use of soil moisture and WRSI (chapter 3). The results indicate that farmers planting date choice is very diverse spatially reiterating the fact that more factors which are non-climatic are considered for the choice of planting time (section 5.3.1). Comparing the new TAMSAT-ALERT PD with the farmers practice it helps to identify clusters of regions in western Kenya where planting time is similar however the spatial diversity of farmers planting time is not captured (section 5.3.2). The yield comparison between the actual farmers planting date and the planting date that would have been recommended using the new method showed that those farmers who planted later than the prescribed date obtained significantly lower yield hence, the current advice for farmers would be to start planting if they have not started yet (section 5.3.3). Planting time adjustment is one of the ways that can quickly be adopted by farmers to utilise the season effectively without any cost and helps to enhance productivity. Therefore, evidence-based advice on planting date benefits farmers by reducing the risk of crop failure due to water stress during the growing season or germination failure at the beginning of the season. This chapter for the first time introduced an operationally viable planting date decision-making method and evaluated it in western Kenya. The new planting date identification approach is currently being used operationally in Uganda and Zambia (not included in this thesis) and the response of the local advisory service is very positive. The next steps will involve the development of this tool with a user interface and training for the local advisory service providers so that they can operate it in conjunction with other climate services like weather forecasts and season outlooks.

5.1 Introduction

5.1.1 Background

Choosing the right time for planting that would maximise productivity from their crops is a challenge faced every year by many farmers (Sacks et al., 2010). This planting period is very variable as the weather is highly variable and uncertain, especially for Sub Saharan Africa (SSA)

where most of the crop production is based on rainfed agriculture system (Waongo et al., 2014, 2015). In practice, planting date for rainfed farming depends on the onset of rainfall (Wang et al., 2008). For example, in Burkina Faso farmers make planting decision from their experience in the previous year with small adjustment based on short term assessments of the upcoming season (Ingram et al., 2002). However, the occurrence of unexpected and prolonged dry spells after the start of the rain season presents a significant risk for farmers (Wang, 2005; Marteau et al., 2011). The significance of planting date in the season farming calendar emanates from the fact that it determines the timing of other farm operations like land preparation, fertiliser application, weeding, harvesting and even the time of second crop planting if there is one (Hassan, 1996; Wolf et al., 2015). Planting time also has an impact on the yield of crops in combination with other factors (Marteau et al., 2011; Sacks et al., 2010; Bondeau et al., 2007; Stehfest et al., 2007). Planting date selection is also considered one of the adapting strategies in improving productivity in changing future climate (Tubiello et al., 2000) and studies of climate change impact on crop productivity have shown the influence of variation of planting date on yield of crops like maize and wheat (Challinor et al., 2007; Thornton et al., 2014). Srivastava et al. (2016) also shown the response of model crop yield to different planting dates and environments is hugely variable.

Planting dates are very variable both regionally and seasonally and the variability arises from variations in soil moisture availability during planting periods, farming operation practices such as harvest times of the preceding crop, and availability of farming inputs such as seeds, fertiliser and labour (Harrison et al., 2000; Chmielewski et al., 2004). Despite the importance of planting date decision making, there is no operationally viable planting date decision-making tool. Instead, there are tools that are based on local expert knowledge of farmers' practices which are compiled in a lookup table for users to choose depending on their location agroecology where the FAO generic Crop Calendar (`http://www.fao.org/agriculture/seed/cropcalendar/welcome.do`, last accessed: August 2018) and Global Yield Gap (`http://www.yieldgap.org/`, last accessed: August 2018) are good examples (Wolf et al., 2015). The FAO Crop Calendar provides information for more than 130 crops, located in 283 agroecological zones of 44 countries whereas Global Yield Gap has collected local planting date of eight major crops including wheat, rice, maize and sorghum over the world and for about 15 countries in SSA. These data sets on planting date are available for users, but the drawbacks of this approach are that similar planting dates are advised year after year, irrespective of the variability in rainfall and there is no consideration for

local variation in varieties of crops. Also, these planting dates are subjective as they depend on local expert knowledge of farmers' practices (Wolf et al., 2015). Another global crop planting date available for use is based on ten years (1990-2000) average of planting date recorded from six different sources over the globe for 19 major crops (Sacks et al., 2010). The main similarity between the above planting date sources is that all of them are not operational tools; instead, they are records based on local practice making it difficult to update to changes in local conditions. An alternative approach in choosing optimum planting date at a global level is to select a planting date based on optimising the yield obtained using a crop model (Stehfest et al., 2007; Liu et al., 2007). However, such a methodology relies on the crop models in question capturing the observed relationship between crop yield and planting date.

Besides local planting records, other approaches use measurable climatic variables (rainfall and temperature) to determine optimal planting dates for different crops at global and regional scales. For example, Waha et al. (2012) presented climate-driven global planting date for 11 major crops based on climatic conditions and crop-specific temperature requirements. The results showed that planting dates estimated from climatic conditions agree over 60% of the cultivated area with a difference of less than one month compared to observed planting date indicating that planting date for rainfed farming could be estimated from climatic conditions for large parts of the earth. The methodology used for this research is based on the assumption that planting date is dependant on the inter-annual variability of precipitation and temperature, and the temperature of the coldest month ($T_{cm} = 10$°C). With this, it created a set of criteria to determine precipitation seasonality and temperature seasonality from annual variation coefficient values calculated as the ratio of the standard deviation to the mean (CV_{precip} = 0.4 and CV_{temp} = 0.01) from which planting dates were estimated (Waha et al., 2012). Sacks et al. (2010) provide a global planting date data for crops by identifying the precipitation and temperature limited regions through an examination of local planting date with temperature, precipitation and potential evapotranspiration from a 30-years climatology. The data defined locations of precipitation and temperature limited planting dates over the globe for 19 crops.

There is also research on the estimation of planting date with a focus on individual countries and crops. For example, Dobor et al. (2016) used soil temperature and soil moisture to determine planting date under climate change using 4M crop model to set soil specific variables. Eight

criteria were used to determine planting date of Maize over Hungary whereby the criteria combine average daily air temperature at 2 m (aT), total precipitation amount of the last three days (3dayTprec), the normalised water content of the topsoil (NWC) and temperature of the topsoil ($soilT$). The result showed maize planting should follow when aT >12°C for 5 days and 20% <NWC <80% and $soilT$ >10°C for 5 days. Studies have tried to establish criteria to identify optimal planting dates for crops at local levels in sub-Saharan Africa too. For instance, different approaches have attempted to optimise planting date for maize and millet in Africa, which are among the staple crops in many African communities (Sultan et al., 2005; Waongo et al., 2014; Kamara et al., 2009). Wolf et al. (2015) found that in Burkina Faso, model-based planting date determination worked very well for maize and sorghum. The study used the WOrld FOod Studies crop simulation model (WOFOST) to simulate maize and sorghum and applied different rules for setting the planting date. The planting rules were determined based on available soil water (cm), the cumulative amount of rainfall (cm, as counted between earliest and latest possible sowing date), and initially available soil water (cm) in initial rooting depth. The planting date identified for the region should use a maximum of a 40-day window around the estimated planting date given by the FAO Crop Calendar and maize should be sown from day 160 to 200 of the year with a 30 mm cumulative rainfall within the planting window and a 20 mm available soil moisture in central Burkina Faso. For the humid regions in the southern part of Burkina Faso, a 20 mm or more cumulative rainfall within the planting window and 10 mm available soil moisture level should be used (Wolf et al., 2015). A study conducted in Ghana used LINTUL5 crop model embedded into SIMPLACE (Scientific Impact Assessment and Modelling Platform for Advanced Crop and Ecosystem Management) combined with a soil water balance model (SLIM) maize yield in central Ghana to simulate maize yield by assuming eight planting dates based on different criteria that are deterministic and involving probabilistic values. The results showed that probabilistic planting date determination approaches with the assumption of normally distributed sowing dates around the sowing day estimated with a rainfall based rule (20 mm rainfall within seven days) was found to capture the spatial and temporal variability of maize yields in central Ghana than deterministic approaches (Srivastava et al., 2016).

In general, the discussions above indicate the importance of identifying an optimum planting date for crops in every region. Delaying planting due to lack of a reliable method to define the season onset, for instance, force farmers to plant late in the Sahel (Bussmann et al., 2016). Consequently,

such planting delays result in ineffective utilisation of the growing season and leads to low yield (Bussmann et al., 2016; Wolf et al., 2015). Whereas in Burkina Faso, using an optimum planting date results in an increase in maize yield (Waongo et al., 2014). The planting decision-making approaches discussed earlier are focused on identifying an invariant planting date that optimises crop yield, retrospectively. Some are based on climatic data, some are based on expert's judgment and others use crop models to determine a planting date that gives higher crop yield. However, in SSA, where the climatic conditions, soil type and crop varieties planted are very diverse, the planting date of crops will also vary spatially and seasonally.

5.1.2 Study objectives

The previous discussion indicates it is crucial to have an operational planting date decision-making tool that considers local conditions. Therefore, this chapter tries to address the need for an operationally viable decision-making method on planting date in Africa. The study evaluates the difference in planting date decision made by three methods which have a significant level of variation in complexity and data requirement as well as how these methods can be operationally available for users to make decisions on planting date. The primary research question for the chapter is:

How can historical weather information and numerical models be integrated for deciding on the optimal planting date?

The objectives of this study include to:

- Design a methodology for operationally viable decision making on planting date based on the framework TAMSAT-ALERT.
- Explore the link between environmental conditions and optimal planting date to identify decision-making criteria for planting date in western Kenya.
- Demonstrate the application of the new system in western Kenya and compare it with planting decision made based on local advisory, objectively defined season onset method and farmers practices.

5.2 Data and methods

5.2.1 Study area

The research was conducted in western Kenya between 1.5°N and 1.5°S latitudes and 34.0°E and 35.5°E longitude. The choice of the region for the case study emanates from the availability of field data regarding farmers planting time and observed crop yield from One Acre Fund (`https://oneacrefund.org/`) for further evaluation of the new planting date decision-making tool developed in this study. The region is characterized by mountains to the east and flat land to the west reaching to Lake Victoria. Figure 5.1 shows the study area with the topography map of the region where the colors represent height above sea level. The climate of the region is humid to sub-humid , shown on Figure 5.2, with average annual rainfall of about 1100 to 1800 mm with a bi-modal seasonal cycle, average temperature 15°C –18°C and a growing period of 180–270 days for sub-humid and above 270 days for humid regions (Kamoni et al., 2007; Kinyanjui et al., 2014). Figure 5.3 indicates the average daily rainfall of the study area. The long rainy season occurs from March to May whereas a short rainy season is not distinct in the region as the region receives rainfall June throughout November. Planting takes place mainly during the March to May rainy season and our research thus focuses on this rainy season (Jaetzold et al., 2006; Mutiga et al., 2015). The explanation of the seasonal cycle of precipitation in the eastern Africa region is discussed in section 4.2.

5.2.2 Data used

The meteorological variables required for the planting date decision-making tool we propose are long-term daily records of precipitation, surface temperature, air temperature, pressure, wind speed, specific humidity and diurnal temperature range. All these data sets, except precipitation, are obtained from the National Center for Environmental Prediction (NCEP) re-analysis (`ftp://ftp.cdc.noaa.gov/Datasets/ncep.reanalysis/surface\_gauss/`, last accessed: August 2018) (Kanamitsu et al., 2002). These data sets are used to drive a soil moisture model (chapter 3) to estimate soil moisture levels and calculate water requirement satisfaction index (WRSI) for Maize. These reanalysis data are chosen because they are updated frequently and are easily accessible. The daily precipitation estimates are obtained from Climate Hazards Group InfraRed Precipitation with Station data (CHIRPS) which is derived based

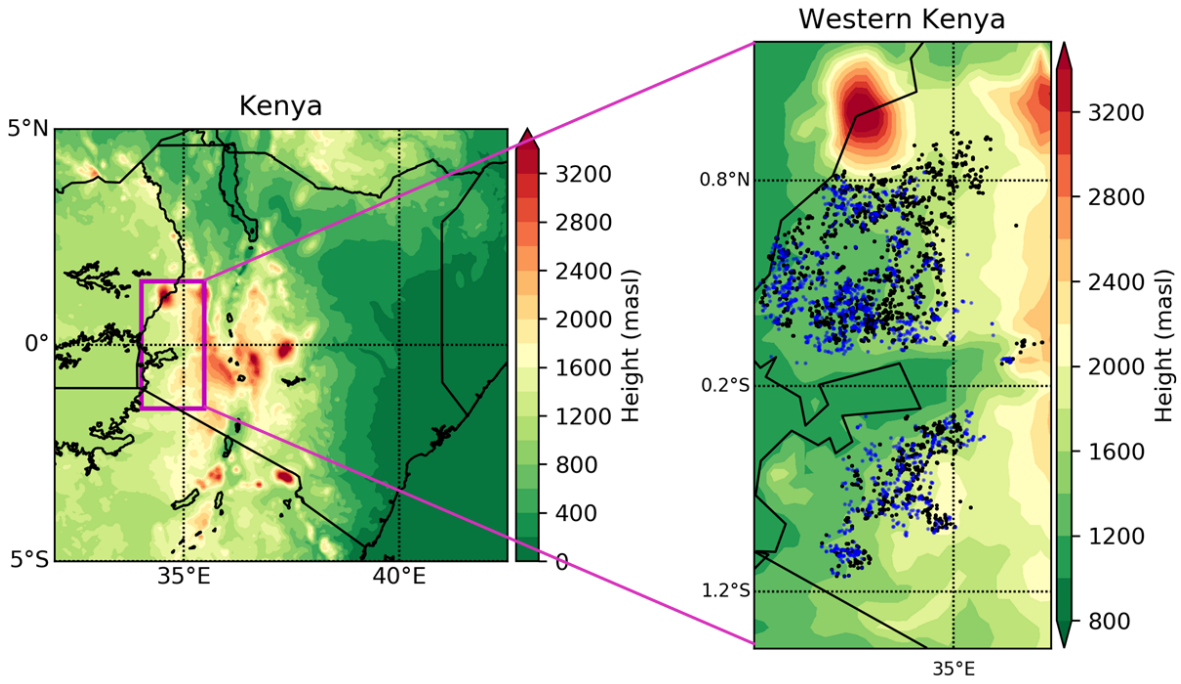

Figure 5.1: Study area with the topography of the region (color representing height above sea level in meters) and farmers field locations for 2016 season (black dots) and 2017 season (blue dots).

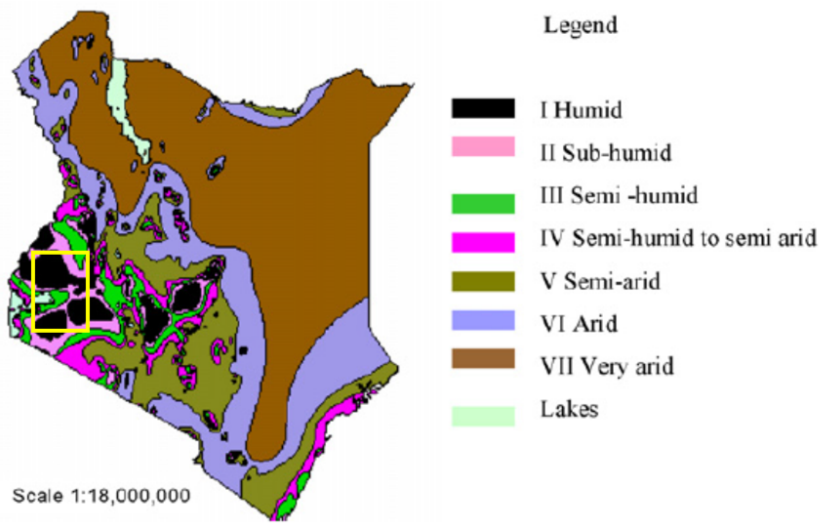

Figure 5.2: Map depicting the climate-zones of Kenya and the location of the study area (yellow box), Figure adapted from (Kamoni et al., 2007)

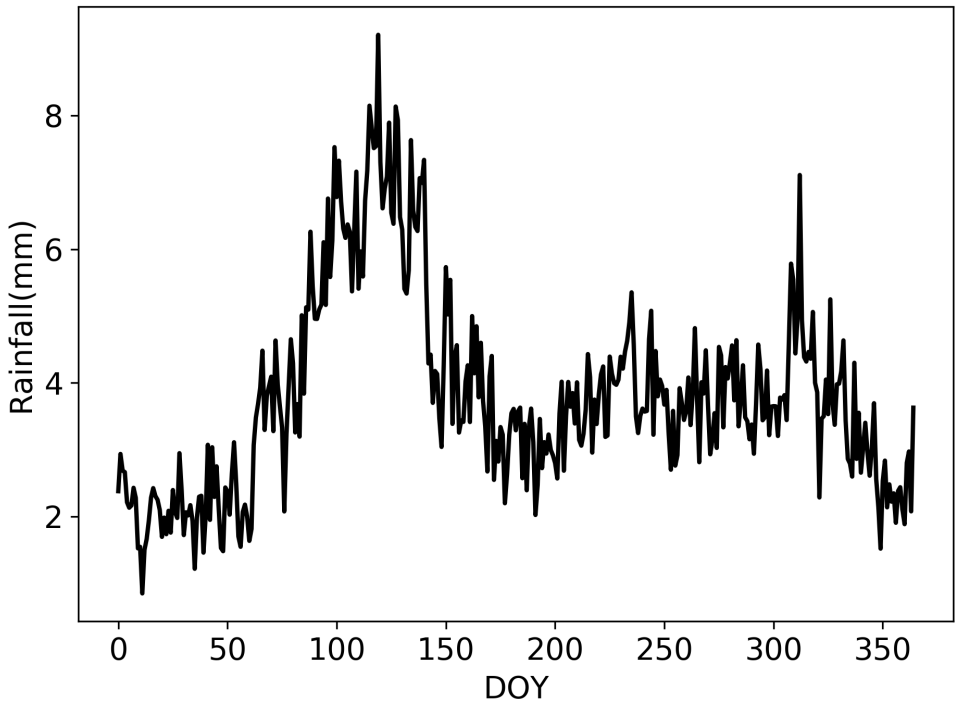

Figure 5.3: Climatological daily average rainfall of western Kenya (1983–2012). The main farming practice in the region is conducted in the long rainy season period of MAM where most of the annual rain occur.

on a combination of satellite rainfall estimates derived using Infrared satellite observation of cold cloud duration (CCD) and gauge data from Global Teleconnections systems (GTS) and privately held records (`ftp://ftp.chg.ucsb.edu/pub/org/chg/products/CHIRPS-2.0/global\_daily/netcdf/p05/`, last accessed: August 2018) (Funk et al., 2015). CHIRPS is one of the widely used rainfall products in Africa in areas of designing drought monitoring and global environmental changes (Funk et al., 2015). The product provides a daily rainfall estimate at a 0.05° spatial resolution. CHIRPS combines a 0.05° resolution of satellite images and data from ground stations to form a gridded rainfall time series. The second version of CHIRPS provides an improved daily rainfall time series (1981-present) with a spatial resolution of 0.05° ranging from 50° S to 50° N and the product is updated regularly (Funk et al., 2015). CHIRPS has been used for applications like drought monitoring (Funk et al., 2015), impacts of climate change and global environmental applications (Abiodun et al., 2017; Zambrano-bigiarini et al., 2017), development of improved precipitation estimate (Ceccherini et al., 2015) and species distribution modelling (Deblauwe et al., 2016).

Planting date and yield data from 4686 farmers for the 2016 season and 1489 farmers for the 2017

season over the study area were provided by One Acre Fund (`https://oneacrefund.org/`, last accessed: August 2018) which is a non-governmental institute working in eastern Africa providing farming advice. One Acre Fund collected this data during field visits by extension workers. The data contain farmers location, planting date of crop (Maize), different agronomic practices used (fertilizer applied, compost amount applied), problems that were encountered in the season (drought and poor germination) as well as yield values estimated by crop cuts from two $40m^2$ areas of each farmers field selected randomly by the extension workers of One Acre Fund. During pre-processing of this data, incomplete data records were removed and therefore, only 2647 farmers from 2016 season and 1404 farmers from 2017 were used for this study.

5.2.3 Methodological approach

This study presents an estimate of optimal planting date for western Kenya using three methods based on local expert judgment for the start of the season, objective estimation of season onset and a combination of soil moisture and Water Requirement Satisfaction Index (WRSI). The methods for optimal planting date estimation are:

1. One Acre Fund method (1AF)
2. Onset method
3. TAMSAT-ALERT planting date method (TAMSAT-ALERT PD)

The first approach is taken from One Acre Fund, which provides farming advisory services to farmers in the region. The fact that most farmers and agricultural agents working on the field use rainfall onset as a critical factor for making their decision on planting date, but there are no defined rules on how to make this decision except a rule of thumb like planting after three days of consecutive rainfall. The second approach emanates from the onset of a season determined in an objective way as described in Dunning et al. (2016), where rainfall onset is determined by evaluating the cumulative rainfall anomaly. This onset method is proved to be useful in identifying the onset date of the season and it can be used to assess agricultural risk besides its advantage of using only daily rainfall as a parameter. The third approach, TAMSAT-ALERT PD, is based on the idea that when deciding planting date farmers face the risk of losing seedling germination ability by planting early and the risk of passing the main rain period to meet the water need by the crop

during the flowering period if they plant their crop late. Therefore, it assumes that the optimum planting time is always balancing these two risks. Section 5.2.3.1, section 5.2.3.2 and section 5.2.3.3 present details of the methods.

5.2.3.1 Method 1: One Acre Fund planting advisory method

The One Acre Fund planting advisory method (1AF) consider a three-day consecutive rainfall ($\geq 5mm$ rainfall on each day) after the rainy season starts which is in March for the region on average as planting date. This is the current planting advisory provided by One Acre Fund for farmers in the study area.

5.2.3.2 Method 2: Onset method

This method uses the rainy season onset to determine planting date. Identification of the onset of the season is based on the cumulative rainfall anomaly where the season starts at the minimum of the anomaly and ends at the maximum point of the anomaly (Dunning et al., 2016). The onset method is based only on a single parameter of daily rainfall and it is proved to determine season onset effectively (Dunning et al., 2016; Liebmann et al., 2012). Moreover, the method accounts for false onset, which might lead to a prolonged dry spell forcing crop germination failure. Figure 5.4 shows how the method of rainy season onset work as described in (Dunning et al., 2016). The technique follows a two-step approach to identify the season onset where initially the climatological water season (i.e. the period of the year when the wet season occurs) is determined (green line in Figure 5.4) by cumulating climatological daily mean precipitation anomaly (blue line in Figure 5.4). The climatological daily mean precipitation anomaly is calculated by subtracting the climatological daily mean rainfall from the climatological daily mean precipitation (red line in Figure 5.4). The minimum and the maximum (the magenta dots) of the cumulative daily mean rainfall anomaly (green line in Figure 5.4) mark the extent of the climatological water season. At the second stage, onset dates are identified for any year by computing the daily cumulative rainfall anomaly minimum value between -50 to +50 days from the start of the climatological water season (Dunning et al., 2016).

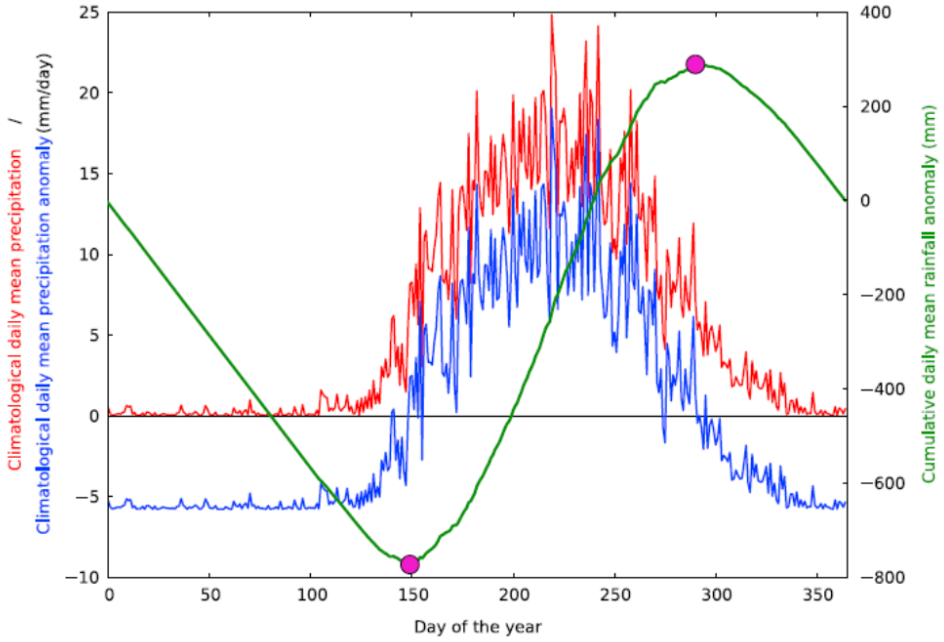

Figure 5.4: Climatological daily mean rainfall for each day of the year (red), climatological daily mean rainfall anomaly (blue), and climatological cumulative daily mean rainfall anomaly (green) for 9.5°N, 14.5°W from GPCP averaged over 1997-2014. The magenta dots mark the extent of the climatological water season. Figure adopted from (Dunning et al., 2016).

5.2.3.3 Method 3: TAMSAT-ALERT planting date method

TAMSAT-ALERT planting date method (TAMSAT-ALERT PD) considers two factors to identify optimum planting date. First Water Requirement Satisfaction Index (WRSI) of crops calculated from historical weather data and the second the topsoil layer (0.1 m) moisture during planting (chapter 3). Based on the two factors, TAMSAT-ALERT PD answers the following two questions:

a) What is the climatological WRSI for a given planting date?

b) What percentage of the topsoil layer field capacity (PFC) of the soil water is expected to be available in the next 14 days after planting?

The specific criteria used for this study in western Kenya are described in detail below.

Water Requirement Satisfaction Index (WRSI)

WRSI refers to the ratio of cumulative actual crop evapotranspiration to the cumulative potential evapotranspiration over the growing period of a crop (Senay and Verdin, 2003). WRSI describes how much water is available for plants to grow without water stress where a value of one indicates no water stress and zero value indicate complete dryness (section 3.2.3). Figure 5.5 shows WRSI

values for a single location in western Kenya. For each planting date of the year, WRSI value for maize crop was calculated based on a climatological period of 30 years (1983–2012). The grey lines represent the ensemble WRSI value and the red line shows the climatological mean WRSI value for the location. The climatological mean WRSI value can then be used to determine the planting window period based on a user-defined threshold percentage of WRSI from the maximum amount of WRSI for any location so that planting occur within a reasonable period where sufficient water satisfaction rate could be found. Figure 5.6 shows the maximum value of WRSI value that can be achieved in western Kenya. The southwestern part of the region there is a higher WRSI value and in the northern part the maximum level WRSI is low indicating lower rainfall in the area.

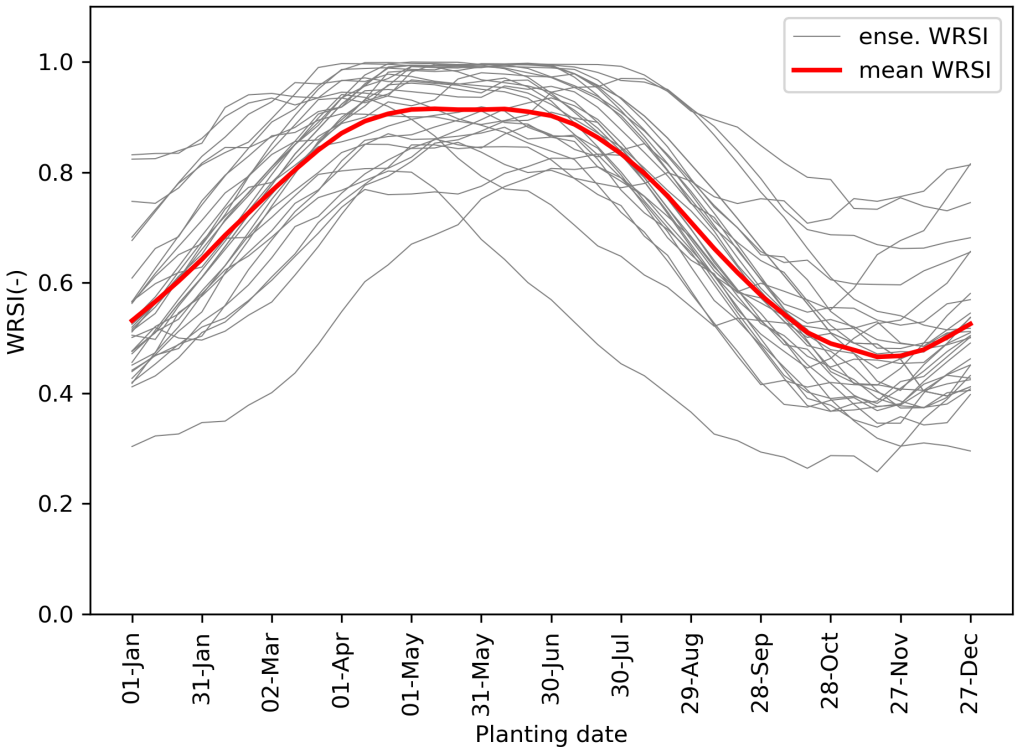

Figure 5.5: Historical WRSI for a location in western Kenya ($0.88°N, 34.88°E$). The grey lines represent the ensemble of WRSI for a climatological period of 30 years (1983–2012) and the red line indicate the mean WRSI value (Figure D.1.1 for other locations in Appendix D).

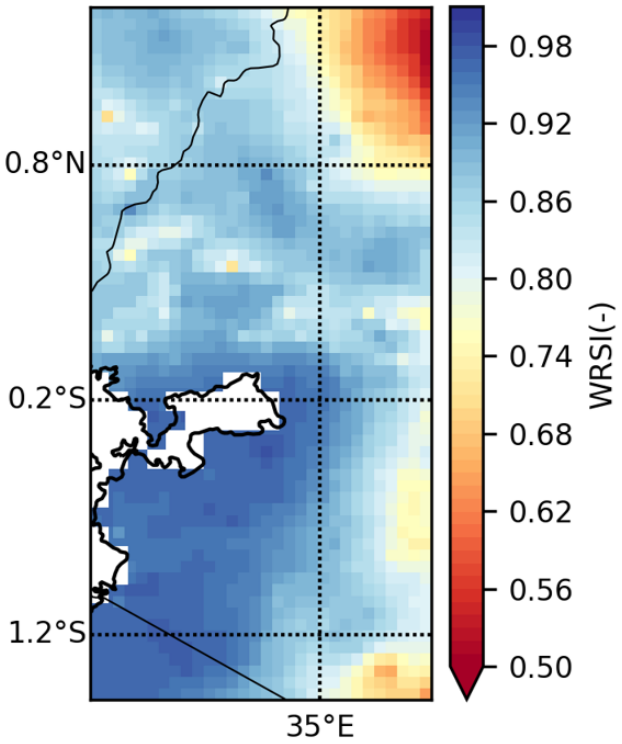

Figure 5.6: The maximum climatological WRSI value that can be achieved in the study area.

Percentage Field Capacity (PFC) of the soil

For seeds to properly germinate, the moisture in the soil needs to be enough and no drying should occur at all. In general, it would take five to seven days for germination depending on the crop and temperature and water content of the soil. The seedling survival depends on what happened with in the first two weeks after planting; therefore, the first 14 days soil moisture were considered. The critical level of soil moisture for crops is different, but it needs to be sufficient enough to facilitate seed germination and survival until the plant roots are strong enough to utilise the moisture in the lower soil layers. First, the percentage field capacity (PFC), which is the ratio of the soil moisture of the top 0.1-meter soil and the field capacity of the soil in the same soil layer, was calculated using Equation 5.1. The PFC of the soil is predicted using the soil moisture model discussed in chapter 3. After identifying the PFC of the soil, users can set a critical percentage field capacity (crPFC) to determine when planting can take place. This crPFC is dependent on the willingness of farmers to take a risk and their experience in the past season hence choosing low critical value results in early planting within the planting window determined by the WRSI and choosing higher value results in late planting within the planting window. Figure 5.7 shows an example of the TAMSAT-ALERT PD method.

$$PFC = (\frac{\theta}{\theta_{fc}}) * 100 \tag{5.1}$$

where θ Soil moisture of the first layer and θ_{fc} represent the soil moisture level at field capacity where field capacity of the soil is 80% of soil saturation.

The TAMSAT-ALERT approach described in chapter 2 was used to forecast the 14-day soil moisture level starting from a forecast day. Soil moisture forecasting is done by running the soil moisture model with historical data up to the date of the forecast to obtain a realistic representation of the antecedent soil moisture and after that by using 30 years of climatological data (1983–2012) from the day of forecast onward, creating 30 ensemble members. The mean of the ensembles of PFC is compared with a different critical PFC (crPFC) value to identify a single optimum planting date for recommendation.

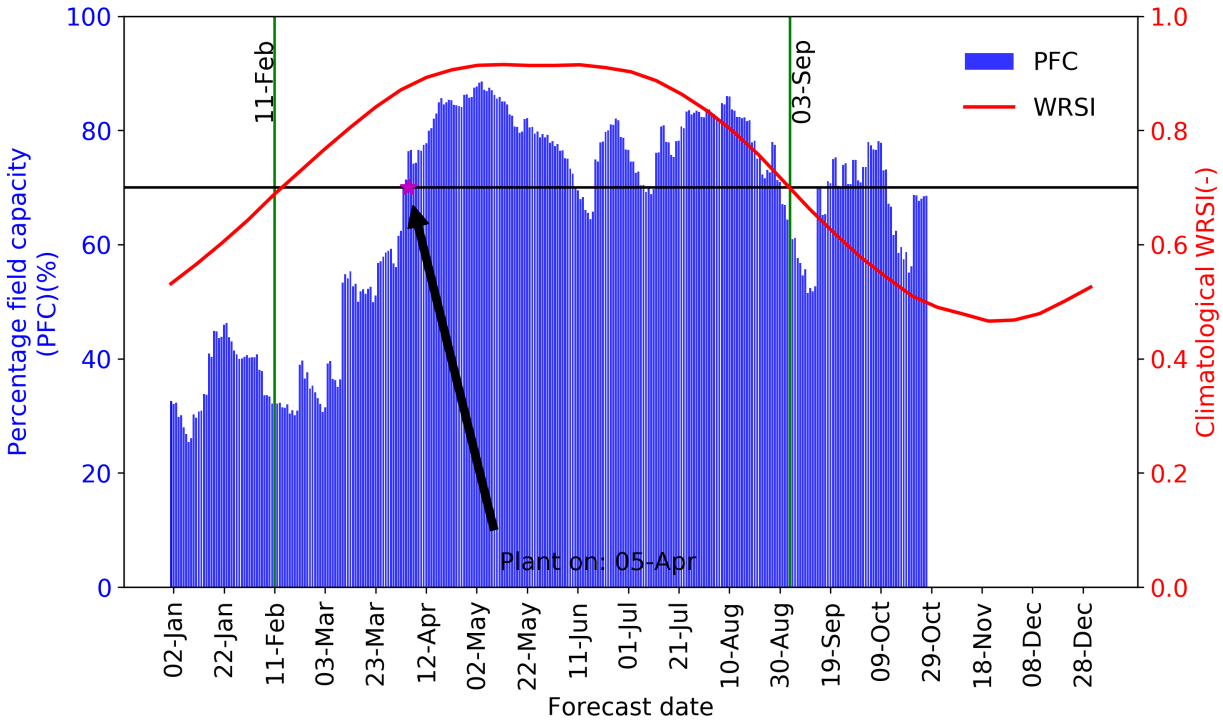

Figure 5.7: TAMSAT-ALERT planting date decision-making methodology example for a location in western Kenya ($0.88°N, 34.88°E$). Red line indicates the climatological WRSI which will be used to define a planting window in the location by considering a critical WRSI value of 75% of the maximum WRSI. This gives a planting window of $February\ 11^{th}$ till $September\ 3^{rd}$ which is represented by the two green vertical lines. The blue bars represent the percentage field capacity of the 14 days average soil moisture forecast and will be used to determine the planting date within the planting window specified. The black solid horizontal line shows crPFC of 70% and the planting date would be $April\ 5^{th}$ as indicated by the star (Figure D.1.2 for other locations in Appendix D).

TAMSAT-ALERT PD decision making criteria

Based on planting date and maize yield data of farmers in the study area provided by One Acre Fund, the study identified a set of recommended specific decision-making criteria. The two factors used as decision-making criteria are:

1. The planting date should be within the window where critical Water Requirement Satisfaction Index (crWRSI) level is 75% of the maximum for the location (Figure 5.6). The value indicates the level of water stress that a crop will face throughout the growing period that means for a crop planted within the window identified by this critical value, there will be at least 75% of moisture available to supply crop growth. The 75% is an arbitrary choice identified through trial and error for the region so that there will be enough days as a planting window. The crWRSI can be changed by the user depending on the local conditions and willingness to take the risk for planting early or late; by increasing the crWRSI, the number of days in the planting window will be reduced and vice-versa. This criterion was chosen to account that crops will not fail due to moisture stress during the flowering period where water demand is high by the plant and using the 75% matches well with the main growing period in the region.

2. Within the planting window identified in step 1, the first date where the mean of ensembles of the 14-day percentage field capacity (PFC) forecast exceeds a critical percentage field capacity (crPFC) is taken as the recommended optimum planting date. The specific crPFC for the area is set to be 70%. The 70% crPFC value was derived from a sensitivity study for the region and a range of planting dates determined for six crPFC values is shown in Figure 5.10 and Figure 5.11 for the 2016 and 2017 seasons respectively (Appendix D.2).

Figure 5.8 shows the flow chart for the process of optimum planting date decision-making developed (TAMSAT-ALERT PD) for the trial in western Kenya. The process is a two-step process where the first criteria of identifying planting window based on WRSI is run once as it is climatology and it is fixed (represented by the black ellipse). The second step is forecasting soil moisture, which is done every time of the day until obtaining an equal value of the crPFC for each location (represented by the blue ellipse). Blue rectangles represent the input data variables, which include precipitation, surface temperature, air temperature, wind speed, pressure, specific

humidity, and diurnal temperature.

The first step is indicated by the black ellipse. Here, the soil moisture model is run with the crop variables for each day of the year as a planting date. The GDD is the growing degree days for the specific crop used (in this case, maize). The soil texture is the percentage of sand, silt and clay content of the soil, which is used while modelling the soil moisture (here it is set to be loam soil). Based on the input data variables in the blue rectangle, the soil moisture model will be run (chapter 3). The outputs from the first step model run are historical WRSI which will be used to generate the climatological WRSI values. The climatological WRSI values are used to identify a planting window based on a critical WRSI (crWRSI) value of 75% of the maximum WRSI. Those days where crWRSI is satisfied are considered planting widow and the rest will be considered outside planting window (Figure 5.7).

The second step, which is marked by the blue ellipse, is based on bare soil moisture model run (chapter 3) for each forecast date based on similar input data. The model run output in this step are historical and forecasted soil moisture, which will be used to get 14 days mean Percentage Field Capacity (PFC). From this, a decision was made based on the 70% crPFC within the planting window obtained from the first step. Red and green rectangles are the decisions made by the model; green signals recommend planting on the date and red signals to wait.

5.2.4 Implementation of TAMSAT-ALERT PD in western Kenya

Planting window

Planting window in the study area for a maize crop with 160 days average growing period length was identified using a critical water requirement satisfaction index (crWRSI) of 75% of the maximum WRSI. The choice of 75% of the maximum WRSI is to allow a wider planting window in the region and make sure that every location will have a specific window based on the climatological maximum of the area. In western Kenya, regions receive a different amount of more rainfall throughout the year- this results in varying WRSI where in some part there is enough water to supply for crop and some areas there will not be sufficient water to provide for the crop. Therefore, the choice of planting window needs to be site-specific because waiting for the highest WRSI value will not work everywhere. Figure 5.9 indicates the identified start of planting, end of planting and the window length for western Kenya, which is based on climatological (1983–2012)

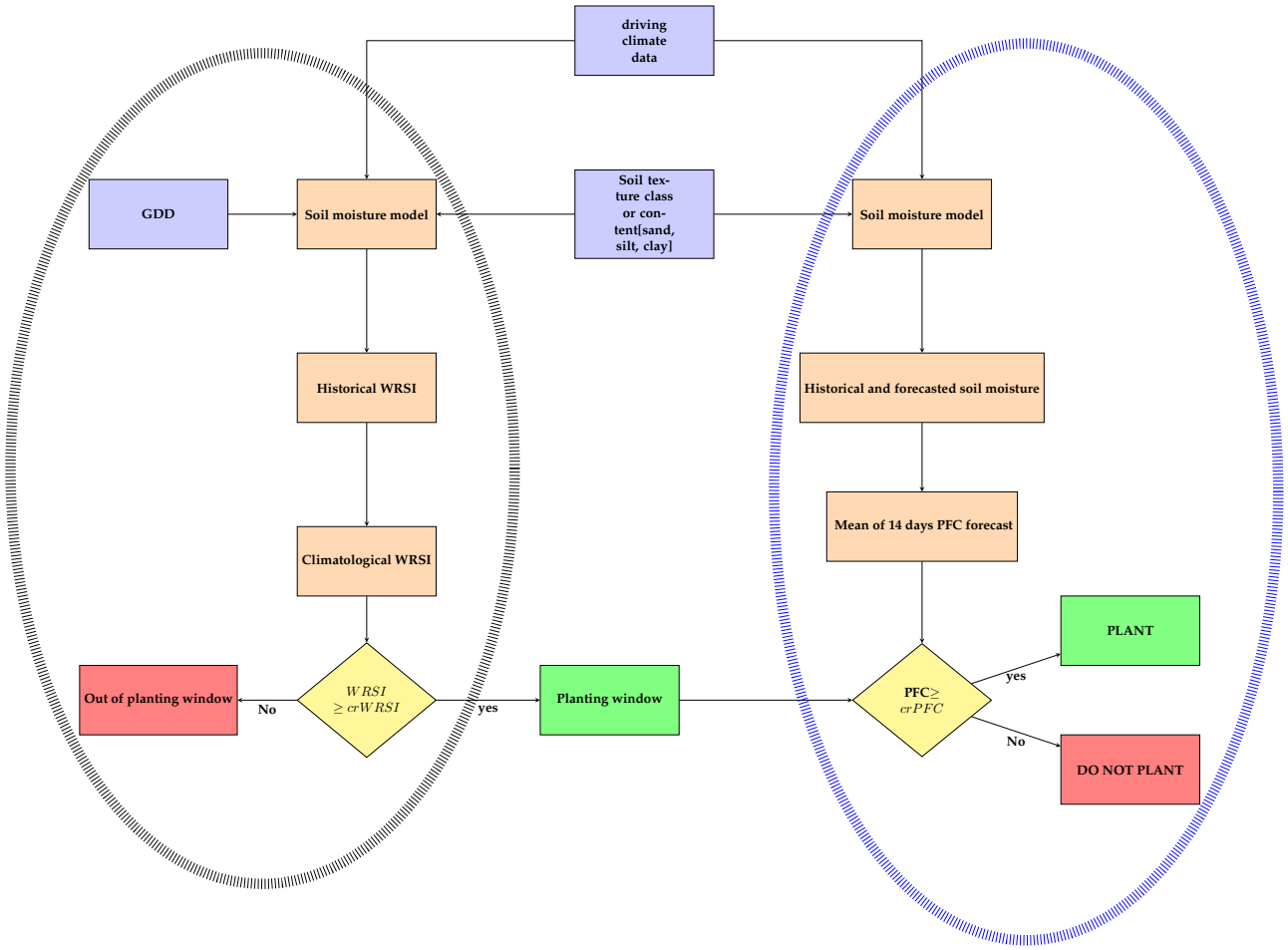

Figure 5.8: TAMSAT-ALERT planting date decision-making (TAMSAT-ALERT PD) model flow chart. TAMSAT-ALERT PD run in two steps where the black ellipse represents the first step where planting window is identified, whereas the blue ellipse is the second step where the optimum planting date is identified. Blue rectangles represent the input data variables to the model, while the orange rectangles are the model processes with the final output of the processes. Yellow diamond boxes are where decisions are made based on the criteria given in the boxes. Red and green rectangles are the decisions made by the model, where green recommend planting on the date and red indicates to wait.

mean WRSI values. The figure indicates that in western Kenya planting can start as early as January and end very late in August with all the region having planting window of over 150 days.

Comparing the planting window and the farmer's practice described in section 5.3.1, even though there is a possibility to plant early in the season most farmers prefer to plant late into the season in 2016 (Figure 5.13(a)). But for the 2017 season, farmers shifted their planting earlier by almost a month (Figure 5.13(b)) and this is in line with the planting window start

date. The FAO crop calendar for the region (Nyanza and Western provinces of Kenya) suggest that the primary growing season planting for maize is from day 59 to day 115 of the year (`http://www.fao.org/agriculture/seed/cropcalendar/welcome.do`). This window is short compared to what is suggested based on the WRSI- this is because the WRSI system is identifying a one season maize growth while FAO calendar identifies two seasons growing where a second season planting starts from day 213 to day 304. The contributing factors for the wide planting window are the maize variety, set by the total GDD required until maturity (section 3.2.3), which results in a 160 days total length of growing period, the region is wet with a large amount of rainfall and the choice of 75% of the maximum WRSI.

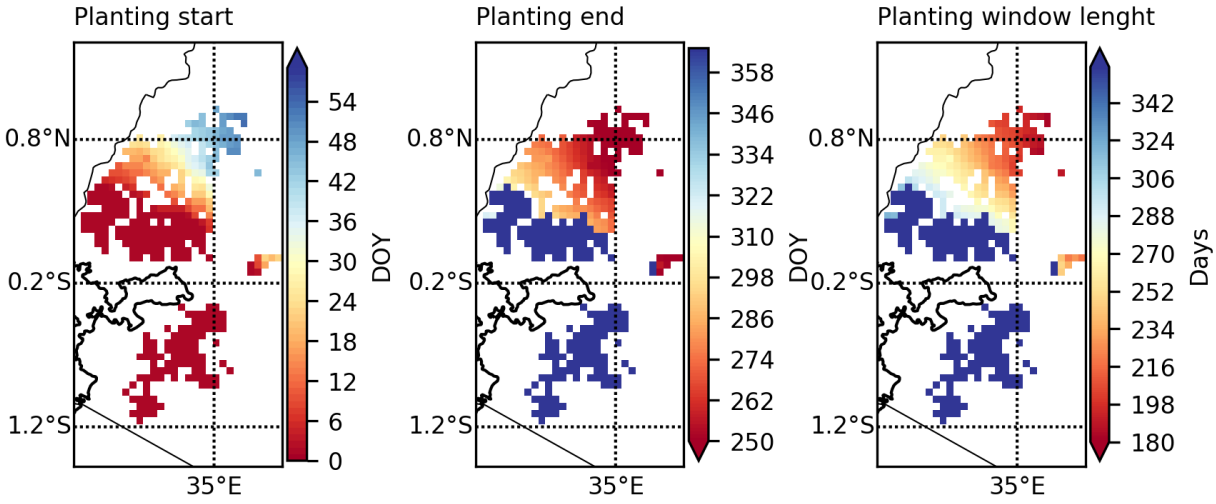

Figure 5.9: Start of planting, end of planting and planting window for maize crop with a 160 days total length of growing period and a critical WRSI value set at 75% of the maximum WRSI.

Optimum planting date

Identifying an optimum planting date for a recommendation was done using three methods as described in section 5.2.3. One Acre Fund method and Onset method are based on the precipitation only whereas the third method involves the use of WRSI and soil moisture. For the third method, additional critical values for critical WRSI (crWRSI) and the percentage field capacity (crPFC) are required (section 5.2.3.3). In western Kenya, there is a wide planting window allowing planting to start as early as January. Figure 5.10 and Figure 5.11 show the planting date identified for 2016 and 2017 season using six crPFC values (55%, 60%, 65%, 70%, 75% and 80%). The figures indicate that lower crPFC result in early planting recommendation, while higher crPFC values result in late planting. Based on the relatively lower moisture requirement for maize germination compare to other crops and comparison of the farmers yield data obtained from One Acre Fund (Appendix

D.2), a crPFC value 70% is considered for detail comparisons of planting date advisory based on TAMSAT-ALERT PD method. Section 5.3.2 discusses the comparison of the planting date recommendation from the three methods.

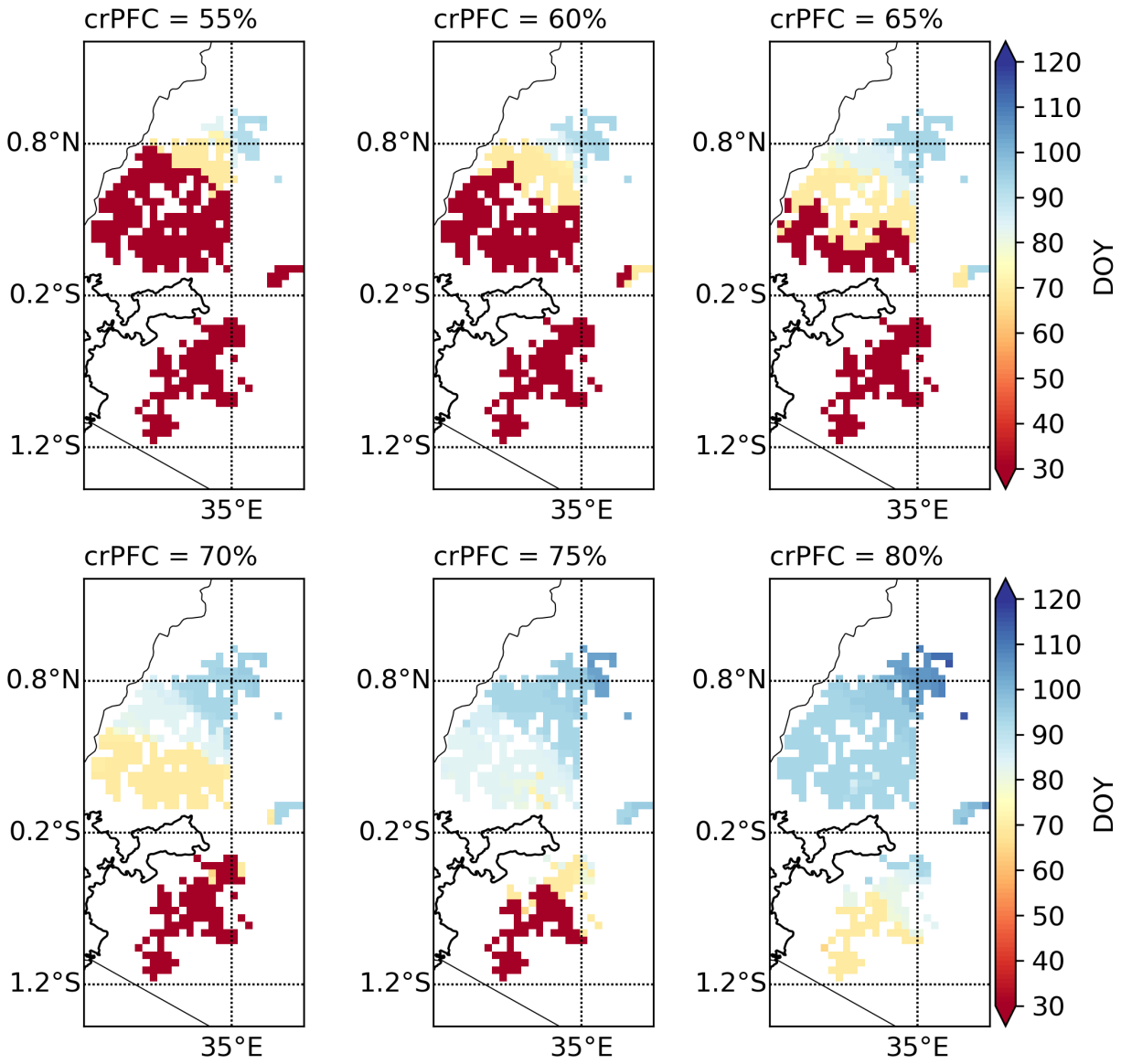

Figure 5.10: Planting dates determined based of 6 levels of critical percentage values ranging from 55% to 80% for 2016 season. (DOY represent day of year)

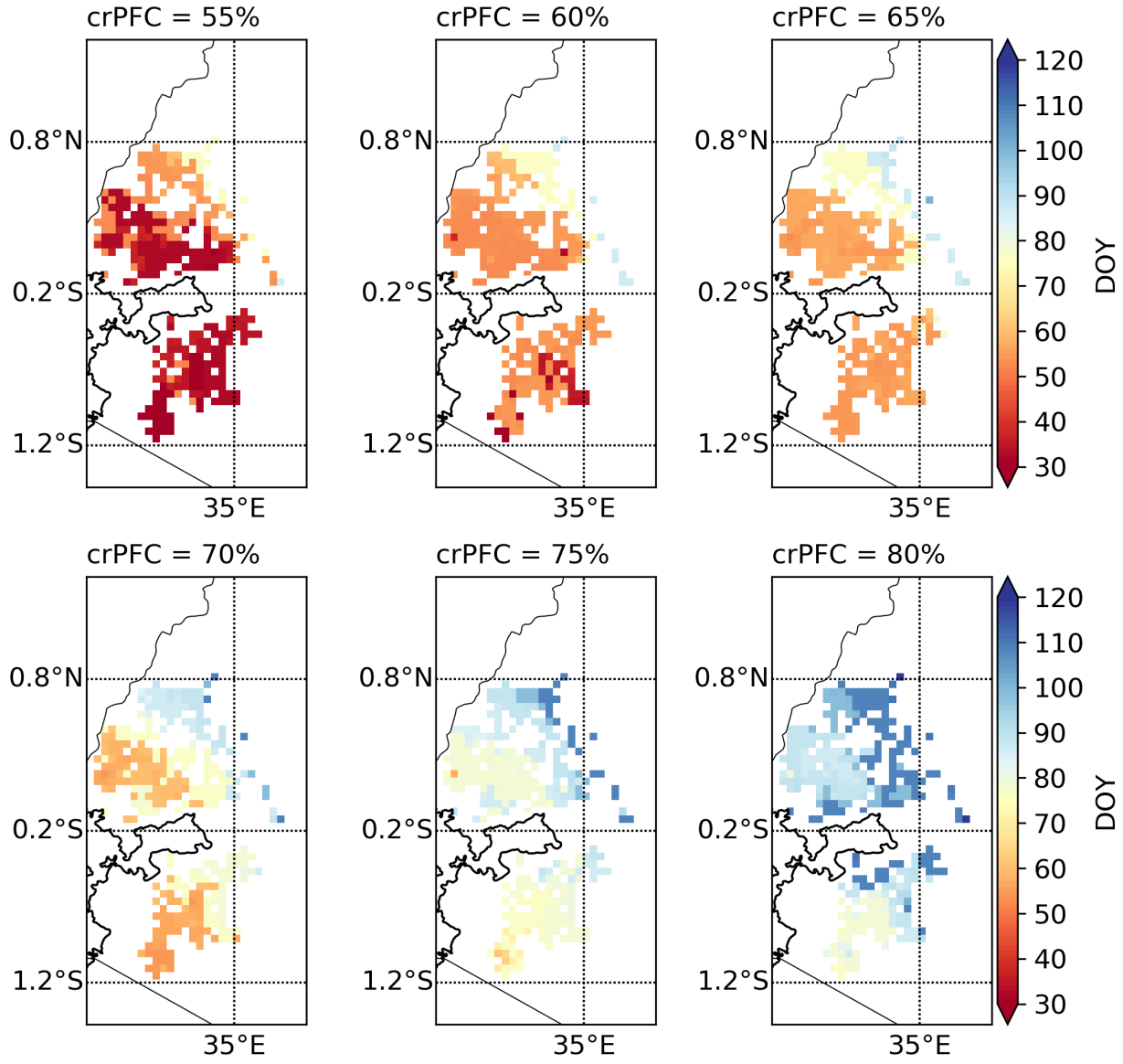

Figure 5.11: Planting dates determined based of 6 levels of critical percentage values ranging from 55% to 80% for 2017 season. (DOY represent day of year)

5.3 Results

An assessment was done in western Kenya based on rainfall data from CHIRPS rainfall data (Funk et al., 2015) and other climatic variables from NCEP reanalysis (Kanamitsu et al., 2002) for western Kenya region planting date recommendation at a 0.05 degrees of spatial resolution using three methods described in section 5.2.3. Two growing seasons (2016 and 2017), for which farmers planting information was available from the region, were analysed against farmers choice of planting time to evaluate the method.

5.3.1 Farmers practice on planting date

Figure 5.12(a) shows the cumulative rainfall from January to June for the season 2016. In the early part of the season from mid-February to end of March, rainfall was below the climatology, but starting end of March to April, the cumulative rainfall values show a rapid increase and most farmers start planting during this time as indicated in Figure 5.12(b). Figure 5.12(c) shows a similar cumulative rainfall for 2017 season and the season was dry from January until the start of March, but there were high rainfall amounts which increase the cumulative rainfall followed by a dry period in last weeks of February. The farmers preference to plant early in the last two weeks of February and early two weeks of March (Figure 5.12(d)) matches with the increase in cumulative rainfall for the season. In general, these figures indicate that farmers in the region follow the rainfall pattern to start planting which reiterate that the region is a precipitation limited area for maize planting forcing farmers to plant around the start of the rain (Sacks et al., 2010).

Comparing the two seasons, in 2016 farmers plant starting late in March through April while in 2017 most farmers plant very early in February and first two weeks of March. This corresponds with the sharp increase in rainfall for starting planting time, but the early planting in 2017 was followed by dry periods which could have a significant impact on the germination and proper growth of seedlings in the early stage of crops. Even though there could be many reasons for farmers to shift their planting time like availability of labour, seed, fertiliser and desire to plant a second crop after the harvest of first crop (Hassan, 1996); previous year experience could also be one reason as the case of farmers in Burkina Faso (Ingram et al., 2002). Though it is hard to conclude based on two seasons of data for western Kenya farmers, in 2015 the rainfall was significantly lower than the climatology and farmers probably remember this experience and tend to avoid the risk of planting early in 2016. Whereas for 2017 the previous season 2016 had a normal rainfall amount hence this experience might give farmers in the region to plant earlier in 2017.

Figure 5.13 shows the spatial variability of farmers planting time in 2016 and 2017 season. In both seasons, the farmers planting is spatially variable which reiterates the fact that there are more factors than just the rainfall condition in farmers planting time preference (Hassan, 1996), and in many regions of SSA, farmers use indigenous knowledge mostly of non-climatic reasons for planting (Waongo et al., 2015).

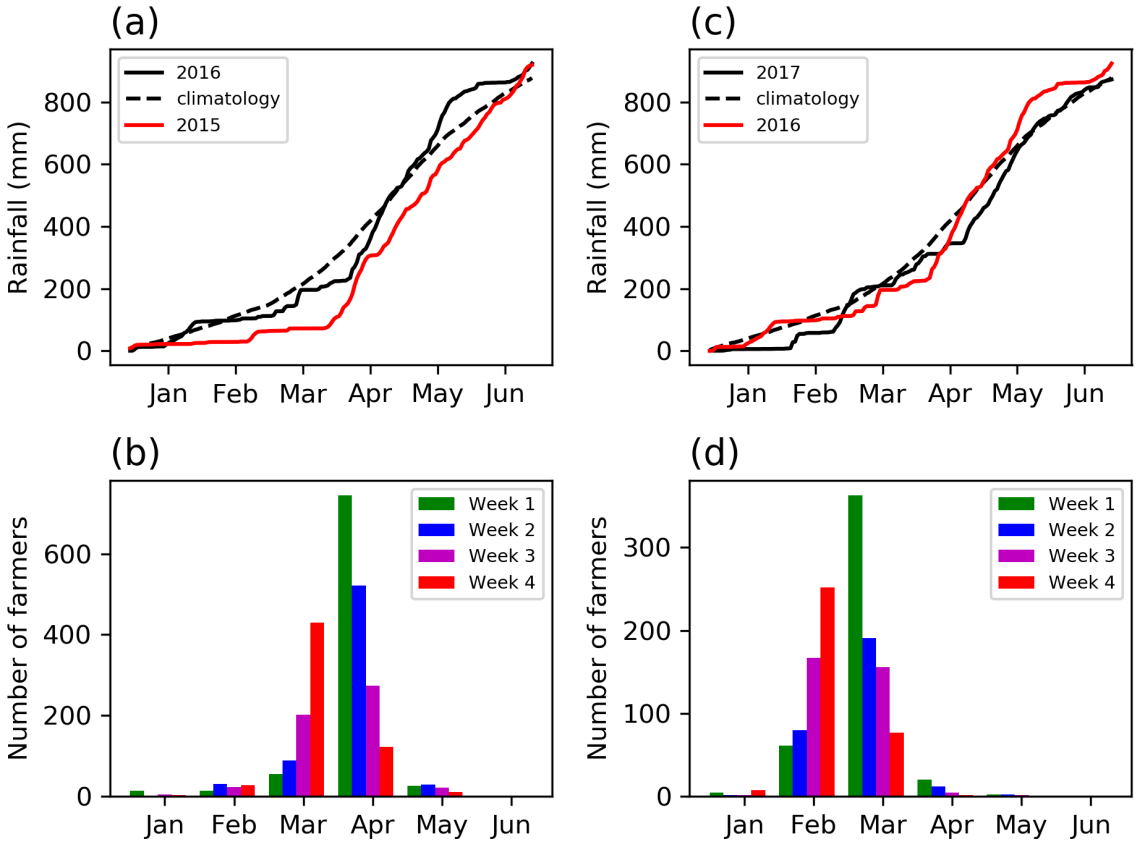

Figure 5.12: (a) 2016 season cumulative rainfall, (b) Farmers planting time by week for 2016 season, (c) 2017 season cumulative rainfall and (d) Farmers planting time by week for 2017 season.

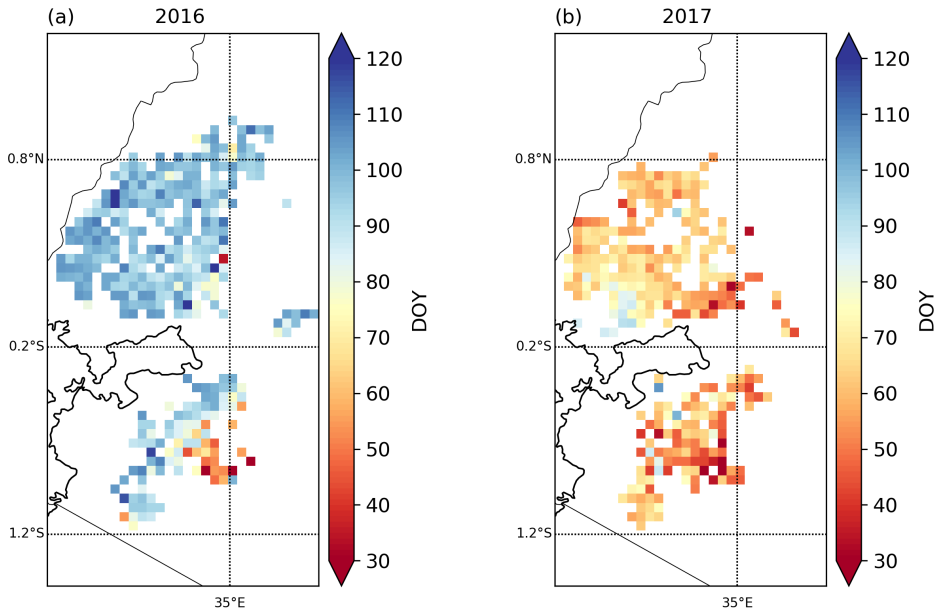

Figure 5.13: Spatial distribution of farmers planting date for (a) 2016 and (b) 2017 season.

5.3.2 Comparison of planting dates

Figure 5.14 shows the spatial and temporal distribution of planting date recorded for framers and the three methods used to define planting date. The figure indicates that farmers planting date choice is spatially diverse, whereas the planting date recommendation given by all the three methods show less variability; however, the methods identify a cluster of regions with different planting date for western Kenya. In 2016 season the farmer's planting time was from February to May ($\sim$ day 30-150) (Figure 5.12(a)), whereas the recommendation from One Acre Fund method shows two distinct planting periods ($\sim$ day 70-75 in the south and central part and $\sim$ day 100-110 for the north-west part of the region). The result is expected as the planting recommendation by this method is fixed to be after March in line with One Acre Fund practice. The rainfall onset method provides a single planting time for all the region ($\sim$ day 90-100) except for few grid points in the south, which indicate much earlier planting time. Rainfall onset is based on objective criteria; hence, it provides a similar onset for the region for this season. Though the farmers planting practice is diverse, majority of the farmers start planting after the onset of the season, which is a common practice of farmers in SSA (Ingram et al., 2002; Wang et al., 2008; Marteau et al., 2011). TAMSAT-ALERT PD provides an early planting recommendation in the southern part of the region (before $\sim$ day 30), $\sim$ day 70-80 for the central part and $\sim$ day 85-95 for the northern part of the region. TAMSAT-ALERT PD shows a clear pattern of late planting as we move from south to north, creating clusters of regions with similar planting time recommendation. In 2017 season, on the other hand, farmers plant their crop earlier than the 2016 season (Figure 5.12(c)) while One Acre Fund method identifies two planting time recommendations $\sim$ day 90-100 in the south and northeast of the region and $\sim$ day 60-70 in the northwest area. The rainfall onset method, on the other hand, identifies planting to be $\sim$ day 45-50 in the northwest part and few locations in the south. Other than this, it recommends planting in $\sim$ day 70-75 in the south and late planting ($\sim$ day 100-105) in the northwest part. TAMSAT-ALERT PD showed the planting time to be in three distinct times for different regions similar to the 2016 season. Early planting in the south and northwest ($\sim$ day 55-65), second region in southwest and north with planting recommendation in $\sim$ day 70-75 and lastly a late planning recommendation ($\sim$ day 90-95) northeast part.

The rainfall onset method is better in identifying the season onset as the farmers planting time better matches with the onset method for 2016 season and has only a slight variation for 2017 sea-

son (Figure 5.14). This indicates that the 1AF method of identifying season onset is not a viable approach compare to the more objective-based method of onset identification described by Dunning et al. (2016). However, both methods rely on rainfall onset, making the practicality of using it for operational planting date identification difficult as forecasting rainfall amount is hard. Here the methods are only presented to see what farmers had followed in the past in retrospective. The new method TAMSAT-ALERT PD accounts WRSI and soil moisture for deciding on planting date; hence, it is different from the other two methods mentioned. Compared to farmers practice, TAMSAST-ALERT PD was not able to replicate the planting time diversity of the farmers, but it helps to identify regions where we could recommend similar planting time.

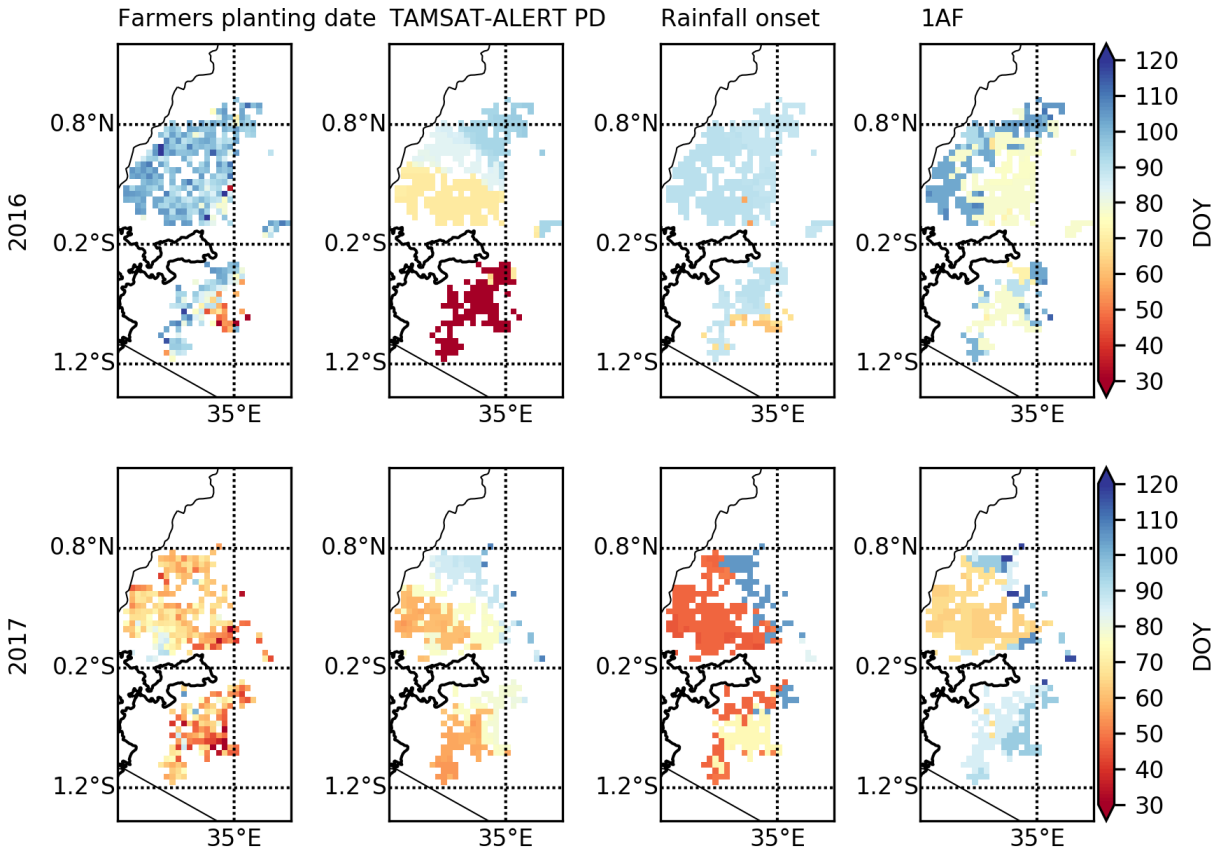

Figure 5.14: Farmers planting date and recommended planting dates based on the three methods TAMSAT-ALERT PD, Rainfall onset method and One Acre Fund method.

The optimal planting time is considered to be the time that reduces the risk of replanting during the first stage of the crop and that will lead to relatively low moisture stress during the period where the plant is more sensitive to water stress (Waongo et al., 2014; Sacks et al., 2010). Figure 5.15 shows WRSI values for farmers and recommended planting dates by the three methods. In 2016 season the WRSI values for the three methods show that the northwest region had over 0.90 WRSI

and parts of the south and northeast region had a slightly lower WRSI of 0.75–0.85. A similar result is observed for 2017 season too where WRSI value is above 0.80 throughout the area. The figure indicates that in western Kenya, there will be enough water for the plants despite the difference in planting time. However, this does not mean the planting time recommendation is optimal; instead, comparing farmers maize yield with the recommended planting time is important in understanding the impact of planting time.

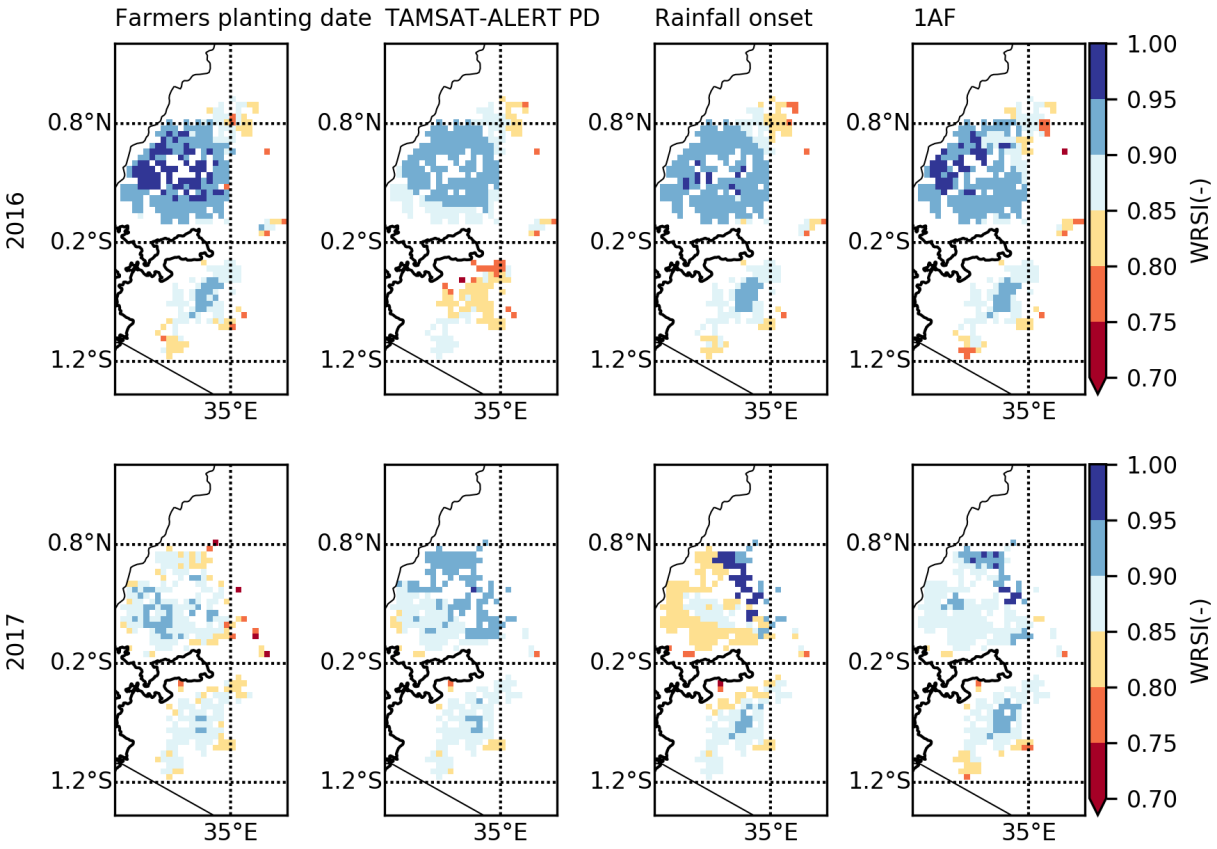

Figure 5.15: WRSI values for a maize crop with 160 days average growing period for the different planting dates identified by the methods for 2016 and 2017 seasons.

5.3.3 Yield comparison

Comparing planting date from the recommendation by the three methods with what farmers are using as planting date does not give a full representation of the optimum planting date. Therefore, to assess the value of the recommendations, a comparison between reported farmer yield against the difference between the actual date of planting and the date that would have been recommended by each of the three methods was made. For the comparison, the yield data were binned based on the difference between actual and recommended planting date (using 10-day

bins) and Figure 5.16 and Figure 5.17 show the results related to the number of farmers and yield respectively. Figure 5.16(a) indicates that in 2016, most farmers plant their crop later than the recommended planting date by TAMSAT-ALERT PD method. The average yield obtained declined for those farmers who planted late by >20 days, while the yield obtained makes no significant difference for those farmers who planted within 20 days from the recommended date (Figure 5.17(a)). Similarly, Figure 5.16(b) shows in 2017, most of the farmers plant within a ten days range from the recommended planting date or earlier than the recommended date. Those farmers who plant earlier than the recommended date obtain high yield compared to those who plant later than the recommended planting time by TAMSAT-ALERT PD. Especially those farmers who were late by >20 days got significantly reduced yield as shown in Figure 5.17(b).

Table 5.1 and Table 5.2 show the statistical comparison for the yield obtained by farmers who planted after the recommended planting dates by the three methods. Based on TAMSAT-ALERT PD, it indicates that for 2016, those farmers who plant very late (over +30 days) obtain significantly lower yield (yield reduction of up to 0.75 tha^{-1} which is 26% of the average yield for the season) and those farmers who plant within the first 30 days after the recommended date did not improve their yield. In 2017 those farmers who plant late (over +30 days) did not get significantly low yield even though the amount is still lower than those who planted on the recommended date. However, the number of farmers who planted in this period was less than 40; hence, the yield result is not necessarily an indicator. For the other two methods based on rainfall (One Acre Fund and onset method), the results indicate a mixed feature. In 2016 the One Acre Fund method show farmers who plants late get higher yield value and the onset method for the same season show those who plant over +50 days get significantly lower yield and those who planted before this time get a higher yield. In 2017, those who plant after One Acre Fund and onset method recommendation got substantially lower yield. However, looking at the number of farmers who planted over 40 days from the recommended date by the two methods, the number of farmers were low (<100 farmers) compared to those who planted before this period. This signifies that in the comparison of yield obtained, the first 30 days after the recommended date is more crucial. In those early 30 days from the recommended time by One Acre Fund and onset methods, the yield makes no significant difference in 2016 season and reduced significantly in the 2017 season.

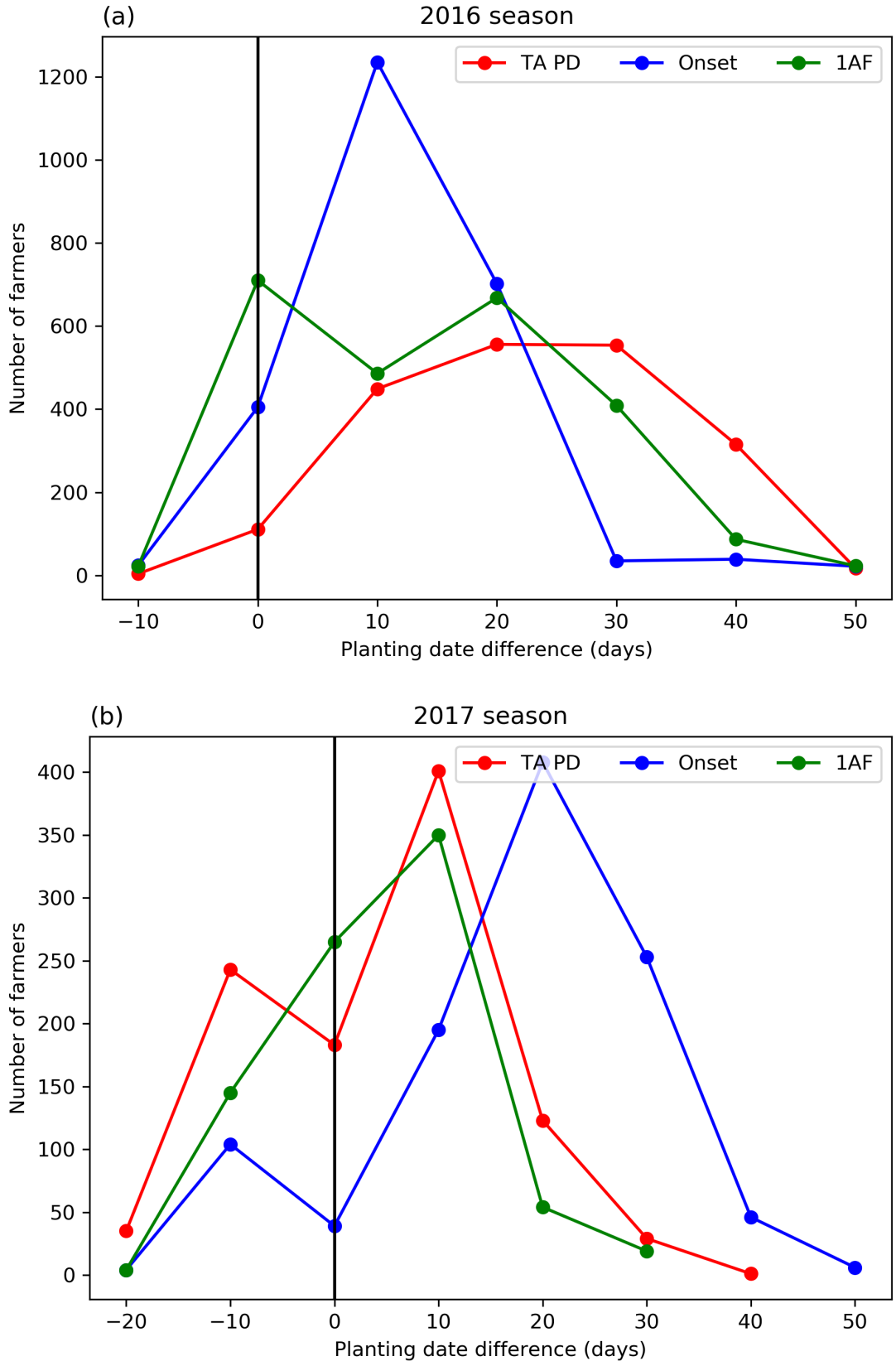

Figure 5.16: Comparison of number of farmers and difference between farmers and recommended planting dates. The black solid line indicate the recommended planting date by the three methods and negative values in the $x-axis$ indicate early planting by farmers while positive values indicate late planting.

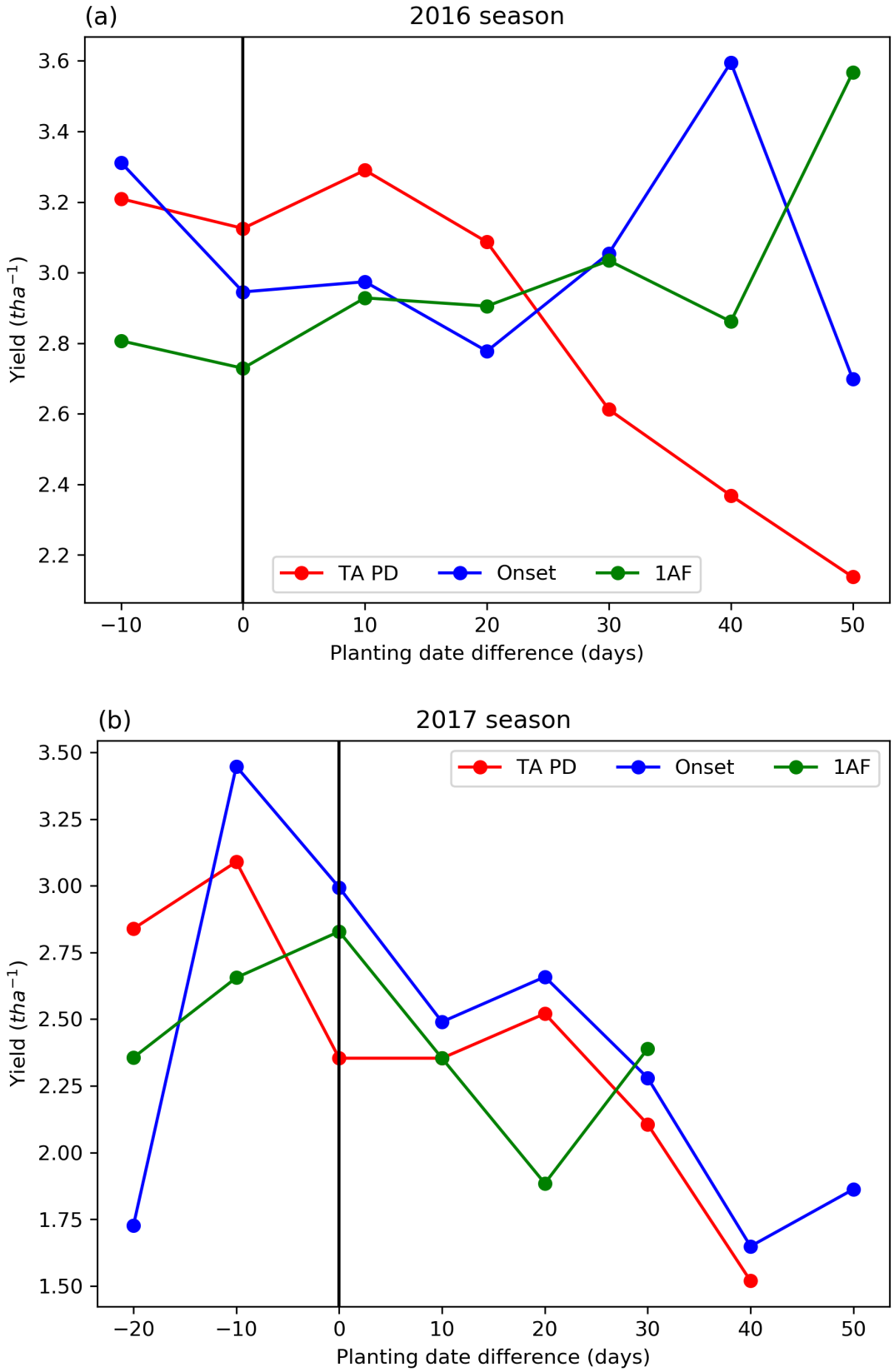

Figure 5.17: Comparison of average yield and difference between farmers and recommended planting dates. The black solid line indicate the recommended planting date by the three methods and negative values in the $x - axis$ indicate early planting by farmers while positive values indicate late planting.

Table 5.1: 2016 season average maize yield (tha^{-1}) and p-values for yield comparison obtained by farmers after the recommended planting date by the three methods.

Days from recommendation	2016 season								
	1AF			Onset			TA-PD		
	#farmer	yield	p-val	#farmer	yield	p-val	#farmer	yield	p-val
+ 0 days	710	2.73	-	405	2.94	-	111	3.12	-
+ 10 days	486	2.93	1.0	1235	2.97	0.91	449	3.29	0.90
+ 20 days	668	2.90	1.0	702	2.77	2.9E-13	556	3.08	0.38
+ 30 days	409	3.03	1.0	35	3.05	0.69	554	2.61	2.9E-5
+ 40 days	87	2.86	0.91	39	3.59	0.99	315	2.36	1.3E-7
+ 50 days	23	3.56	1.0	22	2.69	4.9E-4	17	2.13	6.0E-7

Table 5.2: 2017 season average maize yield (tha^{-1}) and p-values for yield comparison obtained by farmers after the recommended planting date by the three methods.

Days from recommendation	2017 season								
	1AF			Onset			TA-PD		
	#farmer	yield	p-val	#farmer	yield	p-val	#farmer	yield	p-val
+ 0 days	265	2.82	-	390	2.99	-	183	2.35	-
+ 10 days	350	2.35	0.0	195	2.49	1.2E-4	401	2.35	0.50
+ 20 days	54	1.88	4.8E-15	408	2.65	3.9E-3	123	2.52	0.99
+ 30 days	19	2.39	0.04	253	2.28	2.3E-8	29	2.10	0.11
+ 40 days	-	-	-	46	1.64	6.6E-16	1	1.52	-
+ 50 days	-	-	-	6	1.86	8.2E-5	-	-	-

5.4 Discussion and Summary

Information regarding optimum planting date is crucial and many methods have been developed to optimise planting date to maximise yield (Sacks et al., 2010; Waongo et al., 2015; Dobor et al., 2016; Bussmann et al., 2016). These methods are based on different approaches of using climatic information (rainfall and temperature) and continuous evaluation of planting dates through

using crop models and selecting dates that result in higher yield. There are also methods based on expert judgment and others based on statistical probability distributions around local planting time. This chapter presented a new method of identifying optimum planting date using Water Requirement Satisfaction Index (WRSI) to define a planting window to assure sufficient water availability from the rainfall throughout the season and enough soil moisture for the first two weeks after planting for the survival of seedlings. A comparison between the new method (TAMSAT-ALERT PD) and two other methods (1AF and Rainfall Onset), which are based on rainfall onset, was made. Based on farmers practice for two seasons (2016 and 2017) of maize crop planting time, the methods were evaluated in western Kenya.

The results indicate that in western Kenya, where there is no concrete rule for planting date decision except a rule of thumb recommendation by agricultural advisory service providers like One Acre Fund, farmers tend to follow their own rule despite the recommendation given by farming advisory service providers. This is evident from the results shown in Figure 5.12 and Figure 5.13, where farmers planting time is temporally and spatially variable. Farmers planting time tends to peak in a single week; first week of April in 2016 and the first week of March in 2017 (Figure 5.12(b) and Figure 5.12(d)) however planting starts from February and extends to end of May making it a wide window used by farmers for planting maize in the region. The planting time of farmers follows the rainfall pattern in the area. In 2016, for instance, farmers plant late as the season was a normal season with no significant high rainfall events. In 2017 they started planting earlier due to high rainfall conditions, but a dry spell followed the planting time (Figure 5.12) and this prolonged dry spell at the beginning of the season is the main concern of farmers in SSA resulting a major risk of replanting and crop failure in the first stage of the plant development (Waongo et al., 2014). Despite the risk farmers face with dry spells, western Kenya is a region where rainfall plays a significant role in limiting crop growth compared to temperature and in areas which are precipitation limited for farming, farmers tend to plant around the start of the rainy season (Sacks et al., 2010). Comparing the planting date recommendation that would have been given based on the three methods presented in this chapter, all the three methods were not able to replicate the variability of planting time choice by farmers (Figure 5.14). This is mainly due to other factors associated with farmers planting date decision making at an individual level like seed and labour availability.

The rainfall based methods used for planting date estimation in this chapter use different criteria for setting the onset season. One Acre Fund season onset is a very general method compared to the more objective season onset method by (Dunning et al., 2016). The results of planting recommendation from these methods show that the peak number of farmers planting time coincide with One Acre Fund method recommendation for 2016 and deviates by 10-days for 2017, whereas the objective-based season onset method recommendation deviates 10-days in 2016 and 20-days in 2017 from the farmers practice, indicating farmers were inclined to plant after some rainfall occurrence (Figure 5.16). However, the recommended planting dates that would have been given to the farmers did not result in yield difference had the farmers followed it. The result of this was presented and discussed in section 5.3.3. The farmers who planted during the recommended time or after the recommended time showed no significant difference or resulted in a high yield decreased (Figure 5.17). The results also indicate that even though farmers base their planting time on the onset of the season, they were not following any of the advice given to them by One Acre Fund.

The new method TAMSAT-ALERT PD utilises WRSI and PFC (soil moisture) (section 5.2.3.3) where these two criteria are basic decision criteria that link the environment with planting time. The method accounts for the historical weather condition in the region and soil moisture instead of using only rainfall. Rainfall does not immediately translate to available soil moisture for crops; hence, using soil moisture, as a parameter to define planting time is close to the crop. Since the method uses estimated soil moisture, the value of the antecedent moisture from previous weeks and months is accounted for. A high antecedent soil moisture at the beginning of the season allows for better germination of crops even when the rainfall is deficient. Murungu et al. (2003) evaluated the effect of soil matric potential on emergence of maize and showed that low matric potential (-10KPa) (wet soil) results in a 100% emergence of maize seeds whereas high matric potential (-50KPa) (dry soil) results in only a 2% seed emergence. Similarly, during planting date decision making a wet soil moisture anomaly allows for early planting and better utilisation of the rainy season than a season with dry soil moisture anomaly in which the initial few days and weeks of rainfall will infiltrate to replenish the deeper soil layer which takes more time. This will delay planting and result in a short growing season, which could lead to crop failure due to moisture shortage during the flowering time of the crop. The results of planting date recommendation form TAMSAT-ALERT PD identified clusters of regions with

similar planting time over the western Kenya region (Figure 5.14). However, the method was not able to replicate the farmers planning time variability. The mismatch between farmers practice and the recommended planning date by TAMSAT-ALERT PD is expected because farmers planting decision is not solely based on weather conditions, but also determined by the availability of labour for farm work, seeds and fertiliser (Sacks et al., 2010). Dobor et al. (2016) also discussed a similar condition where objective methods of identifying planting date based on climatic factors do not reproduce observed planting time as farmers decision on planting is highly subjective. Also, comparing planting time and maize yield obtained by farmers in the area TAMSAT-ALERT PD identifies the optimum planting date that results in higher yield and showed that those farmers who planted after what would have been given as a recommended date by TAMSAT-ALERT PD obtained a significantly decreased yield or found no significant difference (Figure 5.17). Therefore, the recommendation using the TAMSAT-ALERT PD would be to advise farmers to take the risk of planting earlier. By planting earlier farmers will also benefit through the extra period in which they can plan a second crop planting in the remaining season.

In summary, planting date optimisation is a common strategy for improving yield even though there are many known crop management practices to enhance crop productivity mainly because changing planting date incurs no cost on farmers and farmers are in full control of it. Hence, better-informed advice on planting date can benefit farmers by reducing the risk of crop failure, which will occur due to moisture shortage at the beginning of the season as a result of prolonged dry spells after plating or during the flowering period due to missing the primary rainy season. Here, a new method is presented to estimate planting date for rainfed agriculture and demonstrated the potential to be used operationally in western Kenya. The method indicates that only using the rainfall as criteria might not lead to correct date of planting, instead combining soil moisture into the system can improve to effectively identify planting date allowing to control false alarms of season start that might lead to the wrong conclusion of planting date decision. The method also showed the potential to incorporate historical weather data into an operational system that can support practical decision making in the farming practice. TAMSAT-ALERT PD is a generic method that can be applied to any region and crop type. It can be run on any personal computer and requires only a few hours to run hence it can be an additional tool for climate service providers to generate valuable information on planting time for their users out of the climate data they provide.

Chapter 6

Summary and future work

6.1 Summary

In Sub-Saharan Africa, countries are facing higher climate risk associated with climate variability; the need for climate service providers to make usable climate information available on time for end-users to make an informed decision based on climatic data is paramount. With this in mind, the overall theme of this work focused on developing and accessing new ways determining meteorological risk on agriculture at short and long time scale and the information that can be provided to end-users to make an informed agricultural decision. To achieve the overall theme, the following research questions were developed:

1. What information about meteorological risk on agriculture can be derived from local and regional meteorological observations and forecasts?
2. Can simplified versions of a complex land surface model be used to represent agricultural risk decision metrics?
3. How robustly do model outputs such as soil moisture and Water Requirement Satisfaction Index (WRSI) represent agricultural drought compared to meteorological based metrics such as Standardized Precipitation Index (SPI)?
4. How can historical weather information and numerical models be integrated for deciding on the optimal planting date?

This thesis developed a new framework for assessing climatic risk on agriculture and demon-

strated the application of the new framework for seasonal scale agricultural risk assessment like low crop yield and drought as well as short term critical decision like choosing a planting time. This chapter summarised the key outcomes of the thesis and answers each of the research questions.

6.1.1 Developing a new framework for assessing climate risk on agriculture

In sub-Saharan Africa, where many people build their livelihood in farming and animal husbandry the role of climatic information is significant. Especially, with increased climatic variability and changes that have occurred in the past three decades over African; climate and weather-related information that is specific, timely, and easy to understand plays a vital part in supporting farmers, policymakers and aid agencies mitigate devastating risk associated with the climate. The major players of such climatic information provision in Africa are the national meteorological services, regional climate centres and global institutes run by different agencies such as NASA-CPC. These institutes utilise satellite data, ground-based measurements and weather forecasts from numerical models at a regional and global scale to monitor the risks and adverse events like drought and flood over the continent. Chapter 2 discusses the development of a new operational framework called Tropical Applications of Meteorology using SATellite data and ground-based measurements-AgricuLtural EaRly warning sysTem (TAMSAT-ALERT) and answer the first research question:

What information about meteorological risk on agriculture can be derived from local and regional meteorological observations and forecasts?

TAMSAT-ALERT is a new framework which provides early warning of meteorological risk to agriculture. TAMSAT-ALERT combines information on land surface properties, seasonal forecasts and historical weather to quantitatively assess the likelihood of adverse weather-related outcomes, such as low yield (chapter 2) and drought occurrence (chapter 4). The result demonstrates how monitoring and forecasting information can be combined to identify the climatological risk to maize yield as early as 6–8 weeks before harvesting, whereas incorporating tercile seasonal forecasts of rainfall and temperature showed no impact on maize yield (chapter 2) even though these tercile forecasts are routinely provided. Chapter 2 also showed that the new framework could be used as a test-bed for assessing the value of probabilistic seasonal forecast information.

At a seasonal time scale, TAMSAT-ALERT was used to predict agricultural drought occurrence within a growing season and it anticipates agricultural drought 2–3 months in advance before the end of the growing season (chapter 4). Additionally, at a shot-term timescale, the TAMSAT-ALERT framework helps to address a critical decision on the optimum planting date (chapter 5). The result indicates that farmers in western Kenya can take the risk and plant earlier than their current practice.

Overall, the newly developed framework – TAMSAT-ALERT helps to derive climate risk on maize yield and agricultural drought occurrence within the growing season and identify an optimum planting time from the historical weather data, the current state of the land surface from numerical models and seasonal forecasts. Such an operational framework has a wide range of potential application in advancing the information provided to farmers and decision-makers in Africa. TAMSAT-ALERT is a simple and adaptable platform for any impact model to measure meteorological risk; hence, national climate service centres can easily adapt the framework as part of their current agricultural advisory service. Moreover, TAMSAT-ALERT can serve as an early warning system and provide guidance for decision-makers. This work is presented in (Asfaw et al., 2018).

6.1.2 Developing soil moisture model

Complex land surface models require skilled personnel and computational power to operate most of them are developed accounting global or regional spatial scale making them more generalised in terms of the output they provide. Meteorological service providers in sub-Saharan Africa are also required to cope up with this ever changing subject of utilising numerical models, but their capacity is limited making them more dependent in other institutes results and only engaged in downscaling results rather than tailoring the products to their need. A key reason for this arises from the complexity of the land surface models, legal issues with accessing the model code and above all, the lack of skilled experts. Hence, chapter 3 focus in extracting a portion of the more complex JULES model and developing a new lightweight version of the soil hydrology model with additional features allowing for a more tailored output that is relevant to African countries like drought monitoring metrics (chapter 4) and planting time decision metrics (chapter 5). Chapter 3 describes the new soil moisture model and evaluate the results against JULES output, answering the second research question:

Can simplified versions of a complex land surface model be used to represent agricultural risk decision metrics?

First of all, the new soil moisture model developed is written in Python with low computing power requirement but running much faster than the JULES model with resolution comparable to the driving data provided. This is a crucial benefit to users in African countries climate service centres, as many of them lack the high computational power and skill required to operate more complex global models fully. The soil moisture estimate from both the new soil moisture model and JULES model are found to be similar in terms amount and distribution except few variations in the deeper soil layer (chapter 3). The differences in the deeper layers are not significant since the objective of the thesis is related to agricultural risk where the soil moisture in the top 0.35 meters is more significant. Above all the critical outputs soil moisture availability (β) used for decision making on agricultural drought occurrence (chapter 4) and the topsoil layer (0.1 meters) used to make planting date decision making (chapter 5) resulted in similar values that would not change the final decision to be made based on the model output. The additional output variable, Water Requirement Satisfaction Index (WRSI), derived from β in the new soil moisture model correlates well with observed maize yield and helps to anticipate agricultural drought within a growing season (chapter 4).

In general, in addition to its simplicity and low computational resource requirement, the new soil moisture model was able to replicate JULES soil moisture (chapter 3) and proved to be used for predicting climatic risk on agriculture (agricultural drought) within the growing season (chapter 4). Chapter 5 also provide a significant result on using the topsoil layer moisture to make a critical decision like planting date where the decision-making criteria developed helped to identify optimum planting time. Therefore, chapter 3 concludes that the simplified soil moisture model can be used for assessing climatic risk on agriculture.

6.1.3 Drought monitoring within the growing season

Climate variability is affecting African countries through the frequent occurrence of extreme events such as drought and flooding. The Agriculture sector is at the full front of the impact from these extreme events resulting in loss of productivity and subsequently food insecurity for farming communities. Chapter 4 focused on examining the relationship between drought monitoring

metrics and crop productivity as well as monitoring agricultural drought within the growing season. The chapter addressed the third research question:

How robustly do model outputs such as soil moisture and Water Requirement Satisfaction Index (WRSI) represent agricultural drought compared to meteorological based metrics such as Standardized Precipitation Index (SPI)?

Even though there are several drought monitoring tools available to monitor drought (section 1.2.2), monitoring the risk of whole season drought at a regular interval within the growing season has not been done before. Chapter 4 demonstrated drought monitoring within the growing season using TAMSAT-ALERT (chapter 2) in the seasonal time scale for early warning of agricultural drought risk over Kenya. The result indicated that meteorological drought indicator SPI at a 3 months aggregate has a weak correlation with the overall country maize yield. However, correlation improved with 6 months aggregate timescale SPI. The improvement is expected since the meteorological drought indicator like SPI should only be used at a higher time-scale to be used as a proxy for agricultural drought. Using WRSI values estimated by the soil moisture model (chapter 3) over Kenya and relating it with countrywide maize yield the correlation improved a lot compared to the SPI value relationship with maize yield. Therefore, the chapter concludes that WRSI is preferable for agricultural drought indicator than SPI. Chapter 4 also demonstrated drought prediction within the growing season based TAMSAT-ALERT drought forecast for a strong drought season of 2009 over Kenya; the result showed that TAMSAT-ALERT could anticipate drought 2–3 months ahead of the end of the season. Comparing the drought forecast of 2009 from TAMSAT-ALERT at the end of May 2009 with FEWSNET outlook issued in August 2009 TAMSAT-ALERT forecast depicts the picture on the food insecurity that was looming for the season indicating a higher probability value.

Overall, chapter 4 showed that soil moisture based drought metrics is better in representing agricultural drought and answers the call for integrating probabilistic impacts of climate risk on agriculture which is updated through the growing season in African climate service provision (Ingram et al., 2002; Luseno et al., 2003; Hansen et al., 2011). The chapter indicated the possibility to integrate additional products on drought monitoring within the season by using already available climatic data and provide impending drought information for aid agencies and government to

allocate resources for drought mitigation and support.

6.1.4 Identifying optimum planting date

Choosing planting time is one critical decision that every farmer makes in a growing season. The time of planting influence the length of the growing season, the timing of other farming practices like fertiliser application, weeding and harvesting; subsequently, this will contribute to the productivity of the crop planted. However, planting time is also significantly variable depending on the variability in weather, availability of farming equipment, labour and seed. Especially for Sub-Saharan Africa (SSA) where most of the crop production is based on rainfed agriculture system planting time is mainly governed by the start of the season. Maize being one of the staple crops produced in SSA deciding the planting date for this crop is vital for farmers. With this in mind chapter 5 focused on the last research question:

How can historical weather information and numerical models be integrated for deciding on the optimal planting date?

Chapter 5 demonstrates the use of TAMSAT-ALERT framework (chapter 2) in making critical decisions at a shorter time scale by integrating climatological WRSI for determining planting window (historical information) and 14-day soil moisture forecast (numerical model output) for identifying an optimum planting date. The basis of the method is that planting date decision making consider planting date decision is an optimisation between matching the crop period with high water satisfaction and ensuring sufficient moisture in the soil for proper germination and survival of seedlings in the first two weeks after planting. Therefore, the planting decision making tool works by combining water requirement satisfaction index (WRSI) and high soil moisture probability in the top 0.1 meters soil layer determined from soil moisture model explained in chapter 3.

The criteria were evaluated against two growing seasons (2016 and 2017) field data on planting date from western Kenya. The results indicate that farmers planting date is very diverse in western Kenya though there is a peak planting week in both seasons. Comparison of the two seasons in choice of planting time by farmers revealed that 2016 planting was late into the rainy season (April) and in 2017 planting start early in February indicating that farmers somehow are willing

to shift their planting time based on their local knowledge. Comparison of three decision-making criteria for planting date including TAMSAT-ALERT PD, Rainfall onset and One Acre Fund (1AF) showed that the rainfall onset method works for one season but not always. On the other hand, using a 75% critical WRSI from the maximum WRSI of a specific location and a 70% percentage field capacity provides a planting time that helps to maximise productivity in western Kenya according to the new method TAMSAT-ALERT PD. In general, the chapter demonstrates that it is possible to modify the TAMSAT-ALERT framework (chapter 2) for a critical short term decision making on planting time.

6.2 General discussion

The World Meteorological Organisation framework for climate services states the importance of providing relevant climate information for individuals and organisations for making decisions on socio-economic sectors that are highly climate-sensitive. The framework stats five main pillars in the development and delivery of climate services by national institutes engaged in the service provision, which includes co-design, co-produce, communicate, deliver and use climate services (WMO, 2018). One pillar of co-production focuses on the transformation of climate data into climate information and tailoring it for the user to make a relevant decision based on the information (WMO, 2018). In this regard, the overarching aim of the thesis for producing a decision support tool that helps to determine climatic risk on agriculture is in line with the global framework that is set by Global Framework for Climate Services (GFCS). In SSA, where the climate service is mainly focused on providing basic weather information bringing the climate service to the front is essential (Naab et al., 2019). However, many of the SSA countries have not set out policies on how climate information is provided to end-users to make an informed decision regarding climate risk (Naab et al., 2019). Though the GFCS encourage the development and dissemination of climate services, the implementation of such systems is faced with challenges in many developing countries due to lack of resources, skilled personnel, and institutional, political and legal setup of the national climate service provider (Mahon et al., 2019). This thesis produced a framework that these African climate service providers can adapt to their existing system to provide impact-oriented forecasts to their users. For example, integrating the seasonal weather forecasts into the prediction and monitoring of drought and subsequent low yield (chapter 2 and chapter 4) helps to generate additional information from already existing climate data.

A relevant issue regarding climate services in SSA is also delivering contest-specific information to end-users. A recent study in Rwanda suggests that specific and tailored climate information provision will have some trad-off between tailoring the information and providing it at scale due to lack of required data to generate the information (Hansen et al., 2018). TAMSAT-ALERT presents climate risk on adverse events like drought and low yield (chapter 2 and chapter 4), which are more relevant at a regional scale to be used by government and aid agencies in providing necessary support to affected areas. In short time scale decision making at community level TAMSAT-ALERT provide a critical planting time recommendation (chapter 5) which is disseminated in collaboration with local farming advisory service provider (One Acre Fund). Such partnership helps to get crucial feedback for further improvement of the system and address participatory communication processes in delivering the information that is relevant to farmers decision making (Hansen et al., 2018).

Knowing the context in which climate information is provided is vital however in the field of climate-sensitive sectors like agriculture the context is always dynamic and complex (Guido et al., 2019) therefore it is always necessary to understand the context on which the climate information is provided. TAMSAT-ALERT being a new framework it requires extensive training on how to operate it, what information comes out of it and how it can be interpreted to guide the decision of a government, organisations and farmers in their context. Training can be done through the national meteorological services where a shared vision is emerging in understanding the importance of climate information for countries development and the role of national meteorological agencies in playing a critical role for the provision of the information to end-users (Harvey et al., 2019). The importance of non-state actors and NGO has also been noticed in supporting climate service sector through data collection, analysis and interpretation of forecasts to a more actionable product. TAMSAT-ALERT collaboration with One Acre Fund can be an example where an actionable product like planting time (chapter 5) is provided for farmers. The limitation involving non-state actors is that most of the time the product delivery is of limited time till the end of the projects (Harvey et al., 2019) hence, TAMSAT-ALERT approach to provide the relevant information through national meteorological services and well-established farming advisory institute like One Acre Fund helps to avoid the issue of sustainability in the provision of climate service. Developing and delivering planting time decision at the operational level through

collaboration with One Acre Fund using TAMSAT-ALERT is an example showing the potential to use non-state actors to support the climate service agenda in SSA and address utilising the full potential of non-governmental actors especially in their ability to communicate, co-produce and understanding of climate information for decision-making.

This thesis presented a simple but effective methodology of transforming the raw weather and climate data into user-oriented relevant information that can be used by government, farmers and aid agencies addressing some of the recommendations given in the GFCS regarding climate service promotion in low-income countries (WMO, 2018). The overarching aim of developing a decision support tool to assess the climatic risk on agriculture is paramount to many of the SSA countries as many of them put climate change and variability as the significant risk threatening sectors like agriculture and exacerbating the food security problem (Naab et al., 2019). The TAMSAT-ALERT decision support tool presented in chapter 2 is a new approach that considers agricultural risk as a function of the climatic condition over the whole season rather than a result of a single event occurrence. Therefore, it explains the climate risk that farmers are facing through monitoring what has happened up to a certain period and what might happen in the remaining season and compare it to a long term climatology for the area. This approach makes use of already existing climatic data available in many of the national meteorological agencies that are mandated in providing weather and climate information. The TAMSAT-ALERT tool is an excellent addition to an already existing information delivery system in which they can transform the climate data into the impact-oriented assessment for crop yield (chapter 2), drought occurrence (chapter 4) and determine short term critical decisions like planting time (chapter 5). TAMSAT-ALERT is also in line with the GFCS in SSA where it can be operated with some training and available computational resources. Impact-oriented and generic nature of the framework allows for more metrics to be developed and adopted. For example, chapter 2 discussed the use of TAMSAT-ALERT for determining climate risk on maize yield, but it can be used for other major crops in SSA like wheat, millet and sorghum. The metrics used for drought monitoring and subsequent yield reduction in chapter 4 can be adapted to estimate the risk of flooding and the short time scale decisions made using the new tool (chapter 5) can be extended to other critical decisions like fertiliser application timing which is also a crucial agronomic practice in a growing season calendar.

TAMSAT-ALERT can integrate any numerical model driven by climate data; however, a thorough evaluation of the numerical model to be incorporated is vital. The system compares forecasts against historical values, and hence the climatology period sensitivity is one limitation of the system. The soil moisture model included bases in single soil types and thus required new research in understanding the sensitivity of the system and the decisions that come out of the system when using different soil types. Other limitations associated with the TAMSAT-ALERT that require further study include mainly the evaluation of the outcome from the system in various countries besides those presented in the thesis. These evaluations will help to build trust among producers and users of climate information which is a crucial part of the GFCS in improving climate information services.

6.3 Future work

This thesis has developed a new framework for agricultural decision support over sub-Saharan Africa and demonstrated its use in monitoring climatic risk on low yield (chapter 2). Chapter 3 indicated the possibility of extracting small portions of complex land surface models to integrate it with the new framework and utilise it in climate service centres with little capacity to produce tailored metrics related to climatic risk. Chapter 4 and chapter 5 demonstrate the use of the new framework for seasonal time scale on drought monitoring within the growing season, and for short term time scale decision on optimum planting date respectively.

The new framework TAMSAT-ALERT shows promise at monitoring climatic risk on agriculture (e.g. low yield and drought) and opens an opportunity to develop new criteria for identifying optimum planting date. Further studies and developments to improve the use of the framework include:

Evaluating the robustness of the system

The new framework developed in this thesis was evaluated using data sets from gauge record for crop yield estimation (chapter 2) and NCEP and TAMSAT for drought monitoring (chapter 4). However, assessing the robustness of the TAMSAT-ALERT framework based on other data sources is something that could be done to evaluate the sensitivity of the decision outcome from the system. Doing so will help to see how decisions change based on the data source and help to

evaluate the different data sources available to African climate service centres and support them in choosing environmental data for different purposes.

In addition to using different data sources, TAMSAT-ALERT is currently being used to produce forecasts of drought for forecast-based financing systems for aid agencies in Africa. The new forecast-based financing approach for providing aid is based on in-depth forecast information and the risk caused by the adverse events (Coughlan De Perez et al., 2015). TAMSAT-ALERT can play a pivotal role in predicting adverse event occurrence within the growing season for the timely provision of support to mitigate the impact caused by the adverse event. The sector of financial resource allocation based on the likelihood of advert event occurrence is a new approach and further study could be done using TAMSAT-ALERT system.

Evaluating the value of seasonal and sub-seasonal forecasts

Most of the climate service providers in Africa present their forecasts as a tercile seasonal forecast and outlooks based on these tercile forecasts. However, the usability of these forecasts in making practical farm level decision is limited (Walker et al., 2019). TAMSAT-ALERT is a tool prepared to account weather forecasts to assess climatic risk on agriculture and showed the limited value of seasonal forecasts on maize yield estimation (chapter 2). Therefore, TAMSAT-ALERT can be used to evaluate the seasonal and sub-seasonal forecasts efficiency at the local level and select those forecasts which support agricultural decision making.

Additional climate risk study

This thesis focuses only on low crop yield and drought as an adverse event occurring during a growing season (chapter 2, chapter 4). However, there are other climatic risks faced by farmers within the crop growing season like flooding. Hence, predicting flood risk is an essential part of preparing for mitigating the impact on farming and property loss. TAMSAT-ALERT framework modularity allows incorporating any numerical models like flood prediction models, so investigating the possibilities of using the system for flood risk assessment is an additional study that could be done. The challenge of using TAMSAT-ALERT for flood prediction comes from the fact that flooding is an instantaneous phenomenon unlike that of drought which occurs slowly. Therefore, the initial condition of the land surface and the rainfall occurrence in the

previous days will have more impact on flood prediction than drought prediction. This forces to incorporate additional systems like the Markov Chain Model (Haan et al., 1976) to assess the rainfall occurrence on the date of the forecast.

TAMSAT-ALERT is a simple system that makes sharing the system with African climate service centres much easier. One of the fundamental problems associated with poor adoption of decision support tools at the local level is that most of the systems developed do not involve the end-users during the development process (section 1.2.5). Hence, through the sharing of the system, a new opportunity opens where African climate service centres will be able to add their required inputs to develop additional tailored climate risk information to their local situation.

Developing a user interface

Developing a user interface for TAMSAT-ALERT to make its usability simpler is vital. Such a user interface makes the system more easily accessible for end-users to conduct their climate risk assessment and integrate the results with any existing monitoring system available.

BIBLIOGRAPHY

Abiodun, B. J., J. Adegoke, A. A. Abatan, and C. A. Ibe, 2017: Potential impacts of climate change on extreme precipitation over four African coastal cities. *Climate Change*, **143**, 399–413, doi:10.1007/s10584-017-2001-5.

Abramowitz, G., 2005: Towards a benchmark for land surface models. *Geophysical research letters*, **32 (August)**, 19–22, doi:10.1029/2005GL024419.

Abramowitz, G., R. Leuning, M. Clark, and A. Pitman, 2008: Evaluating the Performance of Land Surface Models. *Journal of Climate*, **21**, 5468–5481, doi:10.1175/2008JCLI2378.1.

Adams, P., and C. Vaughan, 2015: www.climate-services.org/ethics. Endorsement. Since 2013, the CSP has. **(October)**, URL www.climate-services.org/ethics.

Adikari, Y., and J. Yoshitani, 2009: Global Trends in Water-Related Disasters : an insight for policymakers. Tech. rep., UNESCO, Paris,France, 28 pp.

Agnew, C., 2000: Using the SPI to Identify Drought. *Drought Network News*, **12 (2000)**, 6–12.

Allaby, M., 2007: *Encyclopidia of Weather and Climate Revised Edition*. Volume i ed., Facts On File An imprint of Infobase Publishing, New York,USA.

AMCOMET, 2013: Integrated African Strategy on Meteorology (Weather and Climate Services). Tech. rep., WMO, Geneva, 37 pp. URL https://www.wmo.int/amcomet/en/pages/integrated-african-strategy-meteorology-weather-and-climate-services.

Asfaw, D., and Coauthors, 2018: TAMSAT-ALERT v1: A new framework for agricultural decision support. *Geoscientific Model Development*, **(February)**, 1–28, doi:10.5194/gmd-2017-316.

Bannayan, M., N. M. Crout, and G. Hoogenboom, 2003: Application of the CERES-Wheat model for within-season prediction of winter wheat yield in the United Kingdom. *Agronomy Journal*, **95 (1)**, 114–125, doi:10.2134/agronj2003.0114.

Barnston, A. G., and M. K. Tippett, 2014: Climate information, outlooks, and understandingwhere does the IRI stand? *Earth Perspectives*, **1 (1)**, 20, doi:10.1186/2194-6434-1-20.

Bauer, H., and Coauthors, 2013: The stomatal response to reduced relative humidity requires guard cell-autonomous ABA synthesis. *Current Biology*, **23 (1)**, 53–57, doi:10.1016/j.cub.2012.11.022, URL http://dx.doi.org/10.1016/j.cub.2012.11.022.

Bayissa, Y., S. Maskey, T. Tadesse, S. J. van Andel, S. Moges, A. van Griensven, and D. Solomatine, 2018: Comparison of the Performance of Six Drought Indices in Characterizing Historical Drought for the. *Geosciences*, **8 (81)**, doi:10.3390/geosciences8030081.

Best, M., R. Essery, and P. Cox, 2009: JULES Technical Documentation MOSES 2.2 Technical Documentation.

Best, M., and Coauthors, 2011: The Joint UK Land Environment Simulator (JULES), model description. Part 1: Energy and water fluxes. *Geoscientific Model Development*, **4**, 677–699, doi:10.5194/gmdd-4-641-2011, URL http://nora.nerc.ac.uk/15031/.

Betts, R. A., and Coauthors, 2007: Projected increase in continental runoff due to plant responses to increasing carbon dioxide. *Nature*, **448**, doi:10.1038/nature06045.

Black, E., H. Greatrex, M. Young, and R. Maidment, 2016a: Incorporating satellite data into weather index insurance. *Bulletin of the American Meteorological Society*, **97 (10)**, ES203–ES206, doi:10.1175/BAMS-D-16-0148.1.

Black, E., E. Tarnavsky, R. Maidment, H. Greatrex, A. Mookerjee, T. Quaife, and M. Brown, 2016b: The use of remotely sensed rainfall for managing drought risk: A case study of weather index insurance in Zambia. *Remote Sensing*, **8 (342)**, doi:10.3390/rs8040342.

Blyth, E., J. Gash, A. Lloyd, M. Pryor, G. P. Weedon, and J. Shuttleworth, 2010: Evaluating the JULES Land Surface Model Energy Fluxes Using FLUXNET Data. *Journal of Hydrometeorology*, **11**, 509–519, doi:10.1175/2009jhm1183.1.

Boko, M., and Coauthors, 2008: Africa. *Climate change 2007: Impacts, adaptation and Vulnerability. Constribution of Working Group II to the Fourth Assessment Report of the Intergovernmental Panel on Climate Change*, 433–467, doi:10.2134/jeq2008.0015br, URL https://cgspace.cgiar.org/handle/10568/17019.

Bond, B. J., and K. L. Kavanagh, 1999: Stomatal behavior of four woody species in relation to leaf-specific hydraulic conductance and threshold water potential. *Tree Physiology*, **19 (8)**, 503–510, doi:10.1093/treephys/19.8.503.

Bondeau, A., and Coauthors, 2007: Modelling the role of agriculture for the 20th century global terrestrial carbon balance. *Global Change Biology*, **13 (3)**, 679–706, doi:10.1111/j.1365-2486.2006.01305.x.

Bonelli, L. E., J. P. Monzon, A. Cerrudo, R. H. Rizzalli, and F. H. Andrade, 2016: Maize grain yield components and source-sink relationship as affected by the delay in sowing date. *Field Crops Research*, **198**, 215–225, doi:10.1016/j.fcr.2016.09.003, URL http://dx.doi.org/10.1016/j.fcr.2016.09.003.

Boyd, E., R. J. Cornforth, P. J. Lamb, A. Tarhule, M. Issa Lélé, and A. Brouder, 2013: Building resilience to face recurring environmental crisis in African Sahel. *Nature Climate Change*, **3 (7)**, 631–637, doi:10.1038/nclimate1856.

Brown, M., E. Black, D. Asfaw, and F. Otu-Larbi, 2017: Monitoring drought in Ghana using TAMSAT-ALERT: a new decision support system. *Weather*, **72 (7)**, 201–205, doi:10.1002/wea.3033.

Bussmann, A., N. A. Elagib, M. Fayyad, and L. Ribbe, 2016: Sowing date determinants for Sahelian rainfed agriculture in the context of agricultural policies and water management. *Land Use Policy*, **52**, 316–328, doi:10.1016/j.landusepol.2015.12.007, URL http://dx.doi.org/10.1016/j.landusepol.2015.12.007.

Canal, N., O. Deudon, X. Le Bris, P. Gate, G. Pigeon, M. Regimbeau, and J. C. Calvet, 2017: Anticipation of the winter wheat growth based on seasonal weather forecasts over France. *Meteorological Applications*, **24 (3)**, 432–443, doi:10.1002/met.1642.

Cash, D., W. C. Clark, F. Alcock, N. M. Dickson, N. Eckley, and J. J. Salience, 2003a: Salience , Credibility , Legitimacy and Boundaries : Linking Research , Assessment and Decision Making. *KSG Working Papers Series*, doi:10.2139/ssrn.372280.

Cash, D. W., W. C. Clark, F. Alcock, N. M. Dickson, N. Eckley, D. H. Guston, J. Ja, and R. B. Mitchell, 2003b: Knowledge systems for sustainable development . *PNAS*, **100 (14)**, 8086–8091.

Ceccherini, G., I. Ameztoy, C. Patricia, R. Hernández, and C. C. Moreno, 2015: High-Resolution Precipitation Datasets in South America and West Africa based on Satellite-Derived Rainfall, Enhanced Vegetation Index and Digital Elevation Model. *Remote Sensing*, **7**, 6454–6488, doi:10.3390/rs70506454.

Challinor, A., T. Wheeler, T. Osborne, and J. M. Slingo, 2006: Assessing the vulnerability of crop productivity to climate change thresholds using an integrated crop-climate model. *Avoiding Dangerous Climate Change*, J. Schellnhuber, W. Cramer, N. Nakicenovic, G. Yohe, and T. Wigley, Eds., Cambridge University Press, London, UK, chap. 19, 187 – 194, doi:https://doi.org/10.2277/0521864712.

Challinor, A. J., E. S. Simelton, E. D. Fraser, D. Hemming, and M. Collins, 2010: Increased crop failure due to climate change: Assessing adaptation options using models and socio-economic data for wheat in China. *Environmental Research Letters*, **5 (3)**, doi:10.1088/1748-9326/5/3/034012.

Challinor, A. J., J. M. Slingo, T. R. Wheeler, and F. J. Doblas-Reyes, 2005: Probabilistic simulations of crop yield over western India using the DEMETER seasonal hindcast ensembles. *Tellus, Series A: Dynamic Meteorology and Oceanography*, **57 (3)**, 498–512, doi:10.1111/j.1600-0870.2005.00126.x.

Challinor, A. J., and T. R. Wheeler, 2008: Crop yield reduction in the tropics under climate change: Processes and uncertainties. *Agricultural and Forest Meteorology*, **148 (3)**, 343–356, doi:10.1016/j.agrformet.2007.09.015, 0412138v1.

Challinor, A. J., T. R. Wheeler, P. Q. Craufurd, C. A. T. Ferro, and D. B. Stephenson, 2007: Adaptation of crops to climate change through genotypic responses to mean and extreme temperatures. *Agriculture, Ecosystems and Environment*, **119 (1-2)**, 190–204, doi:10.1016/j.agee.2006.07.009, 0412138v1.

Challinor, A. J., T. R. Wheeler, P. Q. Craufurd, J. M. Slingo, and D. I. Grimes, 2004: Design and optimisation of a large-area process-based model for annual crops. *Agricultural and Forest Meteorology*, **124 (1-2)**, 99–120, doi:10.1016/j.agrformet.2004.01.002.

Chmielewski, F. M., A. Müller, and E. Bruns, 2004: Climate changes and trends in phenology of fruit trees and field crops in Germany, 1961-2000. *Agricultural and Forest Meteorology*, **121 (1-2)**, 69–78, doi:10.1016/S0168-1923(03)00161-8.

Collier, P., C. Gordon, and T. Venables, 2008: Climate change and Africa. *Oxford review of economic policy*, **24 (2)**, 337–353, doi:doi:10.1093/oxrep/grn019.

Cook, K. H., and E. K. Vizy, 2006: Coupled Model Simulations of the West African Monsoon System : Twentieth- and Twenty-First-Century Simulations. *Journal of Climate*, **19**, 3681–3703.

Cooper, P. J. M., J. Dimes, K. P. C. Rao, B. Shapiro, B. Shiferaw, and S. Twomlow, 2008: Coping better with current climatic variability in the rain-fed farming systems of sub-Saharan Africa: An essential first step in adapting to future climate change? *Agriculture, Ecosystems and Environment*, **126 (1-2)**, 24–35, doi:10.1016/j.agee.2008.01.007.

Coughlan De Perez, E., B. Van Den Hurk, M. K. Van Aalst, B. Jongman, T. Klose, and P. Suarez, 2015: Forecast-based financing: An approach for catalyzing humanitarian action based on extreme weather and climate forecasts. *Natural Hazards and Earth System Sciences*, **15 (4)**, 895–904, doi:10.5194/nhess-15-895-2015.

Cox, P. M., R. A. Betts, C. B. Bunton, R. L. H. Essery, P. R. Rowntree, and J. Smith, 1999: The impact of new land surface physics on the GCM simulation of climate and climate sensitivity. *Climate Dynamics*, **15 (3)**, 183–203, doi:10.1007/s003820050276, URL http://link.springer.com/10.1007/s003820050276.

Daron, J., 2015: Challenges in using a Robust Decision Making approach to guide climate change adaptation in South Africa. *Climatic Change*, **132 (3)**, 459–473, doi:10.1007/s10584-014-1242-9.

Deblauwe, V., V. Droissart, R. Bose, and B. Sonké, 2016: Remotely sensed temperature and precipitation data improve species. *Global Ecology and Biogeography*, **25**, 443–454, doi:10.1111/geb.12426.

Dicks, L. V., J. C. Walsh, and W. J. Sutherland, 2014: Organising evidence for environmental management decisions: A '4S' hierarchy. *Trends in Ecology and Evolution*, **29 (11)**, 607–613, doi:10.1016/j.tree.2014.09.004, URL http://dx.doi.org/10.1016/j.tree.2014.09.004.

Dinku, T., P. Block, J. Sharoff, K. Hailemariam, D. Osgood, J. Corral, R. Cousin, and M. C. Thomson, 2014: Bridging critical gaps in climate services and applications in africa. *Earth Perspectives*, **1 (15)**, 1–13, URL http://www.earth-perspectives.com/content/1/1/15.

Dobor, L., Z. Barcza, T. Hlásny, T. Árendás, T. Spitkó, and N. Fodor, 2016: Crop planting date matters: Estimation methods and effect on future yields. *Agricultural and Forest Meteorology*, **223**, 103–115, doi:10.1016/j.agrformet.2016.03.023.

Dorward, P., G. Clarkson, and D. Stern, 2015: *Participatory Integrated Climate Services for Agriculture (PICSA): Field Manual*. 62 pp., doi:10.1007/s13398-014-0173-7.2, arXiv:1011.1669v3.

Dunning, C. M., E. C. Black, and R. P. Allan, 2016: The onset and cessation of seasonal rainfall over Africa. *Journal of Geophysical Research*, **121 (19)**, 11 405–11 424, doi:10.1002/2016JD025428.

Dzotsi, K., A. Agboh-Noaméshie, T. Struif Bontkes, U. Singh, and P. Dejean, 2003: Using DSSAT to Derive Optimum Combinations of Cultivar and Sowing Date for Maize in Southern Togo. *Decision Support Tools for Smallholder Agriculture in Sub-Saharan Africa:A Practical Guide*, T. Struif Bontkes, and M. C. S. Wopereis, Eds., IFDC and CTA, Wageningen, Netherlands, chap. 7, 100–112.

Enenkel, M., and Coauthors, 2016: A combined satellite-derived drought indicator to support humanitarian aid organizations. *Remote Sensing*, **8 (4)**, doi:10.3390/rs8040340.

FAO, 2019: *Handbook on Climate Information for Farming Communities- What farmers need and what is available*. Licence:CC BY-NC-SA 3.0 IGO, Rome, 184 pp., URL http://www.wipo.int/amc/en/mediation/rules.

FAO/WFP-GIEWS, 2002: Special report FAO/WFP crop and food supply assessment mission to northern Ghana. URL www.fao.org/docrep/005/y6325e/y6325e00.htm.

FEWS, 2009: KENYA Food Security Update September 2009. Tech. Rep. August. URL http://fews.net/sites/default/files/documents/reports/Kenya{_}FSU{_}August09{_}final.pdf.

Funk, C., and Coauthors, 2015: The climate hazards infrared precipitation with stations - A new environmental record for monitoring extremes. *Scientific Data*, **2**, 1–21, doi:10.1038/sdata.2015.66, arXiv:1011.1669v3.

GCOS, 2006: Climate information for development needs an action plan for Africa. Report and implementation strategy. Tech. rep., Geneva, Switzerland. URL https://library.wmo.int/doc{_}num.php?explnum{_}id=3814.

Graham, R., and Coauthors, 2015: Scoping , Options Analysis and Design of a Climate Information and Services Programme ' for Africa (CIASA): Literature Review. Tech. rep., UK Met office. doi:DOI:http://dx.doi.org/10.12774/eod_cr.may2015.grahamr.

Guido, Z., C. Knudson, D. Campbell, J. Tomlinson, Z. Guido, C. Knudson, and D. Campbell, 2019: Climate information services for adaptation : what does it mean to know the context ? Climate information services for adaptation : what does it mean to know the context ? **5529**, doi:10.1080/17565529.2019.1630352.

Haan, C., D. Allen, and J. Street, 1976: A Markov Chain Model of daily rainfall. *Water Resources Research*, **12 (3)**, 443–449, doi:10.1029/WR012i003p00443.

Haied, N., A. Foufou, S. Chaab, M. Azlaoui, S. Khadri, K. Benzahia, and I. Benzahia, 2017: Drought assessment and monitoring using meteorological indices in a semi-arid region. *Energy Procedia*, **119**, 518–529, doi:10.1016/j.egypro.2017.07.064, URL http://dx.doi.org/10.1016/j.egypro.2017.07.064.

Hansen, J. W., A. Challinor, A. Ines, T. Wheeler, and V. Moron, 2006: Translating climate forecasts into agricultural terms: Advances and challenges. *Climate Research*, **33 (1)**, 27–41, doi:10.3354/cr033027.

Hansen, J. W., and M. Indeje, 2004: Linking dynamic seasonal climate forecasts with crop simulation for maize yield prediction in semi-arid Kenya. *Agricultural and Forest Meteorology*, **125 (1-2)**, 143–157, doi:10.1016/j.agrformet.2004.02.006.

Hansen, J. W., D. M. Kagabo, and G. Nsengiyumva, 2018: Can rural climate services meet context-specific needs, and still be scalable? Experience from Rwanda. *Conference Proceedings of Adaptation Futures 2018*, D. Petrik, and L. Ashburner, Eds., University of Cape Town, Cape Town, June.

Hansen, J. W., S. J. Mason, and L. Sun, 2011: Review of seasonal climate forecasting for agriculture in sub-Sharan Africa. *Experimental Agriculture*, **47 (M2)**, 205–240, doi:10.1017/S0014479710000876.

Hansen, J. W., C. Vaughan, D. M. Kagabo, T. Dinku, E. R. Carr, J. Körner, and R. B. Zougmoré, 2019: Climate Services Can Support African Farmers ' Context-Specific Adaptation Needs at Scale. **3 (April)**, 1–16, doi:10.3389/fsufs.2019.00021.

Hao, Z., and A. AghaKouchak, 2013: Multivariate Standardized Drought Index: A parametric multi-index model. *Advances in Water Resources*, **57**, 12–18, doi:10.1016/j.advwatres.2013.03.009, URL http://dx.doi.org/10.1016/j.advwatres.2013.03.009.

Harrison, P. A., J. R. Porter, and T. E. Downing, 2000: Scaling-up the AFRCWHEAT2 model to assess phenological development for wheat in Europe. *Agricultural and Forest Meteorology*, **101 (2-3)**, 167–186, doi:10.1016/S0168-1923(99)00164-1.

Harvey, B., L. Jones, and L. Cochrane, 2019: The evolving landscape of climate services in sub-Saharan Africa : What roles have NGOs played ? **157**, 81–98, doi:10.1007/s10584-019-02410-z.

Harvey, B., and R. Singh, 2017: Climate services for resilience : the changing roles of NGOs in Burkina Faso. Tech. Rep. December, Burkina Faso. URL https://asdpn.org/publications/CLIMATE/Climate{_}services{_}for{_}resilience{_}the{_}changing{_}roles{_}of{_}NGOs{_}in{_}Burkina{_}Faso.pdf.

Hassan, R. M., 1996: Planting strategies of maize farmers in Kenya: A simultaneous equations analysis in the presence of discrete dependent variables. *Agricultural Economics*, **15 (2)**, 137–149, doi:10.1016/S0169-5150(96)01194-2.

Hellmuth, M., A. Moorhead, M. Thomson, and J. Williams, 2007: Climate Risk Management in Africa: Learning from Practice. Tech. rep., New York,USA.

Hession, S. L., and N. Moore, 2011: A spatial regression analysis of the influence of topography on monthly rainfall in East Africa. *International Journal of Climatology*, **31 (10)**, 1440–1456, doi:10.1002/joc.2174.

Ingram, K. T., M. C. Roncoli, and P. H. Kirshen, 2002: Opportunities and constraints for farmers of west Africa to use seasonal precipitation forecasts with Burkina Faso as a case study. *Agricultural Systems*, **74**, 331–349, doi:10.1016/S0308-521X(02)00044-6.

Isaac, M. E., E. Dawoe, and K. Sieciechowicz, 2009: Assessing local knowledge use in agroforestry management with cognitive maps. *Environmental Management*, **43 (6)**, 1321–1329, doi:10.1007/s00267-008-9201-8.

Jacobs, K., 2002: *Connecting Science , Policy , and Decision-making :*. NOAA Office of Global Programs.

Jacobs, K., G. Garfin, and M. Lenart, 2005: More thanJust Talk:Connecting Science and Decisionmaking. *Environment:Science and Policy for Sustainable Development*, **47 (9)**, 6–21, doi:10.3200/ENVT.47.9.6-21.

Jaetzold, R., H. Schmidt, B. Hormetz, and C. Shisanya, 2006: *Farm management handbook of Kenya: Part A Western Province*, Vol. II. 2nd ed., Kenyan Ministry of Agriculture, Nairobi, Kenya.

Jiménez, C., D. B. Clark, J. Kolassa, F. Aires, and C. Prigent, 2013: A joint analysis of modeled soil moisture fields and satellite observations. *Journal of Geophysical Research:Atmospheres*, **118**, 6771–6782, doi:10.1002/jgrd.50430.

Jones, L., E. Carabine, and L. Schipper, 2015: (Re)Conceptualising Maladaptation in Policy and Practice: Towards an Evaluative Framework. Tech. rep. doi:10.2139/ssrn.2643009.

Kalnay, E., and Coauthors, 1996: ncep_1.pdf. *Bulletin of the American Meteorological Society*, **77**, 437–471, doi:https://doi.org/10.1175/1520-0477(1996)077%3C0437:TNYRP%3E2.0.CO;2.

Kamara, A. Y., F. Ekeleme, D. Chikoye, and L. O. Omoigui, 2009: Planting date and cultivar effects on grain yield in dryland corn production. *Agronomy Journal*, **101 (1)**, 91–98, doi:10.2134/agronj2008.0090.

Kamoni, P. T., P. T. Gicheru, S. M. Wokabi, M. Easter, and E. Milne, 2007: Predicted soil organic carbon stocks and changes in Kenya between 1990 and 2030. **122**, 105–113, doi:10.1016/j.agee.2007.01.024.

Kanamitsu, M., W. Ebisuzaki, J. Woollen, S.-k. Yang, J. Hnilo, M. Fiorino, and G. L. Potter, 2002: Ncep-doe amip-ii reanalysis (r-2). *Bulletin of the American Meteorological Society*, **(November)**, 1631–1643, doi:10.1175/BAMS-83-11.

Kassie, B. T., S. Asseng, R. P. Rotter, H. Hengsdijk, A. C. Ruane, and M. K. Van Ittersum, 2015: Exploring climate change impacts and adaptation options for maize production in the Central Rift Valley of Ethiopia using different climate change scenarios and crop models. *Climatic Change*, **129 (1-2)**, 145–158, doi:10.1007/s10584-014-1322-x.

Kassie, B. T., M. K. Van Ittersum, H. Hengsdijk, S. Asseng, J. Wolf, and R. P. Rötter, 2014: Climate-induced yield variability and yield gaps of maize (Zea mays L.) in the Central Rift Valley of Ethiopia. *Field Crops Research*, **160**, 41–53, doi:10.1016/j.fcr.2014.02.010, URL http://dx.doi.org/10.1016/j.fcr.2014.02.010.

Keyantash, J. A., and J. A. Dracup, 2004: An aggregate drought index: Assessing drought severity based on fluctuations in the hydrologic cycle and surface water storage. *Water Resources Research*, **40 (9)**, 1–14, doi:10.1029/2003WR002610.

Kinyanjui, M. J., C. A. Shisanya, O. K. Nyabuti, M. A. Ojwala, and W. P. Waqo, 2014: Assessing

Tree Species Dominance along an Agro Ecological Gradient in the Mau Forest Complex, Kenya. *Open Journal of Ecology*, **04 (11)**, 662–670, doi:10.4236/oje.2014.411056.

Kirtman, B. P., and Coauthors, 2014: The North American multimodel ensemble: Phase-1 seasonal-to-interannual prediction; phase-2 toward developing intraseasonal prediction. *Bulletin of the American Meteorological Society*, **95 (4)**, 585–601, doi:10.1175/BAMS-D-12-00050.1.

Kistler, R., and Coauthors, 2001: The NCEP-NCAR 50-Year Reanalysis : Monthly Means CD-ROM and Documentation. *Bulletin of the American Meteorological Society*, **82**, 247–267.

Knox, J., T. Hess, A. Daccache, and T. Wheeler, 2012: Climate change impacts on crop productivity in Africa and South Asia. *Environmental Research Letters*, **7 (3)**, doi:10.1088/1748-9326/7/3/034032.

Lana, M. A., F. Eulenstein, S. L. Schlindwein, F. Graef, S. Sieber, and H. V. H. Bittencourt, 2017: Yield stability and lower susceptibility to abiotic stresses of improved open-pollinated and hybrid maize cultivars. **37 (30)**, doi:10.1007/s13593-017-0442-x.

Lee, C., 2011: Corn Growth Stages and Growing Degree Days : A Quick Reference Guide. *Cooperative Extension Service, University of Kentucky, College of Agriculture*, 2.

Leipprand, A., and D. Gerten, 2006: Global effects of doubled atmospheric CO 2 content on evapotranspiration , soil moisture and runoff under potential natural vegetation evapotranspiration , soil moisture and runoff under potential natural vegetation. *Hydrological Science Journal*, **51 (1)**, 171–185, doi:10.1623/hysj.51.1.171.

Li, K., M. Coe, and N. Ramankutty, 2005: Investigation of Hydrological Variability in West Africa Using Land Surface Models. *Journal of Climate*, **18**, 3173–3188.

Liebmann, B., I. Bladé, G. N. Kiladis, L. M. Carvalho, G. B. Senay, D. Allured, S. Leroux, and C. Funk, 2012: Seasonality of African precipitation from 1996 to 2009. *Journal of Climate*, **25 (12)**, 4304–4322, doi:10.1175/JCLI-D-11-00157.1.

Liu, J., J. R. Williams, A. J. Zehnder, and H. Yang, 2007: GEPIC - modelling wheat yield and crop water productivity with high resolution on a global scale. *Agricultural Systems*, **94 (2)**, 478–493, doi:10.1016/j.agsy.2006.11.019.

Lobo, C., N. Chattopadhyay, and K. Rao, 2017: Making smallholder farming climate-smart. *Economic and Political Weekly*, **52 (1)**, 53–58.

Lötter, D., and Coauthors, 2018: Climate information needs in Southern Africa: a review, URL http://www.lse.ac.uk/GranthamInstitute/wp-content/uploads/2018/07/working-paper-300-Lotter-et-al.pdf.

Luseno, W. K., J. G. McPeak, C. B. Barrett, P. D. Little, and G. Gebru, 2003: Assessing the value of climate forecast information for pastoralists: Evidence from Southern Ethiopia and Northern Kenya. *World Development*, **31 (9)**, 1477–1494, doi:10.1016/S0305-750X(03)00113-X.

MacCarthy, D. S., S. G. K. Adiku, B. S. Freduah, F. Gbefo, and A. Y. Kamara, 2017: Using CERES-Maize and ENSO as Decision Support Tools to Evaluate Climate-Sensitive Farm Management Practices for Maize Production in the Northern Regions of Ghana. *Frontiers in Plant Science*, **8 (January)**, doi:10.3389/fpls.2017.00031, URL http://journal.frontiersin.org/article/10.3389/fpls.2017.00031/full.

MacCarthy, D. S., J. Kihara, P. Masikati, and S. G. Adiku, 2018: Decision support tools for site-specific fertilizer recommendations and agricultural planning in selected countries in Sub-Sahara Africa. *Nutrient Cycling in Agroecosystems*, **110**, 343–359, doi:10.1007/978-3-319-58792-9_16.

Machado, S., and Coauthors, 2002: Spatial and Temporal Variability of Corn Growth and Grain Yield: Implications for Site-Specific Farming. *Crop Science*, **42 (5)**, 1564, doi:10.2135/cropsci2002.1564.

Mafongoya, P., and O. Ajayi, 2017: *Indigenous Knowledge Systems and Climate Change Management in Africa*. CTA, Wageningen, The Netherlands, 316 pp., URL www.cta.int{\%}0ACover.

Mahon, R., and Coauthors, 2019: Fit for purpose ? Transforming National Meteorological and Hydrological Services into National Climate Service Centers. *Climate Services*, **13 (February)**, 14–23, doi:10.1016/j.cliser.2019.01.002.

Maidment, R. I., and Coauthors, 2017: A new, long-term daily satellite-based rainfall dataset for operational monitoring in Africa. *Scientific Data*, **4**, 1–19, doi:10.1038/sdata.2017.63, URL http://dx.doi.org/10.1038/sdata.2017.63.

Makondo, C. C., K. Chola, and B. Moonga, 2014: Climate Change Adaptation and Vulnerability: A Case of Rain depenedent Small-holder Farmers in Selected Districts in Zambia. *American Journal of Climate Change*, **3 (4)**, 388–403, doi:10.4236/ajcc.2014.34034.

Marteau, R., B. Sultan, V. Moron, A. Alhassane, C. Baron, and S. B. Traoré, 2011: The onset of the rainy season and farmers' sowing strategy for pearl millet cultivation in Southwest Niger. *Agricultural and Forest Meteorology*, **151 (10)**, 1356–1369, doi:10.1016/j.agrformet.2011.05.018, URL http://dx.doi.org/10.1016/j.agrformet.2011.05.018.

Martey, E., A. N. Wiredu, P. M. Etwire, M. Fosu, S. S. J. Buah, J. Bidzakin, B. D. K. Ahiabor, and F. Kusi, 2014: Fertilizer Adoption and Use Intensity Among Smallholder Farmers in Northern Ghana: A Case Study of the AGRA Soil Health Project. *Sustainable Agriculture Research*, **3 (1)**, 24, doi:10.5539/sar.v3n1p24, URL http://www.ccsenet.org/journal/index.php/sar/article/view/32958.

Masih, I., S. Maskey, F. E. F. Mussá, and P. Trambauer, 2014: A review of droughts on the African continent: a geospatial and long-term perspective. *Hydrol. Earth Syst. Sci*, **18 (Table 1)**, 3635–3649, doi:10.5194/hess-18-3635-2014, URL www.hydrol-earth-syst-sci.net/18/3635/2014/.

Matthies, M., C. Giupponi, and B. Ostendorf, 2007: Environmental decision support systems : Current issues , methods and tools Environmental decision support systems : Current issues , methods and tools. *Environmental Modelling and Software*, **22**, 123–127, doi:10.1016/j.envsoft.2005.09.005.

McAdam, S. A., F. C. Sussmilch, and T. J. Brodribb, 2016: Stomatal responses to vapour pressure deficit are regulated by high speed gene expression in angiosperms. *Plant Cell and Environment*, **39 (3)**, 485–491, doi:10.1111/pce.12633.

Mckee, T. B., N. J. Doesken, and J. Kleist, 1993: The relationship of drought frequency and duration to time scales. *AMS 8th Conference on Applied Climatology*, **(January)**, 179–184, doi:citeulike-article-id:10490403, URL http://ccc.atmos.colostate.edu/relationshipofdroughtfrequency.pdf.

Mcmaster, G. S., and W. W. Wilhelm, 1997: AGRICULTURAL AND FOREST METEOROLOGY Growing degree-days: one equation, two interpretations. *Agricultural and Forest Meteorology*, **87 (1)**, 300, URL https://ac.els-cdn.com/S0168192397000270/1-s2.0-S0168192397000270-main.pdf?{_}tid=eafb1c04-3820-44b3-aa6d-a04e10f4b3cd{\&}acdnat=1540378117{_}06fe7f2955ffe80fae9ee9e2b9a39448.

McNally, A., and Coauthors, 2015: Calculating Crop Water Requirement Satisfaction in the West Africa Sahel with Remotely Sensed Soil Moisture. *Journal of Hydrometeorology*,

16 (1), 295–305, doi:10.1175/JHM-D-14-0049.1, URL http://journals.ametsoc.org/doi/10.1175/JHM-D-14-0049.1.

McNie, E. C., 2007: Reconciling the supply of scientific information with user demands : an analysis of the problem and review of the literature. *Environmental Science and Policy*, **10**, 17–38, doi:10.1016/j.envsci.2006.10.004.

Mishra, A. K., and V. P. Singh, 2010: A review of drought concepts. *Journal of Hydrology*, **391 (1-2)**, 202–216, doi:10.1016/j.jhydrol.2010.07.012, URL http://dx.doi.org/10.1016/j.jhydrol.2010.07.012.

Monfreda, C., N. Ramankutty, and J. A. Foley, 2008: Farming the planet: 2. Geographic distribution of crop areas, yields, physiological types, and net primary production in the year 2000. *Global Biogeochem. Cycles*, **22**, GB1022, doi:doi:10.1029/2007GB002947.

Muller, C., W. Cramer, W. L. Hare, and H. Lotze-Campen, 2011: Climate change risks for African agriculture. *Proceedings of the National Academy of Sciences*, **108 (11)**, 4313–4315, doi:10.1073/pnas.1015078108.

Muller, W. A., C. Appenzeller, F. J. Doblas-Reyes, and M. A. Liniger, 2005: A debiased ranked probability skill score to evaluate probabilistic ensemble forecasts with small ensemble sizes. *Journal of Climate*, **18 (10)**, 1513–1523, doi:10.1175/JCLI3361.1.

Murungu, F. S., P. Nyamugafata, C. Chiduza, L. J. Clark, and W. R. Whalley, 2003: Effects of seed priming, aggregate size and soil matric potential on emergence of cotton (Gossypium hirsutum L.) and maize (Zea mays L.). *Soil and Tillage Research*, **74 (2)**, 161–168, doi:10.1016/j.still.2003.06.003.

Mutiga, S. K., V. Hoffmann, J. W. Harvey, M. G. Milgroom, and R. J. Nelson, 2015: Assessment of Aflatoxin and Fumonisin Contamination of Maize in Western Kenya. *Phytopathology*, **105 (9)**, 1250–1261, doi:10.1094/PHYTO-10-14-0269-R, URL http://apsjournals.apsnet.org/doi/10.1094/PHYTO-10-14-0269-R.

Naab, F. Z., Z. Abubakari, and A. Ahmed, 2019: The role of climate services in agricultural productivity in Ghana : The perspectives of farmers and institutions. *Climate Services*, **13 (November 2018)**, 24–32, doi:10.1016/j.cliser.2019.01.007.

Narasimhan, B., and R. Srinivasan, 2005: Development and evaluation of Soil Moisture Deficit Index (SMDI) and Evapotranspiration Deficit Index (ETDI) for agricultural drought monitoring. *Agricultural and Forest Meteorology*, **133 (1-4)**, 69–88, doi:10.1016/j.agrformet.2005.07.012.

Nesheim, I., L. Barkved, and N. Bharti, 2017: What Is the Role of Agro-Met Information Services in Farmer Decision-Making? Uptake and Decision-Making Context among Farmers within Three Case Study Villages in Maharashtra, India. *Agriculture*, **7 (8)**, 70, doi:10.3390/agriculture7080070.

Nicholson, S. E., 2017: Climate and climatic variability of rainfall over eastern Africa. *Reviews of Geophysics*, **55 (3)**, 590–635, doi:10.1002/2016RG000544.

Nidumolu, U. B., M. Lubbers, A. Kanellopoulos, M. K. van Ittersum, D. M. Kadiyala, and G. Sreenivas, 2016: Engaging farmers on climate risk through targeted integration of bio-economic modelling and seasonal climate forecasts. *Agricultural Systems*, **149**, 175–184, doi:10.1016/j.agsy.2016.09.011, URL http://dx.doi.org/10.1016/j.agsy.2016.09.011.

Niemeyer, S., 2008: New drought indices. *Drought Managment: scientific and technological innovations*, A. Lopez-Francos, Ed., Vol. 80, CIHEAM, Zaragoza, 267–274, doi:10.1017/CBO9781107415324.004, arXiv:1011.1669v3.

Obeng-Antwi, K., A. H. Manfred Ewool, T. Abate, A. Menkir, B. Badu-Apraku, and T. Abdoulaye, 2013: New Drought Tolerant Maize Varieties for Ghana. *A Quarterly Bulletin of the Drought Tolerant Maize for Africa Project*, **2 (1)**, 1–4.

Osborne, T., J. Gornall, J. Hooker, K. Williams, a. Wiltshire, R. Betts, and T. Wheeler, 2015: JULES-crop: a parametrisation of crops in the Joint UK Land Environment Simulator. *Geoscientific Model Development*, **8 (4)**, 1139–1155, doi:10.5194/gmd-8-1139-2015, URL http://www.geosci-model-dev.net/8/1139/2015/.

Osborne, T., G. Rose, and T. Wheeler, 2013: Variation in the global-scale impacts of climate change on crop productivity due to climate model uncertainty and adaptation. *Agricultural and Forest Meteorology*, **170**, 183–194, doi:10.1016/j.agrformet.2012.07.006, URL http://dx.doi.org/10.1016/j.agrformet.2012.07.006.

Osborne, T. M., D. M. Lawrence, A. J. Challinor, J. M. Slingo, and T. R. Wheeler, 2007: Development and assessment of a coupled crop-climate model. *Global Change Biology*, **13 (1)**, 169–183, doi:10.1111/j.1365-2486.2006.01274.x.

Owusu, K., and P. Waylen, 2009: Trends in spatio-temporal variability in annual rainfall in Ghana (1951-2000). *Weather*, **64 (5)**, 115–120, doi:10.1002/wea.255.

Owusu, K., and P. R. Waylen, 2013: The changing rainy season climatology of mid-Ghana. *Theoretical and Applied Climatology*, **112 (3-4)**, 419–430, doi:10.1007/s00704-012-0736-5.

PARI, 2015: Potentials and Possibilities for German Collaboration in Agriculture. *Program of Accompanying Research for Agricultural Innovation*, **(September)**, URL http://research4agrinnovation.org/wp-content/uploads/2016/03/Ghana.pdf.

Parkes, B., A. Challinor, and K. Nicklin, 2015: Crop failure rates in a geoengineered climate: Impact of climate change and marine cloud brightening. *Environmental Research Letters*, **10 (8)**, doi:10.1088/1748-9326/10/8/084003.

Patt, A., P. Suarez, and C. Gwata, 2005: Effects of seasonal climate forecasts and participatory workshops among subsistence farmers in Zimbabwe. *Proceedings of the National Academy of Sciences*, **102 (35)**, 12 623–12 628, doi:10.1073/pnas.0506125102.

Pinnington, E., T. Quaife, and E. Black, 2018: Impact of remotely sensed soil moisture and precipitation on soil moisture prediction in a data assimilation system with the JULES land surface model. *Hydrology and Earth System Sciences*, **22**, 2575–2588.

Pitman, A., 2003: The evolution of , and revolution in , land surface schemes designed for climate models. *International Journal of Climatology*, **23**, 479–510, doi:10.1002/joc.893.

Ragasa, C., A. Dankyi, P. Acheampong, A. N. Wiredu, and A. Chapo, 2013: Patterns of Adoption of Improved Maize Technologies in Ghana. *GSSP Working Paper 35*, **(July)**, 33, URL https://www.ifpri.org/publication/patterns-adoption-improved-maize-technologies-ghana.

Ramadas, M., and R. S. Govindaraju, 2015: Probabilistic assessment of agricultural droughts using graphical models. *Journal of Hydrology*, **526**, 151–163, doi:10.1016/j.jhydrol.2014.09.026, URL http://dx.doi.org.idpproxy.reading.ac.uk/10.1016/j.jhydrol.2014.09.026.

Ramirez-Villegas, J., and A. J. Challinor, 2016: Towards a genotypic adaptation strategy for Indian groundnut cultivation using an ensemble of crop simulations. *Climatic Change*, **138 (1-2)**, 223–238, doi:10.1007/s10584-016-1717-y, URL http://dx.doi.org/10.1007/s10584-016-1717-y.

Ramirez-Villegas, J., J. Watson, and A. J. Challinor, 2015: Identifying traits for genotypic adaptation using crop models. *Journal of Experimental Botany*, **66 (12)**, 3451–3462, doi:10.1093/jxb/erv014.

Ranger, N., A. Millner, S. Dietz, S. Fankhauser, A. Lopez, and G. Ruta, 2010: F126-58P-SX 5-IS Model (1).pdf. **(September)**, doi:10.1063/1.368390.

Raoult, N. M., T. E. Jupp, P. M. Cox, and C. M. Luke, 2016: Land-surface parameter optimisation using data assimilation techniques : the adJULES system V1 . 0. *Geoscientific Model Development*, **9**, 2833–2852, doi:10.5194/gmd-9-2833-2016.

Refsgaard, J. C., J. P. van der Sluijs, A. L. Hojberg, and P. A. Vanrolleghem, 2007: Uncertainty in the environmental modelling process e A framework and guidance. *Environmental Modelling and Software*, **22**, 1543–1556, doi:10.1016/j.envsoft.2007.02.004.

Reichert, P., M. Borsuk, M. Hostmann, S. Schweizer, C. Spörri, K. Tockner, and B. Truffer, 2007: Concepts of Decision Support for River Rehabilitation. *Environmental Modelling & Software*, **22 (2)**, 188–201.

Rose, D. C., and Coauthors, 2016: Decision support tools for agriculture: Towards effective design and delivery. *Agricultural Systems*, **149**, 165–174, doi:10.1016/j.agsy.2016.09.009, URL http://dx.doi.org/10.1016/j.agsy.2016.09.009.

Rosenzweig, C., J. Elliott, D. Deryng, A. C. Ruane, C. Müller, and A. Arneth, 2014: Assessing agricultural risks of climate change in the 21st century in a global gridded crop model intercomparison. *PNAS*, **111 (9)**, 3268–3273, doi:10.1073/pnas.1222463110.

Rosenzweig, C., and Coauthors, 2018: Coordinating AgMIP data and models across global and regional scales for 1 . 5 C and 2 . 0 C assessments Subject Areas :. *Philosophical Transactions of the Royal Society A*, **376 (20160455)**, doi:http://dx.doi.org/10.1098/rsta.2016.0455.

Sacks, W. J., D. Deryng, J. A. Foley, and N. Ramankutty, 2010: Crop planting dates: An analysis of global patterns. *Global Ecology and Biogeography*, **19 (5)**, 607–620, doi:10.1111/j.1466-8238.2010.00551.x.

Sato, H., A. Ito, A. Ito, T. Ise, and E. Kato, 2015: Current status and future of land surface models. *Soil Science and Plant Nutrition*, **61**, 34–47, doi:10.1080/00380768.2014.917593, URL http://dx.doi.org/10.1080/00380768.2014.917593.

Schlenker, W., and D. B. Lobell, 2010: Robust negative impacts of climate change on African agriculture. *Environmental Research Letters*, **5 (1)**, doi:10.1088/1748-9326/5/1/014010.

Schreck III, C. J., and F. H. M. Semazzi, 2004: Variability of the recent climate of eastern africa. *International Journal of Climatology*, **24**, 681–701, doi:10.1002/joc.1019.

Sellers, P. J., and Coauthors, 1997: Modeling the Exchanges of Energy , Water , and Carbon Between Continents and the Atmosphere. *Science*, **275 (January)**.

Semenov, M. A., and F. J. Doblas-Reyes, 2007: Utility of dynamical seasonal forecasts in predicting crop yield. *Climate Research*, **34 (1)**, 71–81, doi:Doi10.3354/Cr034071.

Senay, G. B., and J. Verdin, 2003: Characterization of yield reduction in Ethiopia using a GIS-based crop water balance model. *Canadian Journal of Remote Sensing*, **29 (6)**, 687–692, doi:10.5589/m03-039.

Sheffield, J., and Coauthors, 2014: A Drought Monitoring and Forecasting System for Sub-Sahara African Water Resources and Food Security. *Bulletin of the American Meteorological Society*, **95 (6)**, 861–882, doi:10.1175/BAMS-D-12-00124.1, URL http://journals.ametsoc.org/doi/abs/10.1175/BAMS-D-12-00124.1.

Shim, J. P., M. Warkentin, J. F. Courtney, and D. J. Power, 2002: ScienceDirect.com - Decision Support Systems - Past, present, and future of decision support technology. *Decision support ...*, **33**, 111–126, doi:10.1016/S0167-9236(01)00139-7, URL http://www.sciencedirect.com/science/article/pii/S0167923601001397{\%}5Cnpapers2://publication/uuid/505B2C33-4520-4547-BFBB-5E707E4F2721.

Sidibé, Y., T. O. Williams, and S. Kolavalli, 2016: Flood Recession Agriculture for Food Security in Northern Ghana:Literature review on extent, challenges, and opportunities. *GSSP Working paper 42*, **(February)**, URL https://ideas.repec.org/p/fpr/gsspwp/42.html.

Singh, C., J. Daron, A. Bazaz, G. Ziervogel, D. Spear, J. Krishnaswamy, M. Zaroug, and E. Kituyi, 2018: The utility of weather and climate information for adaptation decision-making: current uses and future prospects in Africa and India. *Climate and Development*, **10 (5)**, 389–405, doi:10.1080/17565529.2017.1318744.

Singh, C., P. Urquhart, and E. Kituyi, 2016: From pilots to systems : Barriers and enablers to

scaling up the use of climate information services in smallholder farming communities, URL https://www.idrc.ca/cariaa.

Spinoni, J., G. Naumann, H. Carrao, P. Barbosa, and J. Vogt, 2014: World drought frequency, duration, and severity for 1951-2010. *International Journal of Climatology*, **34 (8)**, 2792–2804, doi: 10.1002/joc.3875.

Srivastava, A. K., C. M. Mboh, T. Gaiser, H. Webber, and F. Ewert, 2016: Effect of sowing date distributions on simulation of maize yields at regional scale - A case study in Central Ghana, West Africa. *Agricultural Systems*, **147**, 10–23, doi:10.1016/j.agsy.2016.05.012, URL http://dx.doi.org/10.1016/j.agsy.2016.05.012.

Stehfest, E., M. Heistermann, J. A. Priess, D. S. Ojima, and J. Alcamo, 2007: Simulation of global crop production with the ecosystem model DayCent. *Ecological Modelling*, **209 (2-4)**, 203–219, doi:10.1016/j.ecolmodel.2007.06.028.

Steiner, A. L., J. L. Bell, N. S. Diffenbaugh, A. Boone, L. C. Sloan, and F. Giorgi, 2009: Land surface coupling in regional climate simulations of the West African monsoon. *Climate Dynamics*, **33**, 869–892, doi:10.1007/s00382-009-0543-6.

Struif Bontkes, T., and M. Wopereis, 2003: Opportunities for the Use of Decision Support Tools for Smallholder Agriculture in Sub-Saharan Africa. *Decision support tools for smallholder agriculture in Sub-Saharan Africa: a practical guide*, T. Struif Bontkes, and M. C. S. Wopereis, Eds., January, IFDC and CTA, Wageningen, Netherlands, chap. 1, 1–23.

Sultan, B., C. Baron, M. Dingkuhn, B. Sarr, and S. Janicot, 2005: Agricultural impacts of large-scale variability of the West African monsoon. *Agricultural and Forest Meteorology*, **128 (1-2)**, 93–110, doi:10.1016/j.agrformet.2004.08.005.

Tarhule, A., and P. J. Lamb, 2003: Climate research and seasonal forecasting for West Africans. *Bulletin of the American Meteorological Society*, **84 (12)**, 1741–1759, doi:10.1175/BAMS-84-12-1741.

Tarhule, A., Z. Saley-Bana, and P. J. Lamb, 2009: Rainwatch: A prototype GIS for rainfall monitoring in West Africa. *Bulletin of the American Meteorological Society*, **90 (11)**, 1607–1614, doi: 10.1175/2009BAMS2697.1.

Taylor, K. E., R. J. Stouffer, and G. A. Meehl, 2012: An overview of CMIP5 and the ex-

periment design. *Bulletin of the American Meteorological Society*, **93 (4)**, 485–498, doi:10.1175/BAMS-D-11-00094.1.

Thornton, P. K., P. J. Ericksen, M. Herrero, and A. J. Challinor, 2014: Climate variability and vulnerability to climate change: a review. *Global change biology*, 1–16, doi:10.1111/gcb.12581, URL http://www.ncbi.nlm.nih.gov/pubmed/24668802.

Tian, L., S. Yuan, and S. M. Quiring, 2018: Agricultural and Forest Meteorology Evaluation of six indices for monitoring agricultural drought in the south- central United States. *Agricultural and Forest Meteorology*, **249**, 107–119, doi:10.1016/j.agrformet.2017.11.024, URL https://doi.org/10.1016/j.agrformet.2017.11.024.

Troccoli, A., 2010: Seasonal climate forecasting. *Meteorological Applications*, **17 (3)**, 251–268, doi:10.1002/met.184.

Tubiello, F. N., M. Donatelli, C. Rosenzweig, and C. O. Stockle, 2000: Effects of climate change and elevated CO2 on cropping systems: Model predictions at two Italian locations. *European Journal of Agronomy*, **13 (2-3)**, 179–189, doi:10.1016/S1161-0301(00)00073-3.

van den Hurk, B., M. Best, P. Dirmeyer, A. Pitman, J. PolcHer, and J. Santanello, 2011: ACCELERATION OF LAND SURFACE MODEL DEVELOPMENT. *Bulletin of the American Meteorological Society*, **(December)**, 1593–1600, doi:10.1175/BAMS-D-11-00007.1.

Venkatasubramanian, K., A. Tall, J. Hansen, and P. Aggarwal, 2014: Assessment of India's Agro-Meteorological Advisory Service from a farmer perspective. CCAFS Working Paper no. 54. Tech. Rep. 54, Copenhagen, Denmark, 65 pp pp. doi:10.2139/ssrn.701181, URL www.ccafs.cgiar.org, arXiv:1011.1669v3.

Verdin, J., and R. Klaver, 2002: Grid-cell-based crop water accounting for the famine early warning system. *Hydrological Processes*, **16 (8)**, 1617–1630, doi:10.1002/hyp.1025.

Vicente-Serrano, S. M., S. Beguería, and J. I. López-Moreno, 2010: A multiscalar drought index sensitive to global warming: The standardized precipitation evapotranspiration index. *Journal of Climate*, **23 (7)**, 1696–1718, doi:10.1175/2009JCLI2909.1.

Vogel, E., M. G. Donat, L. V. Alexander, M. Meinshausen, D. K. Ray, D. Karoly, N. Meinshausen, and K. Frieler, 2019: The effects of climate extremes on global agricultural yields. *Environmental Research Letters*, **14 (054010)**, doi:https://doi.org/10.1088/1748-9326/ab154b.

Waha, K., L. G. Van Bussel, C. Müller, and A. Bondeau, 2012: Climate-driven simulation of global crop sowing dates. *Global Ecology and Biogeography*, **21 (2)**, 247–259, doi:10.1111/j.1466-8238.2011.00678.x.

Walker, D. H., 2002: Decision support, learning and rural resource management. *Agricultural Systems*, **73 (1)**, 113–127, doi:10.1016/S0308-521X(01)00103-2.

Walker, D. P., C. E. Birch, J. H. Marsham, A. A. Scaife, R. J. Graham, and Z. T. Segele, 2019: Skill of dynamical and GHACOF consensus seasonal forecasts of East African rainfall. *Climate Dynamics*, **(0123456789)**, doi:10.1007/s00382-019-04835-9, URL http://link.springer.com/10.1007/s00382-019-04835-9.

Wang, G., 2005: Agricultural drought in a future climate: Results from 15 global climate models participating in the IPCC 4th assessment. *Climate Dynamics*, **25 (7-8)**, 739–753, doi:10.1007/s00382-005-0057-9.

Wang, S., Y. Yang, A. P. Trishchenko, A. G. Barr, T. A. Black, and H. Mccaughey, 2009: Modeling the Response of Canopy Stomatal Conductance to Humidity. *Journal of Hydrometeorology*, **10 (April)**, 521–532, doi:10.1175/2008JHM1050.1.

Wang, Y. M., S. Traore, and T. Kerh, 2008: Computing and modelling for crop yields in Burkina Faso based on climatic data information. *WSEAS Transactions on Information Science and Applications*, **5 (7)**, 832–842.

Waongo, M., P. Laux, and H. Kunstmann, 2015: Adaptation to climate change: The impacts of optimized planting dates on attainable maize yields under rainfed conditions in Burkina Faso. *Agricultural and Forest Meteorology*, **205**, 23–39, doi:10.1016/j.agrformet.2015.02.006, URL http://dx.doi.org/10.1016/j.agrformet.2015.02.006.

Waongo, M., P. Laux, S. B. Traoré, M. Sanon, and H. Kunstmann, 2014: A crop model and fuzzy rule based approach for optimizing maize planting dates in Burkina Faso, West Africa. *Journal of Applied Meteorology and Climatology*, **53 (3)**, 598–613, doi:10.1175/JAMC-D-13-0116.1.

Watson, J., and A. Challinor, 2013: The relative importance of rainfall, temperature and yield data for a regional-scale crop model. *Agricultural and Forest Meteorology*, **170**, 47–57, doi:10.1016/j.agrformet.2012.08.001, URL http://dx.doi.org/10.1016/j.agrformet.2012.08.001.

Weedon, G. P., G. Balsamo, N. Bellouin, S. Gomes, M. J. Best, and P. Viterbo, 2014: Data methodology applied to ERA-Interim reanalysis data. *Water Resources Research*, **50**, 7505–7514, doi:10.1002/2014WR015638.Received.

Weigel, A. P., M. A. Liniger, and C. Appenzeller, 2007: Generalization of the Discrete Brier and Ranked Probability Skill Scores for Weighted Multimodel Ensemble Forecasts. *Monthly Weather Review*, **135 (7)**, 2778–2785, doi:10.1175/MWR3428.1, URL http://journals.ametsoc.org/doi/abs/10.1175/MWR3428.1.

Wilhite, D. A., 2000: Drought as a Natural Hazard: Concepts and definitions. *Drought : A Global Assessment*, D. A. Wilhite, Ed., Vol. I, Routledge, London, UK.

Wilhite, D. A., and M. H. Glantz, 1985: Understanding the Drought Phenomenon: The Role of Definitions. *Water International*, **10 (3)**, 111–120, doi:10.1080/02508068508686328, URL http://digitalcommons.unl.edu/droughtfacpubhttp://digitalcommons.unl.edu/droughtfacpub/20.

WMO, 2006: Drought monitoring and early warning : concepts , progress and future challenges. *World Meteorogical Organization*, **(1006)**, 24, URL http://www.wamis.org/agm/pubs/brochures/WMO1006e.pdf.

WMO, 2012: Standardized Precipitation Index User Guide, URL http://library.wmo.int/opac/index.php?lvl=notice{_}display{\&}id=13682.

WMO, 2018: *Step-by-step Guidelines for Establishing a National Framework for Climate Services*. 1206, World Meteorological Organization (WMO), Geneva, Switzerland.

Wolf, J., K. Ouattara, and I. Supit, 2015: Sowing rules for estimating rainfed yield potential of sorghum and maize in Burkina Faso. *Agricultural and Forest Meteorology*, **214-215**, 208–218, doi:10.1016/j.agrformet.2015.08.262, URL http://dx.doi.org/10.1016/j.agrformet.2015.08.262.

Xu, Y.-p., M. J. Booij, and A. E. Mynett, 2007: An appropriateness framework for the Dutch Meuse decision support system An appropriateness framework for the Dutch Meuse decision support system. *Environmental Modelling and Software*, **22**, 1667–1668, doi:10.1016/j.envsoft.2007.01.002.

Zambrano-bigiarini, M., A. Nauditt, C. Birkel, K. Verbist, and L. Ribbe, 2017: Temporal and spatial evaluation of satellite-based rainfall estimates across the complex topographical and climatic gradients of Chile. *Hydrology and Earth System Sciences*, **21**, 1295–1320, doi:10.5194/hess-21-1295-2017.

Zargar, A., R. Sadiq, B. Naser, and F. I. Khan, 2011: A review of drought indices. *Environmental Reviews*, **19 (NA)**, 333–349, doi:10.1139/a11-013, URL http://www.nrcresearchpress.com/doi/abs/10.1139/a11-013.

Appendix A

Supplementary for paper reproduced as Chapter 2

A.1 Seasonal weather and maize yield

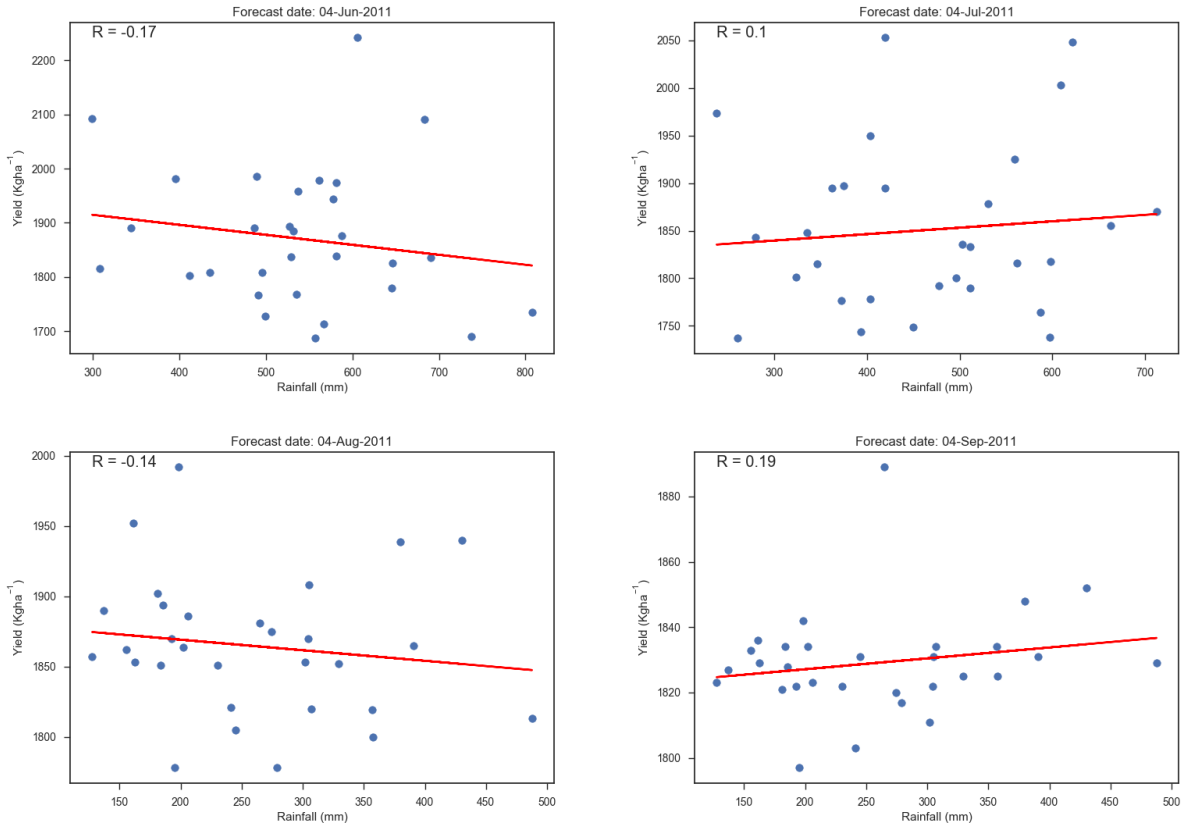

Figure A.1.1: Correlation between Maize yield and 90 days total rainfall after the forecast date.

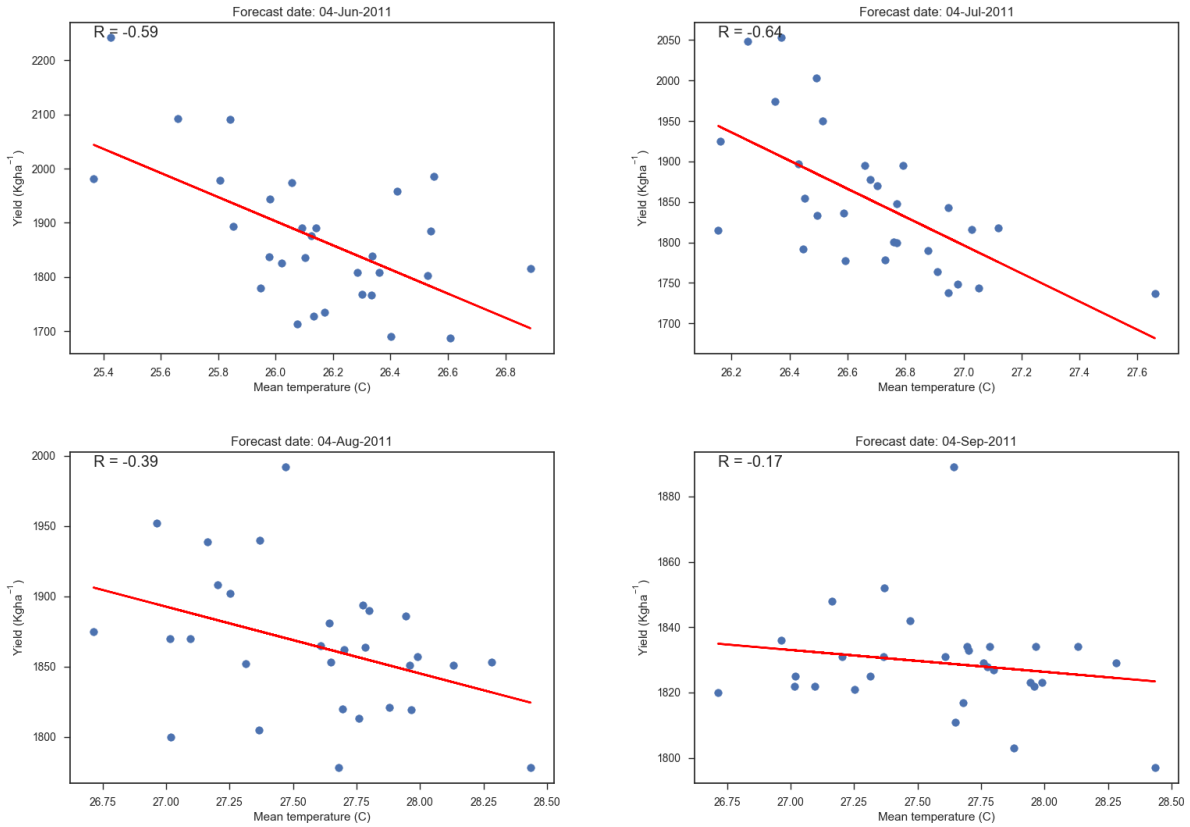

Figure A.1.2: Correlation between Maize yield and the 90 days mean temperature after the forecast date.

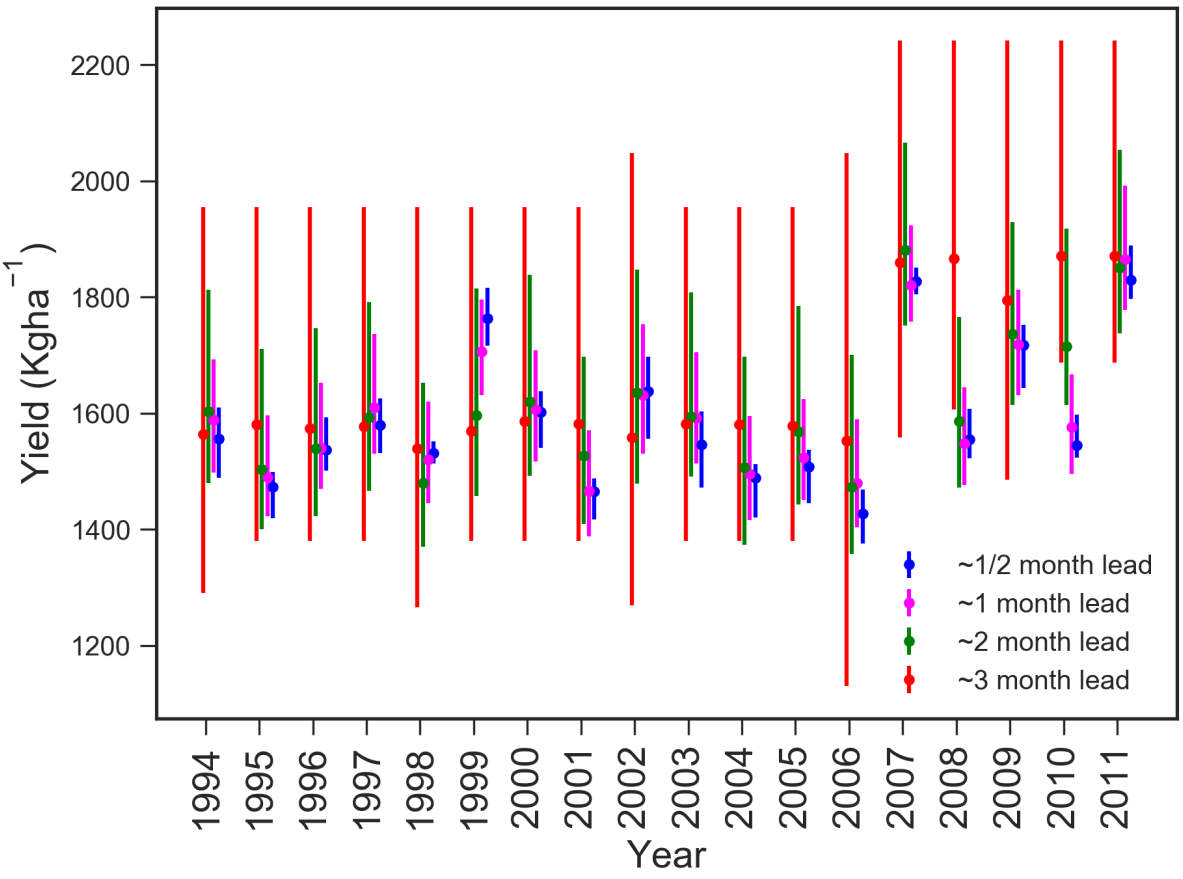

Figure A.1.3: Time series of maize yield forecast in Ghana from 1994 to 2011 with four lead times of forecast. This is done using a hindcast for each year and comparing the plots of 3month lead time (red), 2month lead time (green), 1month lead time (magenta) and 1/2month lead time (blue). The shift in the period 1994 2006 and 2007 -2011 comes due to the change in the crop parameter Transpiration Efficiency (TE) which is implemented to account for the change in drought resistance variety of Maize introduced in Ghana.

Appendix B

Supplementary for Chapter 3

B.1 Driving data disaggregation

JULES take driving data with a higher temporal resolution but insists users use a maximum of hourly time step to run the model however if there driving data is given on daily time scale JULES use different techniques to disaggregate the data to the time step required by the user. Similarly, running the new soil moisture model requires disaggregation of the daily data values to an hourly time step to maintain the numerical stability of the model but, the disaggregation methods used in JULES and the new model are different. For example precipitation disaggregation in the new model was done based on rainfall amount where a value less than 10 mm is represented to fall within one hour, a rainfall amount 10–80 mm is divided into 4 hours with 15%,40%,25% and 20% in each hour, for rainfall above 80 mm the rainfall is distributed over 7 hours with 10%,30%,20% and 20%, 10%,5% and 5% in each hour. This disaggregation is different from JULES hence affecting the amount of water that infiltrates into the soil. Figure B.1.1 and Figure B.1.2 show the hourly interpolated driving data from JULES and the new model. The interpolation method used in the new model matches for wind, temperature and pressure but the rainfall interpolation in JULES tend to allocate a small amount of rainfall values evenly throughout the 24 hours whereas the new model allocates a high amount of rainfall within a maximum of 7 hours. Such a difference in the amount of rainfall distribution through 24 hours will affect the amount of water infiltrating to the top layer at each time step, which leads to more moisture in the first layer of soil in JULES compare to the new model during the peak rainfall periods in the season. The other major difference is the specific humidity variability; the new model uses linear interpolation and the re-

sulting interpolated specific humidity has low variability whereas in JULES the specific humidity hourly variability is higher especially in Kitale where the location is more humid and with rainfall throughout the year. The variability in humidity interpolation of the dry location Wajiri is not very high, as shown in Figure B.1.2. The specific humidity determines the amount of evaporation from the soil, as shown in Equation 3.15. Temperature interpolation is based on a linear increase from the minimum daily temperature value at midnight until the daily maximum temperature at noon and a similar rate decrease after two hours of the maximum temperature in the day time. This approach resulted in a similar interpolation by JULES. For the other variables, pressure and wind speed, the daily values are considered to be constant for all the 24 hours and it showed a similar approach by JULES (Figure B.1.1 and Figure B.1.2).

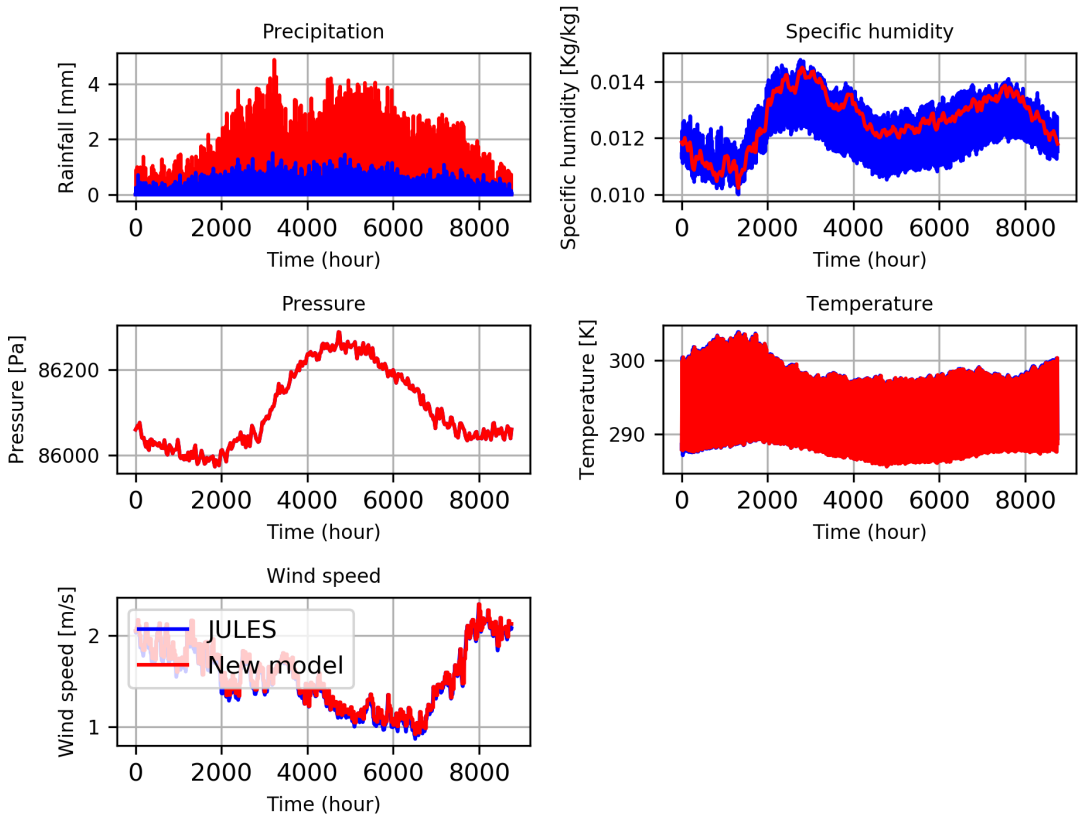

Figure B.1.1: Climatological average of hourly interpolated driving data from JULES and new model (Kitale).

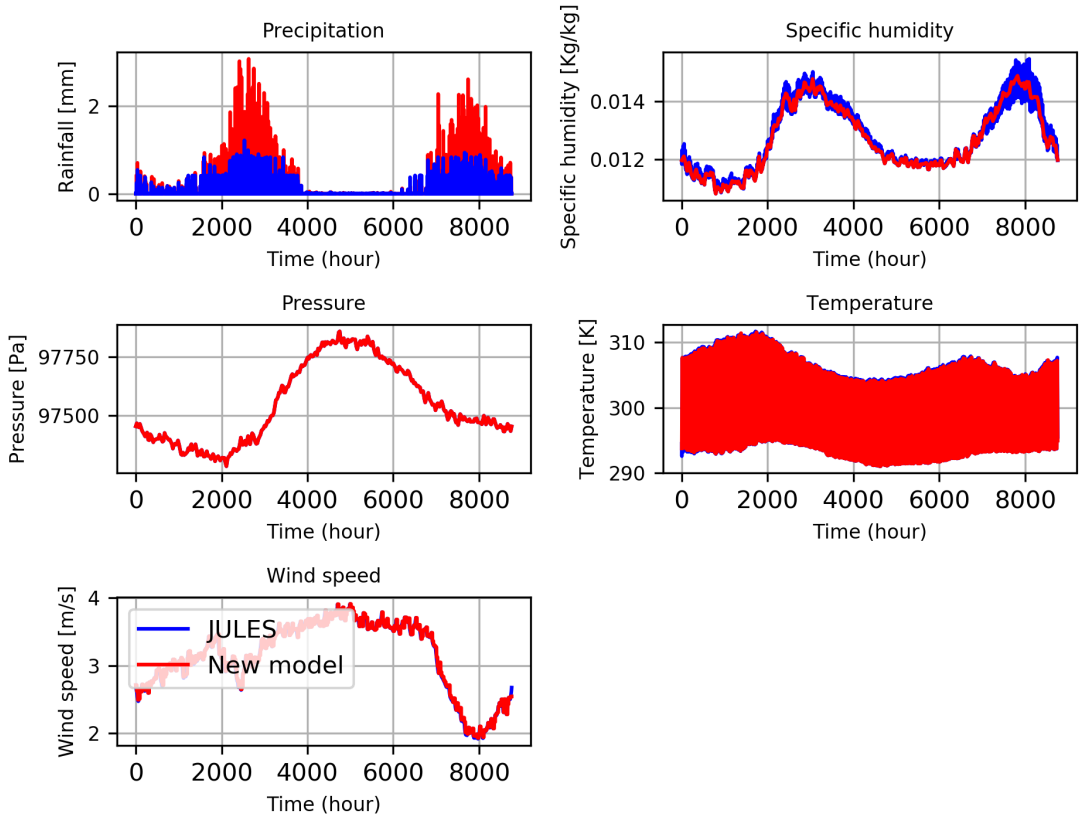

Figure B.1.2: Climatological average of hourly interpolated driving data from JULES and new model (Wajiri).

B.2 Surface temperature difference

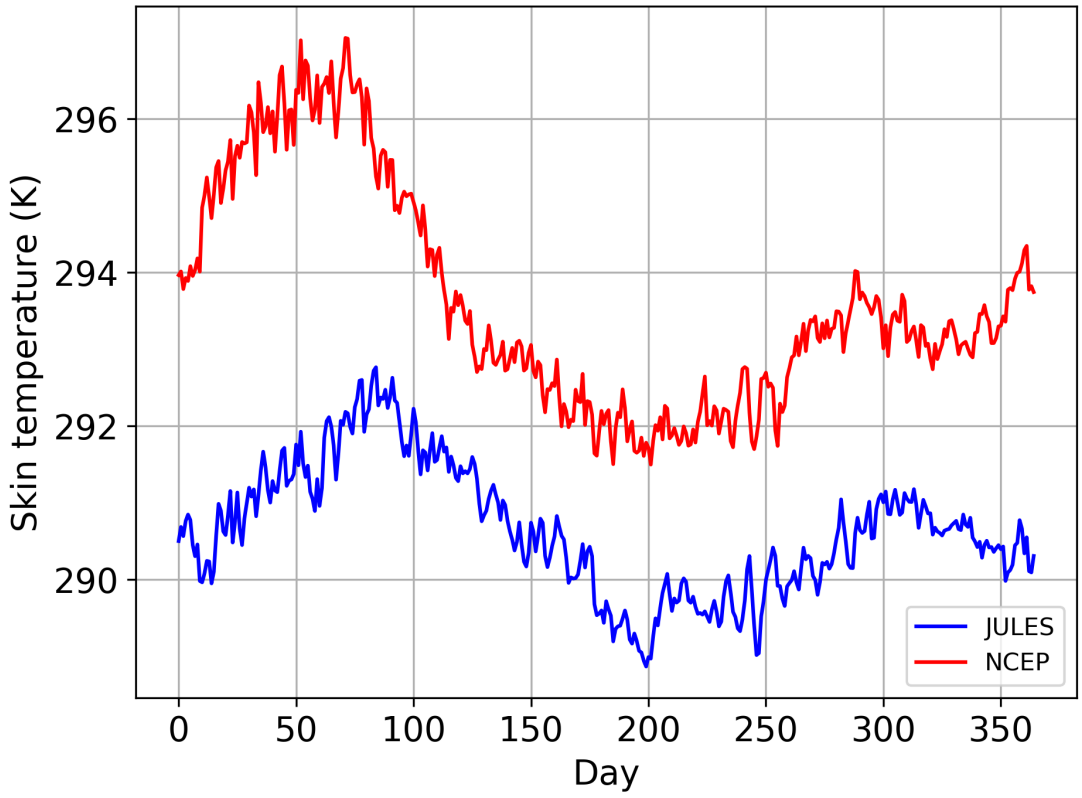

Figure B.2.1: Daily Average (2003-2017) surface temperature (Kitale).

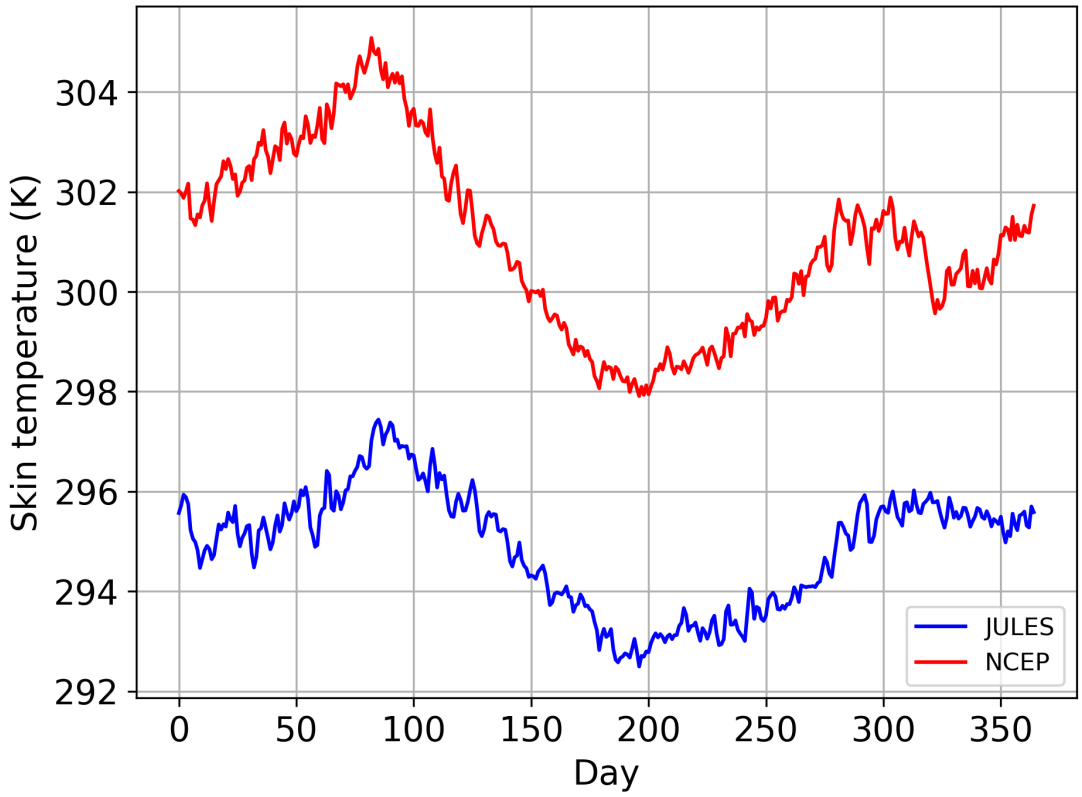

Figure B.2.2: Daily Average (2003-2017) surface temperature (Wajiri).

B.3 Precipitation difference

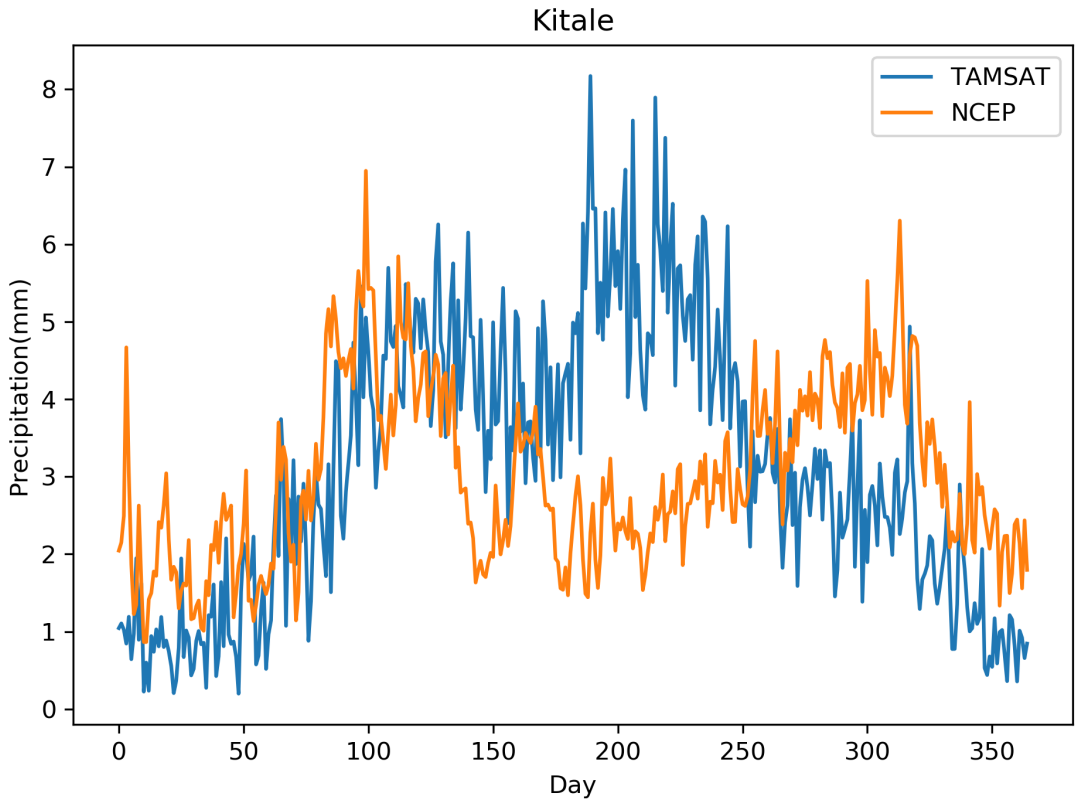

Figure B.3.1: Seasonal mean precipitation for Kitale.

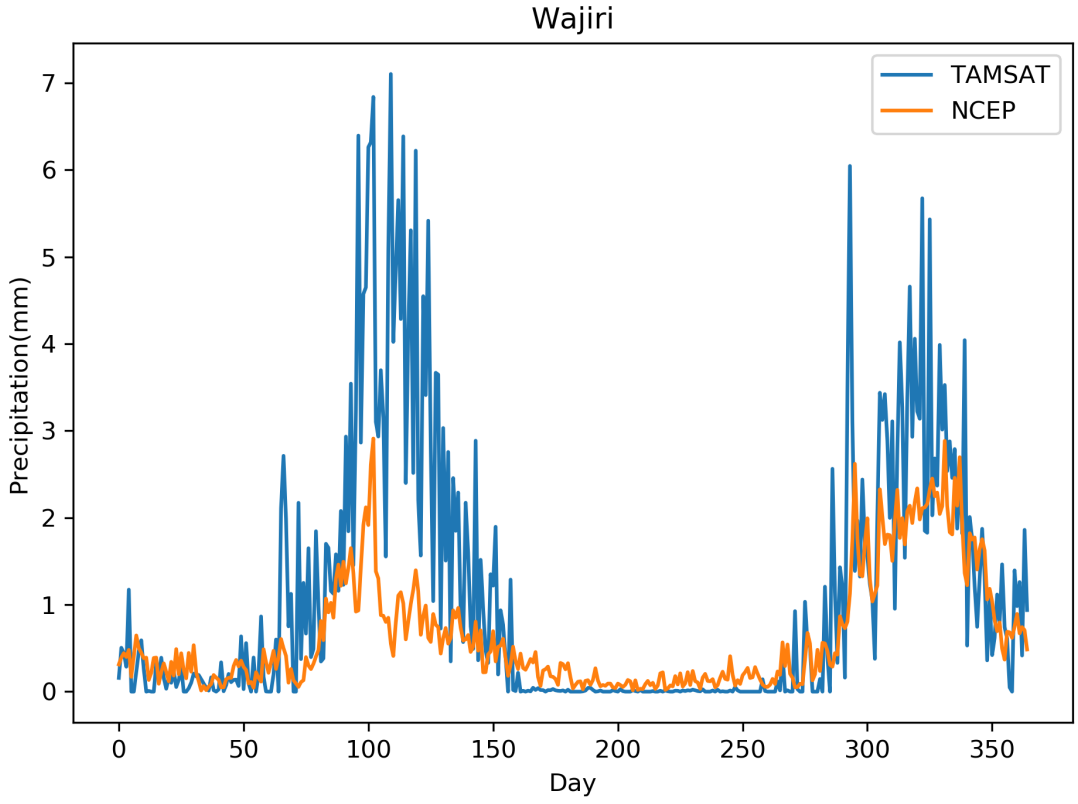

Figure B.3.2: Seasonal mean precipitation for Wajiri.

Appendix C

Supplementary for Chapter 4

C.1 Soil moisture forecast for selected locations in Kenya

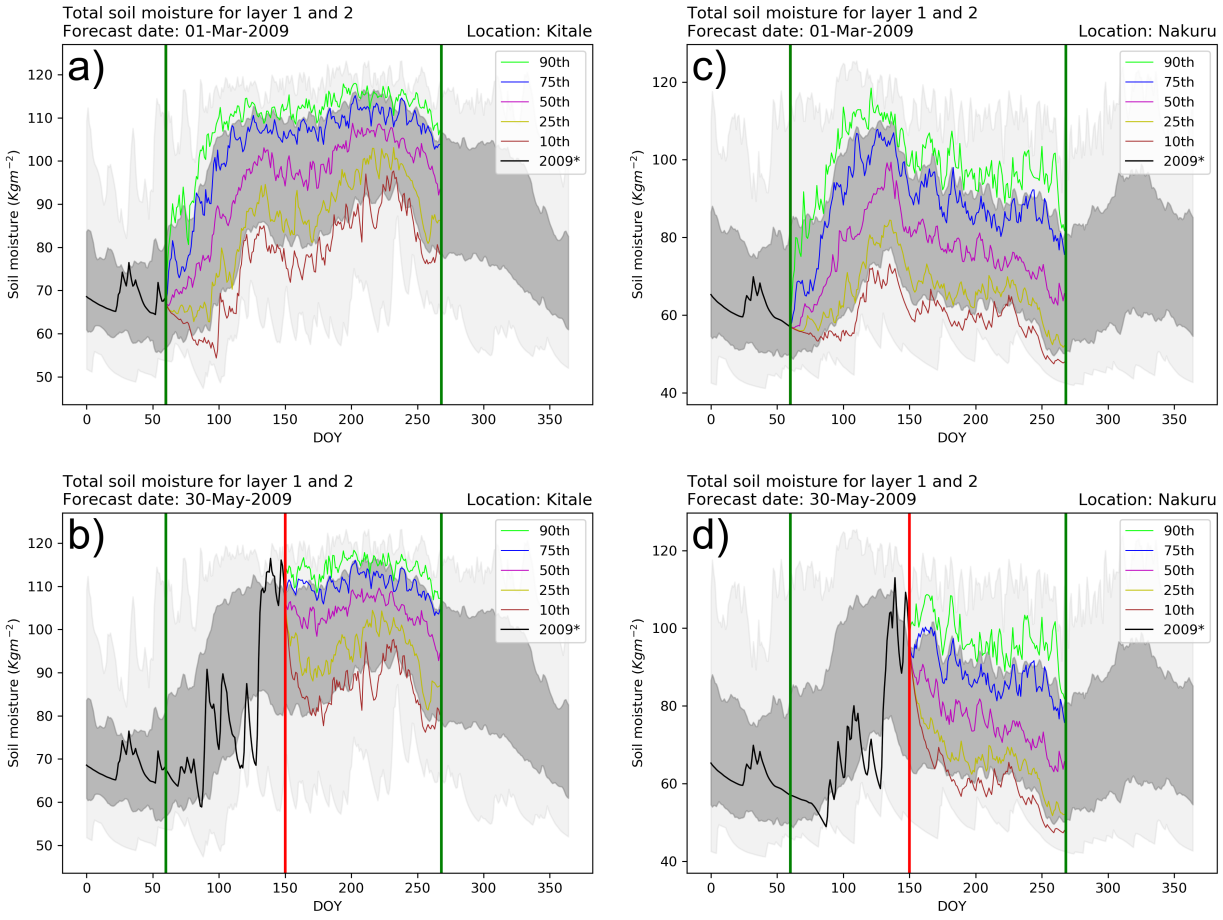

Figure C.1.1: Soil moisture forecast for the first 2 layers. (a) The forecast for Kitale at the beginning of the main rainy season (March) (b) The forecast for Kitale at the end of the main rainy season (May) (c) The forecast for Nakuru in the beginning of the main rainy season (March) (d) The forecast for Nakuru at the end of the main rainy season (May).

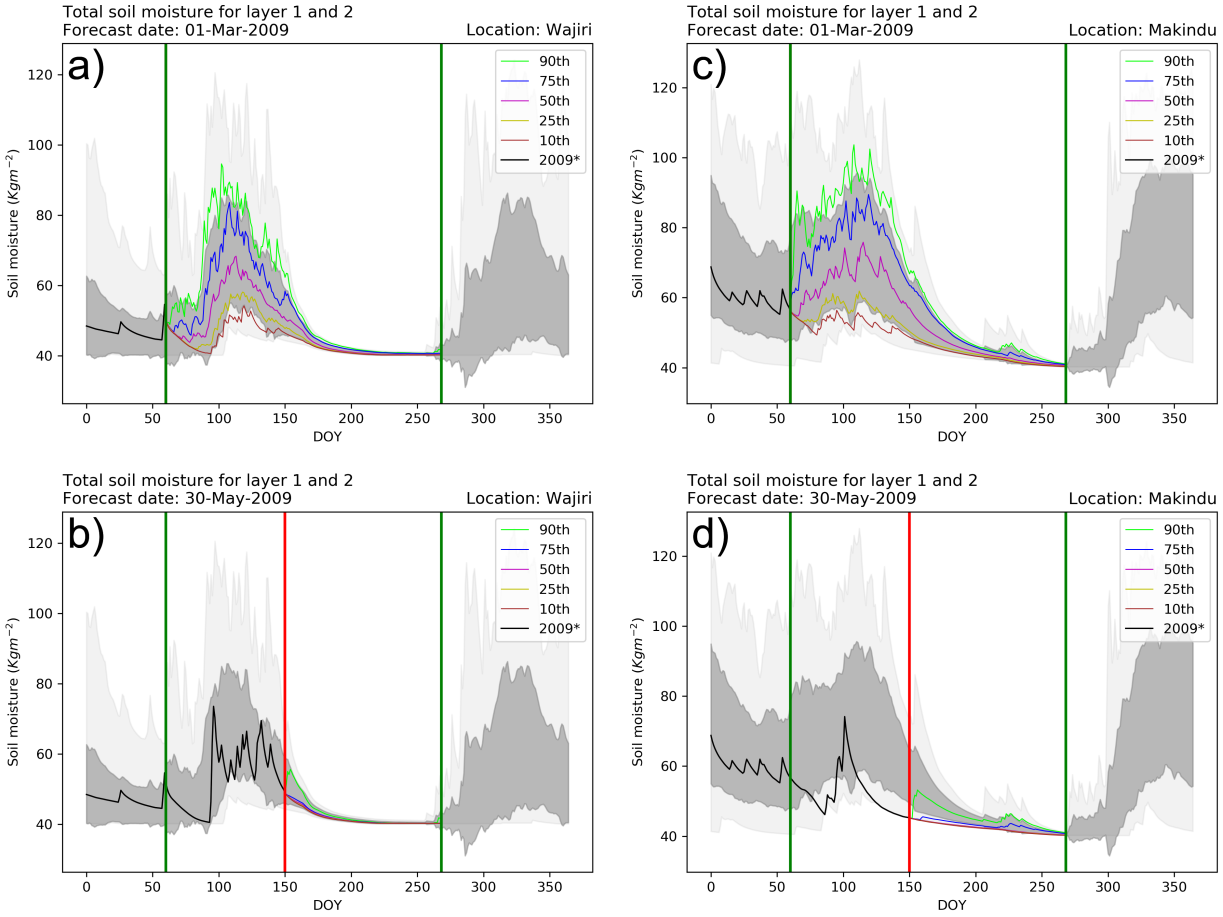

Figure C.1.2: Soil moisture forecast for the first 2 layers. (a) The forecast for Wajiri at the beginning of the main rainy season (March) (b) The forecast for Wajiri at the end of the main rainy season (May) (c) The forecast for Makindu in the beginning of the main rainy season (March) (d) The forecast for Makindu at the end of the main rainy season (May).

Appendix D

Supplementary for Chapter 5

D.1 TAMSAT-ALERT planting date decision making criteria

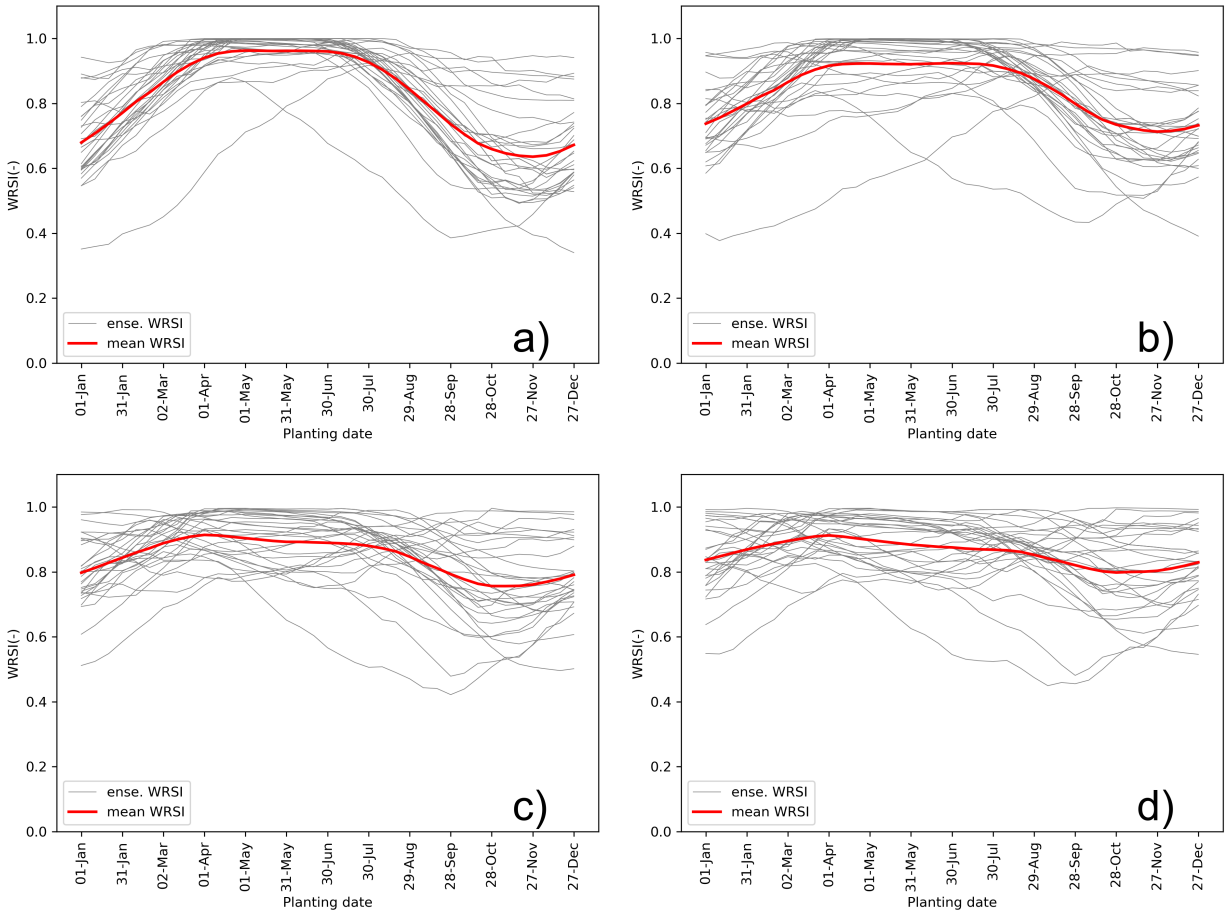

Figure D.1.1: Historical WRSI for different locations in western Kenya. (a) For $0.58°N, 34.55°E$, (b) For $0.0°N, 34.42°E$, (c) For $-0.48°N, 34.85°E$, (d) For $-0.68°N, 34.77°E$. The grey lines represent the ensemble of WRSI for a climatological period of 30 years (1983–2012) and the red line indicate the mean WRSI value.

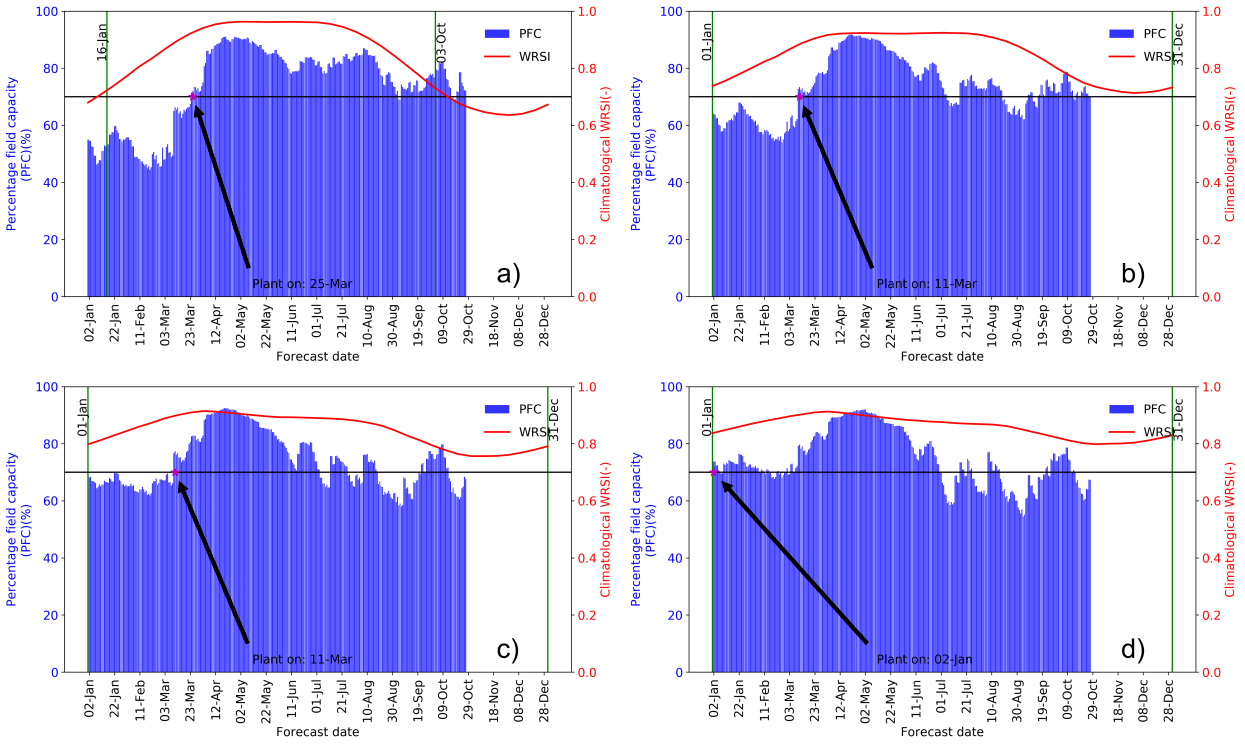

Figure D.1.2: TAMSAT-ALERT planting date decision-making methodology for different locations in western Kenya. (a) For $0.58°N, 34.55°E$, (b) For $0.0°N, 34.42°E$, (c) For $-0.48°N, 34.85°E$, (d) For $-0.68°N, 34.77°E$. In all the plots red line indicates the climatological WRSI which will be used to define a planting window in the location by considering a critical WRSI value of 75% of the maximum WRSI which gives the respected planting window for each point represented by the two green vertical lines. The blue bars represent the percentage field capacity of the 14 days average soil moisture forecast and will be used to determine the planting date within the planting window specified indicated by the black solid horizontal line (crPFC of 70%) and the planting date would be on the day shown by the star.

D.2 Sensitivity test for TAMSAT-ALERT planting date decision making criteria

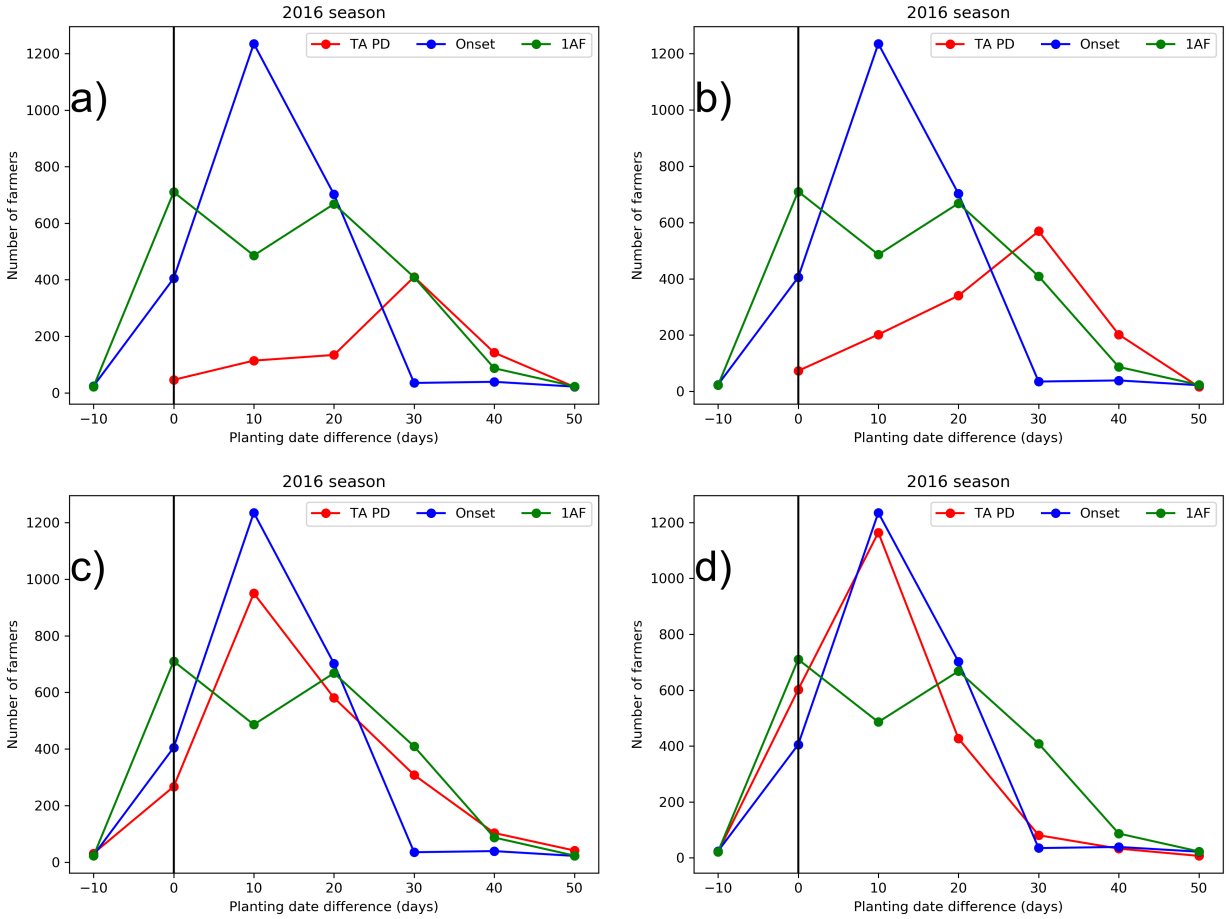

Figure D.2.1: Comparison of number of farmers and difference between farmers and recommended planting dates. The black solid line indicate the recommended planting date by the three methods and negative values in the $x - axis$ indicate early planting by farmers while positive values indicate late planting. Each plot represent different crPFC (a) 60% (b) 65%, (c) 75%, (d) 80% for 2016 season.

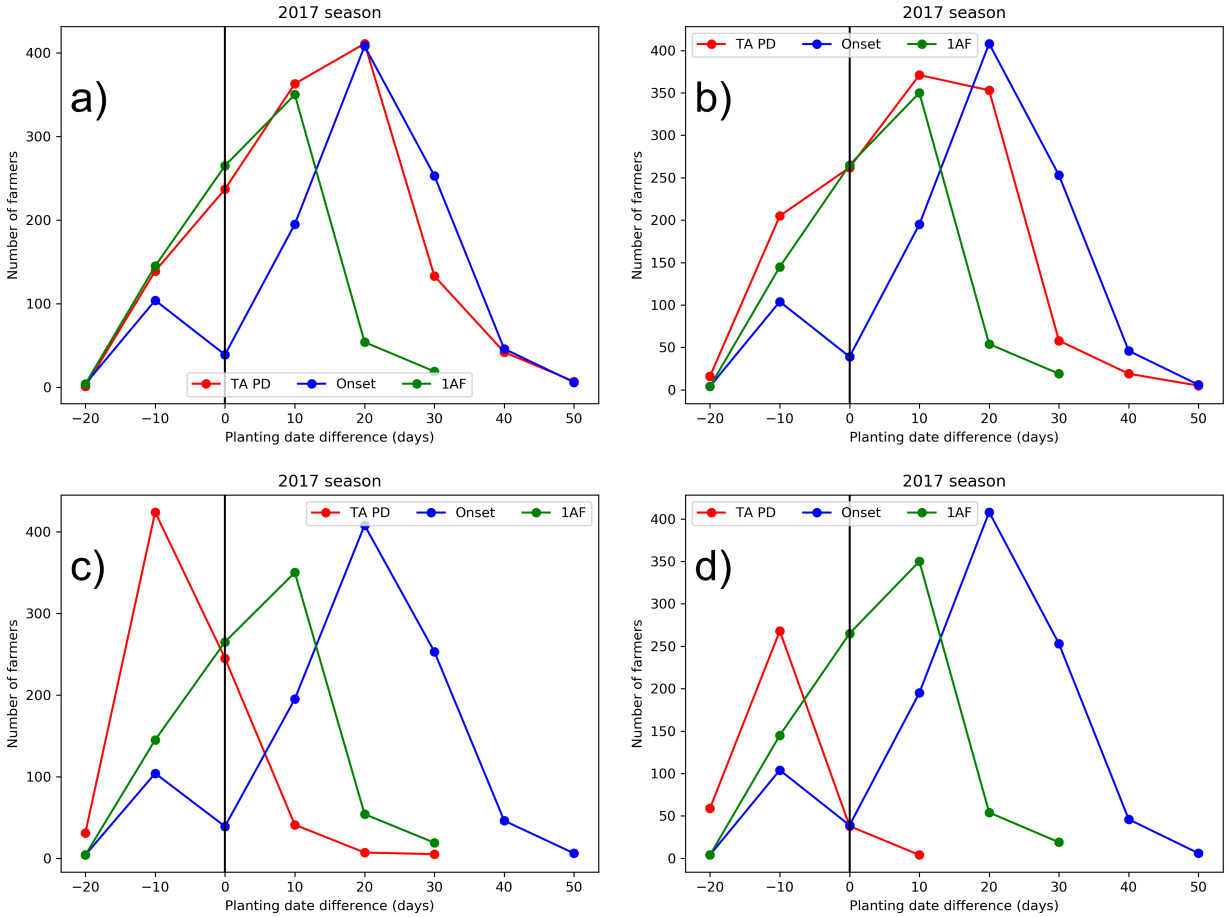

Figure D.2.2: Comparison of number of farmers and difference between farmers and recommended planting dates. The black solid line indicate the recommended planting date by the three methods and negative values in the $x - axis$ indicate early planting by farmers while positive values indicate late planting. Each plot represent different crPFC (a) 60% (b) 65%, (c) 75%, (d) 80% for 2017 season.

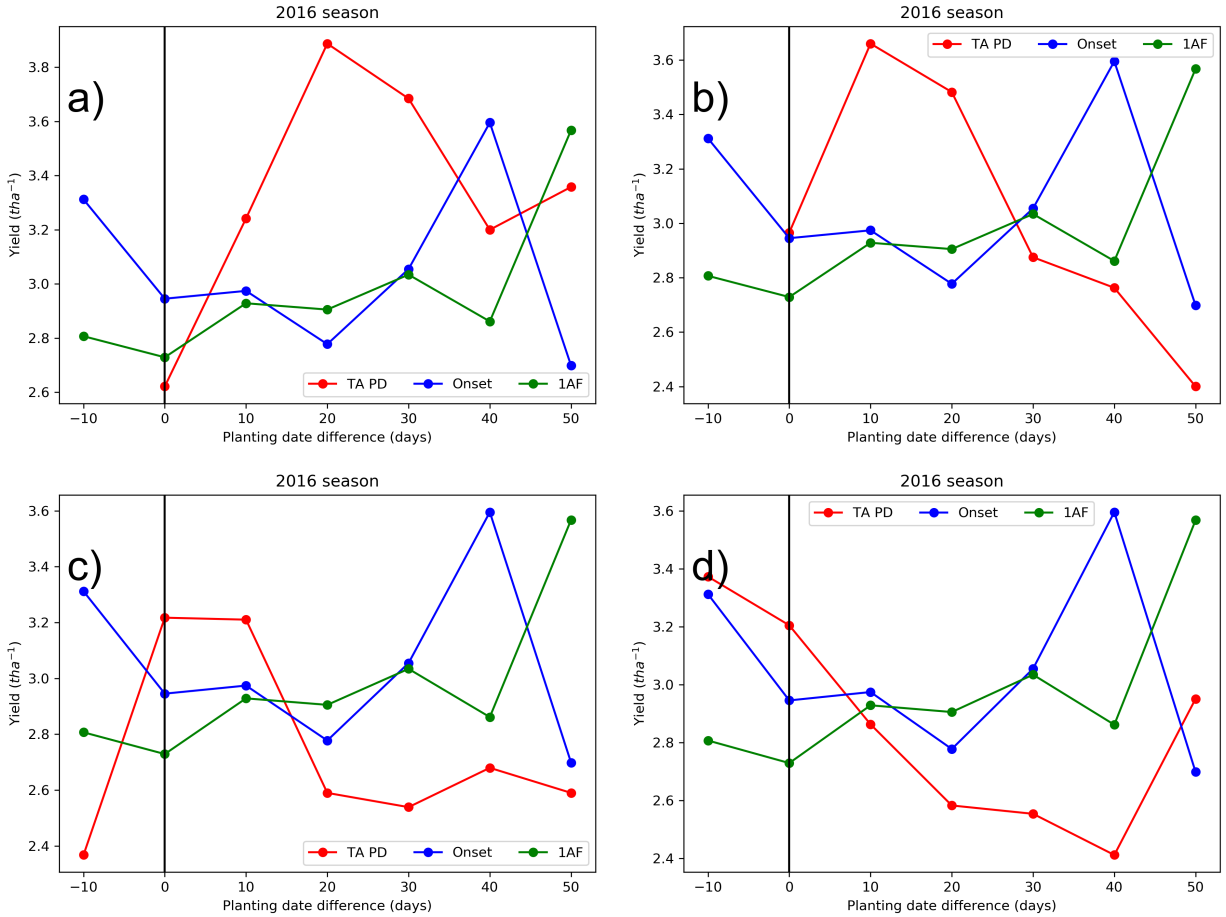

Figure D.2.3: Comparison of average yield and difference between farmers and recommended planting dates. The black solid line indicate the recommended planting date by the three methods and negative values in the $x-axis$ indicate early planting by farmers while positive values indicate late planting. Each plot represent different crPFC (a) 60% (b) 65%, (c) 75%, (d) 80% for 2016 season.

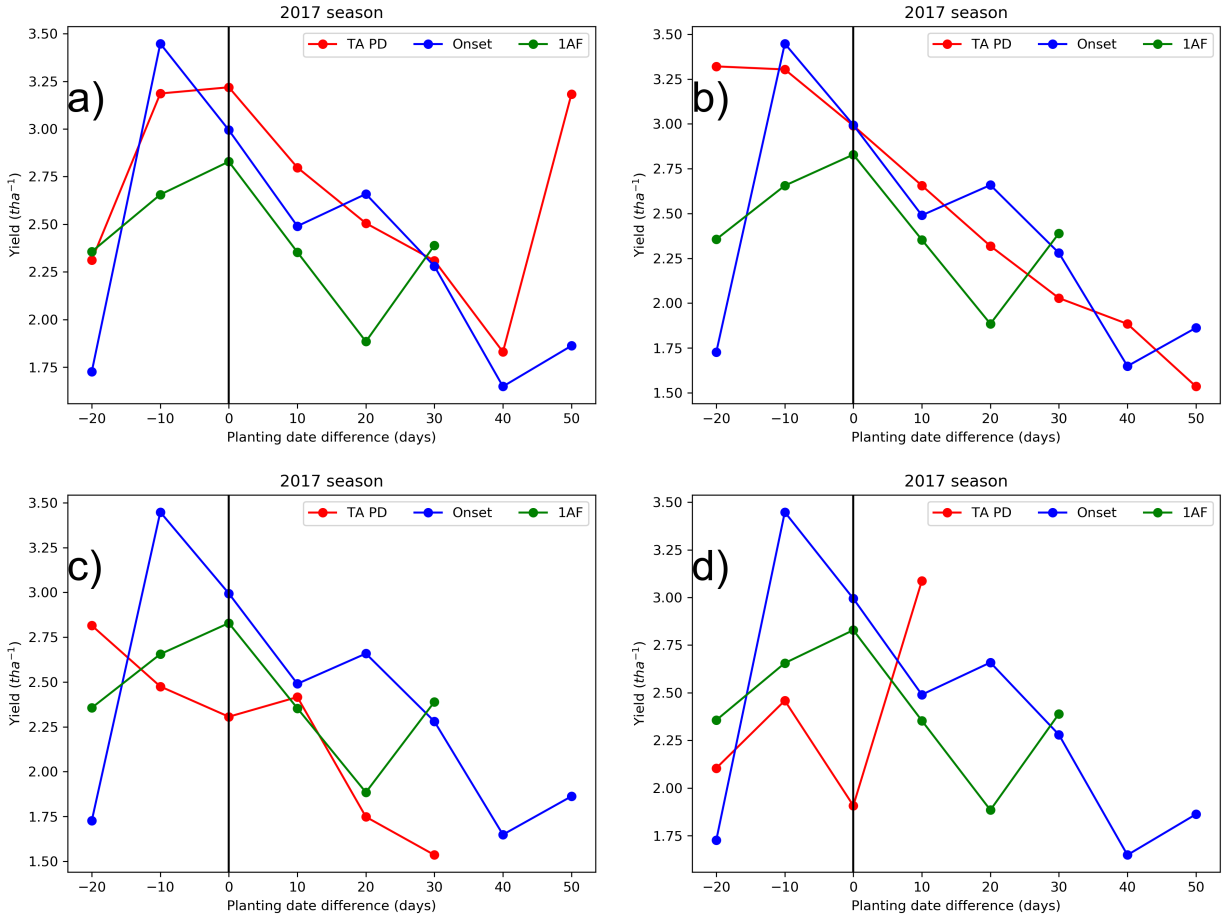

Figure D.2.4: Comparison of average yield and difference between farmers and recommended planting dates. The black solid line indicate the recommended planting date by the three methods and negative values in the $x-axis$ indicate early planting by farmers while positive values indicate late planting. Each plot represent different crPFC (a) 60% (b) 65%, (c) 75%, (d) 80% for 2017 season.